Ministry for Primary Industries
Manatū Ahu Matua

Characterisation and length-based assessment model for scampi (*Metanephrops challengeri*) in the Bay of Plenty (SCI 1) and Hawke Bay–Wairarapa (SCI 2)

New Zealand Fisheries Assessment Report 2016/51

Ian Tuck

ISSN 1179-5352 (online)
ISBN 978-1-77665-390-4 (online)

October 2016

New Zealand Government

Growing and Protecting New Zealand

Requests for further copies should be directed to:

Publications Logistics Officer
Ministry for Primary Industries
PO Box 2526
WELLINGTON 6140

Email: brand@mpi.govt.nz
Telephone: 0800 00 83 33
Facsimile: 04-894 0300

This publication is also available on the Ministry for Primary Industries websites at:
http://www.mpi.govt.nz/news-resources/publications.aspx
http://fs.fish.govt.nz go to Document library/Research reports

TABLE OF CONTENTS

EXECUTIVE SUMMARY

Tuck, I.D. (2016). Characterisation and length-based population model for scampi (*Metanephrops challengeri*) in the Bay of Plenty (SCI 1) and Hawke Bay–Wairarapa (SCI 2).

***New Zealand Fisheries Assessment Report 2016/51.* 188 p.**

Stock assessments of the Bay of Plenty (SCI 1) and Wairarapa–Hawke Bay (SCI 2) scampi stocks have been undertaken through MPI project DEE201508SCI. This work has revised existing models for these stocks, developed within previous MPI projects. The assessments presented for both stocks were accepted by the Shellfish Fisheries Assessment Working Group (SFAWG).

Fishery characterisations were undertaken, and a range of CPUE indices were estimated for each stock, on the basis of spatial and temporal stratification of the previous models. Previous models have examined incorporating considerable spatial structure, but following preliminary investigations, the SFAWG recommended only developing single area models for these stocks, and fitting an annual CPUE index rather than separate time step indices. Sensitivity to natural mortality, revised catchability priors, and data weighting were investigated, with base models for both stocks taken as those with M fixed at 0.25, 0.3 and 0.35.

For SCI 1, SSB is estimated to have increased through the early 1990s, peaking in the mid 1990s, and then declining until the early 2000s. Subsequently, SSB was very stable at around 70% SSB_0, but increased slightly in the most recent years. SSB_{2015} is estimated to be between 72% and 75% of SSB_0 (median values). MCMC posteriors suggest 0% probability that SSB_{2015} is below 40% SSB_0. Annual fishing intensity has consistently been estimated to be below F 40% B_0. Future catches up to 156 tonnes annually (to 2021) are predicted to reduce the SSB relative to SSB_{2015}, but remain above 40% SSB_0.

For SCI 2, SSB is estimated to have increased through the early 1990s, peaking around 1993, and then declined to a minimum in 2003, before increasing slightly to 2005. Subsequently, SSB remained stable until about 2008, then increased rapidly to 2013, and declined slightly after this. SSB_{2015} is estimated to be between 89% and 113% of SSB_0 (median values). MCMC posteriors suggest 0% probability that SSB_{2015} is below 40% SSB_0. Annual fishing intensity peaked in 2002 but has declined considerably in recent years. SSB was at or below 40% SSB_0 between 2002 and 2004, but has increased considerably since this time. Future catches up to 200 tonnes annually (to 2021) are predicted to reduce the SSB relative to SSB_{2012}, but remain above 40% SSB_0.

1. INTRODUCTION

This report undertakes a fishery characterisation for the Bay of Plenty (SCI 1) and Hawke Bay/Wairarapa (SCI 2) scampi stocks, and applies the previously described Bayesian, length-based, two-sex population model to these stocks. Previous characterisations of scampi stocks are described by Tuck (2009) and Tuck (2014). The first attempt at developing a length-based population model for any scampi stock was conducted for SCI 1 (Cryer et al. 2005), implemented using the general-purpose stock assessment program CASAL v2.30 (Bull et al. 2012). This model for SCI 1 was developed further and the same model structure was also applied to SCI 2 in later projects (Tuck & Dunn 2006; Tuck 2014). The current study used CASAL v 2.30 (Bull et al. 2012). Developments in the model implementation and structure have been largely based on suggestions raised at the MFish funded Scampi Assessment Workshop (Tuck & Dunn 2009), and subsequently at Shellfish Fisheries Assessment Working Group (SFAWG) meetings. Assessments for SCI 1 and SCI 2 using this model were accepted in 2011 and 2014 (Tuck & Dunn 2012; Tuck 2014).

We describe the available data and how they were used, the parameterisation of the model, and model fits and sensitivity. This report fulfils Ministry of Primary Industries project DEE201508SCI "*Stock assessment of scampi*", undertaking stock assessments of SCI 1 and SCI 2. The objective of this project was to carry out a stock assessment, including estimating yield, for SCI 1 and SCI 2 in 2015–16.

1.1. The Bay of Plenty (SCI 1) and Hawke Bay/Wairarapa (SCI 2) scampi fisheries

Scampi is fished all around New Zealand, in nine fishery management areas (Figure 1). The SCI 1 and SCI 2 fisheries are two of New Zealand's four main scampi fisheries (the others being SCI 3 and SCI 6A), and over the last five years (2010–11 to 2014–15) have contributed an average of 116 and 118 tonnes annually, with landings from SCI 1 remaining relatively stable while those from SCI 2 have increased in recent years. The TACC for SCI 1 is 120 tonnes, for SCI 2 is 133 tonnes (having been reduced from 200 tonnes to 100 tonnes in 2011, and increased to 133 tonnes in 2014), and the total TACC for all management areas is 1224 tonnes.

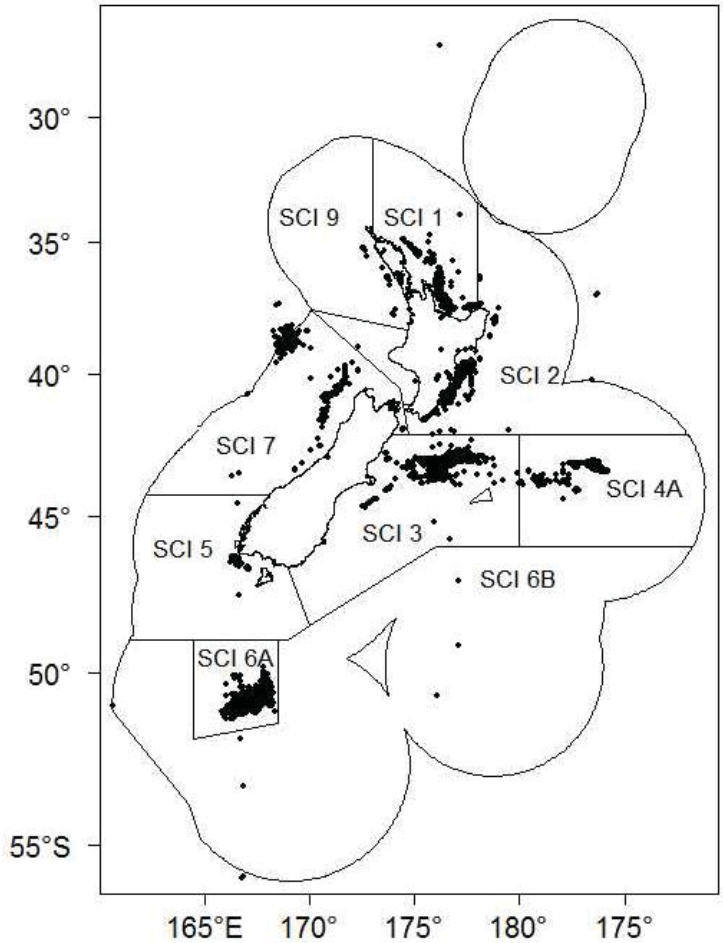

Figure 1: Spatial distribution of the scampi fishery since 1988–89. Each dot shows the mid point of one or more tows recorded on TCEPR with scampi as the target species.

The spatial distribution of the targeted scampi fishing within SCI 1 is focussed in an relatively narrow continuous band (interrupted at Mayor Island) within the Bay of Plenty (Figure 2), generally ranging from 300–500 m depth. More isolated patches have also been fished in some years, to the north and east, but in the same depth range. Targeted scampi fishing in SCI 2 has been focussed in two separate patches, from Hawke Bay to (roughly) Blackhead Point, and from Cape Turnagain to Castle Point, again generally ranging from 300–500 m depth (Figure 3). Smaller isolated patches have also been fished on occasion to the north and south. In both areas, surveys have focussed on the main areas of the fishery, and survey strata coverage is illustrated in the respective figures.

Management areas have remained consistent for SCI 1 and SCI 2 throughout the history of the fishery. Prior to the 1991–92 fishing year there were no limits on scampi catches. For the 1991–92 fishing year, Individual Quotas (IQs) were introduced for both areas (allocated on the basis of the permit holders' catch in 1990–91). These IQs were maintained with the introduction of ICE regulations in 1999, and continued until the Court of Appeal ruled in October 2001 that the scampi ICE regulations were unlawful, after which all scampi stocks were managed under competitive catch limits, until the species was introduced into the QMS (October 2004). Since then all scampi fisheries have been managed with individual quotas.

Previous fishery characterisations have been undertaken for these areas in Cryer & Coburn (2000) and Tuck (2009; 2014).

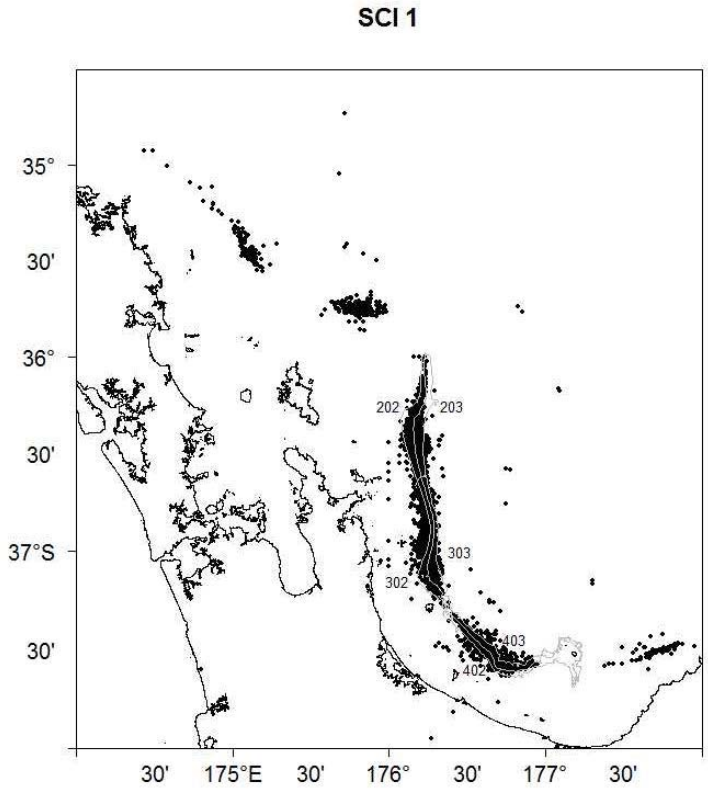

Figure 2: Spatial distribution of the scampi fishery within management area SCI 1 since 1988–89. Each dot shows the mid point of one or more tows recorded on TCEPR with scampi as the target species. The extents of the six scampi survey strata are shown in grey with associated labels.

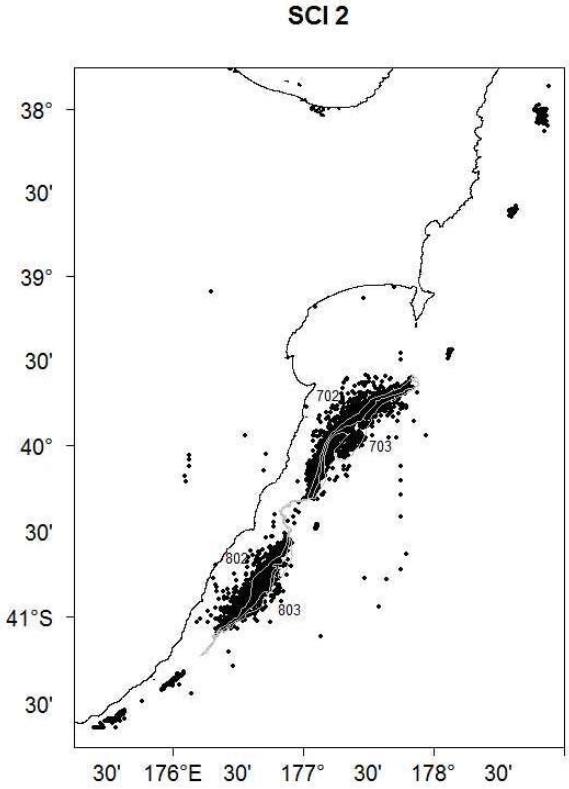

Figure 3: Spatial distribution of the scampi fishery within management area SCI 2 since 1988–89. Each dot shows the mid point of one or more tows recorded on TCEPR with scampi as the target species. The extents of the four scampi survey strata are shown in grey with associated labels.

2. FISHERY CHARACTERISATION AND DATA

2.1. Commercial catch and effort data

Scampi fishers have consistently reported catches on the Trawl Catch, Effort, and Processing Returns (TCEPR) form since its introduction in 1989–90, providing a very valuable record of catch and effort on a tow by tow basis.

Data were extracted from the MPI TCEPR database, requesting all fishing events (from all areas) where scampi (SCI) was the nominated target species, or was reported in the catch from that trip. This resulted in an extract of 318 683 fishing events, but fishing events where scampi was the target species (116 668 events) contributed 99.9% of estimated scampi catches, and so only scampi targeting events were considered further. Errors in TCEPR records are reducing in frequency, but do occur, and the raw records were groomed in the following manner. For each record, the reported data were used to estimate the duration of the trawl shot, the distance between the start and finish locations, and the mid point between the start and finish locations. Tows with zero scampi catch were excluded. All tows with zero hours tow duration recorded (but some scampi catch) were reset to the median tow duration for the trip (51 events). All tows with a tow distance greater than 50 km were reset to the median of the mid point of tows on the same day, adjacent days, or the trip, depending on available data. Once edited, these events were included in the allocation of catch data to area and time step analysis, but not included in the CPUE analysis. Where a vessel only reported start position (rather than start and finish position) for a tow (1583 events), this was used instead of the mid point. Excluding fishing events with no scampi catch reduced the data set to 112 527 events, and removing additional events where the location could not be determined reduced the data set further, to 112 288 events, 2504 of which were those where the original estimated tow distance exceeded 50 km. The data for SCI 1 and SCI 2 were then extracted from this full data set on the basis of latitude and longitude. This dataset represents over 99.8% of estimated scampi catches by the scampi target fishery.

2.1.1. SCI 1

Total annual landings for the fishery, and the percentage by the target scampi fishery, are presented in Table 1. The distribution of fishing activity within the SCI 1 area over time is presented in Figure 4 and Figure 5. The area over which the assessment model is applied is defined as the survey strata (300–500 m depth range in the main area of the fishery) (Figure 2), and over 90% of the targeted scampi catch has been reported from this area in all years except 2002–03 (Table 1). The core area has consistently been fished over the history of the fishery, with smaller isolated patches (particularly to the north) fished in some years. Overall, the core (modelled) area has accounted for 99% of scampi targeted catch. Boxplots of the unstandardized CPUE (Figure 6) show catch rates initially increasing in the mid 1990s, peaking in 1996, declining to about 2000, and remaining relatively stable since then.

The breakdown of catch by survey strata and fishing year is presented for SCI 1 in Figure 7. In general, the shallower strata (202, 302 and 402, i.e., 300–400 m) contributed more catch than the deeper strata, and fishing was less consistent (landings have fluctuated more) in the southern area (strata 402 and 403).

Table 1: Reported commercial landings (tonnes) from the 1986–87 to 2014–15 fishing years for SCI 1, catch estimated from scampi target fishery, and estimated catch from modelled area (survey strata).

	Landings (MHR)	Target catch (TCEPR)	% SCI target	Estimated catch (modelled area)	% catch (modelled area)
1986–87	5.0				
1987–88	15.0				
1988–89	60.0				
1989–90	104.0	104.3	100%	102.5	98%
1990–91	179.0	163.2	91%	162.6	100%
1991–92	132.0	128.6	97%	128.2	100%
1992–93	114.0	116.0	102%	111.2	96%
1993–94	115.0	111.6	97%	109.5	98%
1994–95	114.0	113.6	100%	113.6	100%
1995–96	117.0	116.4	99%	115.3	99%
1996–97	117.0	114.0	97%	112.3	99%
1997–98	107.0	115.3	108%	113.6	98%
1998–99	110.0	112.4	102%	112.2	100%
1999–00	124.0	116.1	94%	116.1	100%
2000–01	120.0	117.1	98%	117.0	100%
2001–02	124.0	117.3	95%	108.3	92%
2002–03	121.0	113.3	94%	95.5	84%
2003–04	120.0	115.9	97%	115.8	100%
2004–05	114.0	100.1	88%	100.1	100%
2005–06	109.0	93.8	86%	93.8	100%
2006–07	110.0	101.3	92%	101.3	100%
2007–08	102.0	93.1	91%	92.9	100%
2008–09	86.0	81.0	94%	81.0	100%
2009–10	111.4	105.0	94%	104.5	100%
2010–11	113.9	107.9	95%	107.7	100%
2011–12	114.5	107.3	94%	107.3	100%
2012–13	126.1	119.4	95%	119.1	100%
2013–14	106.6	100.3	94%	99.9	100%
2014–15	116.9	107.1	92%	107.1	100%

Monthly patterns of effort and catch are presented in Figure 8 and Figure 9. The fishery was managed with competitive catch limits between 2001–02 and 2003–04. During this period, effort and catches were focussed in the first few months of the fishing year, but prior to and since this time, fishing has been distributed throughout the year (particularly more recently).

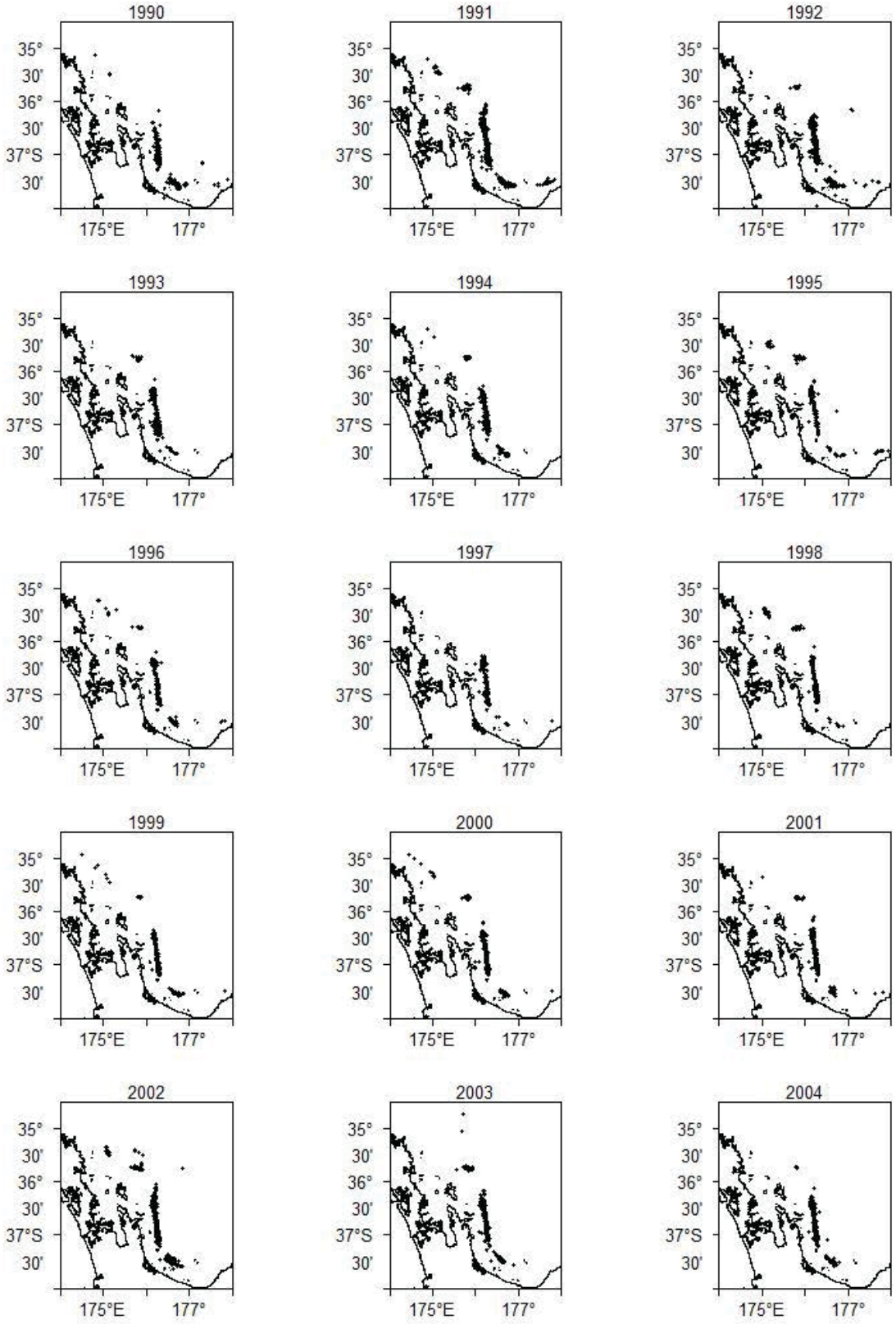

Figure 4: Spatial distribution of the main area of the SCI 1 scampi trawl fishery from 1989–90 to 2003–04. Each dot represents the mid point of one or more tows reported on TCEPR. The general area covered by the plots is indicated within Figure 5.

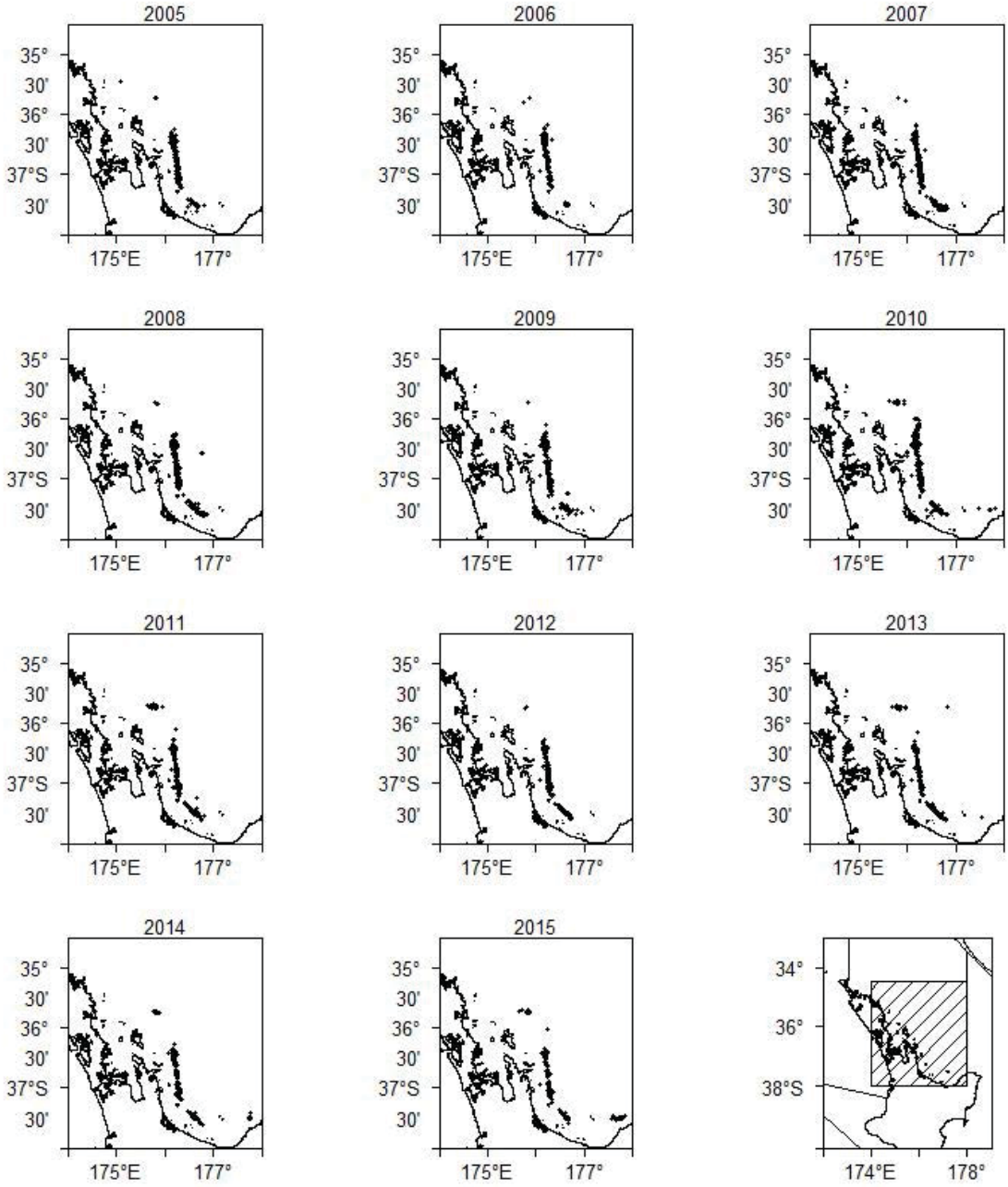

Figure 5: Spatial distribution of the main area of the SCI 1 scampi trawl fishery from 2004–05 to 2014–15. Each dot represents the mid point of one or more tows reported on TCEPR. The general area covered by the plots is indicated by the shaded box in the bottom right plot.

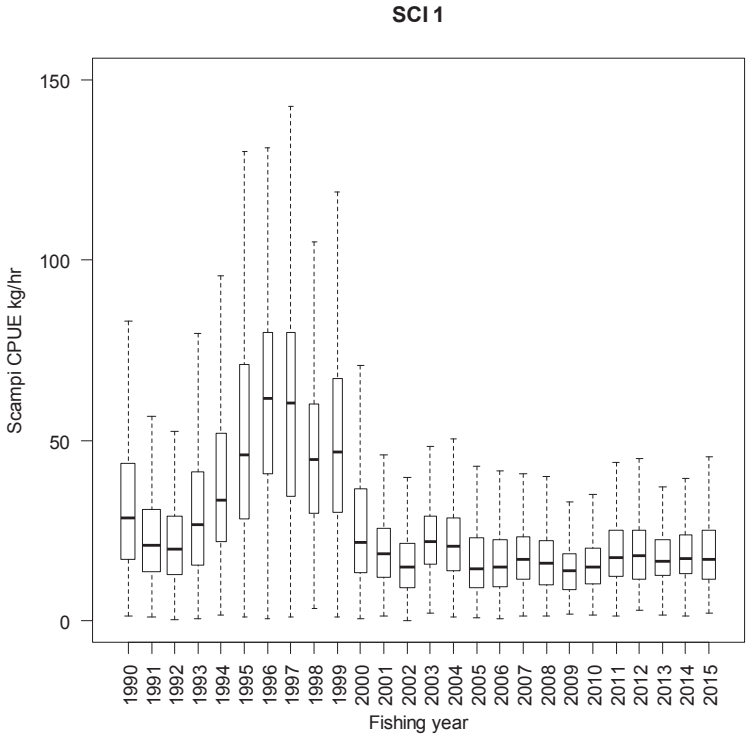

Figure 6: Boxplot (with outliers removed) of individual observations from TCEPR of unstandardized catch rate (catch (kg) divided by tow effort (hours)) with tows of zero scampi catch excluded, by fishing year for the SCI 1 fishery. Box width is proportional to the square root of number of observations.

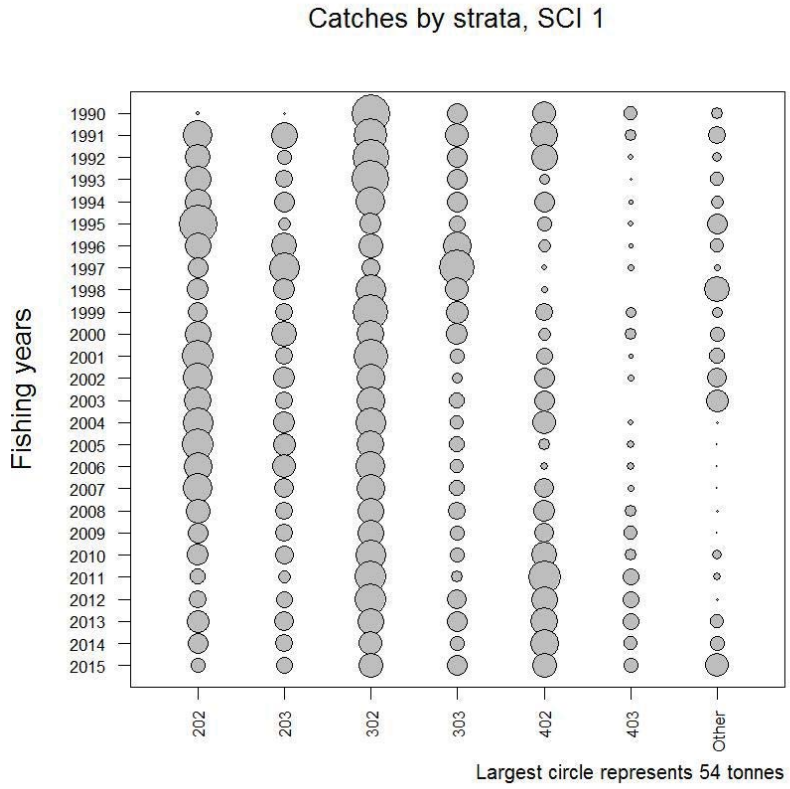

Figure 7: Annual catch breakdown by survey strata (and outside modelled area, 'Other') and fishing year for SCI 1.

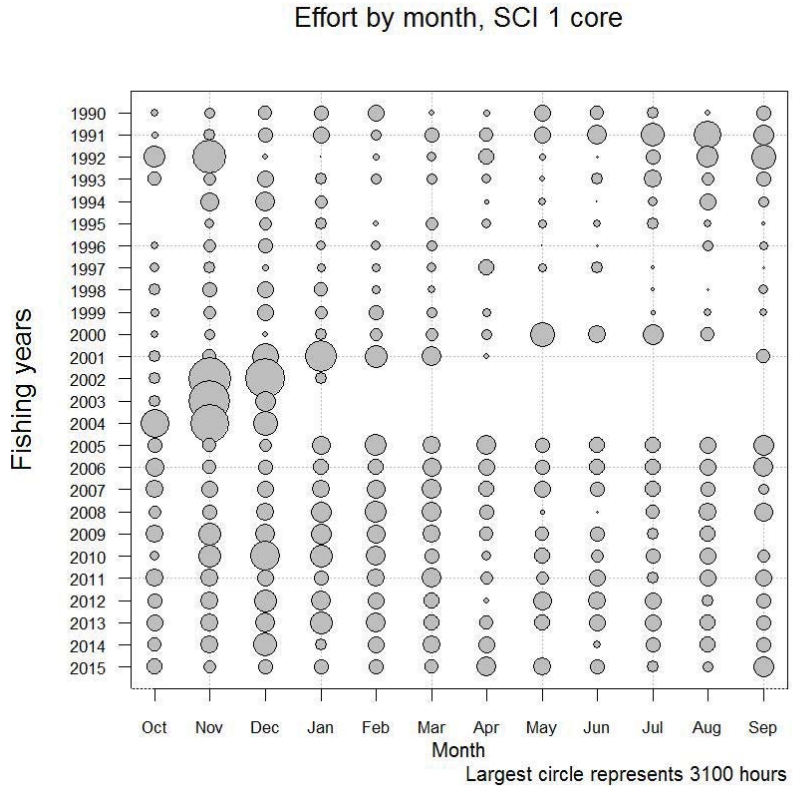

Figure 8: Monthly pattern of fishing effort in the scampi targeted fishery by fishing year for the core (modelled) area of SCI 1.

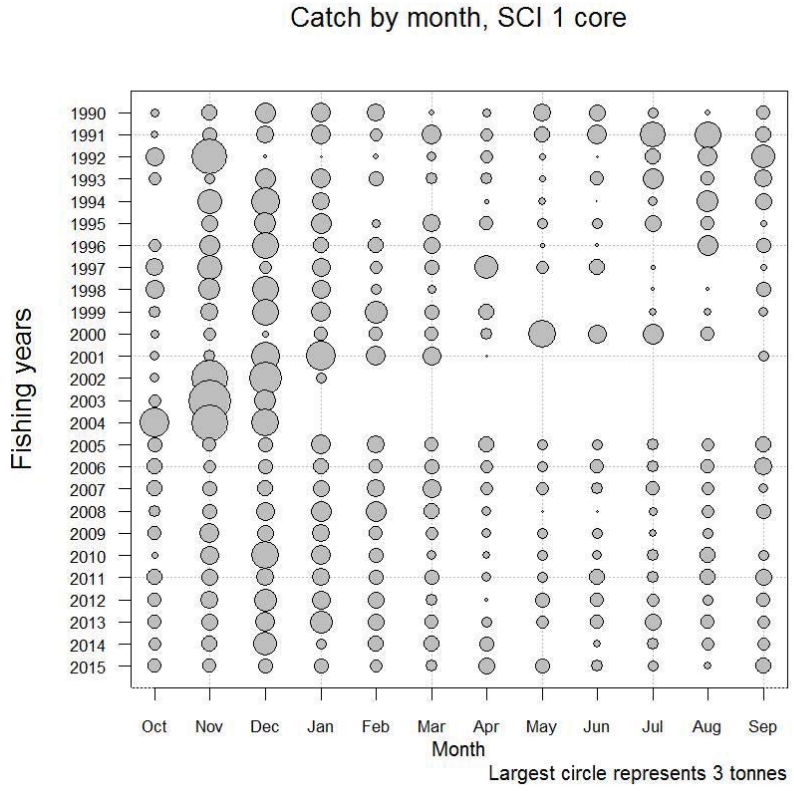

Figure 9: Monthly pattern of scampi catches in the scampi targeted fishery by fishing year for the core (modelled) area of SCI 1.

2.1.2. SCI 2

Total annual landings for the fishery, and the percentage by the target scampi fishery are presented in Table 2, and the distribution of fishing activity within the SCI 2 area over time is presented in Figure 10 and Figure 11. The area over which the assessment model is applied is defined by the survey strata (300–500 m depth range in the main area of the fishery) (Figure 3); over 98% of the targeted scampi catch has been reported from this area (Table 2). The main fishery comprises two distinct grounds (Hawke Bay and Wairarapa), and these core areas have consistently been fished over the history of the fishery, with smaller isolated patches (both to the north and south) fished in some years. A boxplot of the unstandardized CPUE (Figure 12) shows that catch rates were initially stable, increased in 1995, and declined steadily to 2002. This was followed by a slight increase to 2008, and then a rapid increase to a peak in 2014 (at levels similar to those recorded in the early 1990s), before a slight decline in 2015.

Table 2: Reported commercial landings (tonnes) from the 1986–87 to 2014–15 fishing years for SCI 2, catch estimated from scampi target fishery, and estimated catch from modelled area (survey strata).

	Landings (MHR)	Target catch (TCEPR)	% SCI target	Estimated catch (modelled area)	% catch (modelled area)
1986–87	0.0				
1987–88	5.0				
1988–89	17.0				
1989–90	138.0	139.4	101%	138.1	99%
1990–91	295.0	264.7	90%	252.5	95%
1991–92	221.0	212.0	96%	193.5	91%
1992–93	210.0	209.5	100%	200.3	96%
1993–94	244.0	230.5	94%	224.2	97%
1994–95	226.0	233.9	103%	232.1	99%
1995–96	230.0	229.4	100%	227.8	99%
1996–97	213.0	214.1	101%	212.7	99%
1997–98	224.0	228.0	102%	224.3	98%
1998–99	233.0	240.5	103%	216.8	90%
1999–00	193.0	190.3	99%	189.2	99%
2000–01	146.0	190.6	131%	188.9	99%
2001–02	247.0	229.5	93%	224.7	98%
2002–03	134.0	121.8	91%	112.9	93%
2003–04	64.0	56.4	88%	56.4	100%
2004–05	71.0	61.5	87%	60.8	99%
2005–06	77.0	70.3	91%	69.6	99%
2006–07	80.0	73.1	91%	72.7	99%
2007–08	61.0	56.9	93%	56.8	100%
2008–09	52.0	49.2	95%	49.2	100%
2009–10	125.4	119.9	96%	119.3	100%
2010–11	128.2	119.9	94%	119.9	100%
2011–12	98.8	88.2	89%	88.1	100%
2012–13	95.8	90.2	94%	90.0	100%
2013–14	125.4	121.1	97%	121.1	100%
2014–15	142.6	137.4	96%	137.4	100%

The breakdown of catch by survey strata and fishing year is presented for SCI 2 in Figure 13. The two shallower strata (702 and 802, i.e., 300–400 m) contributed far more catch than the deeper strata, with the deeper strata off the Wairarapa coast (strata 803) contributing little in most years.

Monthly patterns of effort and catch are presented in Figure 14 and Figure 15. As with SCI 1, the fishery was managed with competitive catch limits between 2001–02 and 2003–04. During this period, effort and catches were focussed in SCI 2 after the SCI 1 fishery was completed (catch limit taken). Fishing has generally been far less consistently distributed through the year than in SCI 1, and in recent years there has been very little activity in the fishery between April and August.

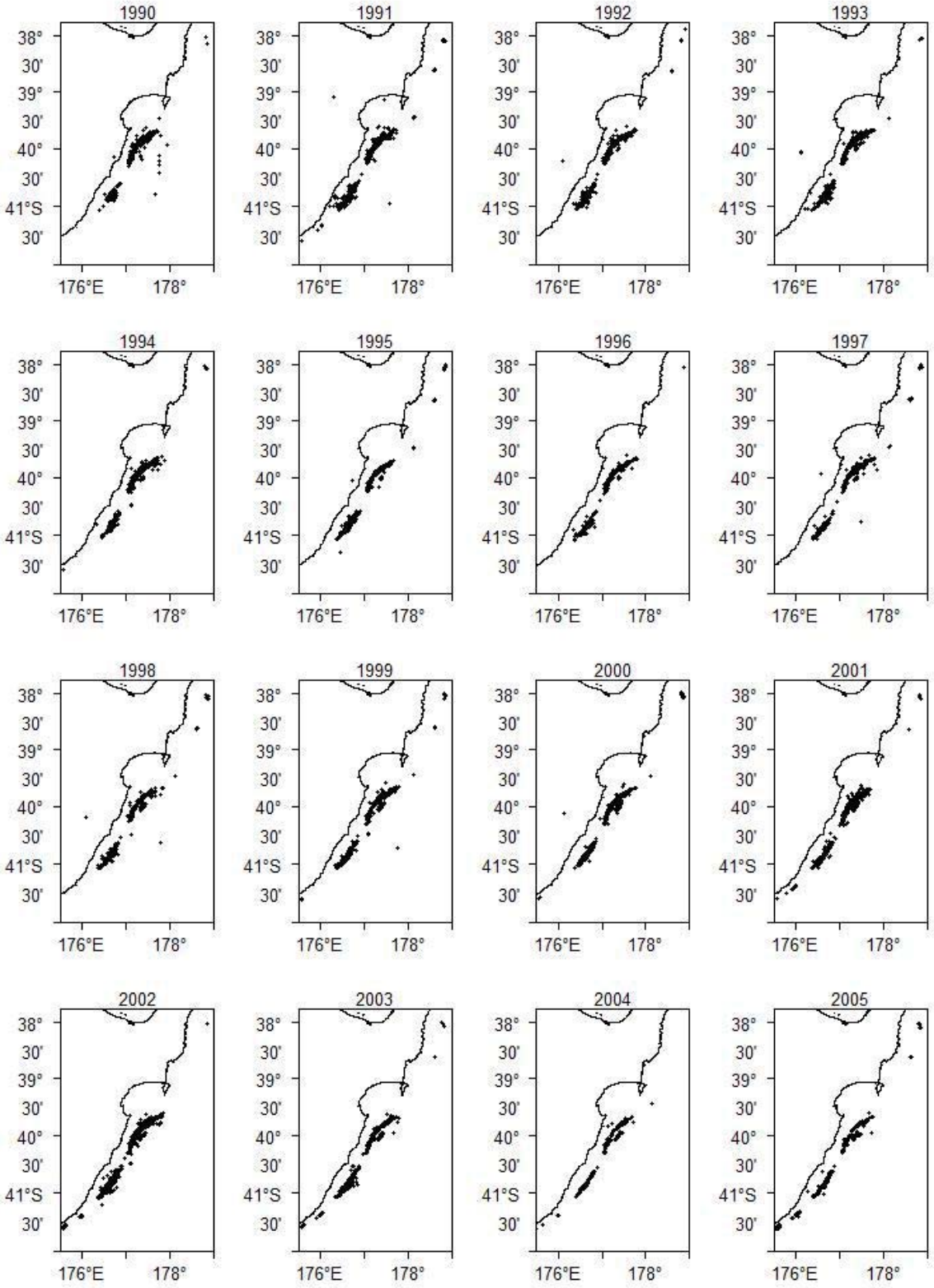

Figure 10: Spatial distribution of the main area of the SCI 2 scampi trawl fishery from 1989–90 to 2004–05. Each dot represents the mid point of one or more tows reported on TCEPR. The general area covered by the plots is indicated within Figure 11.

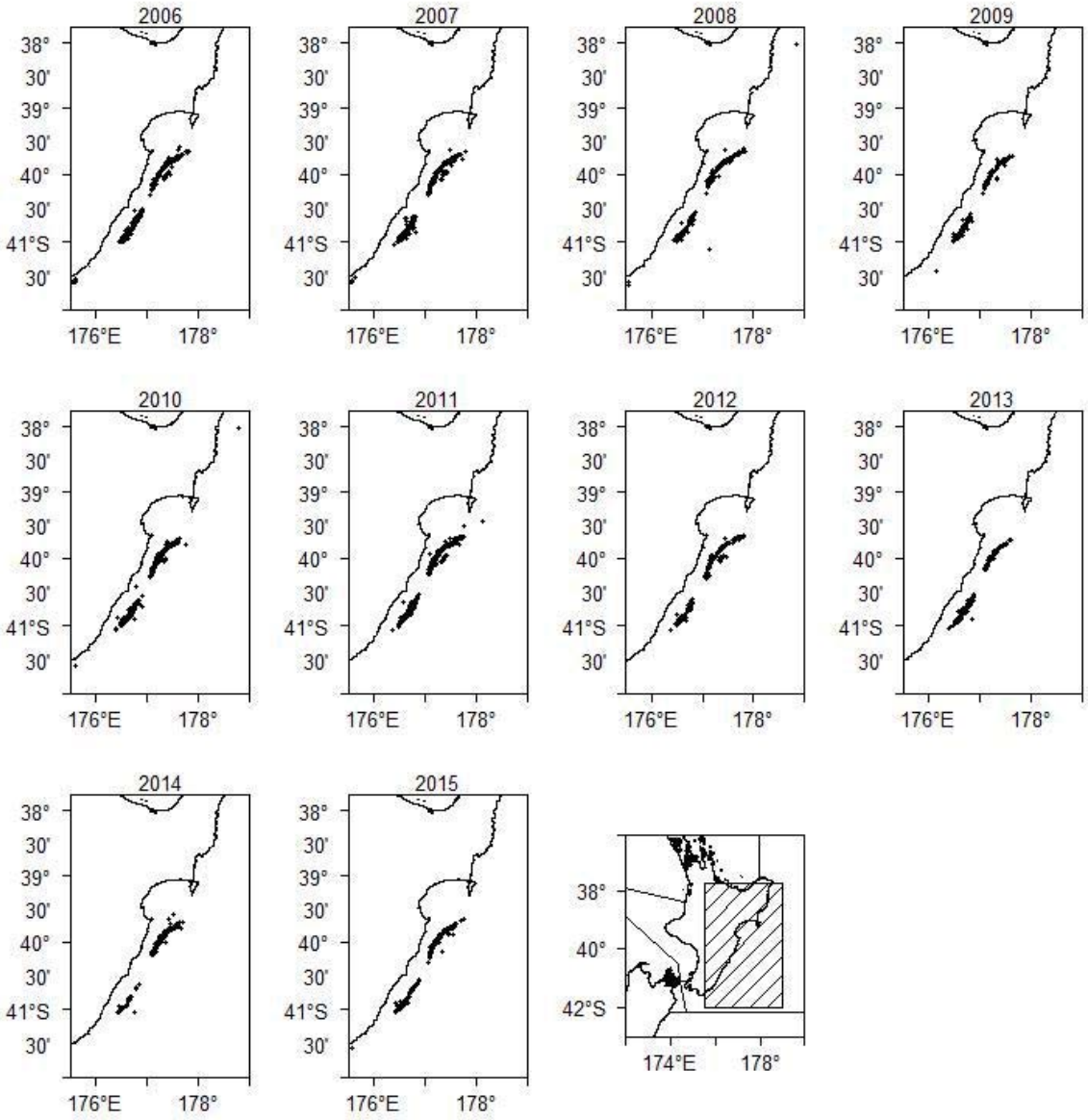

Figure 11: Spatial distribution of the main area of the SCI 2 scampi trawl fishery from 2005–06 to 2014–15. Each dot represents the mid point of one or more tows reported on TCEPR. The general area covered by the plots is indicated by shaded box in the bottom right plot.

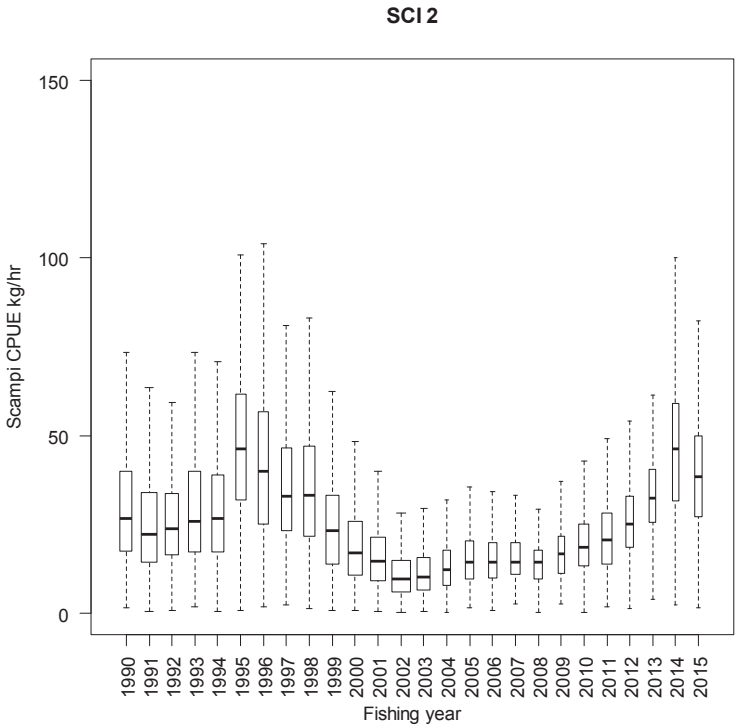

Figure 12: Boxplot (with outliers removed) of individual observations from TCEPR of unstandardized catch rate (catch (kg) divided by tow effort (hours)) with tows of zero scampi catch excluded, by fishing year for the SCI 2 fishery. Box width is proportional to the square root of the number of observations.

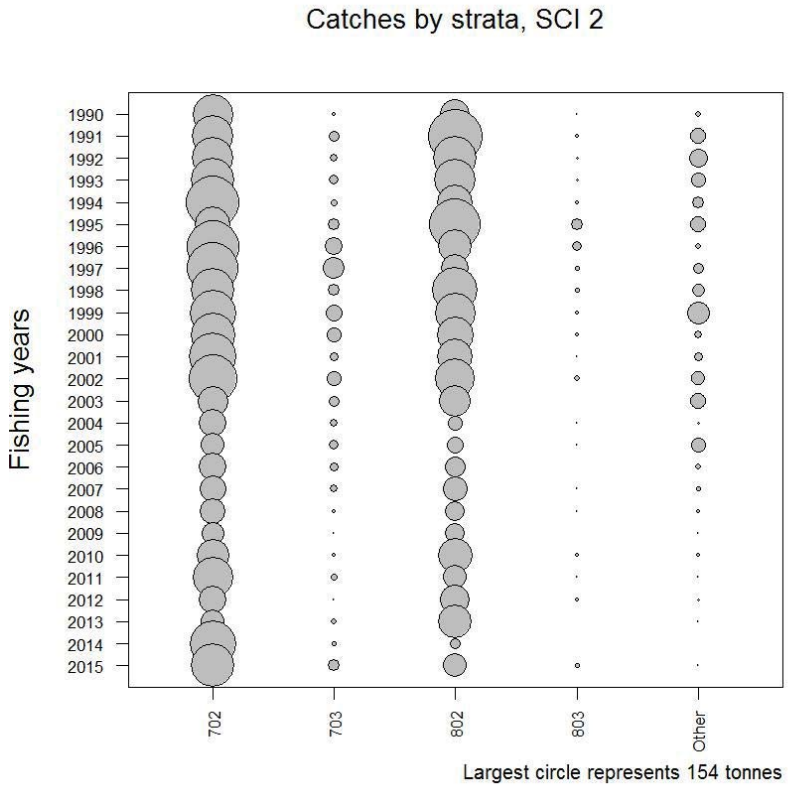

Figure 13: Annual catch breakdown by survey strata (and outside modelled area, 'Other') and fishing year for SCI 2.

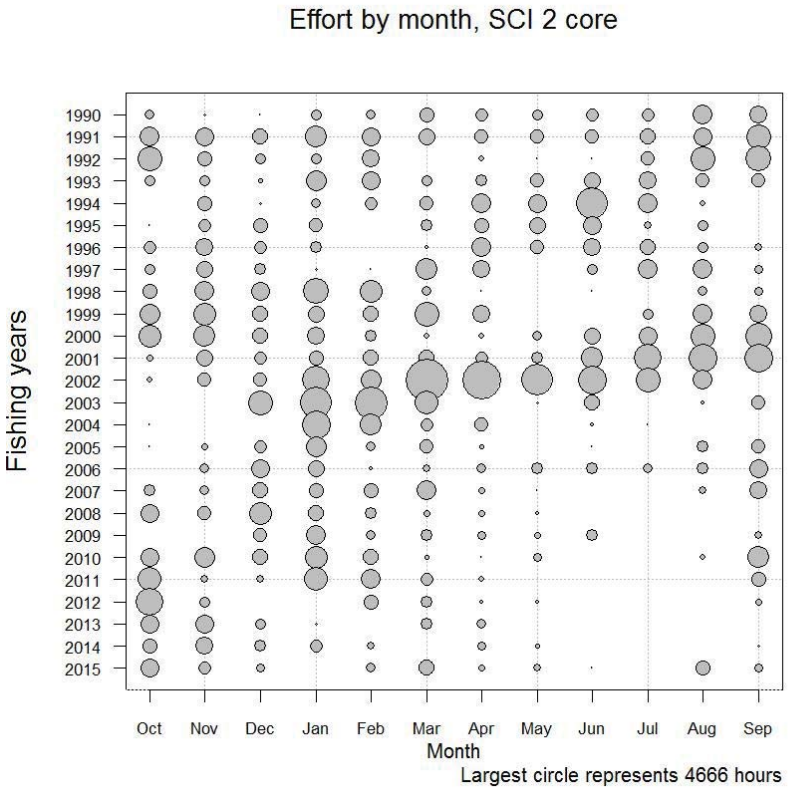

Figure 14: Monthly pattern of fishing effort in the scampi targeted fishery by fishing year for for the core (modelled) area of SCI 2.

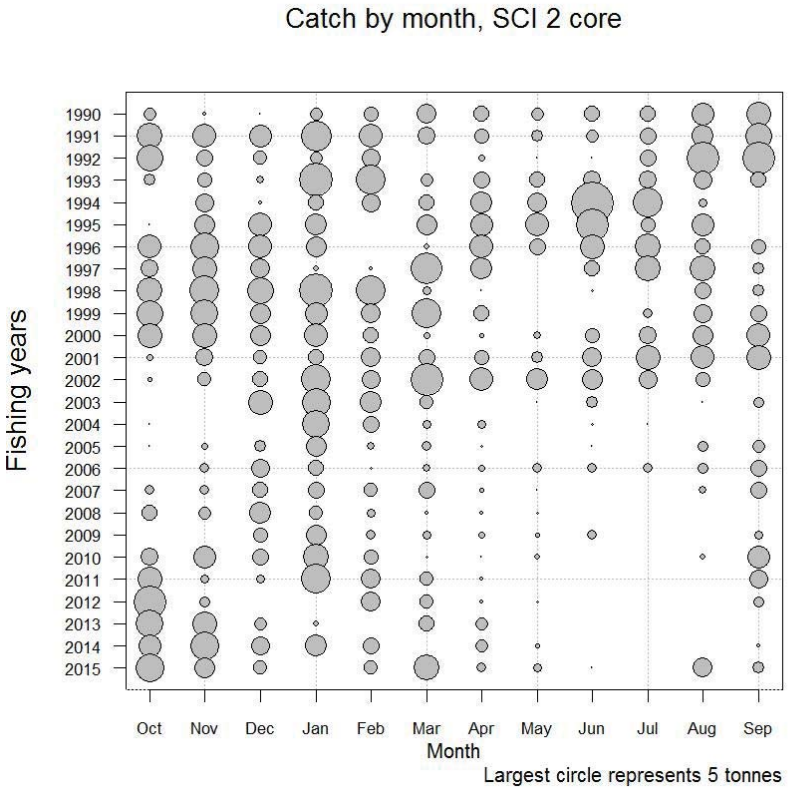

Figure 15: Monthly pattern of scampi catches in the scampi targeted fishery by fishing year for the core (modelled) area of SCI 2.

2.2. Seasonal patterns in scampi biology

Previous development of the length based model for scampi has shown that determination of appropriate time steps for the model is important in fitting to length and sex ratio data in particular (Tuck & Dunn 2006; 2009; 2012). Scampi inhabit burrows, and are not available to trawling when within a burrow. Catchability varies between the sexes on a seasonal basis in relation to moulting and reproductive behaviour, and leads to seasonal changes in sex ratio in catches.

2.2.1. Sex ratio

Current knowledge of the timing of scampi biological processes in SCI 1 and SCI 2 are summarised in Table 3 (Tuck 2010). From patterns in ovary and egg stage observed from commercial and research trawl sampling, along with the proportion of soft animals (Figure 16) and ovigerous females, mature female moulting appears to occur around October and November, just after the hatching period (August and September), with mating occurring at this time and new eggs being spawned onto the pleopods in November – January. The main male moulting is completed well before the female moult (since mating occurs post moult for females, but the males must have completed the moult to mate), and appears to be concentrated in April and May (Figure 17), but may start as early as February. There is also some evidence of male moulting in September–November, generally for smaller (less than 40 mm CL) animals.

The combination of biological processes for males and females lead to different relative availabilities of the two sexes through the year, resulting in the pattern of sex ratio (displayed as proportion males) shown in Figure 18. Males are markedly less abundant than females in catches between February and April (male catches being reduced during their moulting period), but females also dominate catches to a lesser extent between May and September.

Table 3: Summary of scampi biological processes for SCI 1. Source; Tuck (2010) and more recent survey data. X, months when the process is known to occur.

	Jan	Feb	Mar	Apr	May	Jun	Jul	Aug	Sep	Oct	Nov	Dec
Male moult		?	?	X	X				?	?	?	
Female moult										X	X	
Mating										X	X	
Eggs spawn	X										X	X
Eggs hatch								X	X			

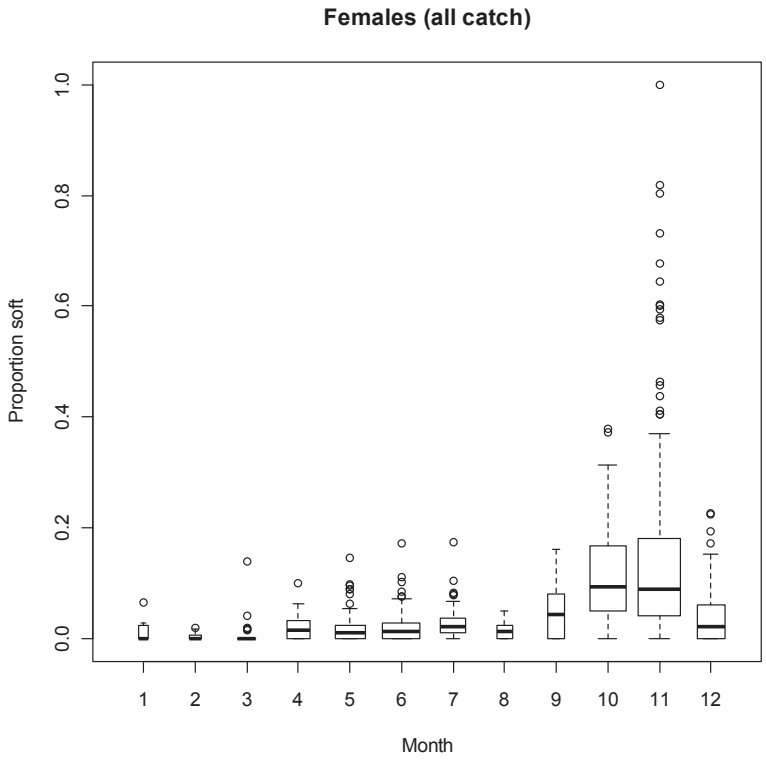

Figure 16: Proportion of females with soft carapace by month, from observer sampling in the SCI 1 and SCI 2 fisheries. Box widths are proportional to the square root of the number of observations.

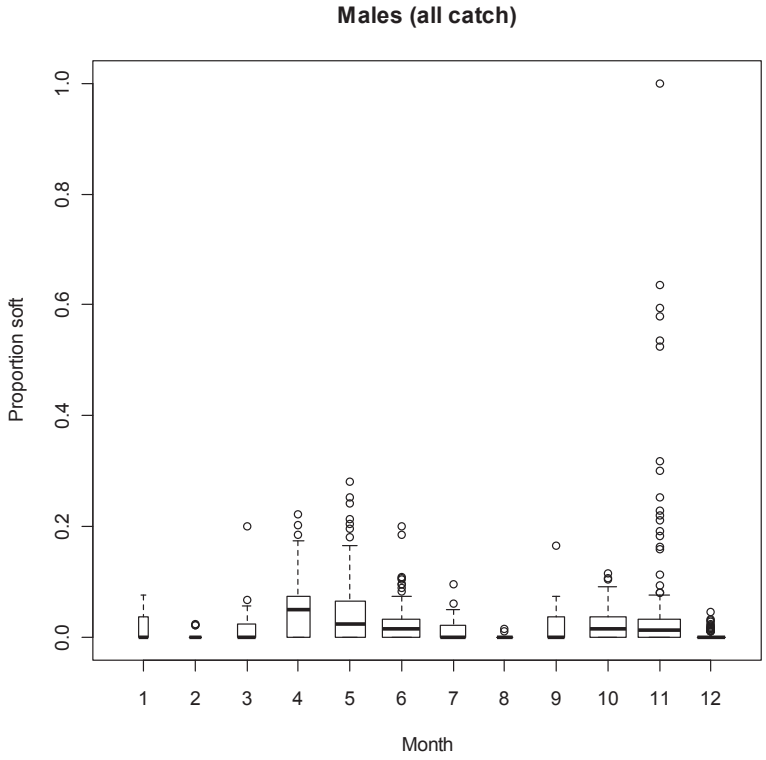

Figure 17: Proportion of males with soft carapace by month, from observer sampling in the SCI 1 and SCI 2 fisheries. Box widths are proportional to the square root of the number of observations.

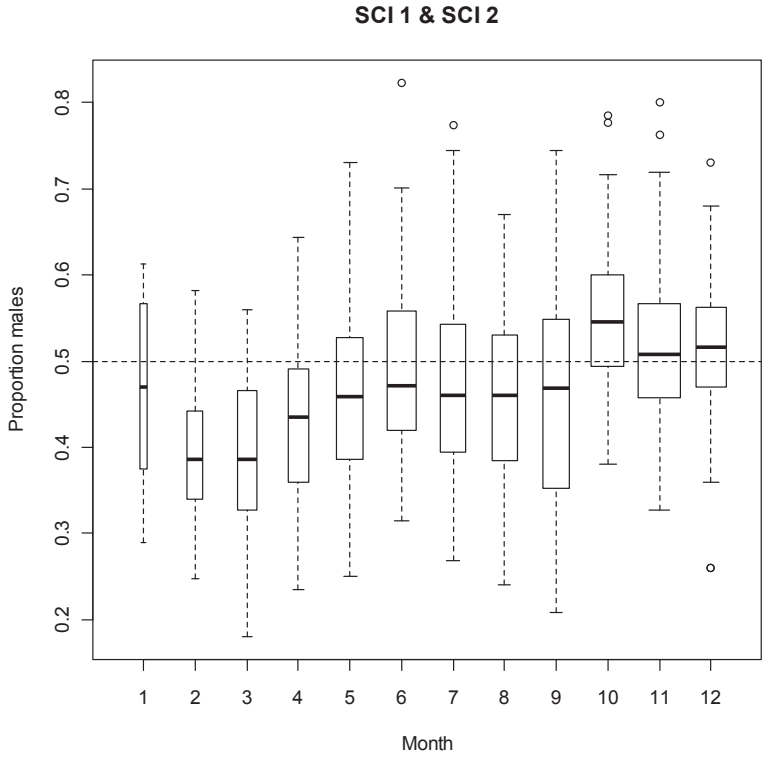

Figure 18: Boxplots of proportion of males in catches by month from observer sampling in the SCI 1 and SCI 2 fisheries. Box widths are proportional to the square root of the number of observations.

2.2.2. Time steps in assessment model

On the basis of our understanding of the timing of biological processes for scampi in this area, and the seasonal pattern in sex ratio, three time steps are proposed for the assessment model, as defined in Table 4. Catch data, stock abundance indices and length frequency distributions have been collated and estimated in relation to these time steps, for inclusion in the assessment model. This is consistent with previous assessments for these areas (Tuck & Dunn 2012; Tuck 2014).

Table 4: Annual cycle of the population model for SCI 1 and SCI 2, showing the processes taking place at each time step, and their sequence within each time step. Fishing and natural mortality that occur together within a time step occur after all other processes, with 50% of the natural mortality for that time step occurring before and 50% after the fishing mortality. Natural mortality is apportioned to time steps in relation to their duration (as a fraction of the year). Fishing mortality is apportioned to time steps according to reported landings.

Step	Period	Process
1	October–January	Growth (both sexes)
		Natural mortality
		Fishing mortality
2	February–April	Recruitment
		Maturation
		Natural mortality
		Fishing mortality
3	May–September	Natural mortality
		Fishing mortality

2.3. Standardised CPUE indices

Vessels have been allocated a letter code to maintain confidentiality, with codes applied consistently between the two fisheries.

2.3.1. Core vessels – SCI 1

A plot of vessel activity (number of scampi targeted tows recorded) over time is presented for SCI 1 in Figure 19. One vessel (H) has been active and dominant throughout the history of the fishery, while some others have contributed for a number of years. Some vessels were only active in the fishery during the late 1990s and early 2000s (partly associated with the period of competitive catch limits between 2001–02 and 2003–04). Only three vessels have been routinely active in the fishery in recent years (H, I, and V).

Figure 20 (upper plot) shows the proportion of the total catch (over the history of the fishery) in relation to number of years vessels contributing that catch have been active in the fishery, and on the basis of this, a cut off of 10 years of activity has been selected to identify seven core vessels (vessels H, I, J, K, L, O, and V), which have contributed over 92% of the targeted scampi catches from SCI 1. These represent the same seven vessels selected as core vessels for SCI 1 in the last assessment (Tuck 2014). The lower plot of Figure 20 shows the proportion of catch accounted for in each year by vessels active for over 5 or 10 years. Other than the first few years, and 2001–02 and 2002–03, the core vessels (active for over 10 years) have accounted for over 90% of annual targeted scampi catches.

2.3.2. Core vessels – SCI 2

A plot of vessel activity (number of scampi targeted tows recorded) over time is presented for SCI 2 in Figure 21. A number of vessels have been regularly active in the fishery, and none is dominant. A few vessels joined the fishery associated with the period of competitive catch limits between 2001–02 and 2003–04, but to a lesser extent than for SCI 1. Four vessels (I, L, O, and U) have been routinely active in the fishery in recent years, with other vessels (H, N and V) occasionally active, and vessel T recently starting (at a very low level) in this fishery.

Figure 22 (upper plot) shows the proportion of the total catch (over the history of the fishery) in relation to number of years those vessels contributing that catch have been active in the fishery, and on the basis of this, a cut off of 10 years of activity has been selected to identify nine core vessels (H, I, J, K, L, N, O, U, and V), which have contributed almost 95% of the targeted scampi catches from SCI 2. These represent the same nine vessels selected as core vessels for SCI 2 in the last assessment (Tuck 2014). The same vessel codes have been used for both fisheries, and all of the core vessels from SCI 1 are included in the SCI 2 list. The lower plot of Figure 22 shows the proportion of catch accounted for in each year by vessels active for over 5 or 10 years (no difference between the lines). Other than the first few years, and 2001–02 and 2002–03, the core vessels (active for over 10 years) have accounted for over 90% of annual targeted scampi catches.

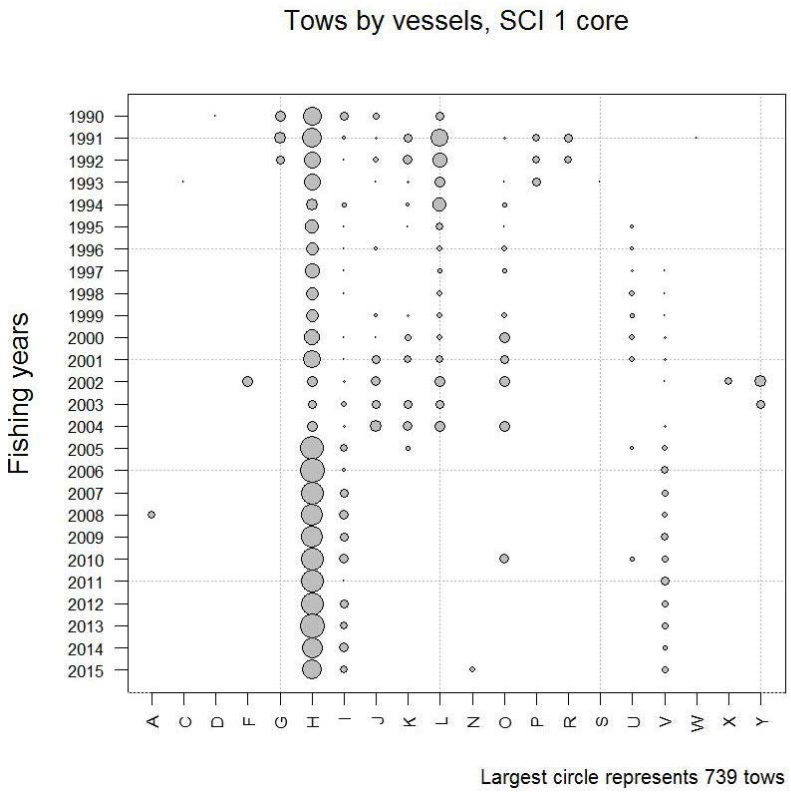

Figure 19: Pattern of fishing activity by vessel and fishing year for SCI 1. The area of the circles is proportional to the number of tows recorded.

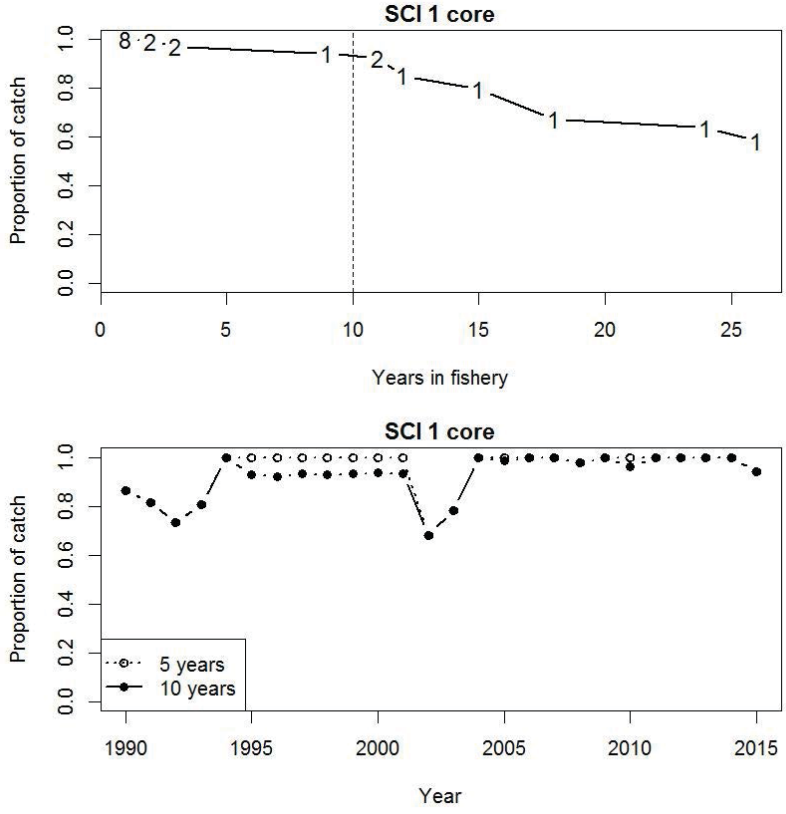

Figure 20: Catch breakdown by vessel. Upper plot - Proportion of total scampi catch (all years) plotted against the number of years the vessels reporting that catch have been active in the fishery. Numbers indicate number of vessels active for that duration. Vertical dotted line represents cut off for core vessels. Lower plot – Proportion of annual catch reported by vessels active in the fishery for over 5 and 10 years.

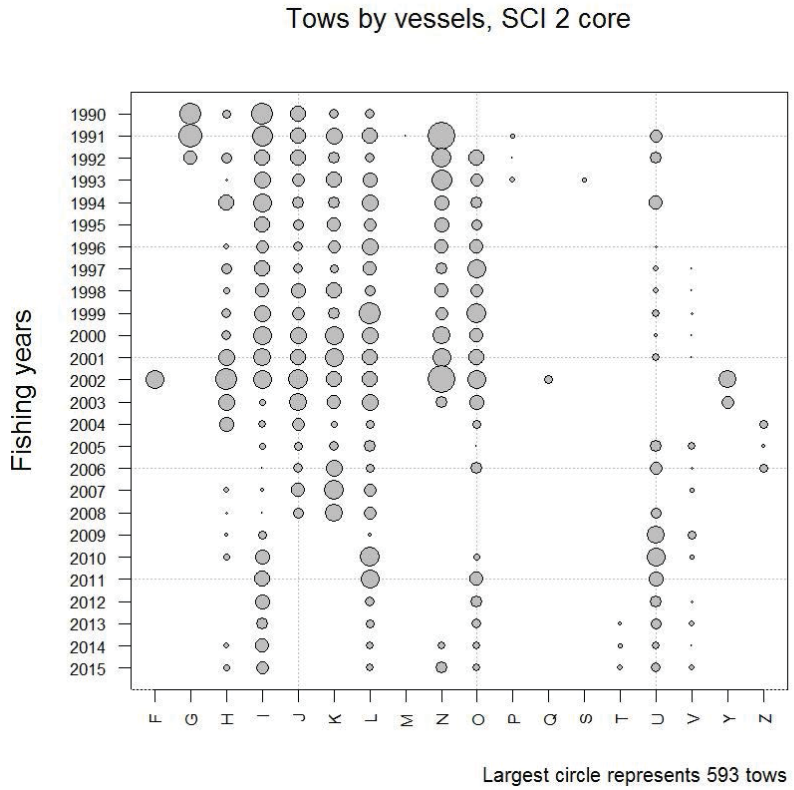

Figure 21: Pattern of fishing activity by vessel and fishing year for SCI 2. The area of the circles is proportional to the number of tows recorded.

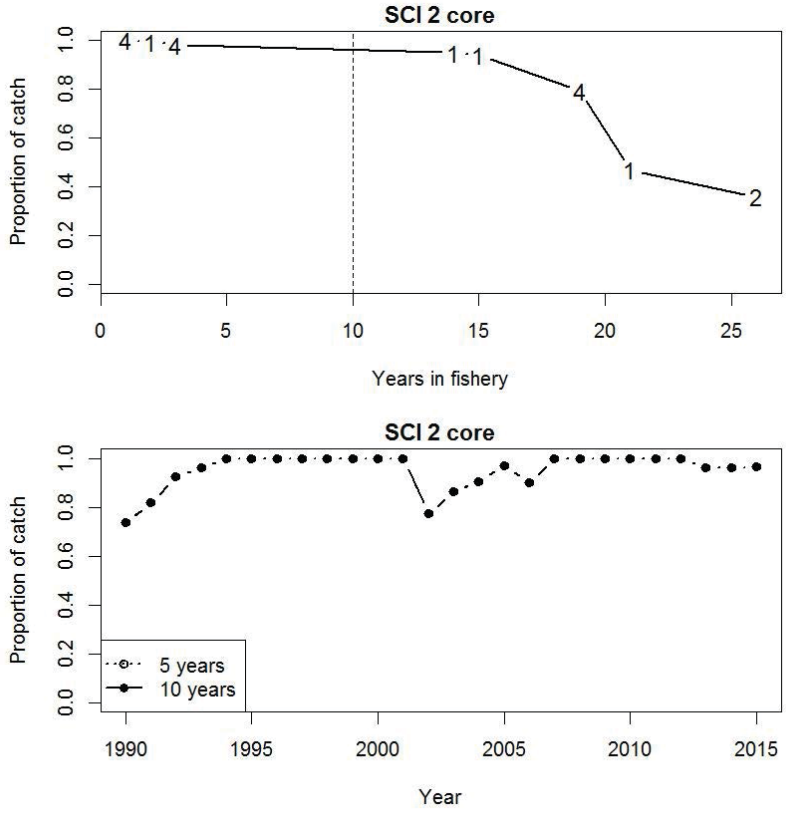

Figure 22: Catch breakdown by vessel. Upper plot - Proportion of total scampi catch (all years) plotted against the number of years the vessels reporting that catch have been active in the fishery. Numbers indicate number of vessels active for that duration. Vertical dotted line represents cut off for core vessels. Lower plot – Proportion of annual catch reported by vessels active in the fishery for over 5 and 10 years.

2.3.3. Exclusion of poorly sampled time periods

Following the approach developed for SCI 3 (Tuck 2013), time steps that were poorly sampled by the core vessels were excluded from the standardisation of the CPUE, on the basis that a small number of tows in an area, or at a particular time, may not provide a good index of abundance. Records were excluded from the analysis when there were less than 10 tows recorded by core vessels within a time step in a year (Figure 23).

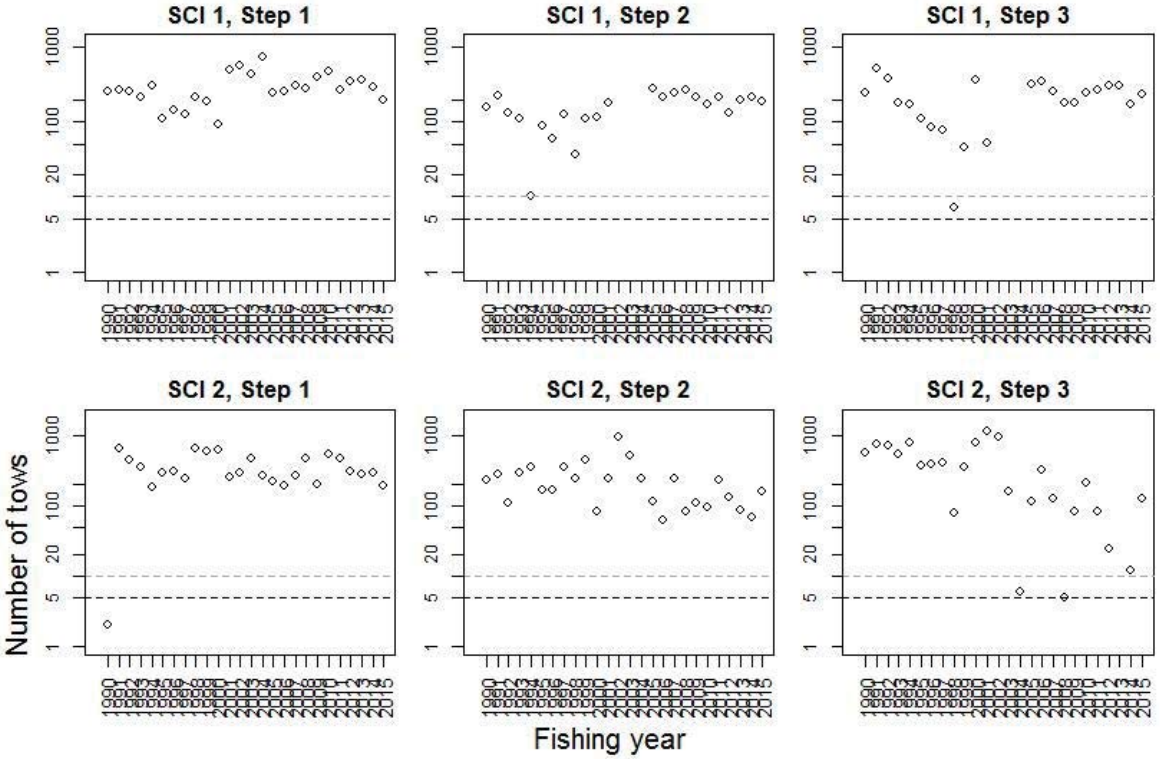

Figure 23: Numbers of commercial tows available within the core vessel dataset by time step and fishing year for SCI 1 (upper row) and SCI 2 (lower row). Dashed lines represent arbitrary cut offs at 5 and 10 tows.

2.3.4. Calculation of indices

The initial assessments of SCI 1 and SCI 2 fitted separate abundance indices for different survey strata and time steps (Tuck & Dunn 2012), but more recently the SFAWG has suggested a simplification of the model structure (Tuck 2014). Therefore, an initial standardisation was conducted to generate an annual index (as applied in Tuck 2014), and this was compared with stratified indices where interaction terms were suggested by the data. For each index, scampi catch of core vessels within the appropriate area and time step was modelled using combined spatial and temporal strata (forced), vessel, time of day, state of moon, depth and fishing duration. For the three time step indices, spatial strata was included in the model as a term, while for the annual index, spatial strata and time step were included.

The indices were calculated from data for core vessels in the modelled area. Core vessels were selected as described above, by examining the scampi fleet's activity over the history of the fishery, and selecting vessels that had consistently contributed over a number of years, and together, had contributed a significant proportion of the overall catches over the whole fishery, and in each year.

Within the core vessels identified, two have changed gear configuration (twin rig to triple rig) in recent years, and two have changed engine power over the history of the fishery. On the basis of previous investigations (Tuck 2013), engine power was fitted within the model (as a factor), and gear configuration as a two level factor (twin or triple rig). Gear configuration for a particular vessel and

date was determined on the basis of information provided by the fishing industry as to when vessels changed from twin to triple, and all tows after this date are defined as triple rig. It is acknowledged that vessels may change configuration within a trip depending on gear damage or fishing conditions, but it is believed that this is not recorded consistently enough over the history of the fishery within the TCEPR records to be useable.

The time of day of each tow was calculated in relation to nautical dawn and dusk (time when the sun is 12 degrees below the horizon in the morning and evening), as calculated by the *crepescule* function of the *maptools* package in R. Individual tows were characterised on the basis of whether they included dawn (shot before dawn, hauled after dawn and before dusk), day (shot after dawn, hauled before dusk), dusk (shot before dusk, hauled after dusk and before dawn) or night (shot after dusk and hauled before dawn). Longer tows including more than one period (i.e. shot before dusk and hauled after dawn) were excluded from this part of the analysis (excluding 34 records from a total of over 16 500 for SCI 1, and 71 records from a total of over 24 400 for SCI 2).

Individual hauls were also categorised in terms of moon state, on the assumption that tidal current strength at the sea floor will be related to the lunar cycle. Tows were categorised by their date in relation to the lunar cycle, as Full moon (more than 26 days since full moon, or less than 3 days since full moon), Waning (4–11 days since full moon), New moon (12–18 days since full moon), and Waxing (19–26 days since full moon).

In addition, examination of the data for SCI 3 (Tuck 2013) identified a distinct shift in trawl duration between 2002–03 and 2006–07 (from about 5 hours to 7 hours). This shift (in SCI 3) was fleet-wide, and associated with a modification to the top of the trawl to reduce the finfish bycatch (John Finlayson, Sanford Ltd., *pers. comm.*), enabling vessels to fish for longer on each tow. The shift in haul duration is not apparent in data from other scampi management areas, but the vessels use the same trawl gear in all their scampi fishing. For each vessel, the timing of the gear modification was estimated from examination of tow durations in SCI 3 (see Tuck 2014), and fitted as a two level factor in the model.

Catch indices were derived using generalised linear modelling (GLM) procedures (Vignaux 1994; Francis 1999), using the statistical software package R. The response variable in the GLM was the natural logarithm of scampi catch. The fishing-year was entered as a categorical covariate (explanatory) term on the right-hand side of the model. Standardised CPUE abundance indices (canonical) were derived from the exponential of the fishing-year covariate terms as described in Francis (1999).

In order to accommodate a non-linear relationship with the response variable (log catch), the continuous variables (effort and depth) were "offered" to the GLM's as third order polynomials. Vessel, time of day, state of tide (i.e., moon state), twin or triple rig, bycatch modification and vessel power were "offered" to the GLM's as factors. A forward fitting, stepwise, multiple-regression algorithm was used to fit GLM's to groomed catch, effort and characterisation data. The stepwise algorithm generates a final regression model iteratively and uses a simple model with a single predictor variable, fishing year, as the initial or base model. The reduction in residual deviance relative to the null deviance is calculated for each additional term added to the base model. The term that results in the greatest reduction in residual deviance is added to the base model if this results in an improvement in residual deviance of more than 1%. The algorithm repeats this process, updating the model, until no new terms can be added. Diagnostic plots for the final models are presented in Appendix 1 and 2 (Bentley et al. 2012).

Preliminary investigations into different error distributions (comparing log normal, gamma and weibull) using a simple standardisation model

$$\text{Log(catch)} \sim \text{fishing\_year}$$

identified that the gamma distribution provided a slight improvement in the distribution of residuals, and this error distribution was used for calculation of the indices reported below. Diagnostic plots for

the three compared error distributions, and for the final standardisation model, are presented in Appendix 1 and 2.

2.3.5. SCI 1 indices

Single annual index

An initial single annual index was estimated, for consistency with the previous assessment (Tuck 2014), and to provide a baseline for comparison of other indices. Stepwise regression analysis of the dataset to estimate an annual CPUE index for SCI 1 resulted in a final model with fishing year, time of day, effort (tow duration), survey strata and time step retained (Table 5). Model diagnostics are presented in Appendix 1. The model explained 42% of the variation in the data. Effort was the most influential variable, at 8.4%, with time of day and time step having influences of 3–4%, and survey strata about 2%. The standardised and unstandardized annual indices are shown in Figure 24. The two indices follow a very similar pattern, although as with the SCI 1 index (Figure 24) standardised index is consistently above the unstandardized during the early part of the series (as fishing duration was increasing), and below the unstandardized in later years (when fishing is more concentrated in time step 1). The relative effects of the explanatory variables (excluding fishing year) are shown in Figure 25. Expected catch rates are highest during the day, and lowest at night, being about half of the daytime rate. Expected catch increases for tow durations up to about 8 hours, but then declines. Catch rates are highest in the southern strata, and are highest in time step 1, falling to about 80% of this level in time steps 2 and 3.

Table 5: Analysis of deviance table and overall influence for the standardisation model selected by a stepwise regression for an annual index for SCI 1.

	Df	Deviance explained	Additional deviance explained (%)	Overall influence (%)*
NULL				
fishing_year	25	1688.78	24.81	
TOD	3	724.51	10.64	3.80
poly(effort, 3)	3	217.25	3.19	8.40
survstrata	5	102.9	1.51	2.20
model_step	2	111.4	1.64	3.05

*- Overall influence as in table 1 of Bentley et al. (2012)

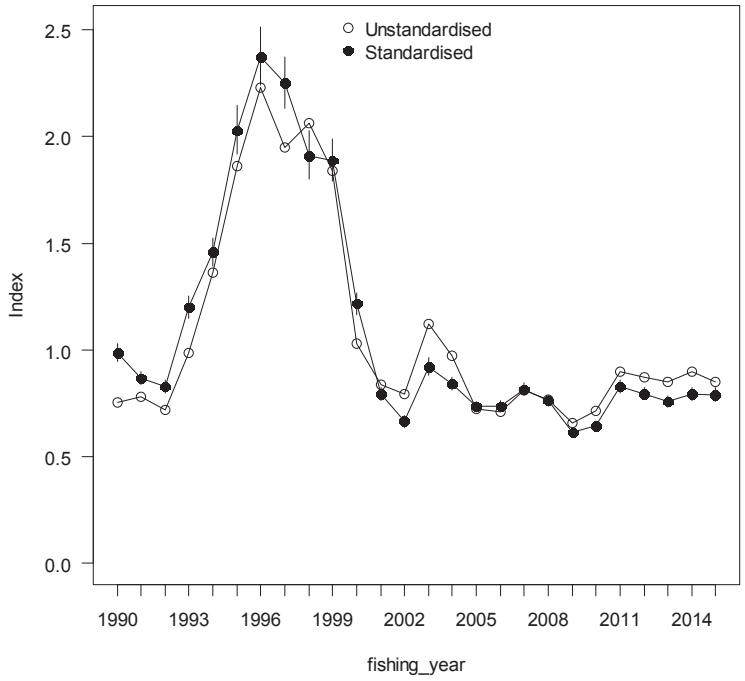

Figure 24: Comparison of standardised (Table 5) and unstandardized annual CPUE index for SCI 1.

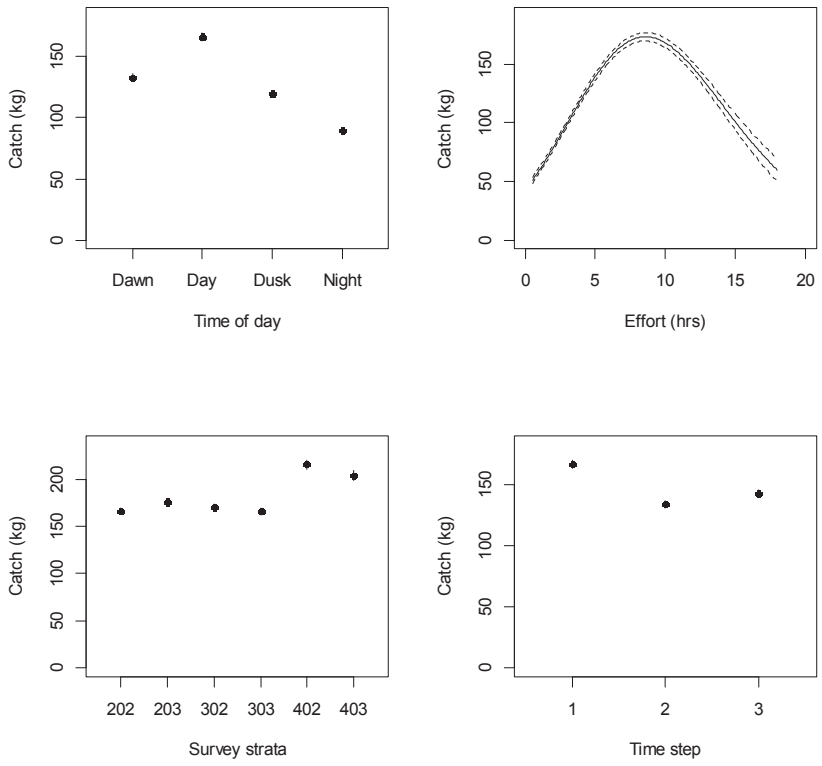

Figure 25: Termplot (in natural space) for annual index standardisation model (Table 5), showing relative effects of time of day, effort (tow duration), survey strata and time step.

Other indices

The inclusion of interaction terms was explored allowing interactions between fishing_year, survey strata and time step, with terms for fishing year (forced), time of day, effort, survey strata and time step retained, along with interaction terms for fishing_year:survey strata and fishing_year:time step (Table 6). This model explained 45% of the variation in the data.

Table 6: Analysis of deviance table for the standardisation model including interactions selected by stepwise regression for SCI 1.

	Df	Deviance explained	Additional deviance explained (%)
NULL			
fishing_year	25	1688.78	24.81
TOD	3	724.51	10.64
poly(effort, 3)	3	217.25	3.19
survstrata	5	102.9	1.51
model_step	2	111.4	1.64
fishing_year:survstrata	122	159.29	2.34
fishing_year:model_step	44	96.49	1.42

Given that interaction terms were retained within the initial model, separate stratum time step indices were estimated within a standardisation model including a fishing_year_strata_step term. This model retained terms for fishing_year_strata_step (forced), time of day and effort (Table 7), and explained 47% of the variance in the data. Individual time step indices are plotted for each survey stratum in Figure 26, along with the single annual index (Table 5). In general, the individual strata time step indices are consistent with the single annual index.

Table 7: Analysis of deviance table for the initial standardisation model including a term for fishing_year_strata_time step selected by stepwise regression for SCI 1.

	Df	Deviance explained	Additional deviance explained (%)
NULL			
fishing_year_strata_step	391	2508.97	36.86%
TOD	3	502.28	7.38%
poly(effort, 3)	3	228.13	3.35%

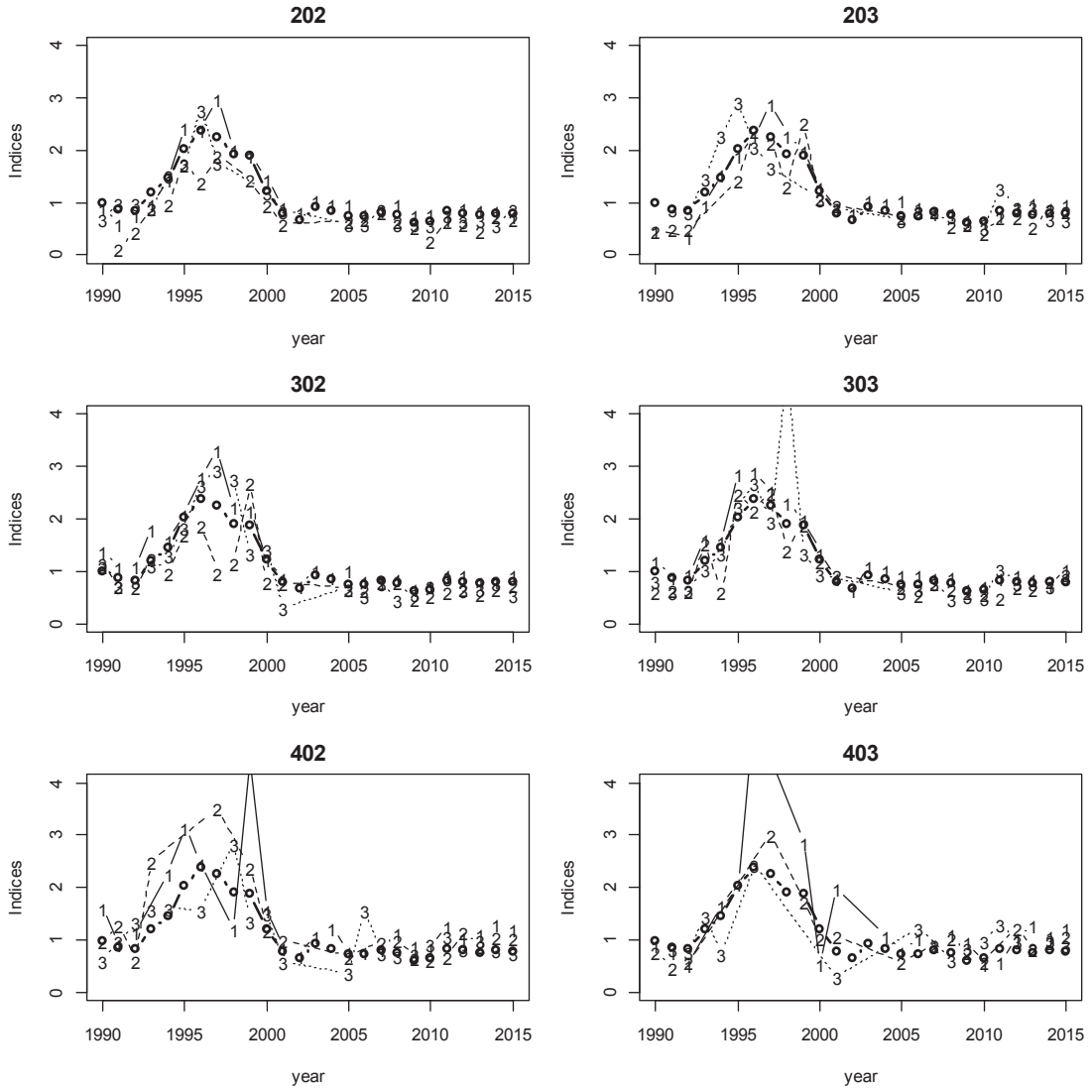

Figure 26: Standardised indices for each time step and strata (Table 7) plotted over the single annual index (Table 5). Annual index represented by thicker line with open symbols, individual time step indices for each strata labelled by time step number.

As discussed, previous assessment models for scampi have fitted indices stratified spatially and temporally (Tuck & Dunn 2012), but more recently the SFAWG has proposed more simplified model structures (Tuck 2014). Given the consistency in the patterns shown in the individual strata time step and single annual index, it was considered that realistic options for weighting individual spatial strata would not generate a composite annual index greatly different from the single index presented in Figure 24, and the Working Group agreed that the annual index (Table 5, Figure 24) should be used within the models as the index of abundance from the CPUE data.

2.3.6. SCI 2 indices

Single annual index

An initial single annual index was estimated, for consistency with the previous assessment (Tuck 2014), and to provide a baseline for comparison of other indices. Stepwise regression analysis of the dataset to estimate an annual CPUE index for SCI 2 resulted in a final model with fishing year, time of day, effort (tow duration), time step and vessel code retained (Table 8). Model diagnostics are presented in Appendix 2. The model explained 41% of the variation in the data. Effort was the most influential

variable, at 8.5%, with time step having about 4% influence, and time of day and vessel about 2%. The standardised and unstandardized annual indices are shown in Figure 27. The two indices follow a very similar pattern, although standardised index is consistently above the unstandardized during the early part of the series (as fishing duration was increasing), and the unstandardized is above the standardised from 2001 to 2004 (when most fishing was concentrated in time step 1), and again in more recent years (as the southern strata have become more important). The relative effects of the explanatory variables (excluding fishing year) are shown in Figure 28. Expected catch rates are highest during the day, and lowest at night. Expected catch increases for tow durations up to about 10 hours, but then declines. Catch rates are highest in time step 1, falling to about 80% of this level in time steps 2 and 3, and performance varies between vessels, with one markedly lower than the others.

Table 8: Analysis of deviance table and overall influence for the standardisation model selected by stepwise regression for an annual index for SCI 2.

	Df	Deviance explained	Additional deviance explained (%)	Overall influence (%)*
NULL				
fishing_year	25	3310.1	28.45	
TOD	3	500.7	4.30	1.82
poly(effort, 3)	3	408.5	3.51	8.52
model_step	2	257	2.21	3.88
vessel_code	8	184.5	1.59	2.17

*- Overall influence as in table 1 of Bentley et al. (2012)

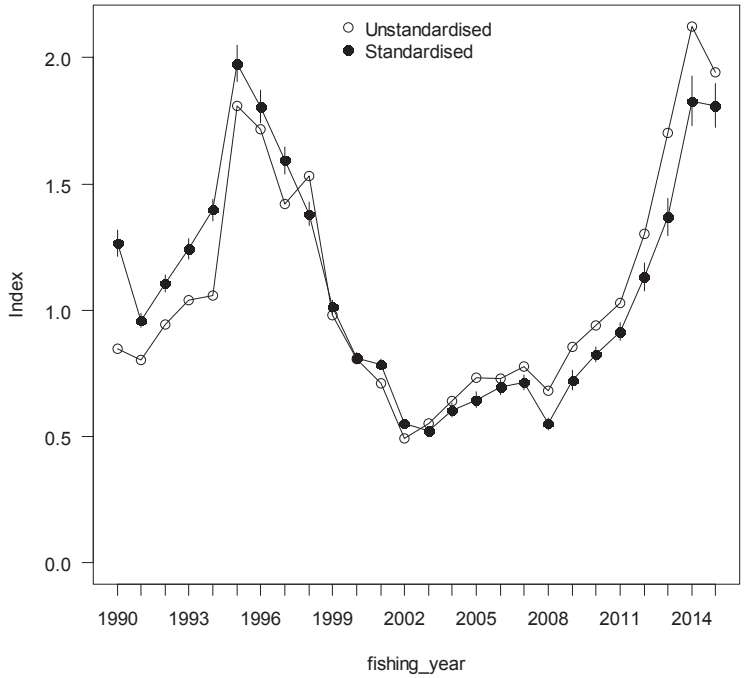

Figure 27: Comparison of standardised (Table 8) and unstandardized annual CPUE index for SCI 2.

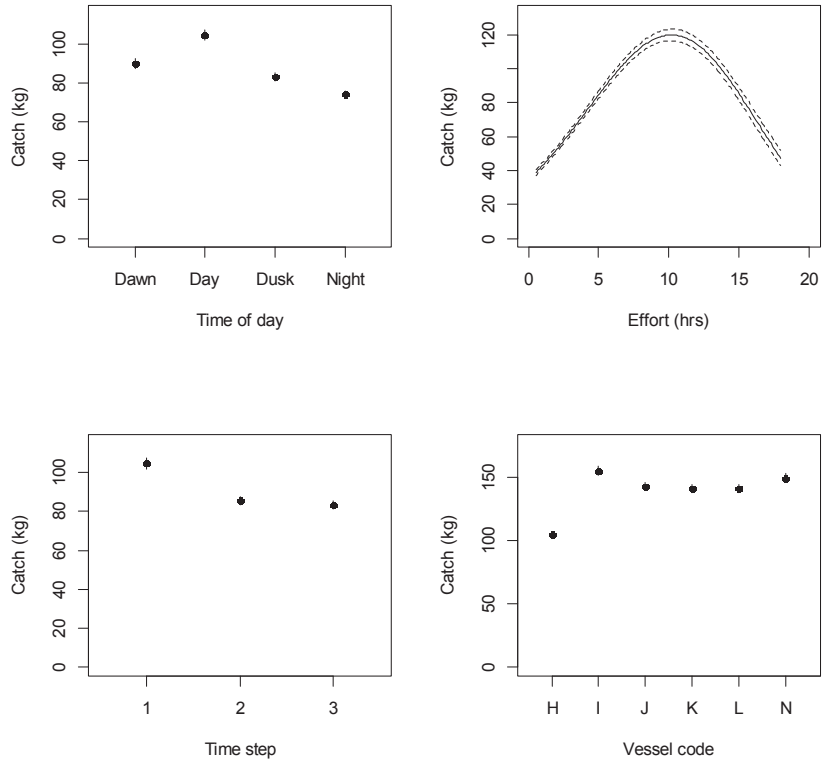

Figure 28: Termplot (in natural space) for annual index standardisation model (Table 8), showing relative effects of effort (tow duration), time of day, time step, and vessel.

Other indices

The inclusion of interaction terms was explored allowing interactions between fishing_year, survey strata and time step, with terms for fishing year (forced), time of day, effort, and vessel retained, along with an interaction term for fishing_year:time step (Table 9). This model explained 44% of the variation in the data.

Table 9: Analysis of deviance table for the standardisation model including interactions selected by stepwise regression for SCI 2.

	Df	Deviance explained	Additional deviance explained (%)
NULL			
fishing_year	25	3310.1	28.45
TOD	3	500.7	4.30
poly(effort, 3)	3	408.5	3.51
model_step	2	257	2.21
vessel_code	8	184.5	1.59
fishing_year:model_step	49	507.5	4.36

Given that interaction terms were retained within the initial model, separate time step indices were estimated within a standardisation model including a fishing_year_step term. This model retained terms for fishing_year_step (forced), effort, time of day and vessel code (Table 10), and explained 44% of the variance in the data. Individual time step indices are plotted in Figure 29, along with the single annual index (Table 8). The individual time step indices are consistent with the single annual index.

Table 10: Analysis of deviance table for the initial standardisation model including a term for fishing_year _time step selected by stepwise regression for SCI 2.

	Df	Deviance explained	Additional deviance explained (%)
NULL			
fishing_year_step	76	4379.7	37.65
poly(fishing_duration, 3)	3	341	2.93
TOD	3	315.5	2.71
vessel_code	8	132.1	1.14

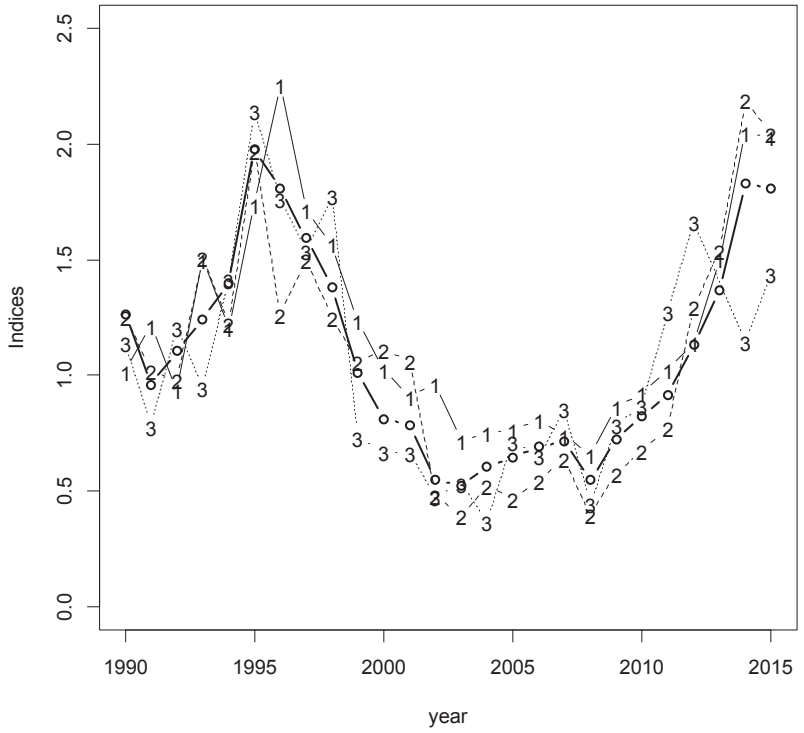

Figure 29: Standardised indices for each time step and strata (Table 10) plotted over the single annual index (Table 8). Annual index represented by thicker line with open symbols, individual time step indices for each strata labelled by time step number.

Given the consistency in the patterns shown in the individual time step and single annual index, it was considered that realistic options for weighting individual time steps would not generate a composite annual index greatly different from the single index presented in Figure 27, and the Working Group agreed that the annual index (Table 8, Figure 27) should be used within the models as the index of abundance from the CPUE data.

2.3.7. Potential for fishing activity to increase scampi catchability

Scampi live in muddy habitats, and share their environment with a number of other burrowing and bioturbating species (Tuck & Spong 2013). A number of these bioturbating species generate mounds through ejecting sediment from their burrows, and mound generation can be quite rapid (up to 97 g

sediment per day) (Smith et al. 1986; Hughes et al. 1996; Hughes et al. 1999), with mounds up to 20 – 30 cm in height common (Nickell & Atkinson 1995; Nickell et al. 1995; Hughes et al. 1999). Seabed video footage collected from an area of the Mernoo Bank (SCI 3) that is currently not fished recorded an extensively mounded seabed.

Scampi catch rates increased rapidly at the start of a number of fisheries, and it has previously been questioned by the Shellfish Working Group as to whether, assuming CPUE reflects abundance, the rate of increase is biologically plausible for a lobster with relatively low fecundity. Further analysis was conducted to investigate the possibility that fishing activity may have flattened the seabed mounds, and thus improved ground contact for scampi trawls, therefore improving catchability.

Historic fishing effort

To estimate historic fishing effort, all fishing events in the scampi targeted fishing effort dataset (described in Section 2.1) were allocated to cells of a 0.1 degree × 0.1 degree grid covering the combined area of SCI 1 and SCI 2. Fishing events were allocated on the basis of their midpoint. Scampi targeted trawling is the main fishing method employed on scampi grounds, and so only scampi targeted effort was included. For each fishing event in the core vessel dataset for each area, all effort from fishing events in the same cell in the previous decade were summed on a weekly basis (weeks 1 to 520 prior to the fishing event in question).

Data analysis

Analysis was conducted on the two fisheries separately. For each fishery, historical fishing effort was offered as an additional term in the standardisation model (Sections 2.3.5 and 2.3.6), to determine if changes in effort patterns over time help explain the patterns in CPUE. It might be expected that more recent effort (relative to the fishing event in question) would have a greater influence on seabed topography than older effort, and so effort was weighted by age and summed, with both linear and exponential decay weighting, and different time periods prior to the fishing event in question considered.

Results

For SCI 1, examining the whole time series, historical effort was only retained as an explanatory variable when weighted over the 2 months prior to the fishing event (both weighting options), explaining just over 1 % of the residual deviance, but having minimal effect on the overall index. When just examining data for the initial period of the fishery (1990 – 1998), historical effort terms were retained when weighted over the previous year, previous 6 months, or previous 2 months, but again with minimal effect on the overall index. For SCI 2, historical fishing effort was not retained in the standardisation models over any of the timescales considered, for either the full dataset or early years.

Overall, the Working Group agreed that there was no strong evidence that historical fishing effort had affected catch rates, or that a historical effort term should be included in the standardisation model.

3. MODEL STRUCTURE

3.1. Spatial and seasonal structure, and the model partition

The model partitions scampi by sex, and length class. Growth between length classes are determined by sex-specific, length-based growth parameters. Individuals enter the partition by recruitment and are removed by natural mortality and fishing mortality. The model's annual cycle is based on the fishing year and is divided into the three time-steps described above (Table 4). The choice of three time steps was based on current understanding of scampi biology and sex ratio in catches. Note that model references to "year" within this report refer to the modelled or fishing year, and are labelled as the most recent calendar year, e.g. the fishing year 1998–99 is referred to as "1999" throughout. Previous models for SCI 1 and SCI 2 have included spatial structure (Tuck & Dunn 2012), but following the characterisation and preliminary model investigation, the SFAWG recommended a single area model for both assessments (Tuck 2014).

The model uses capped logistic length based selectivity curves for commercial fishing and research trawl surveys, assumed constant over years, but allowed to vary with sex and time step (where necessary). While the sex ratio data suggest that the relative catchability of the sexes vary through the year (hence the model time structure adopted), there is no reason to suggest that assuming equal availability, selectivity at size would be different between the sexes. Therefore the two sex selectivity implementation developed within CASAL for the SCI 1 and SCI 2 assessments (Tuck & Dunn 2012) was applied. This allows the L_{50} (size at which 50% of individuals are retained) and a_{95} (size at which 95% of individuals are retained) selectivity parameters to be estimated as single values shared by both sexes in a particular time step, but allows for different availability between the sexes through estimation of different a_{max} (maximum level of selectivity) values for each sex. Previous assessments have examined using double normal capped selectivity curves for the commercial fishery, to allow domed selectivity (no link between the parameters for each sex) (Tuck 2014), but this had little effect on assessment outputs, and has not been repeated here. Photographic survey abundance indices are not sex specific, and a standard logistic length based selectivity curve is applied.

3.2. Biological inputs

3.2.1. Growth

Scampi growth has been estimated from wild-tagged scampi in SCI 1 (Cryer & Stotter 1997; 1999) and aquarium-reared scampi from SCI 2 (Cryer & Oliver 2001) (Figure 30). The aquarium data have been used like tag date, with an initial and subsequent length measurement defining a growth increment, over a known time period.

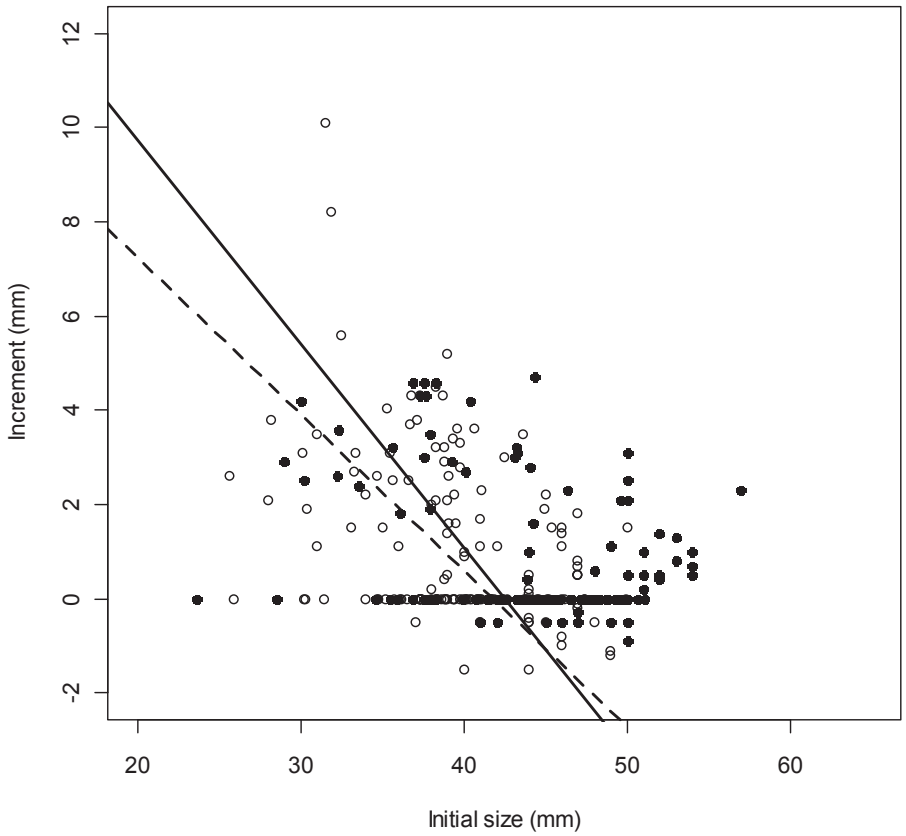

Figure 30: Growth increment data from scampi tagging in SCI 1 and SCI 2, and aquarium studies. Solid and hollow symbols represent males and females, respectively. Solid (males) and dotted (females) lines represent best fits to data from combined growth studies.

In the initial developments of the of the scampi assessment model (Cryer et al. 2005), the combined data set (SCI 1 field studies and SCI 2 aquarium studies) was analysed externally and the estimated growth parameters for each sex fixed within the model. However, given the strong influence growth has on length based models, and the scatter around the externally fitted relationships in Figure 30, more recently the fitting of the growth data has been included within this model (Tuck & Dunn 2012). The growth increment data from SCI 1 and SCI 2 have been combined into a single dataset, and are fitted independently in the two assessment models.

On the basis of the time steps within the model structure, the tag data can be split into three release events (i.e., 1996–7, 2012, 2015). Recaptures of tagged scampi from these releases are tabulated by recapture time step in Table 11. Within the analysis, animals from both wild release and aquarium studies have been combined, although the numbers of animals are provided separately in Table 11.

Table 11: Numbers of scampi recaptured by release and recapture time step (SCI 1 and 2).

Release	Recapture			
	1996-3	1997-1	1997-2	1997-3
1996-2		20	7	13
1996-3*	12	15 (28)	2 (21)	42 (30)
1997-1			15	80
	2012-2	2012-3		
2012-2		2		
	2015-2			
2015-2	10			

* Recapture data from1996-3 release include 79 animals in aquaria and 71 from wild releases. For recaptures, numbers in parenthesis represent aquarium animals.

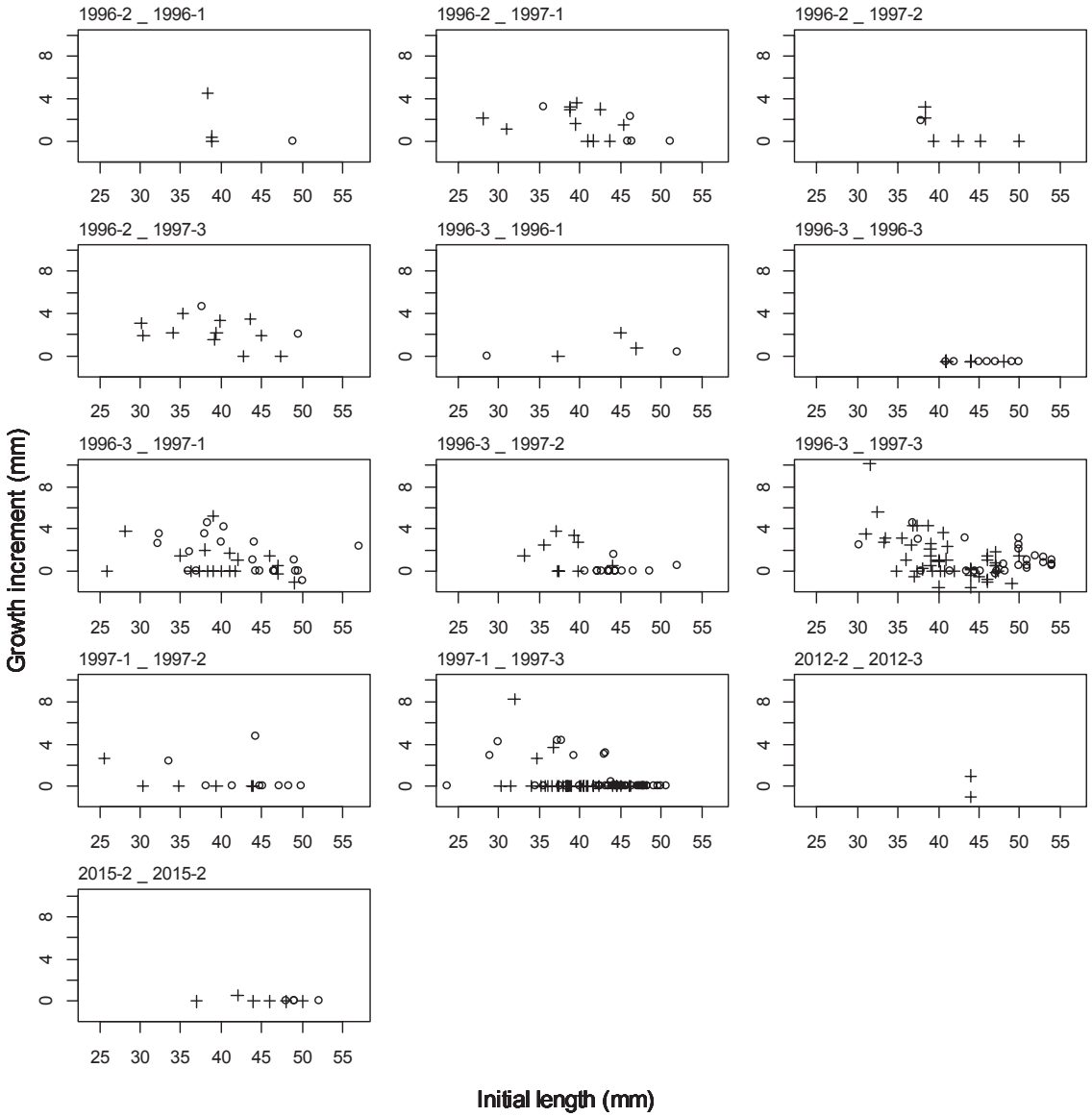

Figure 31: Plot of initial length against growth increment by combination of release and recapture time steps. Males represented by hollow symbols, females represented by crosses.

For the various combinations of release and recapture the length increment is plotted by sex against initial length in Figure 31. The model structure has a growth period assigned to the start of time step 1 for both sexes. Therefore no growth would be expected for those animals not at liberty at the start of time step 1. The data available, particularly for males (Figure 17), suggest some evidence of two periods of moulting. The sensitivity of the model to allowing two growth periods per year was examined in a previous assessment (Tuck & Dunn 2012).

3.2.2. Maturity

The proportion of females mature at each 1 mm size class have been recorded during all research surveys since 1993. These data have been combined for females from SCI 1 and 2, assuming internal gonad stages 2–5 to be mature, and stage 1 to be immature. No data are available for the maturity of male scampi, so their maturity ogive was assumed to be identical to that of females, although studies on *N. norvegicus* have suggested that male maturity may occur at a larger size than (although possibly the same age as) females (Tuck et al. 2000). Maturity is not considered to be a part of the model partition, but proportions mature were fitted within the model based on a logistic ogive with a binomial likelihood (Bull et al. 2008).

Analysis of the proportion ovigerous data, modelled as a function of length, was conducted within a GLM framework, with a quasibinomial distribution of errors and a logit link (McCullagh & Nelder 1989),

$$\text{logit}(m) = a + bL$$

where a and b are constants, and L is the orbital carapace length, which equates to the logistic model. The model was weighted by the number measured at each length. After obtaining estimates for the parameters a and b, the length at which 50% are mature (L_{50}) was calculated from:

$$L_{50} = -\frac{a}{b}$$

with selection range (SR, a_{25} to a_{75}) calculated from:

$$SR = \frac{(2.\ln(3))}{b}$$

Female maturity data for SCI 1 and 2 are summarised in Figure 32 (Tuck & Dunn 2006). The L_{50} estimate for the pooled SCI 1 and SCI 2 data was 29.7 mm, with a selection range of 5.3 mm. The maturity curve fitted to these data is plotted in Figure 33.

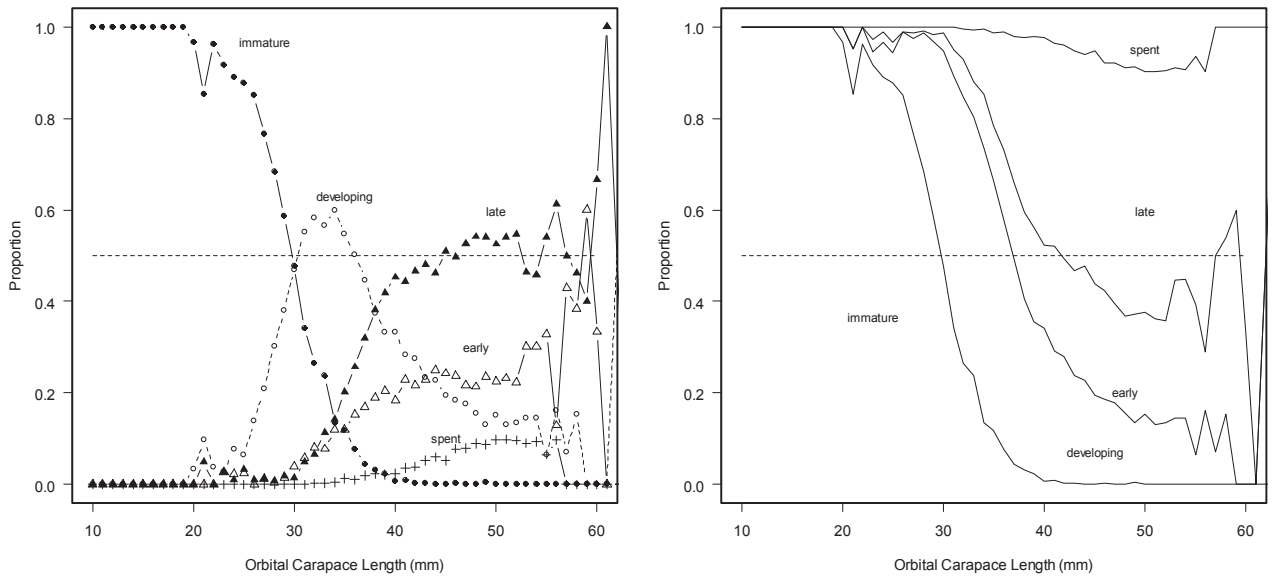

Figure 32: Proportions of female scampi having various developmental stages of internal ovaries. Left panel shows proportions of each stage separately, right panel shows combined proportions. Aggregated data from research voyages in SCI 1 and 2.

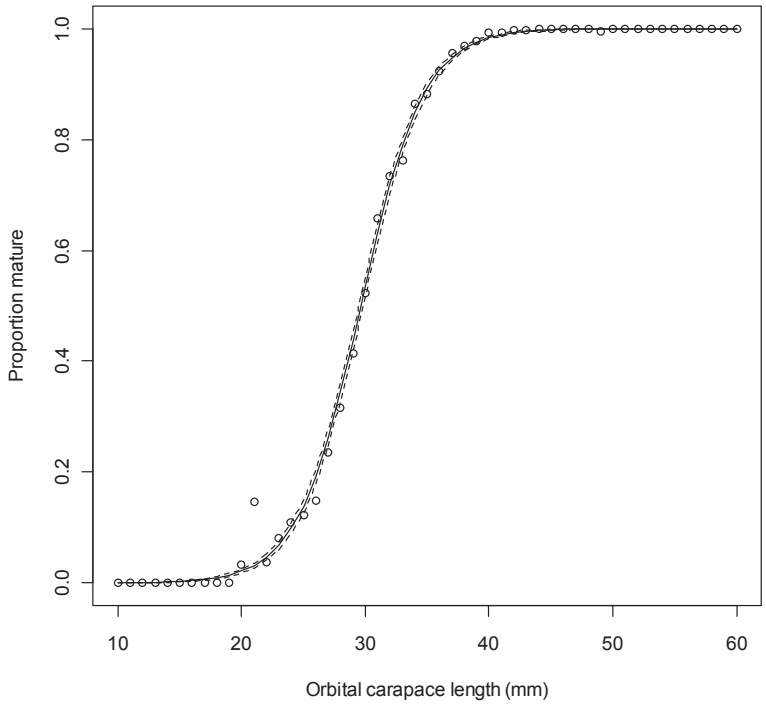

Figure 33: Proportions of female scampi with mature gonad stages at length, from all research trawling in SCI 1 and SCI 2. Solid line represents logistic curve fitted to the data (L_{50} 29.7 mm and selection range 5.3 mm). Dashed lines represent ± 1 s.e.

3.2.3. Natural mortality

The instantaneous rate of natural mortality, M, has not been estimated directly for any scampi species, but estimates have been made based on the estimate of the K parameter from a von Bertalanffy growth curve (Cryer & Stotter 1999) using a correlative method (Pauly 1980; Charnov et al. 1983). Morizur (1982) used length distributions from 'quasi-unexploited' *Nephrops* stocks to obtain estimates for annual *M* of 0.2–0.3. The values most commonly assumed for assessment of *Nephrops* stocks in the Atlantic is 0.3 for males and immature females, and 0.2 for mature females (assumed less vulnerable to predation during the ovigerous period) (Bell et al. 2006). For New Zealand scampi, M has previously been fixed at 0.2 (Tuck & Dunn 2012). Within the current assessment, an attempt was made to estimate M within the model, but sensitivities were also examined with M fixed at 0.2, 0.25 and 0.3.

3.3. Catch data

Data for the model were collated over the spatial and temporal strata as defined in the model structure. Catches in these modelled areas represent over 98% of scampi catches from both SCI 1 and SCI 2. Details of catches by time step, and breakdown by survey strata, are provided for SCI 1 in Table 12, and SCI 2 in Table 13.

Table 12: Catch breakdown by time step for each fishing year for SCI 1, along with breakdown by survey strata within each time step. Catch in tonnes.

	Step 1					Step 2					Step 3				
	Catch	202	203	3/402	3/403	Catch	202	203	3/402	3/403	Catch	202	203	3/402	3/403
1987	2	1%	0%	70%	29%	1	0%	1%	60%	40%	2	1%	0%	90%	10%
1988	7	1%	0%	70%	29%	3	0%	1%	60%	40%	6	1%	0%	90%	10%
1989	28	1%	0%	70%	29%	10	0%	1%	60%	40%	22	1%	0%	90%	10%
1990	48	1%	0%	70%	29%	18	0%	1%	60%	40%	38	1%	0%	90%	10%
1991	44	0%	0%	75%	25%	34	0%	2%	84%	13%	102	36%	29%	21%	14%
1992	68	12%	5%	68%	15%	13	2%	2%	85%	11%	52	32%	10%	45%	12%
1993	44	41%	5%	48%	5%	21	4%	0%	82%	14%	49	15%	21%	40%	24%
1994	75	31%	4%	54%	11%	1	61%	0%	35%	3%	39	12%	35%	28%	25%
1995	54	57%	3%	29%	11%	26	60%	3%	31%	6%	34	51%	15%	18%	17%
1996	65	39%	17%	21%	23%	23	1%	59%	17%	23%	29	6%	4%	43%	47%
1997	58	5%	28%	16%	51%	39	29%	37%	8%	26%	20	12%	29%	10%	49%
1998	87	22%	23%	36%	19%	9	0%	6%	41%	53%	11	2%	2%	66%	30%
1999	62	17%	12%	58%	14%	39	9%	13%	52%	26%	9	0%	0%	53%	47%
2000	22	18%	35%	17%	30%	24	8%	26%	10%	56%	78	31%	19%	43%	8%
2001	82	34%	12%	45%	9%	33	28%	7%	59%	5%	5	41%	16%	42%	1%
2002	124	32%	17%	45%	6%	0					0				
2003	121	29%	12%	49%	10%	0					0				
2004	120	30%	15%	48%	7%	0					0				
2005	46	41%	22%	28%	9%	34	30%	13%	35%	22%	34	39%	20%	38%	4%
2006	40	25%	6%	53%	16%	26	34%	9%	57%	1%	43	36%	44%	12%	8%
2007	43	33%	10%	45%	13%	34	15%	9%	61%	14%	32	45%	24%	26%	5%
2008	49	29%	3%	49%	19%	34	15%	8%	59%	19%	20	25%	44%	20%	11%
2009	50	21%	11%	47%	21%	18	23%	15%	49%	12%	17	9%	18%	53%	20%
2010	65	26%	21%	47%	6%	15	3%	4%	68%	25%	31	2%	2%	77%	19%
2011	48	5%	6%	86%	3%	23	32%	15%	51%	2%	43	1%	1%	64%	34%
2012	58	14%	9%	63%	14%	19	6%	4%	67%	23%	37	9%	14%	41%	35%
2013	59	26%	13%	48%	14%	25	6%	6%	55%	33%	42	10%	17%	44%	29%
2014	50	27%	17%	50%	6%	32	12%	13%	48%	26%	24	2%	4%	72%	21%
2015	44	8%	7%	64%	21%	31	16%	22%	41%	21%	42	6%	8%	48%	38%

Table 13: Catch breakdown by time step for each fishing year for SCI 2, along with breakdown by survey strata within each time step. Catch in tonnes.

	Step 1					Step 2					Step 3				
	Catch	702	703	802	803	Catch	702	703	802	803	Catch	702	703	802	803
1987	0					0					0				
1988	1	99%	0%	1%	0%	1	39%	1%	60%	0%	3	70%	1%	29%	0%
1989	2	99%	0%	1%	0%	5	39%	1%	60%	0%	10	70%	1%	29%	0%
1990	17	99%	0%	1%	0%	39	39%	1%	60%	0%	83	70%	1%	29%	0%
1991	143	34%	0%	66%	0%	58	27%	0%	73%	0%	94	43%	8%	47%	1%
1992	72	58%	1%	42%	0%	22	19%	0%	81%	0%	127	44%	3%	52%	0%
1993	77	69%	3%	28%	0%	62	41%	1%	59%	0%	71	41%	5%	53%	1%
1994	31	67%	3%	30%	0%	55	97%	1%	2%	0%	159	59%	1%	40%	1%
1995	71	35%	9%	57%	0%	45	34%	1%	62%	2%	110	25%	2%	67%	6%
1996	109	67%	13%	19%	1%	27	80%	0%	20%	0%	94	56%	2%	38%	4%
1997	62	70%	7%	23%	0%	71	57%	11%	31%	0%	80	73%	18%	8%	1%
1998	158	53%	4%	43%	0%	45	33%	3%	64%	0%	20	14%	1%	81%	4%
1999	121	56%	7%	36%	1%	76	43%	3%	54%	0%	36	64%	15%	21%	0%
2000	103	43%	8%	49%	1%	15	51%	0%	49%	0%	75	73%	6%	20%	0%
2001	29	61%	0%	38%	0%	33	63%	0%	37%	0%	84	63%	4%	33%	0%
2002	68	64%	2%	31%	2%	102	50%	1%	49%	0%	76	59%	14%	26%	1%
2003	80	45%	3%	52%	0%	39	32%	8%	60%	0%	15	80%	19%	1%	0%
2004	40	72%	8%	19%	0%	24	70%	4%	26%	0%	0	100%	0%	0%	0%
2005	42	65%	9%	25%	0%	11	59%	3%	38%	0%	18	45%	16%	38%	1%
2006	37	48%	1%	51%	0%	6	95%	1%	4%	0%	34	69%	13%	18%	0%
2007	36	37%	4%	59%	0%	26	61%	1%	38%	0%	18	67%	11%	22%	0%
2008	55	61%	2%	37%	0%	5	82%	2%	15%	0%	0	74%	0%	26%	0%
2009	32	55%	1%	44%	0%	11	36%	0%	64%	0%	10	92%	0%	8%	0%
2010	86	41%	0%	58%	1%	11	49%	1%	50%	0%	29	62%	3%	35%	0%
2011	82	76%	3%	21%	0%	30	77%	1%	23%	0%	17	45%	1%	55%	0%
2012	61	48%	1%	51%	1%	31	50%	0%	48%	2%	7	3%	0%	97%	0%
2013	75	40%	2%	58%	0%	20	12%	0%	88%	0%	0				
2014	102	93%	1%	6%	0%	22	100%	0%	0%	0%	2	78%	0%	22%	0%
2015	69	63%	0%	35%	2%	45	99%	1%	1%	0%	28	55%	26%	19%	0%

3.4. CPUE indices

The annual CPUE indices estimated within the standardisation (SCI 1: Figure 24, SCI 2: Figure 27) were fitted within the model as abundance indices. There has been considerable discussion on whether CPUE is proportional to abundance for scampi (Tuck 2009), with rapid increases in both CPUE and trawl survey catch rates for a number of stocks in the early to mid 1990s (and changes in sex ratio in trawl survey catches) initially being considered related to changes in catchability. Later analysis (Tuck & Dunn 2009) suggested that the observed changes in sex ratio were related to slight changes in the survey timing in relation to the moult cycle. Similar patterns in CPUE are observed over the same period for rock lobster (Starr 2009; Starr et al. 2009), and scampi in SCI 3 (Tuck 2013), which may suggest broad scale environmental drivers influencing crustacean recruitment. The CPUE patterns for SCI 1 are mirrored by trawl survey catch rates, suggesting that they do not reflect fisher learning. While not considered appropriate for use as an index in the model (Tuck 2013), the middle depths (*Tangaroa*) trawl survey scampi abundance index shows a very similar temporal pattern to the standardised CPUE indices for SCI 3, also supporting the suggestion that the increases in scampi catch rate observed during the 1990s reflect scampi abundance rather than fisher learning. Also, analysis described above found no evidence that previous fishing effort at a location had a significant effect on scampi catchability (Section 2.3.7).

CPUE standardisation procedures tend to estimate unrealistically low CVs and so we have adopted the approach proposed by Francis (2011), estimating appropriate CVs by fitting a smoother to the index. The smoothers are presented in Appendices 1 and 2 with the relevant standardisation. On the basis of

discussion at the Shellfish Assessment Working Group, initial values for CPUE index CVs were taken as 0.15 for SCI 1 and 0.11 for SCI 2, with sensitivity to these assumptions also being investigated.

3.5. Research survey indices

Trawl surveys were first conducted from the RV *Kaharoa* in SCI 1 and SCI 2 in 1993, and have been conducted intermittently (in conjunction with photographic surveys in more recent years). Surveys have been conducted between January and April, but timing within this period has varied between years.

3.5.1. Photographic surveys

Photographic surveys of SCI 1 and SCI 2 (Cryer et al. 2003; Tuck et al. 2006; Tuck et al. 2009; Tuck et al. 2013; Tuck et al. 2016) have been used to estimate the absolute abundance (in numbers) of burrows thought to belong to scampi in 1998, 2000–2003, 2008, 2012 and 2015 (for SCI 1) and 2003–2006, 2012 and 2015 (for SCI 2). The surveys provide two indices of scampi abundance, one based on major burrow openings, and one based on visible scampi. Both indices are subject to uncertainty, either from burrow detection and occupancy rates (for burrow based indices) or emergence patterns (for visible scampi based indices). The burrow index has been used to date within assessments for SCI 1 and SCI 2 (Tuck & Dunn 2012). Survey estimates are provided for SCI 1 in Table 14 and SCI 2 in Table 15. Surveys of SCI 1 only covered part of the main fishery area until 2012, and the data are fitted within the model as two separate series, with separate *q* values, with the *q* for the total area informed by a prior, and the ratio between the *q*s for the total and part surveys constrained by the @ratio_qs_penalty in CASAL. Details of the estimation of the priors and the ratio are provided in Section 3.7. Although the photographic surveys have occurred in time step 1 and 2, the survey abundance (based on burrow counts) should be relatively insensitive to moult cycle and reproductive behaviour driving the changes in sex ratio in catches, and therefore the indices are fitted as occurring at the end of time step 1.

Table 14: Time series of photo survey scampi stock estimates (millions) and CV for SCI 1. Estimates are provided for survey combined strata 302, 303, 402 and 403 (areas surveyed 1998–2008), and the larger area surveyed in 2012 and 2015 (including survey strata 202 and 203). Time step relates to assessment model, with surveys in December–January allocated to step 1, and those in February–April allocated to step 2.

	302,303,402,403		Total area		
	Abundance	CV	Abundance	CV	Time step
1998	149.6	0.15			1
2000	93.5	0.13			2
2001	131.3	0.12			1
2002	124.6	0.08			2
2003	97.8	0.12			2
2008	103.0	0.08			2
2012	99.6	0.06	149.1	0.06	2
2015	104.6	0.05	161.2	0.05	2

Table 15: Time series of photo survey scampi stock estimates (millions) and CV for SCI 2. Time step relates to assessment model, with surveys in December–January allocated to step 1, and those in February–April allocated to step 2.

	Abundance	CV	Time step
2003	100.4	0.16	2
2004	156.9	0.14	1
2005	92.7	0.17	2
2006	72.3	0.11	2
2012	116.9	0.09	2
2015	234.1	0.06	2

3.5.2. Trawl surveys

Stratified random trawl surveys of scampi in SCI 1 and SCI 2, 200–600 m depth, were conducted in 1993, 1994, and 1995. Formal trawl surveys to estimate relative abundance were discontinued following this, because it was inferred from the results that catchability had varied among surveys, although it was later concluded that the changes were related to slight differences in survey timing (Tuck & Dunn 2009). Despite these concerns, research trawling continued in both areas for a variety of other purposes (in support of a tagging programme to estimate growth in 1995 and 1996, to assess selectivity of research and commercial mesh sizes in 1996, and trawl surveys have been conducted in support of photographic surveys since 1998). Identical gear has been used throughout the survey trawling. Survey coverage in SCI 1 has changed over time, with the early surveys covering the whole modelled area, but surveys in 1998, and from 2001 – 2008 only covering survey strata 302, 303, 402 and 403. Survey estimates (by area) are provided for SCI 1 in Table 16 and SCI 2 in Table 17. As with the photo survey for SCI 1, the trawl survey is fitted as two indices with separate *q*s, with the ratio between the *q*s for the total and part surveys constrained by the @ratio_qs_penalty (Section 3.7). Trawl surveys in both fisheries have occurred in time steps 1 and 2. In SCI 1, surveys in time step 2 have generally been early in the time step, and to reduce complexity, given the two levels of survey coverage, all trawl surveys were assumed to occur at the end of time step 1. In SCI 2, surveys have occurred later in time step 2, and have been fitted as separate indices in each time step.

Table 16: Time series of trawl survey scampi stock estimates (tonnes) by survey strata for SCI 1. Estimates are provided for survey combined strata 302, 303, 402 and 403 (areas surveyed 1998, 2001–2008), and the larger area surveyed in 1993–1995, 2000, 2012 (including survey strata 202 and 203). Time step relates to assessment model, with surveys in December–January occurring in step 1, and those in February–April occurring in step 2, although in the model both are allocated to the end of time step 1. N represents number of research tows in each survey.

	302,303,402,403			Total area			
	N	Biomass	CV	N	Biomass	CV	Time step
1993				36	271.6	0.117	1
1994				33	364.0	0.171	1
1995				37	510.4	0.150	1
1998	18	174.0	0.172				1
2000				15	225.1	0.328	2
2001	12	179.5	0.269				1
2002	13	130.6	0.236				2
2008	10	211.9	0.132				2
2012				19	186.6	0.210	2
2015				18	170.6	0.150	2

Table 17: Time series of raised trawl survey scampi stock estimates (tonnes) by survey strata for SCI 2. Time step relates to assessment model, with surveys in December–January allocated to step 1, and those in February–April allocated to step 2. N represents number of research tows in each survey.

	N	Biomass	CV	Time step
1993	26	238.2	0.12	1
1994	27	170.0	0.16	1
1995	29	216.2	0.18	1
2003	7	28.0	0.33	2
2004	8	46.9	0.20	1
2005	8	50.8	0.35	2
2006	8	22.9	0.19	2
2012	14	164.2	0.28	2
2015	12	224.46	0.19	2

3.6. Length distributions

3.6.1. Commercial catch at length data

Ministry for Primary Industries observers have collected scampi length frequency data from scampi targeted fishing on commercial vessels in SCI 1 and SCI 2 since 1990–91. The numbers of tows for which length data are available are presented by fishing year and month in Table 18 (SCI 1), Table 19 (SCI 2).

For both fisheries, levels of sampling, and the pattern of sampling relative to the pattern of catches, vary between years, and the proportion of landings represented by the observer sampling varies considerably (Table 20). Where size compositions vary markedly between areas, low proportions of landings being represented by observer sampling may lead to biased estimates of catch composition. For both fisheries, mean orbital carapace length (OCL) and proportion males from observer sampling was modelled for each year individually on survey strata and time step with multivariate tree regression. Very few significant splits were detected, and there was no consistent pattern suggesting that length frequencies should be spatially stratified.

Table 18: Number of commercial tows for which length distributions are available for SCI 1, by fishing year, time step and survey strata.

	Step 1				Step 2				Step 3			
	202	203	3/402	3/403	202	203	3/402	3/403	202	203	3/402	3/403
1991									8	60	25	8
1992		1	13	2					15			
1993	2		1									
1994											1	
1995									3			
1996	1		4						1			
1997						7		8				
1998												
1999					3	1	8	2				
2000									6	14	9	2
2001												
2002		2	1									
2003												
2004	1	1										
2005									7	6	2	1
2006	2	2	2	7					8	16		1
2007	4	2	13	1					11	2	5	1
2008	1	4	5	14			21	11				
2009	2	5	14	6								
2010	9		2	2	2		8	5	2	4	12	11
2011	1	3	20	2							20	2
2012			3	3			15	12				
2013												
2014	14	10	9	2								
2015												

Proportional length distributions (and associated CVs) were calculated using CALA (Francis & Bian 2011), using the approaches previously implemented in NIWA's *Catch-at-Age* software (Bull & Dunn 2002). Plots of the proportional length distribution are shown by year for SCI 1 by time step in Figure 34 to Figure 36, and for SCI 2 by time step in Figure 37 to Figure 40.

Table 19: Number of commercial tows for which length distributions are available for SCI 2, by fishing year, time step and survey strata.

	Step 1				Step 2				Step 3			
	702	703	802	803	702	703	802	803	702	703	802	803
1991									33	17	11	1
1992	9		5									
1993		1	2						7	2	18	
1994					1				32	2	24	
1995					4	2	18		7		25	5
1996	13								4		10	1
1997	28		6		1				5			
1998	3	1				2						
1999	51	8	22	1	18	7						
2000												
2001	20	26	29						1			
2002												
2003	36	2	16						7	1		
2004	25		12									
2005	11	2										
2006			6									
2007					3		1		1			
2008	10	2	8		7		3		2		1	
2009					6		6					
2010									4	2	4	
2011	4	1	12						3		3	
2012	45		64	1			2					
2013			11									
2014	1											
2015												

Table 20: Proportion of landings not represented by observer catch sampling.

	SCI 1			SCI 2		
	Step 1	Step 2	Step 3	Step 1	Step 2	Step 3
1991			0%			1%
1992	17%		68%	1%		
1993	59%			72%		1%
1994						1%
1995			49%		2%	2%
1996	79%			33%		6%
1997		38%		7%		27%
1998		100%		47%	97%	
1999		13%		1%	54%	
2000			0%			
2001				0%		
2002	83%					
2003				0%		20%
2004				9%		
2005			4%	25%		
2006	0%		20%	49%		
2007	13%		5%		39%	
2008	29%	23%		0%	2%	26%
2009	0%				0%	
2010	21%	4%	0%	100%	100%	0%
2011	5%		2%	4%		1%
2012	23%	10%		1%	52%	
2013				42%		
2014	0%					
2015						

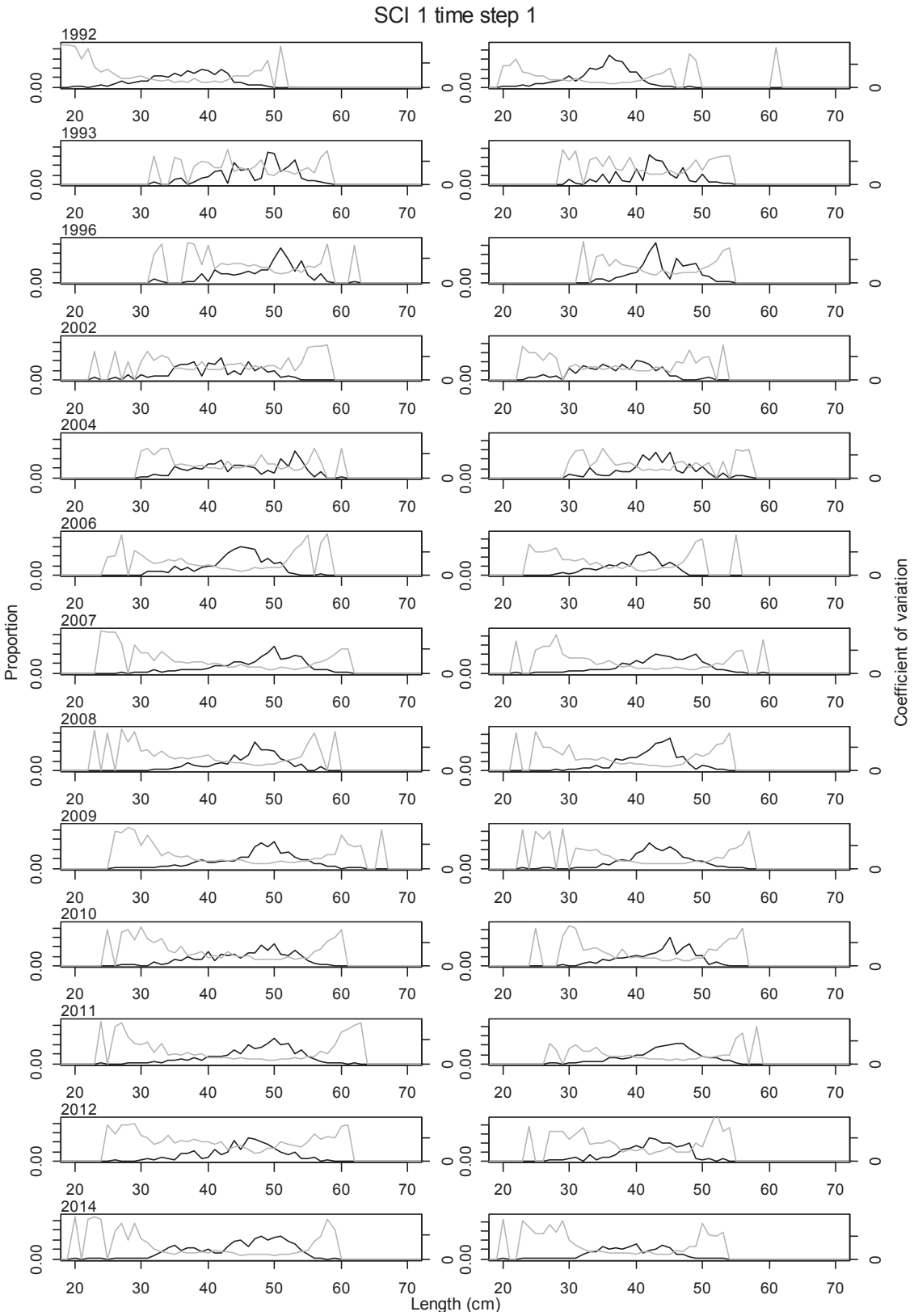

Figure 34: Proportional length frequency distributions (black line) and CVs (grey line) for commercial catches by model year and time step 1 for SCI 1. Males plotted on left, females on right.

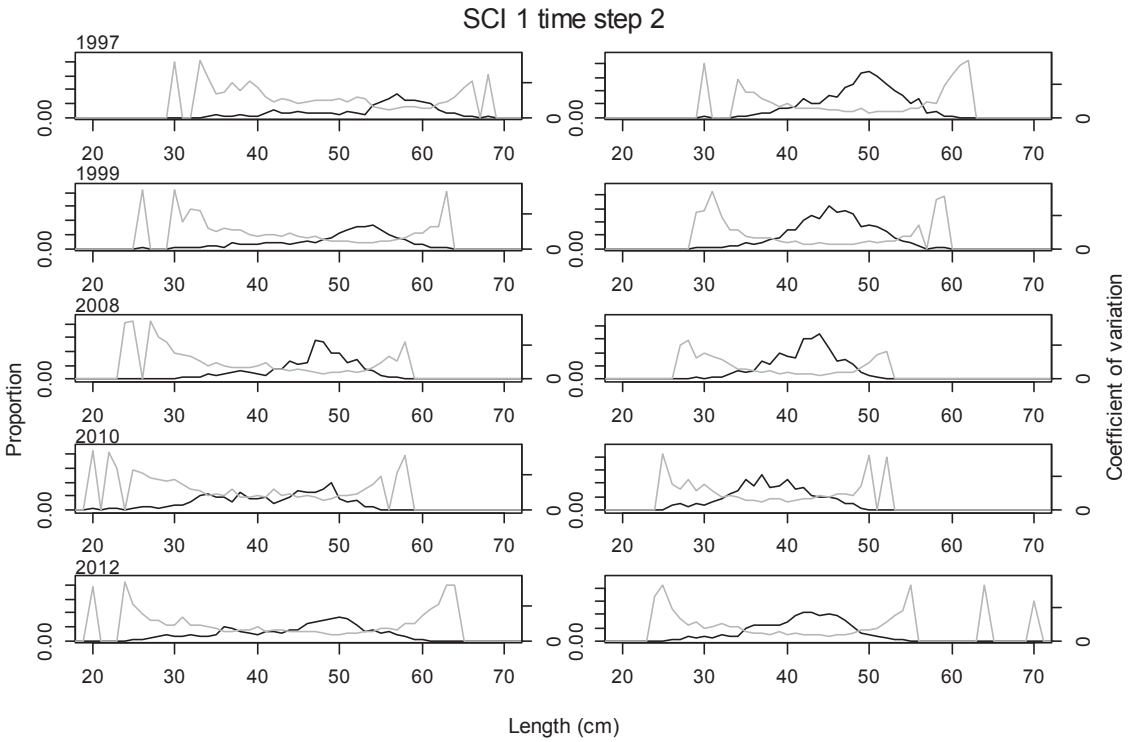

Figure 35: Proportional length frequency distributions (black line) and CVs (grey line) for commercial catches by model year and time step 1 for SCI 1. Males plotted on left, females on right.

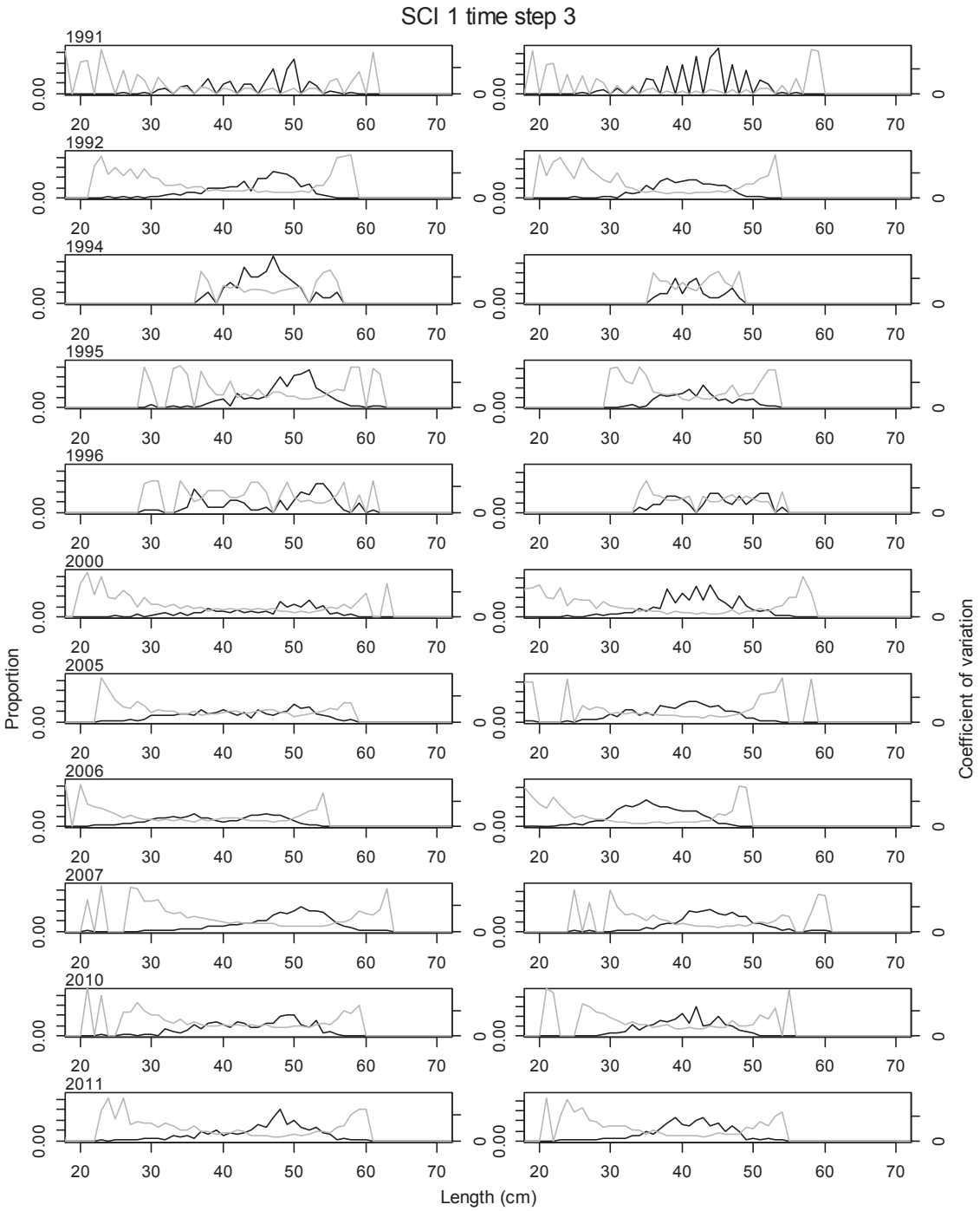

Figure 36: Proportional length frequency distributions (black line) and CVs (grey line) for commercial catches by model year and time step 3 for SCI 1. Males plotted on left, females on right.

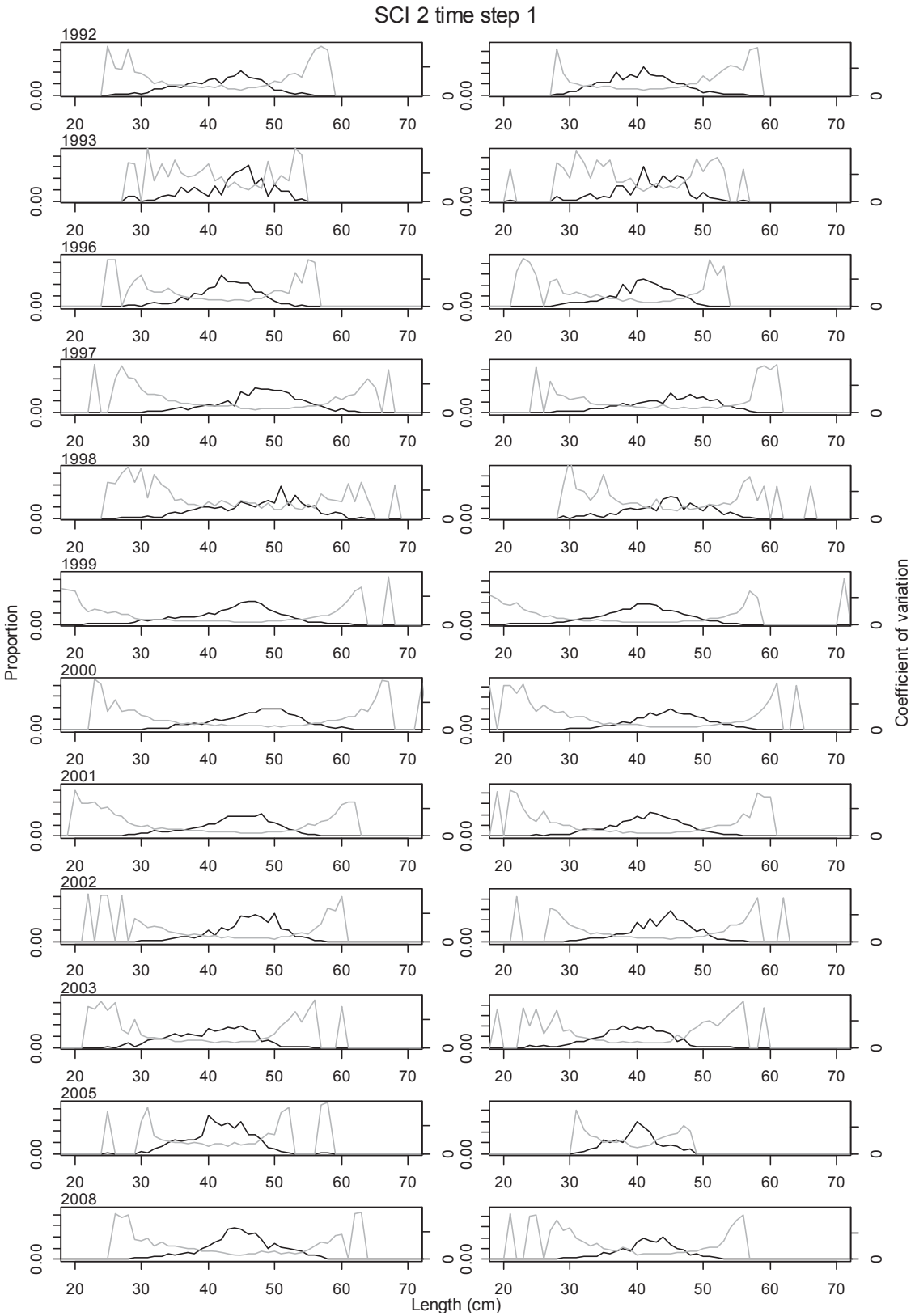

Figure 37: Proportional length frequency distributions (black line) and CVs (grey line) for commercial catches by model year and time step 1 for SCI 2, 1992 to 2008. Males plotted on left, females on right.

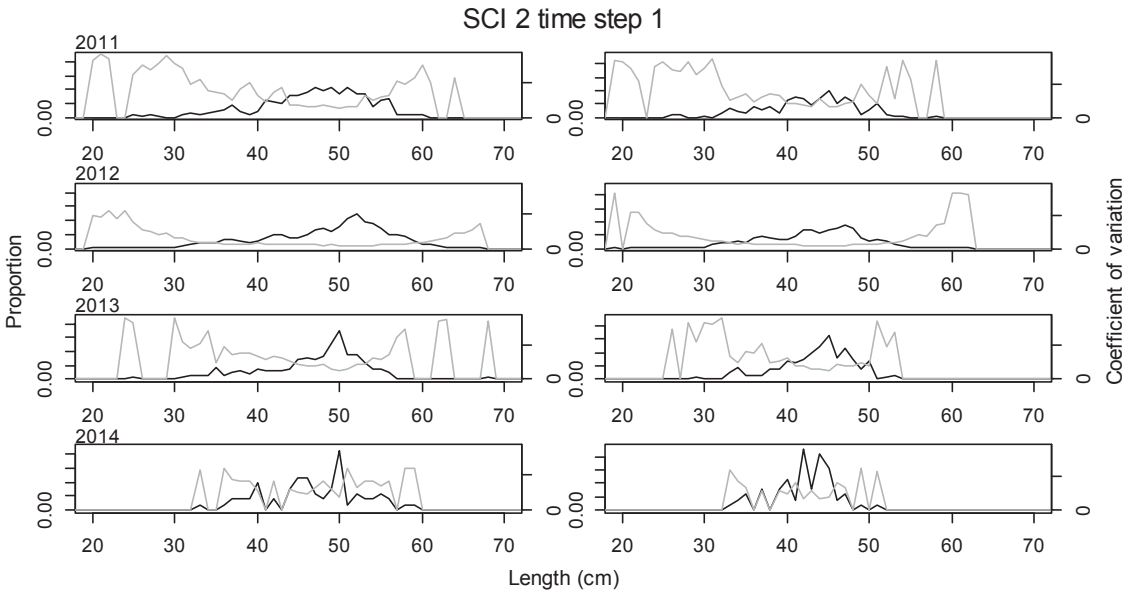

Figure 38: Proportional length frequency distributions (black line) and CVs (grey line) for commercial catches by model year and time step 1 for SCI 2, 2011 to 2014. Males plotted on left, females on right.

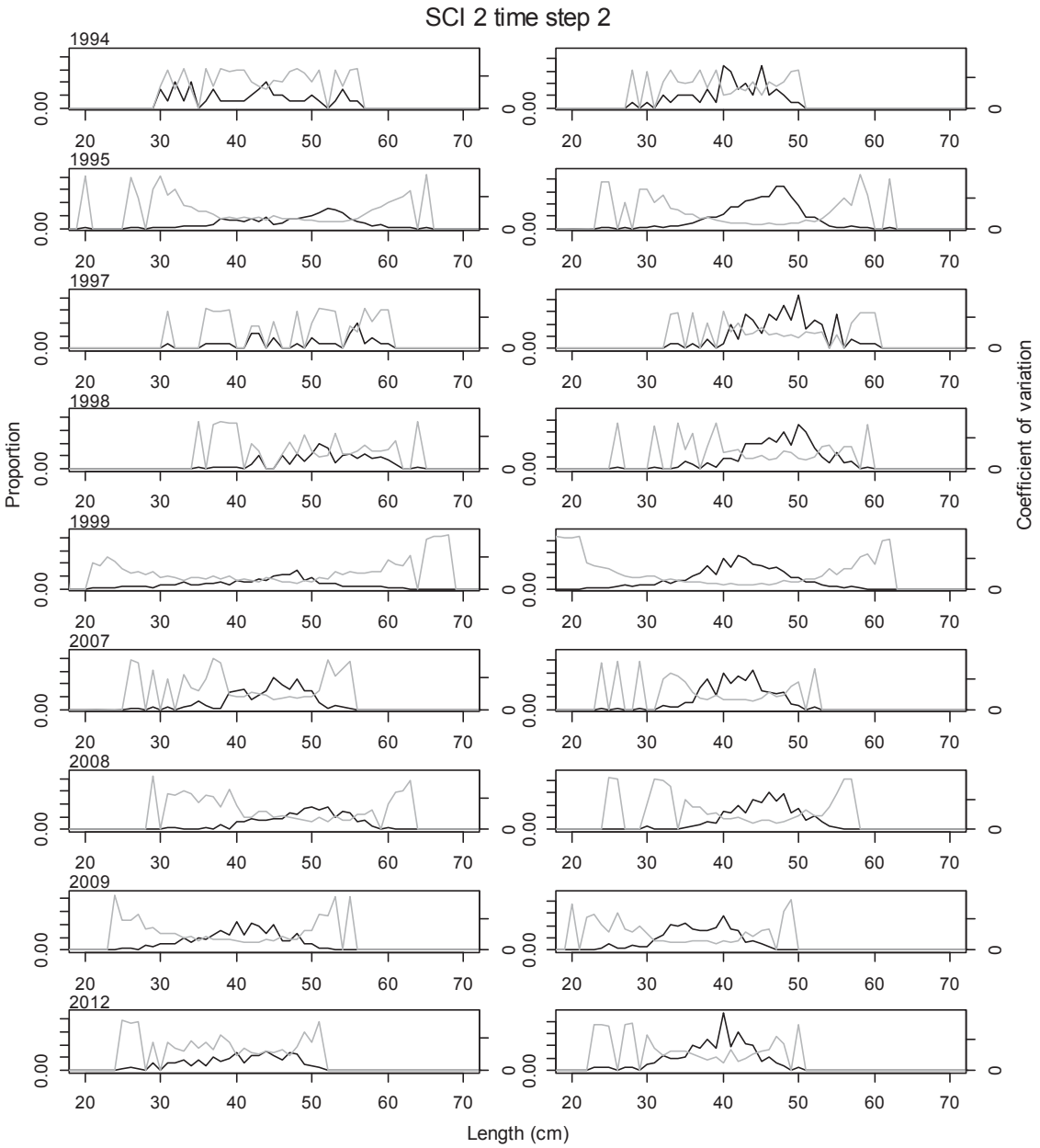

Figure 39: Proportional length frequency distributions (black line) and CVs (grey line) for commercial catches by model year and time step 2 for SCI 2. Males plotted on left, females on right.

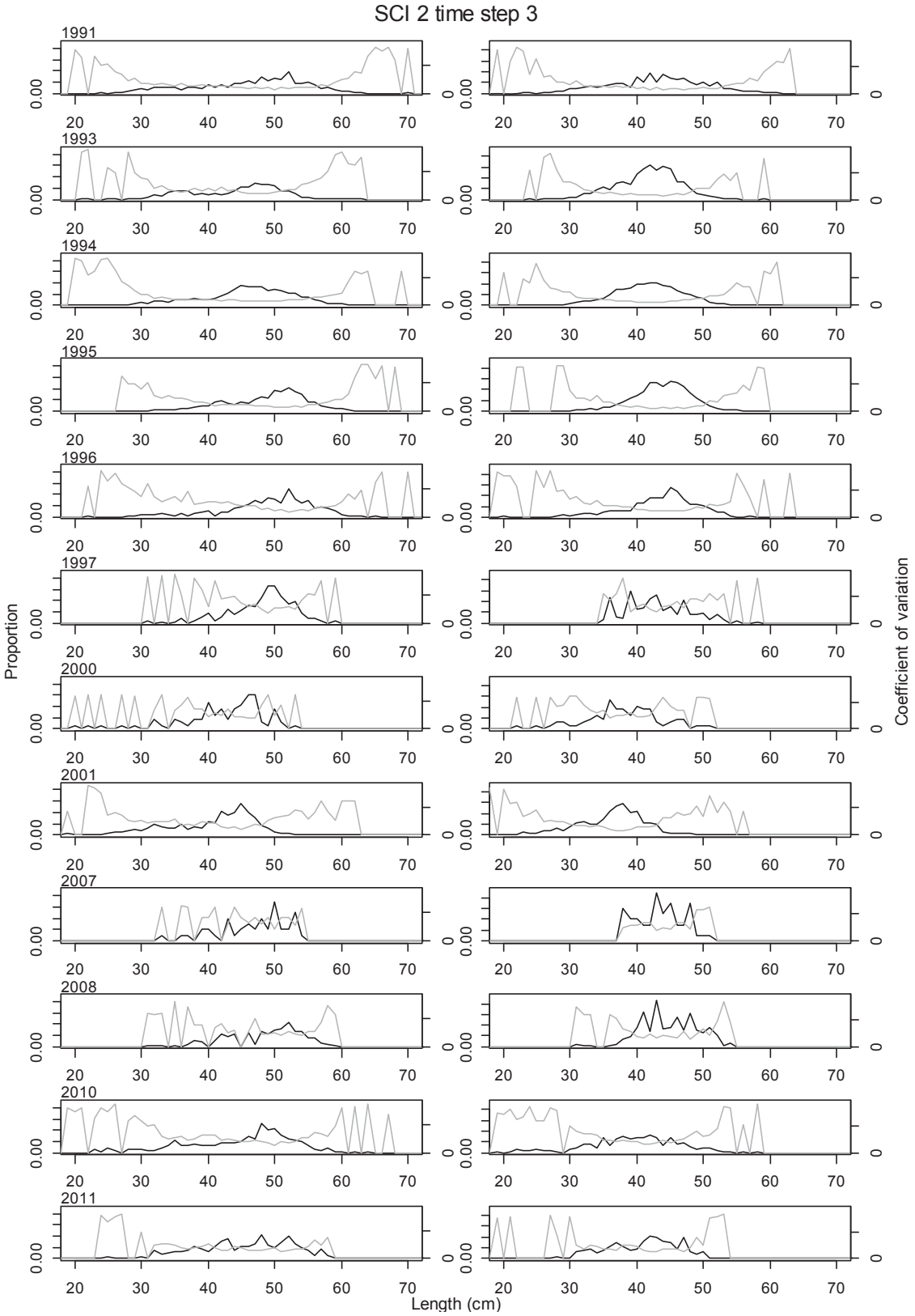

Figure 40: Proportional length frequency distributions (black line) and CVs (grey line) for commercial catches by model year and time step 3 for SCI 2. Males plotted on left, females on right.

3.6.2. Trawl survey length distributions

Length frequency samples from research trawling in both fisheries have been taken by scientific staff since 1993 (Table 16 and Table 17). Estimates of the length frequency distributions (with associated CVs) were derived using the NIWA CALA software (Francis & Bian 2011), using 1 mm OCL (Orbital Carapace Length) length classes by sex, and are presented in Figure 41 (SCI 1) and Figure 42 and Figure 43 (SCI 2).

3.6.3. Photo survey length distributions

Length frequency distributions were estimated for the relative photographic abundance series, by measuring the widths of a large sample of major burrow openings in the images, and converting these to orbital carapace lengths using a regression of OCL on major opening width (Cryer et al. 2005), augmented with additional data collected from more recent surveys. To estimate the CVs at length for each year, we used a bootstrap procedure, resampling with replacement from the original observations of burrow width, converting each observation to an estimated scampi size (in OCL), using an error term sampled from a normal distribution fitted to the regression residuals. Compared with the length frequency distributions from trawl catches, this procedure gave very large CVs, but we think this is realistic given the uncertainties involved in generating a length frequency distribution from burrow sizes. Estimates of the length frequency distributions (with associated CVs) for scampi generating burrows are presented for SCI 1 in Figure 44 and for SCI 2 in Figure 45.

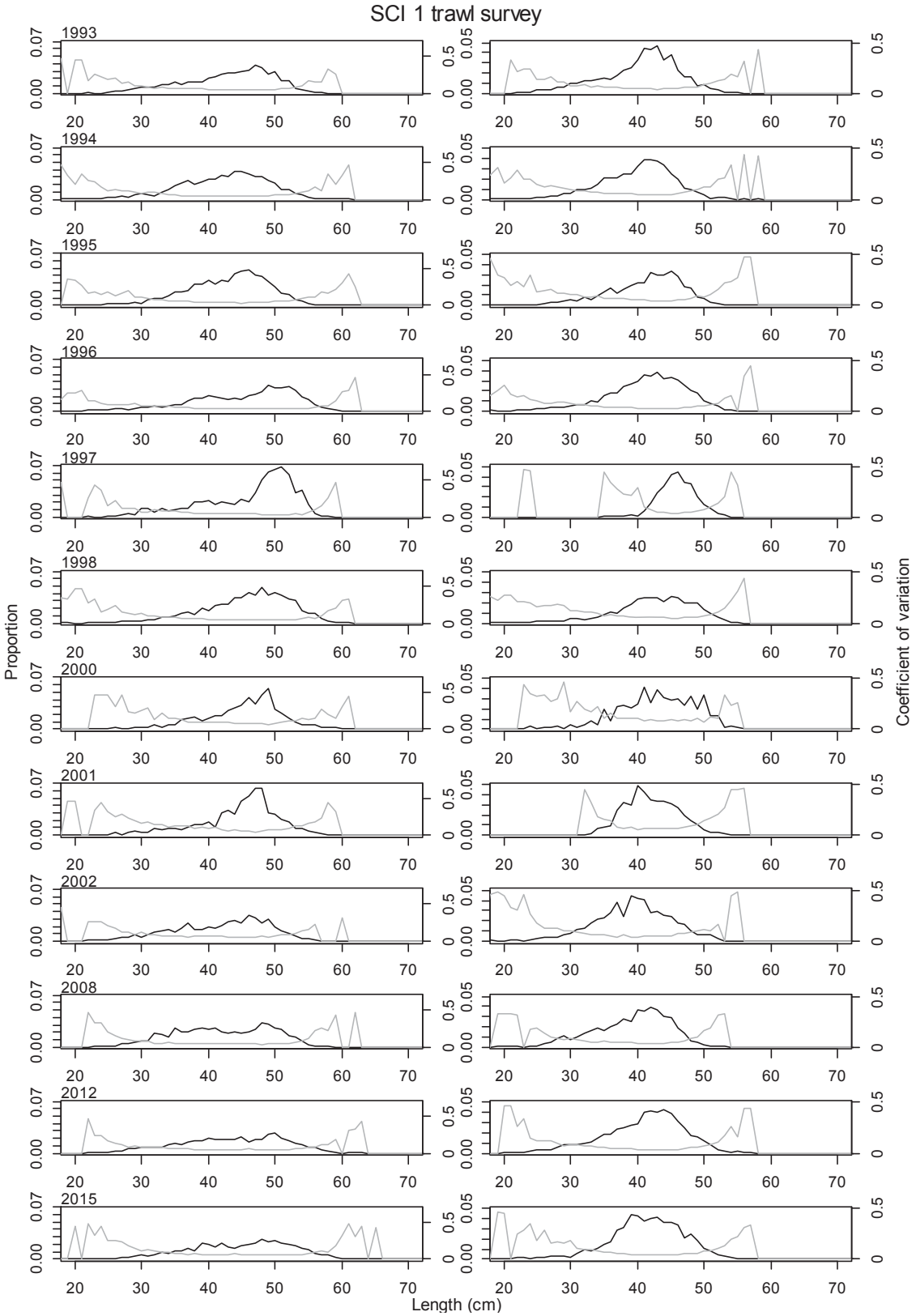

Figure 41: Proportional length frequency distributions (black line) and CVs (grey line) for research survey catches by model year for SCI 1. Males plotted on left, females on right.

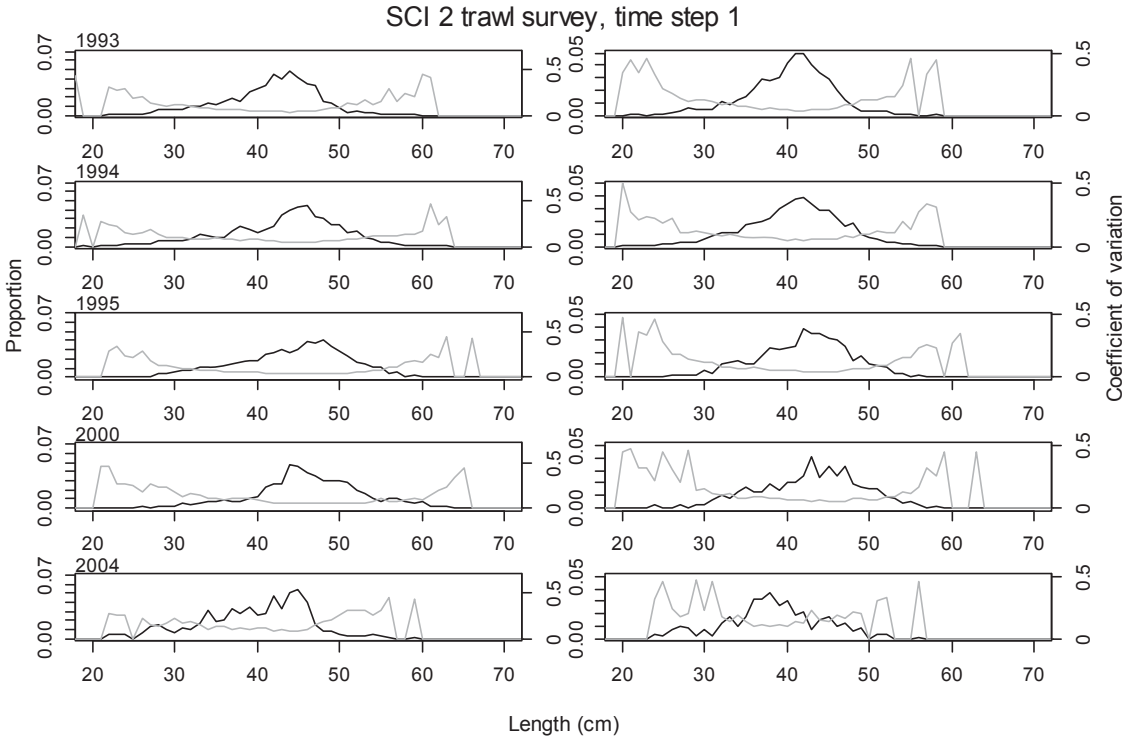

Figure 42: Proportional length frequency distributions (black line) and CVs (grey line) for research survey catches by model year for SCI 2, time step 1. Males plotted on left, females on right.

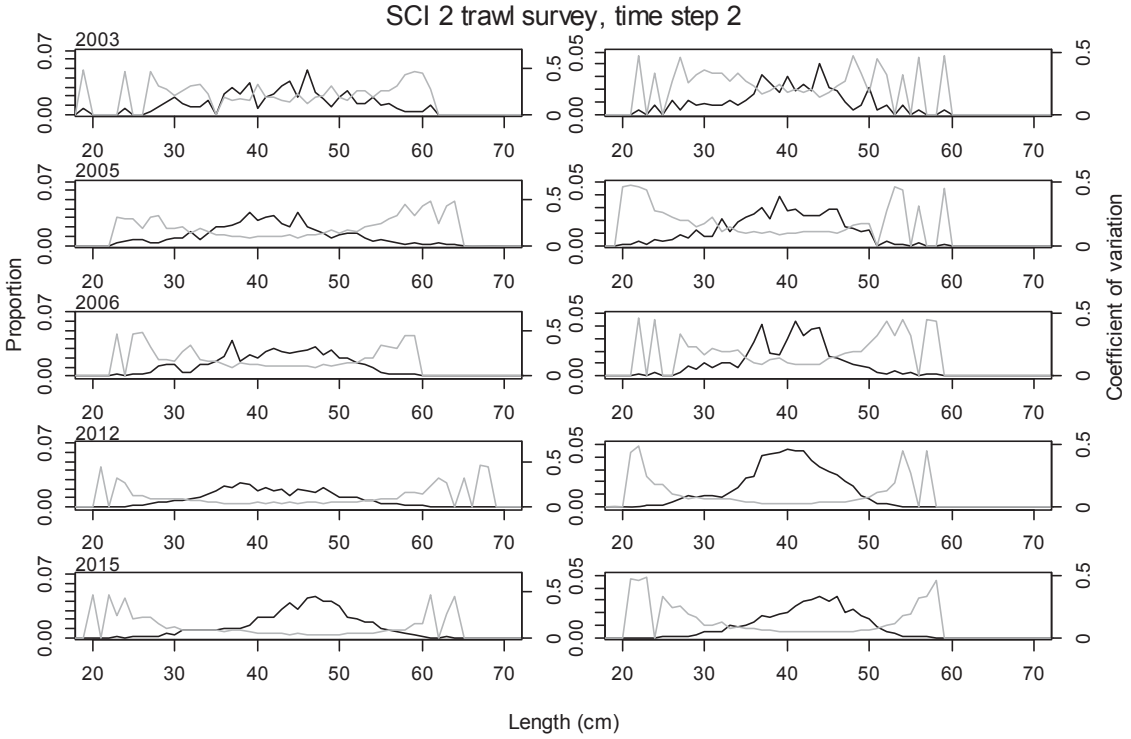

Figure 43: Proportional length frequency distributions (black line) and CVs (grey line) for research survey catches by model year for SCI 2, time step 2. Males plotted on left, females on right.

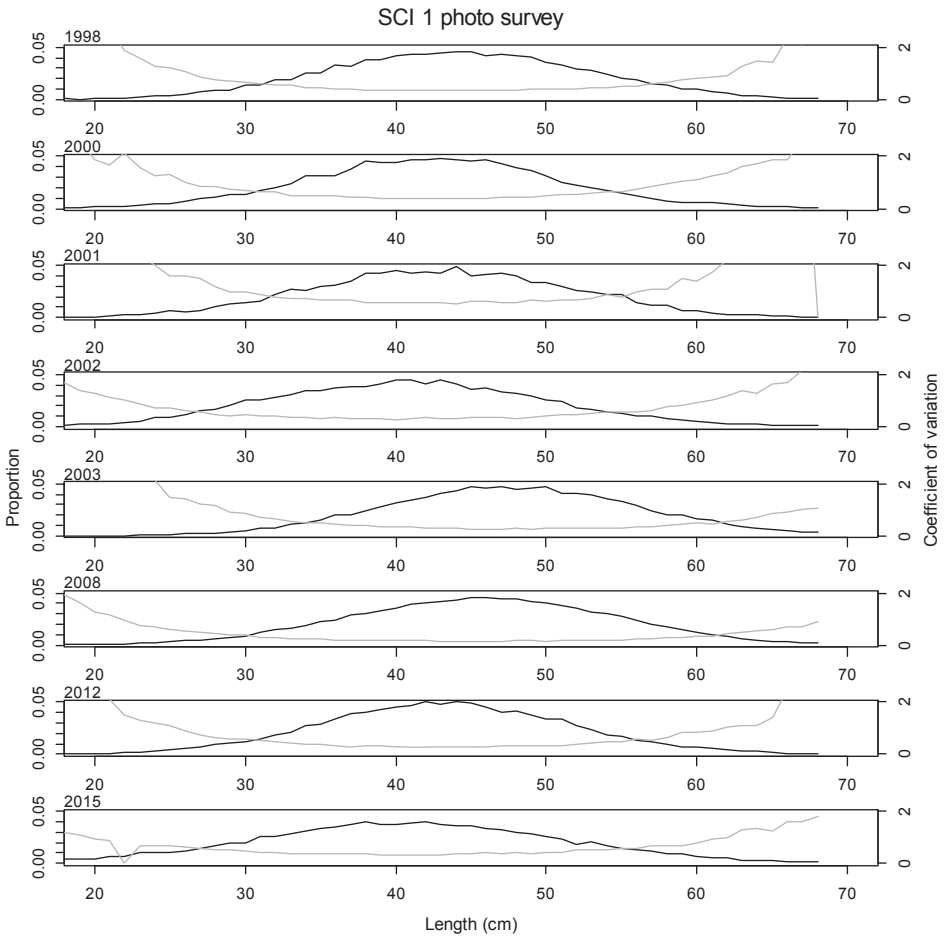

Figure 44: Proportional length frequency distributions (black line) and CVs (grey line) for scampi responsible for burrows counted within photo survey for SCI 1.

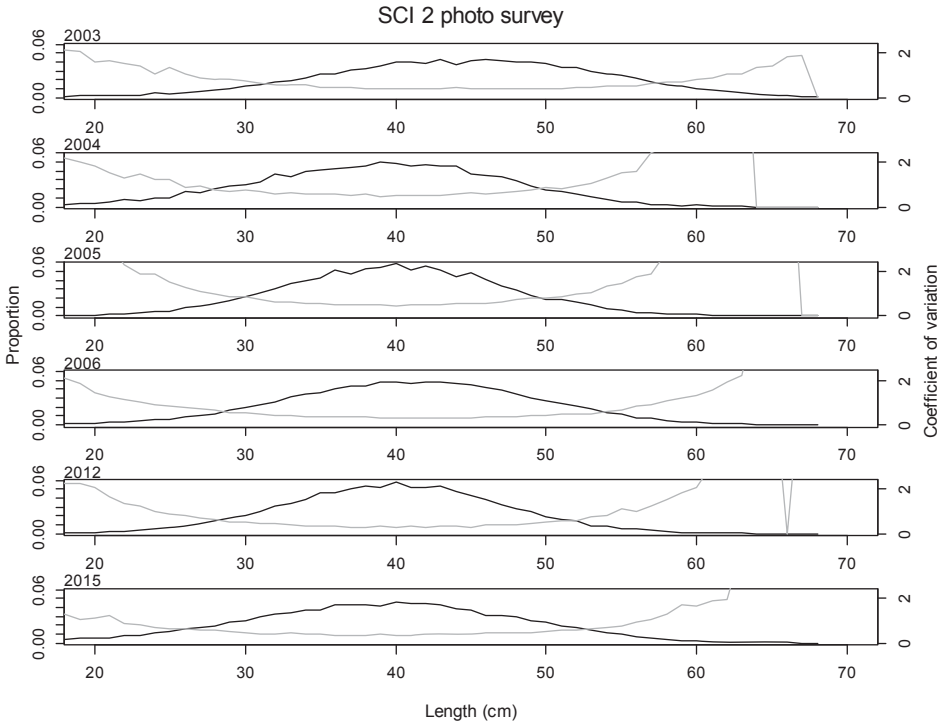

Figure 45: Proportional length frequency distributions (black line) and CVs (grey line) for scampi responsible for burrows counted within photo survey for SCI 2.

3.7. Model assumptions and priors

Maximum Posterior Density (MPD) fits were found within CASAL using a quasi-Newton optimiser and the BETADIFF automatic differentiation package (Bull et al. 2008). Fitting was done inside the model except for the weighting of the abundance and length frequency data. For the length frequency data, observation-error CVs were estimated using CALA, converted to equivalent observation-error multinomial *N*s, and used within the model. The appropriate multinomial *N*s to account for both observation and process error were then calculated from the model residuals (method TA1.8 of Francis 2011), and these final *N*s were used in all models reported. Generally this process resulted in small *N*s for the commercial length frequency data in particular, and therefore relatively low weighting within the model. For the CPUE indices, the approach proposed by Francis (2011) was initially investigated (estimating appropriate CVs by fitting a smoother to the index), although sensitivity to this was examined, and in the final models CVs were fixed at the lower range of the sensitivity runs examined, with additional process error estimated within the model. CASAL was also used to run Monte-Carlo Markov Chains (MCMC) on the base models. MPD output was analysed using the extract and plot utilities in the CASAL library running under the general analytical package R.

The initial model was based on that described by Tuck (2014). The model inputs include catch data, abundance indices (CPUE, trawl and photo surveys) and associated length frequency distributions. The parameters estimated in the base model include SSB_0 and R_0, and time series of SSB and year class strength, selectivity parameters for commercial and research trawling, and the photo survey, and associated catchability coefficients. Catchability coefficients (*q*'s) for commercial fishing, research trawling, and photographic surveys were estimated as free parameters, but as with previous scampi assessments (Tuck 2015; in prep), MCMC diagnostics for these models were poor, and equivalent models with "nuisance" *q*'s were used for final runs. Model results were not sensitive to the estimation of *q*'s as nuisance or free parameters. The only informative priors used in the initial model were for *q-Photo, q-Trawl*, the ratio of *q* values for *q-Photo* and *q-Trawl* for the whole and part areas of SCI 1, and the YCS vector (which constrains the variability of recruitment).

3.7.1. Scampi catchability

Catchability is considered to be the proportion of the scampi population that a particular survey index represents. The priors for scampi catchability used in the initial scampi assessments were largely based on information on *Nephrops* emergence and occupancy rates from European studies conducted in far shallower waters than *Metanephrops* populations inhabit (Tuck & Dunn 2012), but the acoustic tagging study conducted at the Mernoo Bank in October 2010 offered an opportunity to estimate priors for occupancy and emergence from New Zealand data (Tuck 2013). Acoustic tagging was repeated within the SCI 1 and SCI 2 surveys in 2012 and 2015, and the data collected within these studies have been used to estimate priors (Tuck et al. 2013; Tuck et al. 2015).

Acoustic tags were fitted to scampi, and released with a moored hydrophone which recorded tag detections, when animals were emerged from burrows. Data were recorded over a period of up to 46 days for SCI 1, and 61 days for SCI 2 (Tuck et al. 2013; Tuck et al. 2015). Tag detections showed distinct cyclical patterns (tidal and daily), and the proportion of scampi detectable over the duration of the studies varied from 22–67% (2.5^{th} to 97.5^{th} percentile of range), with a median detection of 46%. On the basis of shallow water trials with the acoustic tags, and scampi observations, it is assumed that these detections include scampi in burrow entrances and scampi walking free on the seabed (all of which would be visible to the photographic survey). The 2015 survey in SCI 1 and SCI 2 provided a second opportunity to investigate emergence rates and patterns through acoustic tagging (Tuck et al. 2016). During this study the deployment was less successful (data returned from fewer scampi), and estimated emergence rates were higher. Priors estimated from the 2012 study were taken as the base case, with a sensitivity to inclusion of the 2015 data (using a combination of both data sets, weighted by the number of animals providing data) examined.

Emergence and photographic survey data were combined to estimate catchability for major burrow opening counts, visible animal counts, and trawl catches. Using the overall proportion detectable (over the duration of the mooring deployment) as an estimate of the proportion of scampi that would be visible in photographs (emerged or door keeping) at a particular time of day, the density of visible scampi in each survey can be scaled to a population density estimate. Overall proportion detectable also provides a catchability for estimates of visible scampi. The population density estimate was used in conjunction with photographic survey estimates of scampi burrows, and emerged scampi, to provide estimates of burrow count and trawl survey catchability, respectively. Uncertainty in each component was accounted for through resampling from the original distributions (1000 iterations), and the mean and upper and lower bound (2.5th and 97.5th quantiles) of the estimated catchability distributions were fitted within a binomial GLM (probit link) to estimate the slope and intercept of the cumulative frequency distribution, which in turn were used to estimate the mean and standard deviation of the lognormal distribution of the priors for the various catchability terms used in the assessment model (Table 21).

3.7.2. Priors for *q*s

q-Photo

This is the proportion of the scampi population represented by the count of major burrow openings. The 2012 best estimate is 2.012 (major burrow openings divided by estimated scampi density). The 2012 and 2015 combined best estimate is 2.261. Upper and lower estimates are taken as the 2.5th and 97.5th percentiles of the distribution.

q-Trawl

This is the proportion of the scampi population represented by the trawl survey catches. The 2012 best estimate is 0.094 (scampi out of burrows divided by estimated scampi density). The 2012 and 2015 combined best estimate is 0.097. Upper and lower estimates are taken as the 2.5th and 97.5th percentiles of the distribution.

Ratio of *q*, part : whole survey (SCI 1)

As discussed above (Section 3.5), some surveys in SCI 1 have only covered four of the six survey strata that comprise the modelled area. These limited area surveys have been fitted as a separate index, with *q* constrained as a proportion of *q-Trawl* for the whole area survey, using the @ratio_qs_penalty command. The prior distribution for this ratio was estimated from the distribution of relative catch rates in the two areas by all scampi targeting commercial trips fishing in both areas, scaled by the relative size of the areas. The best estimate was that 80% of the biomass was within the limited survey area.

3.7.3. Estimation of prior distributions

The bounds and best estimate were assumed to represent the 2.5th, 50th and 97.5th percentiles of the prior distribution. These values were fitted within a binomial GLM (probit link) to estimate the slope and intercept of the cfd, which in turn were used to estimate the mean and standard deviation of the lognormal distribution of the prior. The distributions of the priors are presented in Figure 46. The distributions of the priors are similar to those used in the previous assessment (Tuck 2014), although the revised approach takes better account of uncertainty in the component parameters (Tuck et al. 2015).

Table 21: Best estimates of catchability terms for trawl caught scampi, visible scampi and scampi burrows, estimated from 2012 photo survey observations and scampi emergence study. Rows are numbered (1–8) to clarify calculations in "source" column.

Row		2.5th percentile	Best estimate	97.5th percentile	Source
1	Major opening	0.0680 m^{-2}	0.0772 m^{-2}	0.0858 m^{-2}	Survey
2	Visible scampi (Emerged + door keeping)	0.0145 m^{-2}	0.0174 m^{-2}	0.0207 m^{-2}	Survey
3	Emerged scampi	0.0022 m^{-2}	0.0035 m^{-2}	0.0050 m^{-2}	Survey
4	Scampi as % of openings	19.7%	22.6%	26.2%	Visible(2)/openings(1)
5	% of scampi emerged	13.5%	20.3%	27.8%	Emerged(3)/visible(2)
6	Emergence	22.2%	46.0%	66.7%	Acoustic tags
7	Estimated scampi density	0.0240 m^{-2}	0.0373 m^{-2}	0.0757 m^{-2}	Visible(2)/emergence(6)
8	Estimated occupancy	31.9%	49.3%	95.7%	Est den(7)/major(1)
9	q trawl	0.042	0.094	0.156	Emerged(3)/Est den(7)
10	q scampi	0.222	0.460	0.667	Emergence(6)
11	q photo	0.972	2.012	3.054	Major(1)/Est den(7)

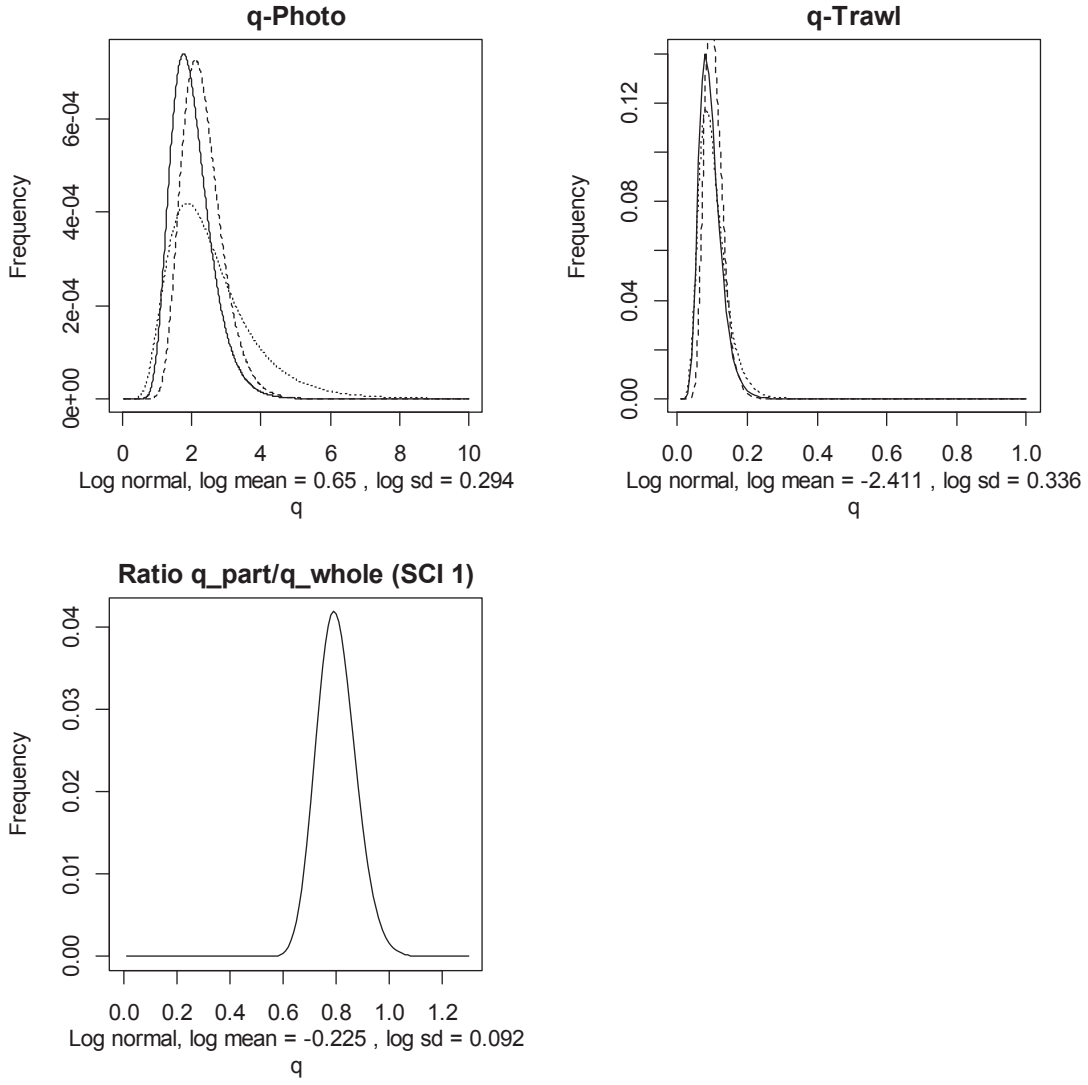

Figure 46: Estimated distribution of *q-Photo*, *q-Trawl*, and the ratio of q_part/q_whole for SCI 1. Dashed lines represent the prior distributions used in the previous assessment, based on a slightly different estimation approach (Tuck 2014). Dotted line represents the prior based on combined 2012 and 2015 data, used for sensitivity.

3.7.4. Recruitment

Few data are available on scampi recruitment. Relative year class strengths were assumed to average 1.0 up to the last two years, and are fixed at 1 for these. In the initial model development (Cryer et al. 2005) lognormal priors on relative year class strengths were assumed, with mean 1.0 and CV 0.2, and the sensitivity of year class strength (YCS) variation was examined in further developments (Tuck & Dunn 2006). More recent model investigations, particularly those fitting the CPUE indices, suggest that the constraint on variability in YCS may be too severe, and the SFAWG suggested increasing the CV (Tuck & Dunn 2012). In the current implementation, lognormal priors on relative year class strengths were assumed, with mean 1.0 and CV 1.0. The relationship between stock size and recruitment for scampi is unknown, and a Beverton Holt relationship with a steepness of 0.8 has been assumed. New Zealand scampi have very low fecundity (Wear 1976; Fenaughty 1989) (in the order of tens to hundreds of eggs carried by each female), so very successful recruitment is probably not plausible at low abundance. Recruitment enters the model partition as a year class, with a normally distributed OCL of mean 10 mm and CV 0.4.

4. SCI 1 - ASSESSMENT MODEL RESULTS

4.1. Initial models

As described in Section 3.1, a single area model was applied, with an annual CPUE index, and the photo and trawl survey data both fitted as two separate indices, both in time step 1, but with different areas covered. Attempts to estimate natural mortality within the model were not considered reliable, and therefore M was fixed, with sensitivity runs examined. Sensitivity runs were also examined to the catchability priors (Section 3.7.1), and the CPUE CV. On the basis of previous scampi assessments, initial values for process error were fixed at 0.2 for trawl surveys, and 0.15 for photographic surveys, but these were also estimated in some sensitivity runs. Some of the selectivity parameters were estimated at values considered to be unrealistic, and so were fixed. Details of differences between models examined within sensitivity analyses are presented in Table 22. Key parameter and quantity estimates from the MPD fits for the models described in Table 23, and stock and recruitment trajectories for the models are presented in Figure 47 to Figure 49.

Table 22: General details of models examined within sensitivity analyses for SCI 1.

Model	M	CPUE CV	Process error
M25	0.25	0.15	Fixed
M30	0.3	0.15	Fixed
M35	0.35	0.15	Fixed
CV10	0.3	0.10	Fixed
CV15	0.3	0.15	Fixed
CV20	0.3	0.20	Fixed
CV30	0.3	0.30	Fixed
PE1	0.3	0.15	Estimated for surveys
PE2	0.3	0.10	Estimated for CPUE and surveys

Table 23: Estimated key parameters and quantities from MPD fits for SCI 1 sensitivity model runs. Italicised values indicate parameters that were fixed rather than estimated.

	M25	M30	M35	CV10	CV15	CV20	CV30	PE1	PE2
SSB_0	5384	5313	5466	5173	5313	5639	5894	5422	5658
SSB_{2015}	3857	3901	4070	3747	3901	4257	4543	4046	4187
SSB_{2015}/SSB_0	0.72	0.73	0.74	0.72	0.73	0.75	0.77	0.75	0.74
q-Photo	2.3917	2.4397	2.3116	2.6862	2.4397	2.2465	2.0938	2.4905	2.2713
q-Trawl	0.0530	0.0533	0.0549	0.0555	0.0533	0.0529	0.0514	0.0523	0.0542
Growth									
Male g20	11.29	14.02	14.79	13.68	14.02	11.95	11.73	13.66	11.60
Male g40	2.39	2.77	2.97	2.79	2.77	2.55	2.43	2.75	2.58
Female g20	10.73	13.06	13.57	12.55	13.06	11.25	11.27	12.71	10.80
Female g40	0.00	0.00	0.00	0.00	0.00	0.00	0.00	0.00	0.00
min_sigma	4.04	4.56	4.70	4.60	4.56	4.19	4.08	4.53	4.22
Selectivity									
step1 L50	38.07	37.86	39.73	37.15	37.86	39.63	41.79	37.73	39.17
step1 a95	10.68	11.96	13.63	10.08	11.96	12.15	15.00	11.43	11.22
step1 amax	0.89	0.90	0.87	0.90	0.90	0.85	0.83	0.90	0.85
step2 L50	*38.00*	*38.00*	*38.00*	*37.00*	*38.00*	*41.00*	*41.00*	*37.00*	*37.00*
step2 a95	12.21	12.83	12.00	12.56	12.83	12.74	12.38	12.03	10.68
step2 amax	0.58	0.58	0.58	0.59	0.58	0.54	0.55	0.59	0.59
trawl L50	34.63	34.74	36.22	35.36	34.74	36.69	36.38	35.60	36.99
trawl a95	12.32	13.59	14.43	12.68	13.59	12.95	13.11	13.59	12.41
trawl amax	1.04	1.04	1.02	1.01	1.04	1.01	1.04	1.03	0.99
photo L50	*35.00*	*35.00*	*35.00*	*35.00*	*35.00*	*35.00*	*35.00*	*35.00*	*35.00*
photo a95	*25.00*	*25.00*	*25.00*	*25.00*	*25.00*	*25.00*	*25.00*	*25.00*	*25.00*

There was little difference between any of the models in terms of fits to observed data. The different levels of natural mortality examined altered the magnitude of the estimated abundance increase and decline in the mid 1990s, but all models suggested that biomass increased to the mid 1990s, declined to about 2000, and remained relatively stable since then (Figure 47). Slight differences in the YCS patterns between models relate to differences in estimated growth. Models were sensitive to the CV on the CPUE index, with lower CV constraining the stock trajectory to better match the index, but estimating lower SSB_0 and SSB_{2015}, although current stock status (SSB_{2015}/SSB_0) was less sensitive (Figure 48, Table 23). Estimation of process error for surveys within the model had minimal effect on model outputs (compared to the fixed value model), while estimation of process error for the CPUE index increased SSB_0 and SSB_{2015}, but had no effect on stock trajectory (relative to SSB_0) (Figure 49). Across all the models examined, estimates of SSB_0 varied from 5100 to 5900 tonnes, and although stock trajectories varied between models over the history of the fishery, the models were very consistent in estimates of SSB_{2015}/SSB_0 (between 72 and 77% SSB_0) (Table 23).

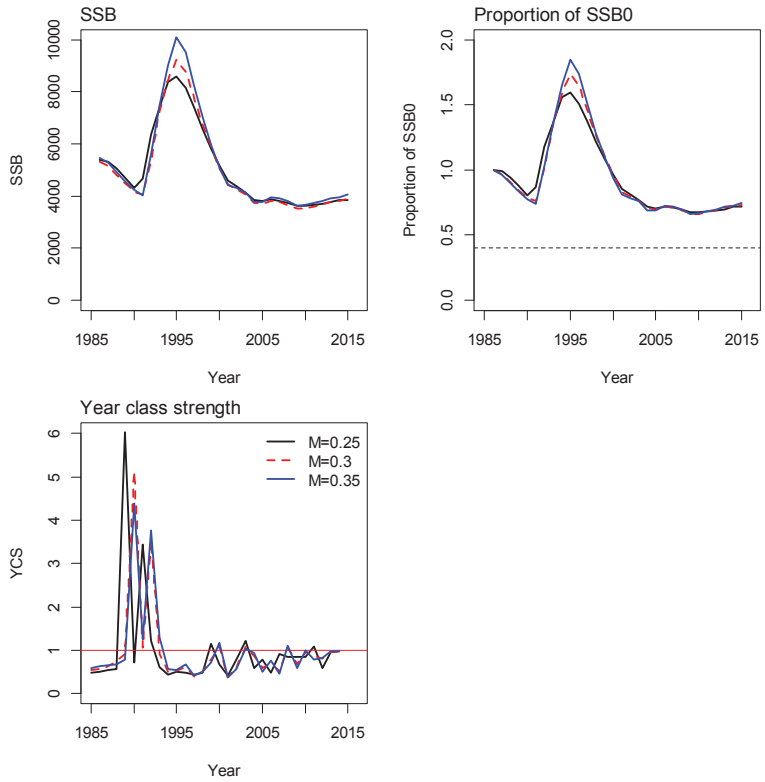

Figure 47: Plots of absolute SSB, SSB as a proportion of SSB_0, and year class strength (YCS) for MPD fits to the SCI 1 sensitivity runs to natural mortality.

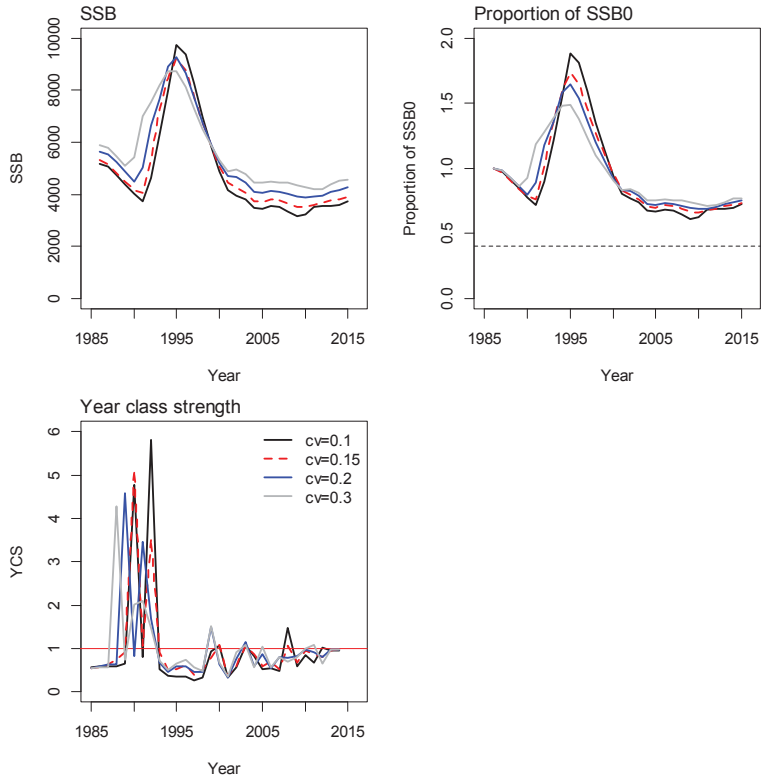

Figure 48: Plots of absolute SSB, SSB as a proportion of SSB_0, and year class strength (YCS) for MPD fits to the SCI 1 sensitivity runs to the assumed CV on the CPUE index.

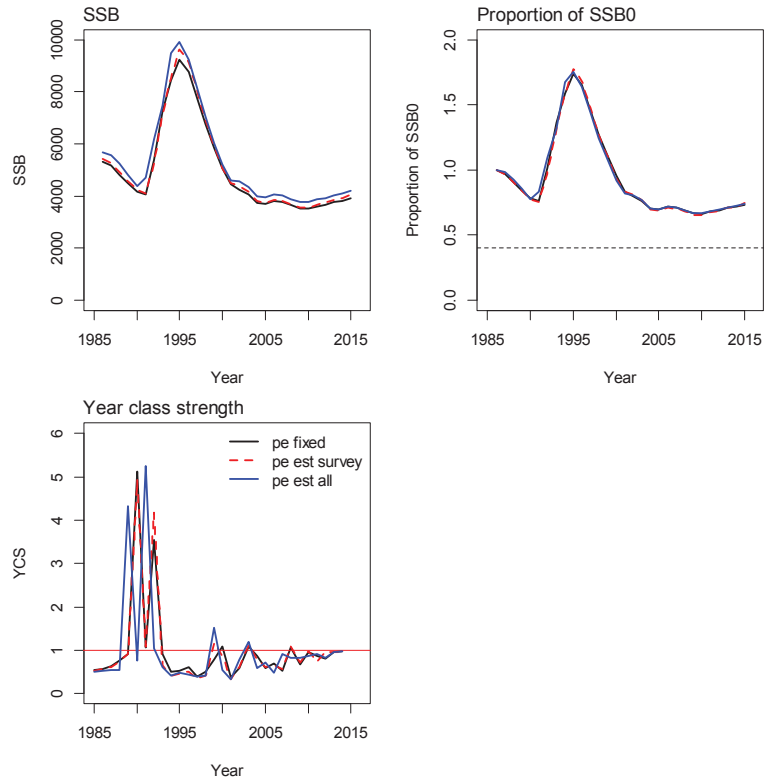

Figure 49: Plots of absolute SSB, SSB as a proportion of SSB_0, and year class strength (YCS) for MPD fits to the SCI 1 sensitivity runs to estimation of process error.

4.2. Base models

On the basis of presentation of the sensitivity runs to the SFAWG, base models with M fixed at 0.25, 0.3 and 0.35 were examined further, with process error for CPUE and abundance indices estimated within the model. Various model output plots and diagnostics are presented as an Appendix for each model.

4.2.1. SCI 1 Base25 (Appendix 5)

The Base25 model (M = 0.25) estimated a SSB_0 of 5687 t, with SSB_{2015} 4352 t, 77% of SSB_0. Fits to the abundance indices and normalised residuals (A5. 1), show that the model did not match the observed increase and decline in CPUE in the mid 1990s, but fits to the trawl and photographic surveys (particularly over more recent years) were better. SSB is estimated to have declined slightly to the late 1980s, increased rapidly to 1995, declined through the later 1990s until about 2003, and then remained relatively stable (A5. 2). Strong year class strengths were estimated in 1988 and 1990–91 (to a lesser extent), with a period of below average recruitment in the mid to late 1990s, followed by a period with recruitment fluctuating generally at or below the long term average. Estimated selectivity curves matched observed changes in sex ratio between time steps, with males less available to trawling during time step 2 (A5. 3). L_{50} for the commercial selectivity in time step 2, and both parameters for the photo selectivity were fixed because estimated values were considered unrealistic. MPD estimates of trawl and photo survey catchability were within the prior distributions (A5. 4). Fits to the observer length frequencies were variable, and the data weighting process down-weighted the length data (particularly the observer data), on the basis of fits to the mean length (A5. 5).

The overall likelihood profile when B_0 is fixed was relatively U shaped (A5. 6), but the majority of the signal appears to come from the priors rather than the data. The CPUE abundance index suggested a smaller SSB_0, the surveys and proportions at length provide little signal, and catchability priors provided

conflicting signals for the photo and trawl surveys. The other data sets provided little information on SSB_0.

MCMC runs

Three independent MCMC chains were started a random step away from the MPD for each model, and run for 2 million simulations, with every one thousandth sample saved, giving a set of 2000 samples. The three chains were examined for evidence of lack of convergence (A5. 7 – A5. 10), and concatenated and systematically thinned to produce a 2000 sample chain for projections. Posterior distributions of trawl and photo survey catchability were within the prior distribution (A5. 11), with the MPD estimates also located within the posterior distributions. The posterior trajectory of SSB (Figure 50) suggests a decline from about 1994 to about 2004, with the stock remaining stable after this. The median estimate of current status (SSB_{2015}/SSB_0) is 72% (95% confidence interval 59%–86%), with 0% probability that SSB_{2015} is below 40% SSB_0.

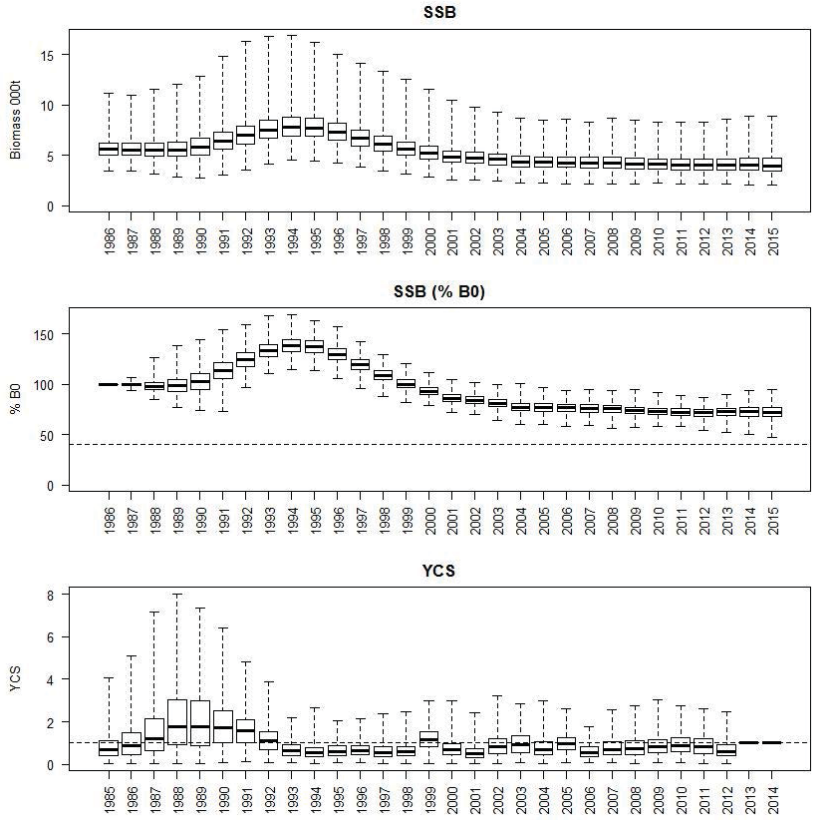

Figure 50: Posterior trajectories of SSB, SSB_{2015}/B_0 and YCS from the MCMC run for the SCI 1 Base25 model.

4.2.2. SCI 1 Base30 (Appendix 6)

The Base30 model (M = 0.3) estimated a SSB_0 at 5660 t, with SSB_{2015} 4207 t, 74% of SSB_0. Fits to the abundance indices and normalised residuals (A6. 1), show that the model fitted the observed increase and decline in CPUE in the mid 1990s better than the Base25 model, and fits to the trawl and photographic surveys (particularly over recent years) were reasonable. SSB is estimated to have increased from 1990 to 1995, declined through the later 1990s until about 2004, and then remained relatively stable (A6. 2). Strong year class strengths were estimated for 1989 and 1991, with a period of below average recruitment around the mid 1990s, followed by a period with recruitment fluctuating around the long term average, and then remaining stable but just below the average since the late 2000s (A6. 3). Estimated selectivity curves were similar to those for the Base25 model, in that they matched

observed changes in sex ratio between time steps, but also that some estimates had to be fixed as estimated values were considered unrealistic. MPD estimates of trawl and photo survey catchability were within the prior distribution (A6. 4). Fits to the observer length frequencies were variable, and the data weighting process down-weighted the length data (particularly the observer data), on the basis of fits to the mean length (A6. 5).

The overall likelihood profile when B_0 is fixed was relatively U shaped (A6. 6), but as with the Base25 model the majority of the signal appears to come from the priors rather than the data. The CPUE abundance index has a strong preference for a smaller SSB_0, the surveys and proportions at length provide little signal, while catchability priors provided conflicting signals for the photo and trawl surveys. The other data sets provided little information on SSB_0.

MCMC runs

Three independent MCMC chains were started a random step away from the MPD for each model, and run for 2 million simulations, with every one thousandth sample saved, giving a set of 2000 samples. The three chains were examined for evidence of lack of convergence (A6. 7 – A6. 10), and concatenated and systematically thinned to produce a 2000 sample chain for projections. Posterior distributions of trawl and photo survey catchability were within the prior distribution (A6. 11), with the MPD estimates also located within the posterior distributions. The posterior trajectory of SSB (Figure 51) suggests a decline from about 1995 to about 2004, with the stock remaining stable after this. The median estimate of current status (SSB_{2015}/SSB_0) is 75% (95% confidence interval 62%–88%), with 0% probability that SSB_{2015} is below 40% SSB_0.

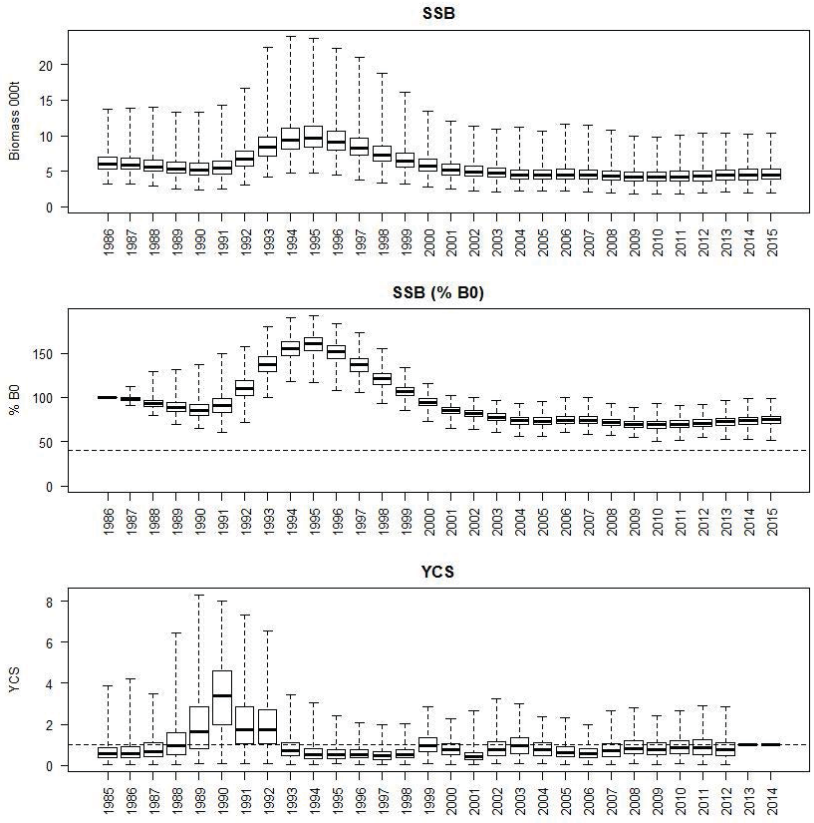

Figure 51: Posterior trajectories of SSB, SSB_{2015}/B_0 and YCS from the MCMC run for the SCI 1 Base30 model.

4.2.3. SCI 1 Base35 (Appendix 7)

The Base30 model (M = 0.3) estimated a SSB_0 at 5553 t, with SSB_{2015} 4128 t, 74% of SSB_0. Fits to the abundance indices and normalised residuals (A7. 1), show that the model fitted the observed increase and decline in CPUE in the mid 1990s better than either of the previous two models, and fits to the trawl and photographic surveys (particularly over recent years) were reasonable. SSB is estimated to have increased from 1990 to 1995, declined through the later 1990s until about 2004, and then remained relatively stable (A7. 2). Strong year class strengths were estimated in 1989 and 1991, with a period of below average recruitment around the mid 1990s, followed by a period with recruitment fluctuating around the long term average (A7. 3). Estimated selectivity curves were similar to those for the other models, in that they matched observed changes in sex ratio between time steps, but also that some estimates had to be fixed as estimated values were considered unrealistic. MPD estimates of trawl and photo survey catchability were within the prior distribution (A7. 4). As with the other models, fits to the observer length frequencies were variable, and the data weighting process down-weighted the length data (particularly the observer data), on the basis of fits to the mean length (A7. 5).

The overall likelihood profile when B_0 is fixed was relatively U shaped (A7. 6), but as with the other models the majority of the signal appears to come from the priors rather than the data. The CPUE abundance index has a strong preference for a smaller SSB_0, the surveys and proportions at length provide little signal, while catchability priors provided conflicting signals for the photo and trawl surveys. The other data sets provided little information on SSB_0.

MCMC runs

Three independent MCMC chains were started a random step away from the MPD for each model, and run for 2 million simulations, with every one thousandth sample saved, giving a set of 2000 samples. The three chains were examined for evidence of lack of convergence (A7. 7 – A7. 10), and concatenated and systematically thinned to produce a 2000 sample chain for projections. Posterior distributions of trawl and photo survey catchability were within the prior distribution (A7. 11), with the MPD estimates also located within the posterior distributions. The posterior trajectory of SSB (Figure 52) suggests a decline from about 1995 to about 2001, with the stock remaining stable after this. The median estimate of current status (SSB_{2015}/SSB_0) is 75% (95% confidence interval 63%–86%), with 0% probability that SSB_{2015} is below 40% SSB_0.

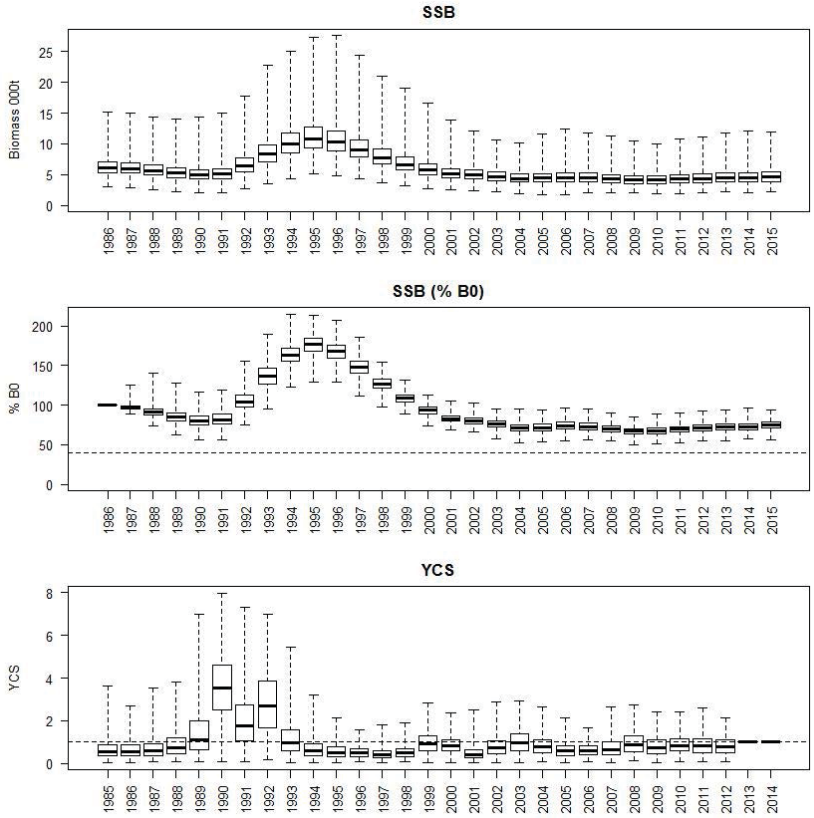

Figure 52: Posterior trajectories of SSB, SSB_{2015}/B_0 and YCS from the MCMC run for the SCI 1 Base35 model.

4.3. Comparison with previous assessment

During the last assessment (Tuck 2014), a range of final models were presented for SCI 1, examining sensitivities to assumptions about natural mortality, and a variety of data weighting approaches were explored, to reduce the standard error of normalised residuals for the abundance indices. Updating the current model included recalculation of the existing data for older years (the CPUE index, and the photographic survey revised on the basis of new reader calibration (Tuck et al. 2016)), the extension of the time series for CPUE, trawl survey, photographic survey, and length frequency data, and updating the catchability priors.

To investigate the effects of the new data and assumptions and data weighting options, a number of models were compared (Table 24), initially removing recent CPUE, survey and length frequency data from the current assessment model (2016-12), then applying the previous version of the catchability priors to the 2016 version of the model (2016_p13), and applying the revised data weighting approach (estimating process error for all indices) to the 2013 assessment (2013_w16). These were compared with the base3 model from Tuck (2014) and the Base30 model from the current study.

Table 24: General details of models examined to compare with previous assessment.

Model	Data	Model years	Process error
2013	Base3 model from Tuck (2014) (M=0.3)	1996–2012	
2016	Base30 model from this report	1996–2015	Estimated
2016_12	Base30 model truncated to 2012 data	1996–2012	Estimated
2016_p13	Base30 model using priors from 2013	1996–2015	Estimated
2013_w16	2013 model with process error estimated	1996–2012	Estimated

Plots of SSB, %SSB0 and YCS are presented for the models described in Table 24 in Figure 53. The inclusion of data from the most recent years and revision/updating of existing indices had minimal effect on model outputs (2016 compared to 2016_12). The revised priors developed on the basis of Tuck et al. (2015) (see Section 3.7.1 and Figure 46) have greater uncertainty (and lower minimum bounds) than the previously applied priors, and resulted in lower estimates of *q-Trawl* and *q-Photo*, and therefore higher biomass estimates, but no change in the stock trajectory (relative to SSB_0) (2016 compared to 2016_p13). The revised weighting approach adopted in the current assessment leads to a slight shift in the biomass trajectory and YCS pattern, but has minimal effect on current stock status (2013 compared to 2013_w16).

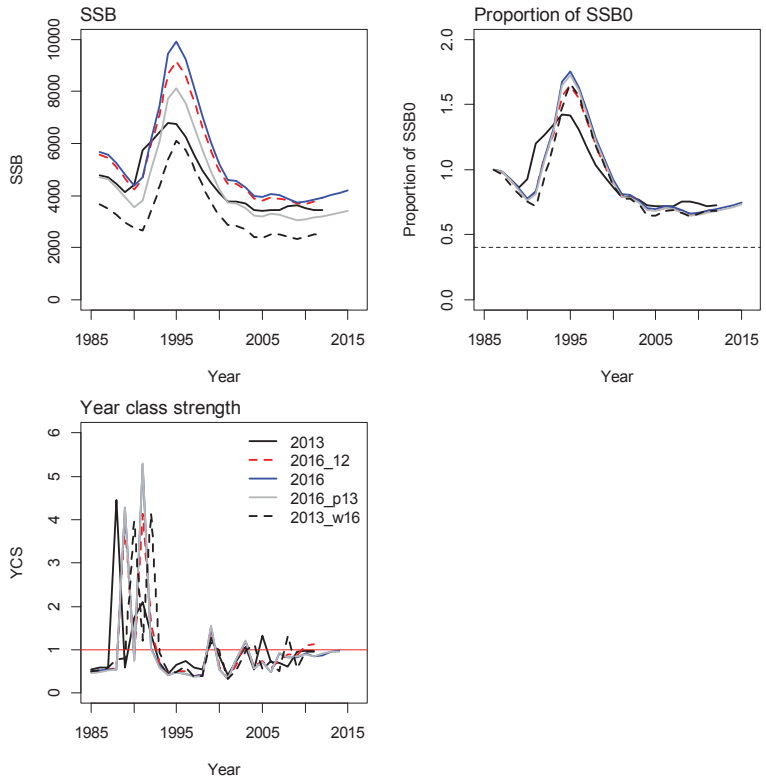

Figure 53: Plots of SSB, SSB as a proportion of SSB_0, and year class strength (YCS) for MPD fits for the SCI 1 base model from the previous assessment, and equivalent models updated with new data or data weighting. See Table 24 for model definitions.

4.4. SCI 1 Fishing Pressure

Annual fishing intensity (equivalent annual F) and the level of fishing that, if applied forever, would result in an equilibrium biomass of 40% SSB_0 (F 40% B_0) were calculated using methods described by Cordue (2012). Plots of annual fishing intensity against proportion SSB_0 (presented for the Base30 model in Figure 54) show that although SSB has declined with the development of the fishery, it remains well above the 40% SSB_0 target, and annual fishing intensity remains well below F 40% B_0. Annual catches of 100–120 tonnes throughout much of the history of the fishery are low relative to the current estimated biomass of around 4000 tonnes, and so estimates of F are low.

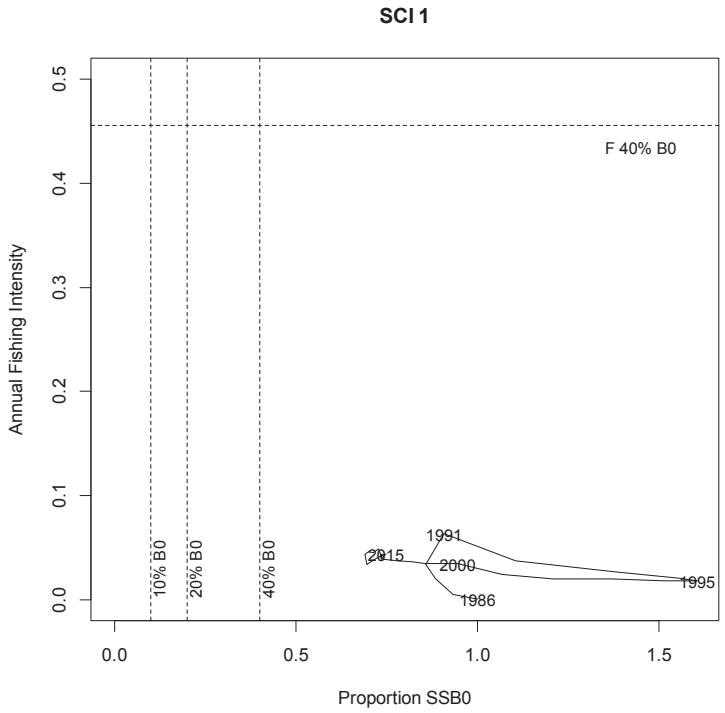

Figure 54: Trajectory of annual fishing intensity (equivalent annual F) plotted against proportion SSB_0 for the SCI 1 Base30 model, in relation to Harvest Strategy Standard target and limit reference points.

4.5. SCI 1 Projections

The assessments reported SSB_0 and $SSB_{current}$ and used the ratio of current and projected SSB to SSB_0 as preferred indicators. Projections were conducted up to 2021 on the basis of a range of catch scenarios (recent average, current TACC of 120 t, and 10% and 30% increases in TACC) (Table 25). Projections have been conducted randomly resampling year class strengths from the last decade of YCS estimated within the model (2003–2012). The probability of exceeding the default Harvest Strategy Standard target and limit reference points are reported (Table 26).

For each of the models presented (M=0.25, M=0.3 and M=0.35), future catches between 116 and 156 tonnes are predicted to reduce the SSB relative to SSB_{2015}, but remain above 40% SSB_0 (the most pessimistic prediction giving a 98% probability of SSB exceeding 40% SSB_0 by 2021).

Table 25: Results from MCMC runs showing B_0, B_{curr} B_{2019} and B_{2021} estimates at varying catch levels for SCI 1.

	Model	M=0.25	M=0.3	M=0.35
	B_0	5571	6009	6148
	B_{curr}	3967	4467	4519
	B_{curr}/B_0	0.72	0.74	0.74
116 tonnes (5 year average)	B_{2019}/B_0	0.71	0.73	0.72
	B_{2019}/B_{curr}	0.98	0.99	0.99
	B_{2021}/B_0	0.70	0.72	0.72
	B_{2021}/B_{curr}	0.98	0.97	0.98
120 tonnes (TACC)	B_{2019}/B_0	0.70	0.73	0.72
	B_{2019}/B_{curr}	0.98	0.98	0.98
	B_{2021}/B_0	0.70	0.72	0.72
	B_{2021}/B_{curr}	0.98	0.97	0.98
132 tonnes (10% increase)	B_{2019}/B_0	0.70	0.72	0.72
	B_{2019}/B_{curr}	0.97	0.98	0.98
	B_{2021}/B_0	0.69	0.71	0.72
	B_{2021}/B_{curr}	0.97	0.96	0.97
156 tonnes (30% increase)	B_{2019}/B_0	0.69	0.71	0.71
	B_{2019}/B_{curr}	0.95	0.96	0.96
	B_{2021}/B_0	0.68	0.70	0.70
	B_{2021}/B_{curr}	0.95	0.94	0.96

Table 26: Results from MCMC runs for SCI 1, showing probabilities of projected spawning stock biomass exceeding the default Harvest Strategy Standard target and limit reference points.

	116 tonnes	120 tonnes (TACC)	132 tonnes (+10%)	156 tonnes (+30%)
M=0.25				
2019				
P(SSB<10% B0)	0.00	0.00	0.00	0.00
P(SSB<20% B0)	0.00	0.00	0.00	0.00
P(SSB>40% B0)	1.00	1.00	1.00	0.99
$P(SSB_{2019} > SSB_{2015})$	0.45	0.44	0.41	0.36
2021				
P(SSB<10% B0)	0.00	0.00	0.00	0.00
P(SSB<20% B0)	0.00	0.00	0.00	0.00
P(SSB>40% B0)	0.99	0.99	0.99	0.98
$P(SSB_{2021} > SSB_{2015})$	0.45	0.44	0.41	0.35
M=0.3				
2019				
P(SSB<10% B0)	0.00	0.00	0.00	0.00
P(SSB<20% B0)	0.00	0.00	0.00	0.00
P(SSB>40% B0)	1.00	1.00	1.00	1.00
$P(SSB_{2019} > SSB_{2015})$	0.46	0.45	0.43	0.40
2021				
P(SSB<10% B0)	0.00	0.00	0.00	0.00
P(SSB<20% B0)	0.00	0.00	0.00	0.00
P(SSB>40% B0)	1.00	0.99	0.99	0.99
$P(SSB_{2021} > SSB_{2015})$	0.43	0.42	0.40	0.36
M=0.35				
2019				
P(SSB<10% B0)	0.00	0.00	0.00	0.00
P(SSB<20% B0)	0.00	0.00	0.00	0.00
P(SSB>40% B0)	1.00	1.00	1.00	0.99
$P(SSB_{2019} > SSB_{2015})$	0.47	0.46	0.45	0.41
2021				
P(SSB<10% B0)	0.00	0.00	0.00	0.00
P(SSB<20% B0)	0.00	0.00	0.00	0.00
P(SSB>40% B0)	0.99	0.99	0.99	0.98
$P(SSB_{2021} > SSB_{2015})$	0.46	0.46	0.44	0.41

4.6. Sensitivity to survey data

Likelihood profiles suggest that the priors may be having undue influence in the estimation of biomass. Following presentation of the SCI 1 models to the MPI Plenary, further investigations were undertaken for the M=0.3 model excluding either the trawl or photographic survey series. As with the previous models, process error was estimated within the model, and length frequency data were reweighted iteratively using method TA1.8 (Francis 2011).

MCMC chains were run for these models in the same way as those described above, and posterior distributions of the stock trajectory and YCS are presented in Figure 55. While the two models provide very similar trajectories of stock status and YCS, the overall level of stock biomass was clearly sensitive to inclusion of the survey data, with exclusion of the photo survey resulting in a lower estimate of biomass.

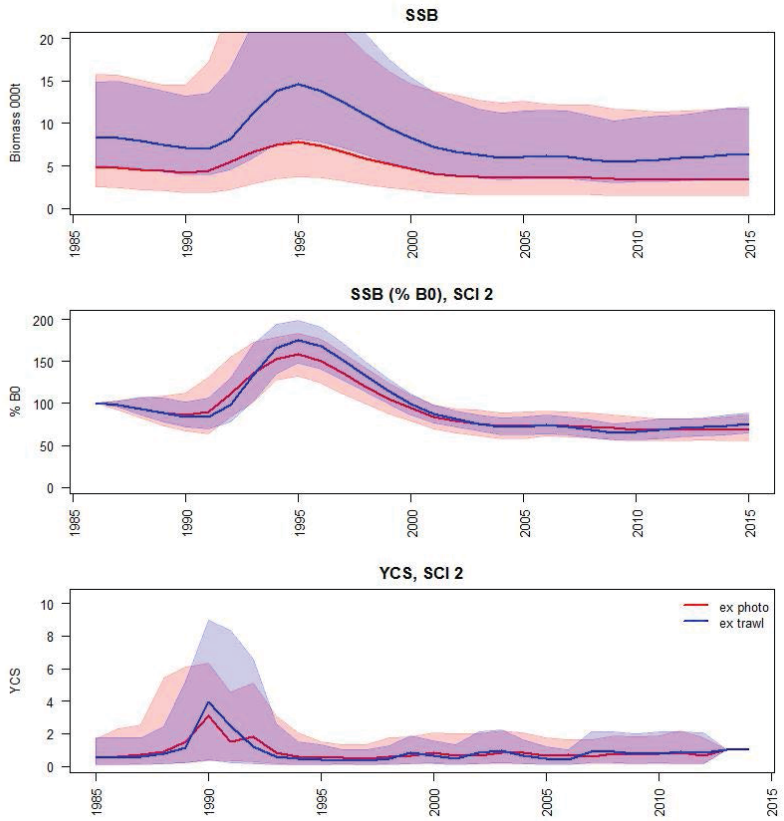

Figure 55: Posterior trajectories of SSB, SSB_{2015}/B_0 and YCS from the MCMC run for the SCI 1 models (M=0.3) excluding either the photo survey or trawl survey series. Shaded areas represent 95% confidence intervals.

5. SCI 2 - ASSESSMENT MODEL RESULTS

5.1. Initial models

A single area model was applied, with an annual CPUE index, and the trawl survey data fitted as two separate indices in different time steps. As with SCI 1, attempts to estimate natural mortality within the model were not considered reliable, and sensitivity to M was examined. As with the SCI 1 model, additional sensitivity runs were also examined in relation to the catchability priors, CPUE CV and process error. Details of differences between models examined within sensitivity analysis are presented in Table 27. Key parameter and quantity estimates from the MPD fits for the models described in Table 28, and stock and recruitment trajectories for the models are presented in Figure 56 to Figure 58.

Table 27: General details of models examined within sensitivity analyses for SCI 2.

Model	M	CPUE CV	Process error
M25	0.25	0.15	Fixed
M30	0.3	0.15	Fixed
M35	0.35	0.15	Fixed
CV10	0.3	0.10	Fixed
CV15	0.3	0.15	Fixed
CV20	0.3	0.20	Fixed
CV30	0.3	0.30	Fixed
PE1	0.3	0.15	Estimated for surveys
PE2	0.3	0.10	Estimated for CPUE and surveys

Table 28: Estimated key parameters and quantities from MPD fits for SCI 2 sensitivity model runs. Italicised values were fixed rather than estimated.

	M25	M30	M35	CV08	CV11	CV15	CV30	PE1	PE2
SSB_0	3117	2960	2915	2899	2960	2575	2843	2846	2775
SSB_{2015}	3409	3501	3680	3199	3501	2496	2591	2967	2829
SSB_{2015}/SSB_0	1.09	1.18	1.26	1.10	1.18	0.97	0.91	1.04	1.02
q-Photo	4.1578	3.9660	3.6815	3.7513	3.9660	4.0839	3.7555	3.7155	3.7932
q-Trawl	0.0702	0.0781	0.0836	0.0850	0.0781	0.0731	0.0531	0.0784	0.0763
Growth									
Male g20	12.53	12.16	11.77	11.58	12.16	12.47	10.80	11.78	12.00
Male g40	2.35	2.44	2.50	2.48	2.44	2.83	2.94	2.50	2.53
Female g20	12.14	11.91	11.69	11.86	11.91	12.86	10.73	12.20	12.45
Female g40	0.00	0.00	0.00	0.00	0.00	0.32	1.05	0.00	0.00
min_sigma	4.49	4.60	4.67	4.54	4.60	4.48	3.73	4.54	4.57
Selectivity									
step1 L50	39.92	42.70	44.95	42.03	42.70	43.78	42.94	43.96	44.30
step1 a95	12.40	13.47	13.90	11.98	13.47	14.67	14.21	13.83	14.38
step1 amax	0.88	0.85	0.83	0.89	0.85	0.86	0.83	0.87	0.87
step2 L50	43.51	45.82	47.30	46.04	45.82	45.30	42.79	46.33	46.82
step2 a95	19.01	18.24	17.27	18.29	18.24	19.02	15.06	18.74	19.36
step2 amax	0.50	0.50	0.49	0.51	0.50	0.50	0.50	0.51	0.50
trawl1 L50	36.27	38.88	40.73	40.35	38.88	35.45	30.89	39.09	38.17
trawl1 a95	15.83	16.08	15.73	15.18	16.08	16.09	9.08	16.62	16.93
trawl1 amax	1.05	1.04	1.03	1.06	1.04	1.10	1.13	1.08	1.09
trawl2 L50	40.74	41.92	42.99	42.08	41.92	39.85	39.43	41.95	41.60
trawl2 a95	19.79	18.64	17.73	16.96	18.64	16.13	14.17	17.08	17.16
trawl2 amax	0.84	0.85	0.85	0.89	0.85	0.92	0.88	0.90	0.91
photo L50	*35.00*	*35.00*	*35.00*	*35.00*	*35.00*	*35.00*	*35.00*	*35.00*	*35.00*
photo a95	*25.00*	*25.00*	*25.00*	*25.00*	*25.00*	*25.00*	*25.00*	*25.00*	*25.00*

As with the SCI 1 models, there was little difference between any of the models in terms of fits to observed data. The different levels of natural mortality examined altered the magnitudes of the estimated abundance increase and decline in the mid 1990s, and the increase since the late 2000s. Higher M resulted in lower estimates of SSB_0 and higher estimates of SSB_{2015}, and a higher SSB_{2015}/SSB_0 (Figure 56). The pattern of estimated YCS was not sensitive to M. Models were sensitive to the CV on the CPUE index, and while the overall stock trajectories were quite similar (except with the largest CV), estimated current stock status (SSB_{2015}/SSB_0) was lower with increasing CV (Figure 57, Table 28). Estimation of process error for surveys within the model reduced the estimate of current stock status (compared to the fixed process error model), while the estimation of process error for the CPUE index had minimal additional effect (Figure 58). Across all the models examined, estimates of SSB_0 varied

from 2500 to 3500 tonnes, and while stock trajectories were reasonably similar through much of the history of the fishery, the estimates of SSB_{2012}/SSB_0 ranged from 91% to 126% SSB_0) (Table 28).

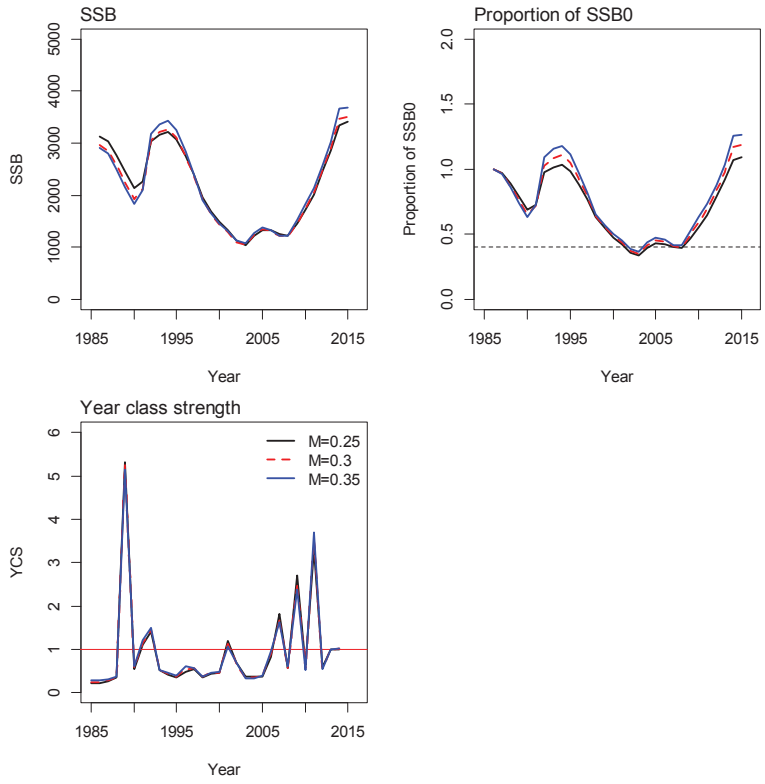

Figure 56: Plots of SSB, SSB as a proportion of SSB_0, and year class strength (YCS) for MPD fits to the SCI 2 sensitivity runs to natural mortality.

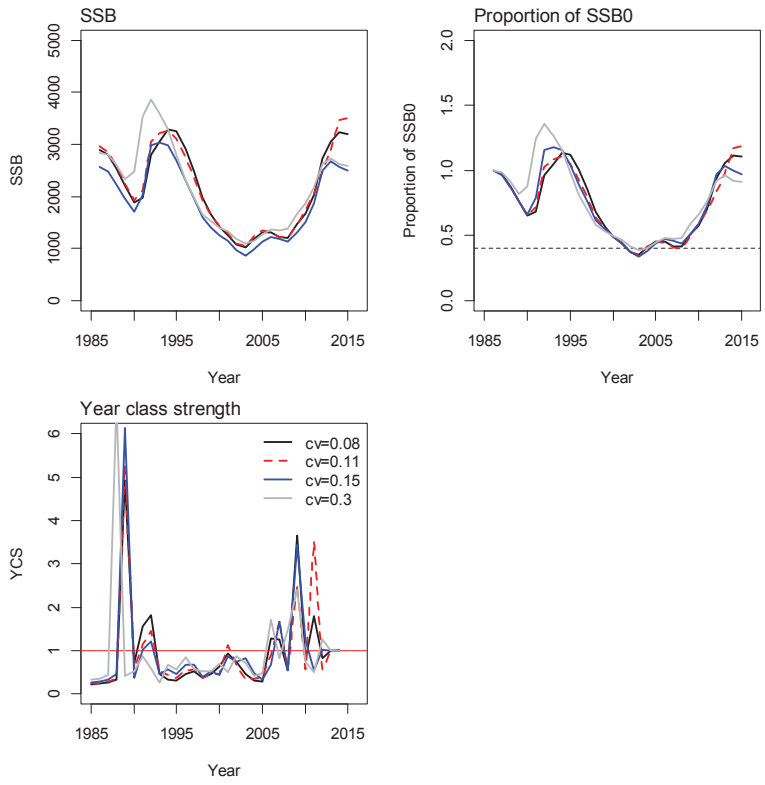

Figure 57: Plots of SSB, SSB as a proportion of SSB_0, and year class strength (YCS) for MPD fits to the SCI 2 sensitivity runs to the assumed CV on the CPUE index.

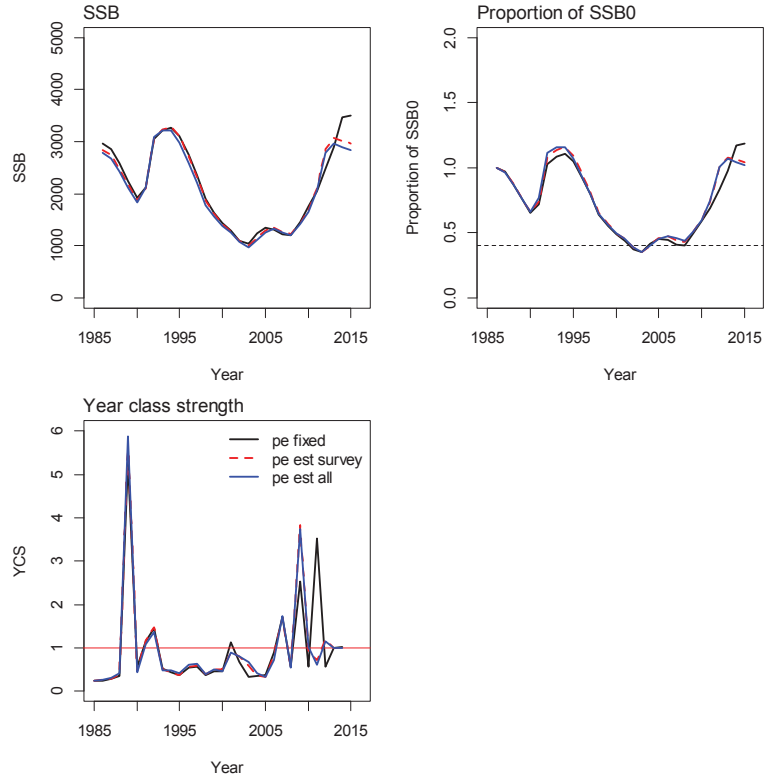

Figure 58: Plots of SSB, SSB as a proportion of SSB_0, and year class strength (YCS) for MPD fits to the SCI 2 sensitivity runs to estimation of process error.

5.2. Base models

On the basis of presentation of the sensitivity runs to the SFAWG, base models with M fixed at 0.25, 0.3 and 0.35 were examined further, with process error for CPUE and abundance indices estimated within the model. Various model output plots and diagnostics are presented as an Appendix for each model.

5.2.1. SCI 2 Base25 (Appendix 8)

The Base25 model (M = 0.25) estimated a SSB_0 of 2546 t, with SSB_{2015} 2200 t, 86% of SSB_0. Fits to the abundance indices and normalised residuals (A8. 1), show that the model did not match the observed increase and decline in CPUE in the mid 1990s, or the increase in the most recent years, but fits to the trawl and photographic surveys were better, although the model was unable to match the recent increase in biomass observed in the trawl survey. SSB is estimated to have increased in the early 1990s, peaking around 1992, and then declined steadily until about 2003. Subsequently, SSB recovered slightly by 2009, and then increased rapidly to peak in 2013, but has declined slightly since then (A8. 2). Particularly strong year class strengths were estimated in 1989 and (to a lesser extent) in 2007 and 2009, with a period of below average recruitment in the intervening period. Estimated selectivity curves matched observed changes in sex ratio between time steps, with males less available to trawling during time step 2 (A8. 3). Unlike the SCI 1 models, L_{50} for the commercial selectivity in time step 2 was estimated, but again, both parameters for the photo selectivity were fixed because estimated values were considered unrealistic. MPD estimates of trawl and photo survey catchability were within the prior distributions (A8. 4), although the estimate for photo catchability was towards the upper limit of the prior distribution. Fits to the observer length frequencies were variable, and the data weighting process down-weighted the length data (particularly the observer data), on the basis of fits to the mean length (A8. 5).

The overall likelihood profile when B_0 is fixed was U shaped (A8. 6), with the majority of the signal appearing to come from the abundance indices, which were in reasonable agreement. There was less signal in the proportion at length data, although in general those data seemed to prefer a lower SSB_0. Catchability priors provided conflicting signals for the photo and trawl surveys.

MCMC runs

Three independent MCMC chains were started a random step away from the MPD for each model, and run for 2 million simulations, with every one thousandth sample saved, giving a set of 2000 samples. The three chains were examined for evidence of lack of convergence (A8. 7 – A8. 10), and concatenated and systematically thinned to produce a 2000 sample chain for projections. Posterior distributions of trawl survey catchability were well within the prior distribution (A8. 11), with the MPD estimates also located within the posterior distributions, but the posterior distribution for the photo survey catchability was towards the upper range of the prior. The posterior trajectory of SSB (Figure 59) suggests a decline from about 1994 to about 2003, with the stock increasing slightly to 2005, remaining stable to 2008, and then increasing to a peak in 2013, declining slightly in more recent years. The median estimate of current status (SSB_{2015}/SSB_0) is 89% (95% confidence interval 74%–103%), with 0% probability that SSB_{2015} is below 40% SSB_0.

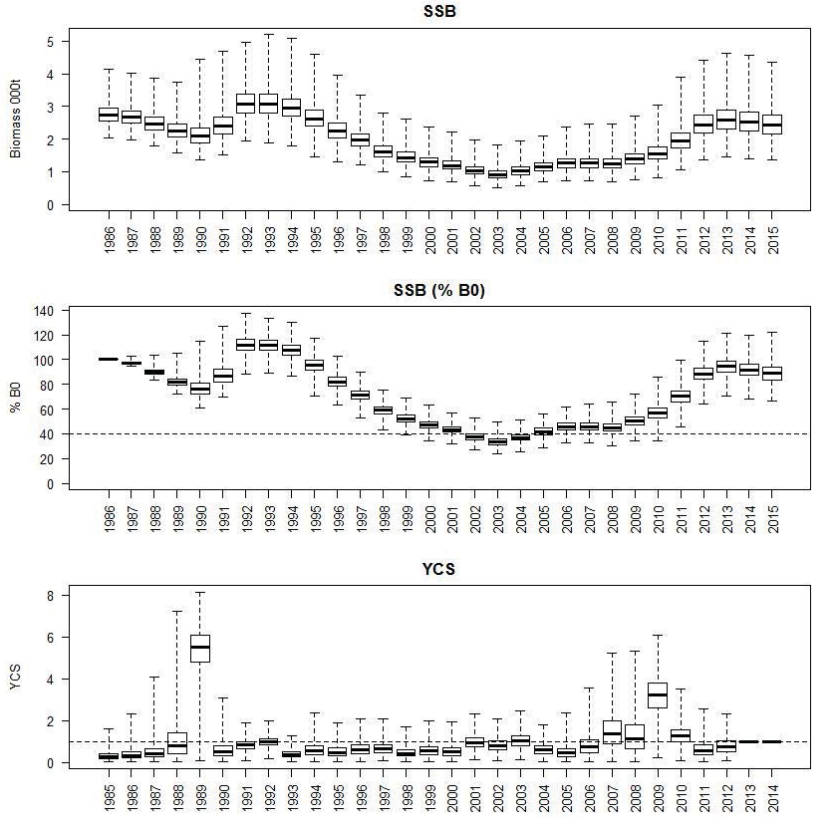

Figure 59: Posterior trajectories of SSB, SSB/B_0 and YCS from the MCMC run for the SCI 2 Base25 model.

5.2.2. SCI 2 Base30 (Appendix 9)

The Base30 model (M = 0.3) estimated a SSB_0 at 2749 t, with SSB_{2015} 2779 t, 101% of SSB_0. Fits to the abundance indices and normalised residuals (A9. 1), show that the model was slightly better able to match the observed increase and decline in CPUE in the mid 1990s and the increase in the most recent years, compared to the Base25 model (A8. 1), but fits to the photographic survey were slightly worse, and as with the Base25 model, the model was unable to match the recent increase in biomass observed

in the trawl survey. SSB followed a similar pattern to the previous model, and is estimated to have increased in the early 1990s, peaking around 1992, and then declining steadily until about 2003, recovering slightly by 2009, and then increasing rapidly to peak in 2013, but declining slightly since then (A9. 2). Particularly strong year class strengths were estimated in 1989 and (to a lesser extent) in 2007 and 2009, with a period of below average recruitment in the intervening period. Estimated selectivity curves matched observed changes in sex ratio between time steps, with males less available to trawling during time step 2 (A9. 3), although both parameters for the photo selectivity were fixed because estimated values were considered unrealistic. MPD estimates of trawl and photo survey catchability were within the prior distributions (A9. 4), and although the estimate for photo catchability was towards the upper limit of the prior distribution, it was lower than for the Base25 model. Fits to the observer length frequency distributions were variable, and the data weighting process down-weighted the length data (particularly the observer data), on the basis of fits to the mean length (A9. 5).

The overall likelihood profile when B_0 is fixed was U shaped (A9. 6), with the majority of the signal appearing to come from the abundance indices, which were in reasonable agreement, although there was relatively little contrast in the likelihood from the abundance indices between SSB_0 values of 2500 and 5500 tonnes. There was less signal in the proportion at length data, although in general those data seemed to prefer a lower SSB_0. Catchability priors provided conflicting signals for the photo and trawl surveys.

MCMC runs

Three independent MCMC chains were started a random step away from the MPD for each model, and run for 2 million simulations, with every one thousandth sample saved, giving a set of 2000 samples. The three chains were examined for evidence of lack of convergence (A9. 7 – A9. 10), and concatenated and systematically thinned to produce a 2000 sample chain for projections. Posterior distributions of trawl survey catchability were well within the prior distribution (A9. 11), with the MPD estimates also located within the posterior distributions, but the posterior distribution for the photo survey catchability was again towards the upper range of the prior, but lower than the Base25 model. The posterior trajectory of SSB (Figure 60) suggests a decline from about 1994 to about 2003, with the stock increasing slightly to 2005, remaining stable to 2008, and then increasing to a peak in 2013, before declining slightly in more recent years. The median estimate of current status (SSB_{2015}/SSB_0) is 101% (95% confidence interval 86%–118%), with 0% probability that SSB_{2015} is below 40% SSB_0.

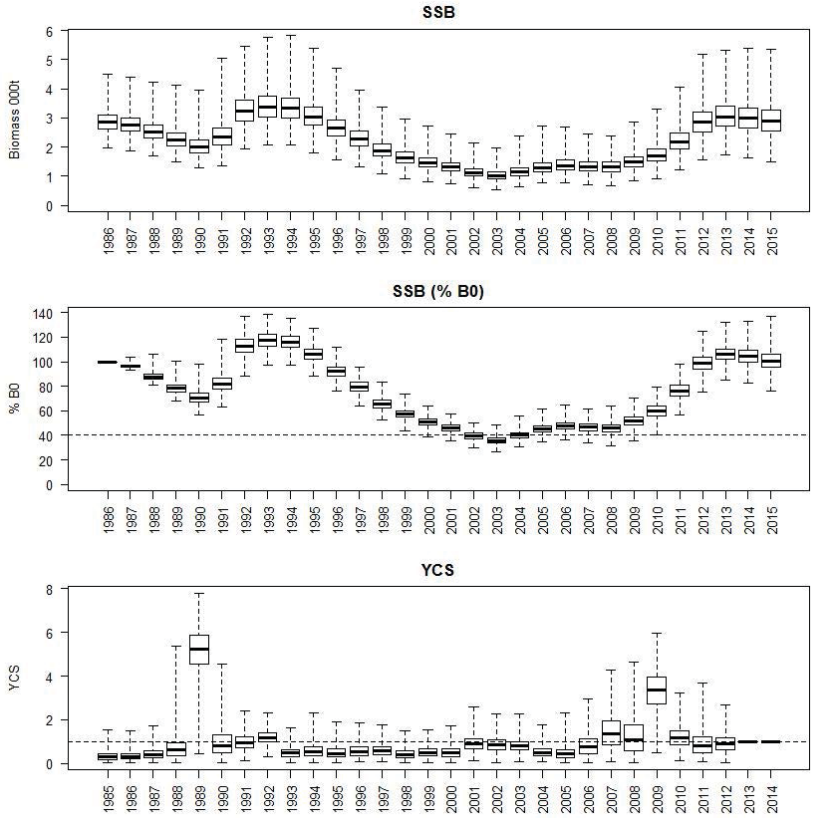

Figure 60: Posterior trajectories of SSB, SSB/B_0 and YCS from the MCMC run for the SCI 2 Base30 model.

5.2.3. SCI 2 Base35 (Appendix 10)

The Base35 model (M = 0.35) estimated a SSB_0 at 2841 t, with SSB_{2015} 3176 t, 112% of SSB_0. Fits to the abundance indices and normalised residuals (A10. 1) show that the model was able to match the observed increase and decline in CPUE in the mid 1990s and more recent increase better than either of the previous two models, although the model was unable to match the recent increase in biomass observed in the trawl survey. SSB is estimated to have increased in the early 1990s, peaking around 1994, and then declining steadily until about 2003, recovering slightly by 2009, and then increasing rapidly to peak in 2013–14, before declining slightly since then (A10. 2). Particularly strong year class strengths were estimated in 1989 and (to a lesser extent) in 2009, with a period of below average recruitment in the intervening period. Estimated selectivity curves were very similar to those for the previously described models, and matched observed changes in sex ratio between time steps, with males less available to trawling during time step 2 (A10. 3), although both parameters for the photo selectivity were fixed because estimated values were considered unrealistic. MPD estimates of trawl and photo survey catchability were within the prior distribution (A10. 4), and although the estimate for photo catchability was towards the upper limit of the prior distribution, it was lower than for either of the previously described models. Fits to the observer length frequencies were variable, and the data weighting process down-weighted the length data (particularly the observer data), on the basis of fits to the mean length (A10. 5).

The overall likelihood profile when B_0 is fixed was U shaped (A10. 6), with the majority of the signal appearing to come from the abundance indices, but the individual indices were not consistent, with the CPUE index preferring a SSB_0 of 2000 tonnes, while the trawl survey suggested between 2000 and 8000 tonnes, and the photo survey just indicated a preference for SSB_0 greater than 2000 tonnes. There was less signal in the proportion at length data, and the individual data sets appeared less consistent than the previously discussed models.

MCMC runs

Three independent MCMC chains were started a random step away from the MPD for each model, and run for 2 million simulations, with every one thousandth sample saved, giving a set of 2000 samples. The three chains were examined for evidence of lack of convergence (A10. 7 – A10. 10), and concatenated and systematically thinned to produce a 2000 sample chain for projections. Posterior distributions of trawl survey catchability were well within the prior distribution (A10. 11), with the MPD estimates also located within the posterior distributions, but the posterior distribution for the photo survey catchability was again towards the upper range of the prior, but lower than the other models. The posterior trajectory of SSB (Figure 61) suggests a decline from about 1994 to about 2003, with the stock increasing slightly to 2005, remaining stable to 2008, and then increasing to a peak in 2014, before declining slightly in 2015. The median estimate of current status (SSB_{2015}/SSB_0) is 113% (95% confidence interval 97%–131%), with 0% probability that SSB_{2015} is below 40% SSB_0.

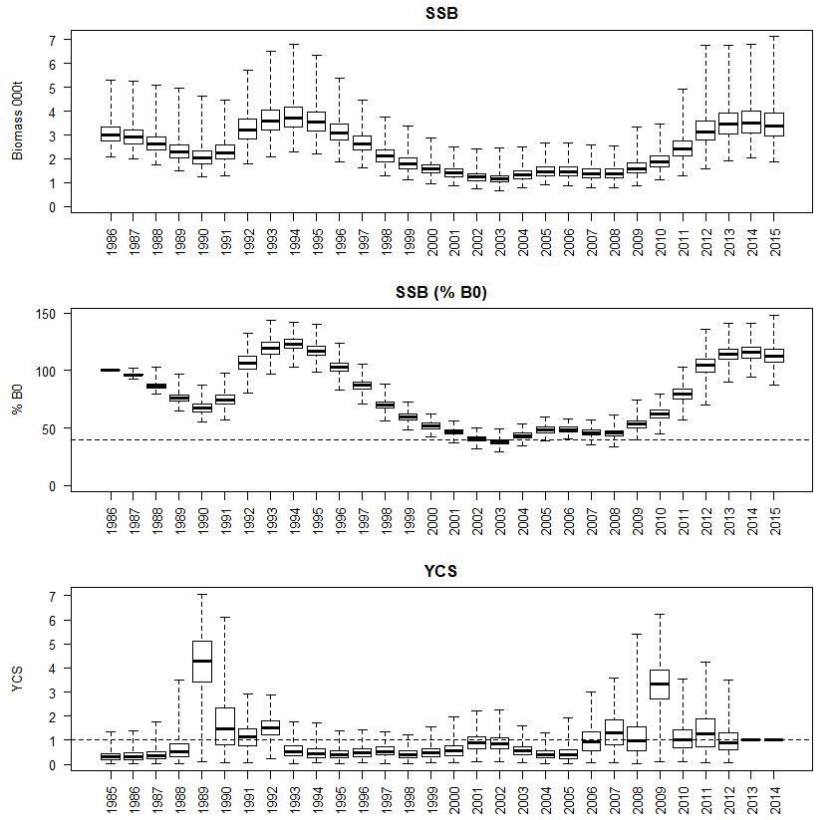

Figure 61: Posterior trajectories of SSB, SSB/B_0 and YCS from the MCMC run for the SCI 2 Base35 model.

5.3. Comparison with previous assessment

As with SCI 1, during the last SCI 2 assessment (Tuck 2014) a range of final models was presented, examining sensitivity to assumptions about natural mortality, and a variety of data weighting approaches were explored, to reduce the standard error of normalised residuals for the abundance indices. Updating the current model involved the same data sets as for SCI 1 (see Section 4.3), and investigation of the effects of the updated data series, new priors and revised data weighting were examined using the same set of model configurations (Table 24).

Plots of SSB, %SSB0 and YCS are presented (Figure 62) for the equivalent SCI 2 models described in Table 24. The inclusion of data from the most recent years and the revision or updating of existing

indices (2016 compared to 2016_12) influenced the stock trajectory and YCS pattern, in that the biomass was estimated to decline further in the early years of the fishery before peaking (at a lower level) in the mid 1990s, and then declining (again to a lower level) during the 2000s. Inclusion of the new data also produces a more rapid biomass increase after 2008. The revised priors developed on the basis of Tuck et al. (2015) (see Section 3.7.1 and Figure 46) had minimal influence on the SCI 2 assessment, estimating slightly lower biomass estimates, but having no effect on the stock trajectory (relative to SSB_0) (2016 compared to 2016_p13). The revised weighting approach adopted in the current assessment leads to the estimation of slightly lower SSB, but has minimal effect on current stock status (2013 compared to 2013_w16) or YCS patterns.

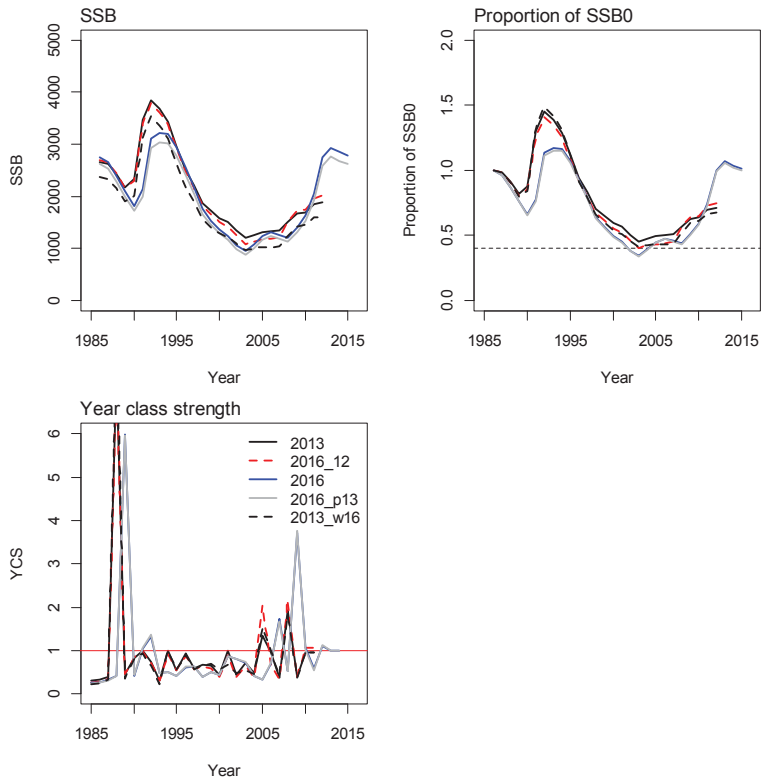

Figure 62: Plots of SSB, SSB as a proportion of SSB_0, and year class strength (YCS) for MPD fits for the SCI 2 base model from the previous assessment, and equivalent models updated with new data or data weighting. See Table 24 for model definitions.

5.4. SCI 2 Fishing Pressure

Annual fishing intensity (equivalent annual F) and the level of fishing that, if applied forever, would result in an equilibrium biomass of 40% SSB_0 (F 40% B_0) were calculated using methods described by Cordue (2012). Plots of annual fishing intensity against proportion SSB_0 (presented for the Base30 model in Figure 63) show that although SSB declined to a low level between 2002 and 2004 (and may have been below the 40% SSB_0 target), following the peak in fishing intensity observed in 2002, it has increased in more recent years, and is currently well above the 40% SSB_0 target, with annual fishing intensity well below F 40% B_0.

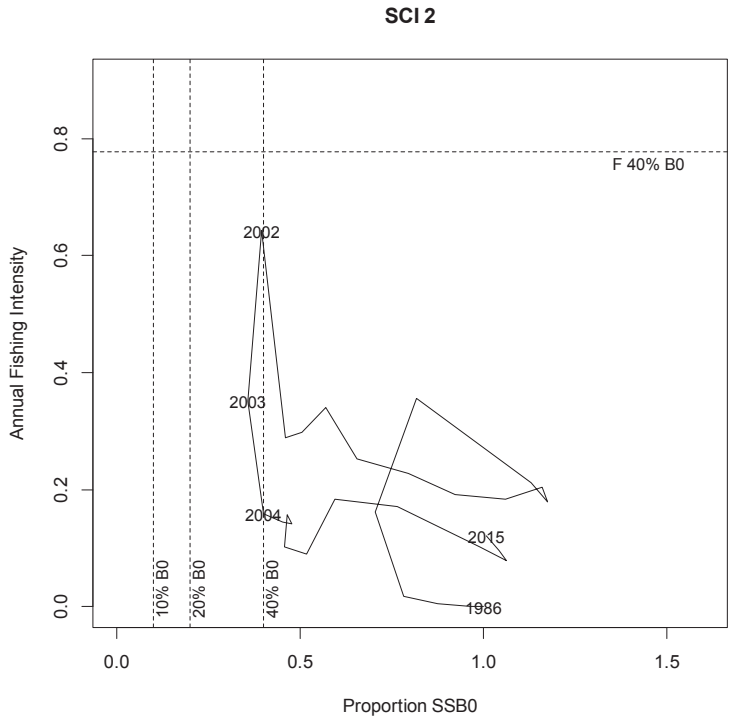

Figure 63: Trajectory of annual fishing intensity (equivalent annual F) plotted against proportion SSB_0 for the SCI 2 Base30 model, in relation to Harvest Strategy Standard target and limit reference points.

5.5. SCI 2 Projections

The assessments reported SSB_0 and $SSB_{current}$ and used the ratio of current and projected SSB to SSB_0 as preferred indicators. Projections were conducted up to 2021 on the basis of a range of catch scenarios (recent average, current TACC of 120 t, and 10%, 30% and 50% increases in TACC) (Table 29). Projections have been conducted randomly resampling year class strengths from the last decade of YCS estimated within the model (2003–2012). The probability of exceeding the default Harvest Strategy Standard target and limit reference points are reported (Table 30).

For each of the models presented (M=0.25, M=0.3 and M=0.35), future catches between 118 and 200 tonnes are predicted to reduce the SSB relative to SSB_{2015}, but remain above 40% SSB_0 (the most pessimistic prediction giving a 97% probability of SSB exceeding 40% SSB_0 by 2021).

Table 29: Results from MCMC runs showing B_0, B_{curr} B_{2019} and B_{2021} estimates at varying catch levels for SCI 2.

	Model	M=0.25	M=0.3	M=0.35
	B_0	2728	2867	3005
	B_{curr}	2431	2888	3391
	B_{curr}/B_0	0.89	1.01	1.13
118 tonnes (5 year average)	B_{2019}/B_0	0.87	0.95	1.04
	B_{2019}/B_{curr}	0.97	0.93	0.91
	B_{2021}/B_0	0.89	0.97	1.03
	B_{2021}/B_{curr}	1.00	0.95	0.90
133 tonnes (TACC)	B_{2019}/B_0	0.85	0.93	1.03
	B_{2019}/B_{curr}	0.95	0.92	0.90
	B_{2021}/B_0	0.87	0.95	1.01
	B_{2021}/B_{curr}	0.98	0.93	0.89
146 tonnes (10% increase)	B_{2019}/B_0	0.84	0.92	1.02
	B_{2019}/B_{curr}	0.94	0.91	0.89
	B_{2021}/B_0	0.85	0.94	1.00
	B_{2021}/B_{curr}	0.95	0.91	0.88
173 tonnes (30% increase)	B_{2019}/B_0	0.81	0.90	1.00
	B_{2019}/B_{curr}	0.91	0.88	0.87
	B_{2021}/B_0	0.82	0.90	0.97
	B_{2021}/B_{curr}	0.91	0.88	0.85
200 tonnes (50% increase)	B_{2019}/B_0	0.79	0.88	0.98
	B_{2019}/B_{curr}	0.87	0.86	0.85
	B_{2021}/B_0	0.78	0.87	0.95
	B_{2021}/B_{curr}	0.87	0.85	0.83

Table 30: Results from MCMC runs for SCI 2, showing probabilities of projected spawning stock biomass exceeding the default Harvest Strategy Standard target and limit reference points.

	118 tonnes	133 tonnes (TACC)	146 tonnes (+10%)	173 tonnes (+30%)	200 tonnes (+50%)
M=0.25					
2019					
P(SSB<10% B0)	0	0	0	0	0
P(SSB<20% B0)	0	0	0	0	0
P(SSB>40% B0)	1.00	1.00	1.00	1.00	0.99
$P(SSB_{2019} > SSB_{2015})$	0.45	0.42	0.40	0.35	0.32
2021					
P(SSB<10% B0)	0	0	0	0	0
P(SSB<20% B0)	0	0	0	0	0
P(SSB>40% B0)	1.00	1.00	0.99	0.98	0.97
$P(SSB_{2021} > SSB_{2015})$	0.50	0.46	0.44	0.38	0.32
M=0.3					
2019					
P(SSB<10% B0)	0	0	0	0	0
P(SSB<20% B0)	0	0	0	0	0
P(SSB>40% B0)	1.00	1.00	1.00	1.00	1.00
$P(SSB_{2019} > SSB_{2015})$	0.41	0.39	0.38	0.35	0.32
2021					
P(SSB<10% B0)	0	0	0	0	0
P(SSB<20% B0)	0	0	0	0	0
P(SSB>40% B0)	1.00	1.00	1.00	0.99	0.98
$P(SSB_{2021} > SSB_{2015})$	0.43	0.40	0.38	0.34	0.31
M=0.35					
2019					
P(SSB<10% B0)	0	0	0	0	0
P(SSB<20% B0)	0	0	0	0	0
P(SSB>40% B0)	1.00	1.00	1.00	1.00	1.00
$P(SSB_{2019} > SSB_{2015})$	0.37	0.35	0.34	0.31	0.29
2021					
P(SSB<10% B0)	0	0	0	0	0
P(SSB<20% B0)	0	0	0	0	0
P(SSB>40% B0)	1.00	1.00	0.99	0.99	0.98
$P(SSB_{2021} > SSB_{2015})$	0.36	0.34	0.33	0.31	0.27

6. COMBINED AREA (SCI 1 & SCI 2) MODEL

On the basis of suggestions from previous Working Group and Plenary meetings, a combined area (SCI 1 and SCI 2) model was developed. This was a two stock/area model, with no migration of animals between areas, and shared parameters for growth, selectivity and natural mortality. It was initially hoped that by combining and fitting to the two area data sets in a single model that more realistic estimates for some of the parameters (in particular, natural mortality and some of the SCI 1 selectivity terms) would be provided, but this did not prove to be the case. A single base model (M=0.3, process error estimated) was explored.

6.1.1. Combined area Base30 (Appendix 11)

The combined area model (M = 0.3) estimated SCI 1 SSB_0 at 5067 t, with SSB_{2015} 3808 t, 75% of SSB_0, and SCI 2 SSB_0 at 3053 t, with SSB_{2015} 3266 t, 107% of SSB_0. Fits to the abundance indices and normalised residuals (A11. 1 and A11. 2) show that the model fits were very similar to the equivalent single area models. SSB followed a very similar pattern to the equivalent single area models, and while the absolute biomass values for SCI 1 were slightly lower than the single area model, the values for SCI 2 were more noticeably greater than the single area model (A11. 3). YCS for SCI 1 were slightly offset from the single area model, but identical for SCI 2 (A11. 3). Estimated selectivity curves matched observed changes in sex ratio between time steps, with males less available to trawling during time step 2, and were generally similar to single area models (A11. 4). For time step 2, however, the fishery selectivity was strongly influenced by the SCI 1 data, and it may have been more appropriate to fix this. MPD estimates of trawl and photo survey catchability were similar to single area estimates (A11. 5), although slightly lower for SCI 2, and higher for SCI 1 (particularly for *q-Photo*). Fits to the observer length frequency distributions were variable, and the data weighting process down-weighted the length data (particularly the observer data), on the basis of fits to the mean length (A11. 6).

The overall likelihood profiles when B_0 is fixed were U shaped (A11. 7 and A11. 8), but as for the single area models, little of the SCI 1 signal appeared to come from the abundance indices.

MCMC runs

Three independent MCMC chains were started a random step away from the MPD for each model, and run for 2 million simulations, with every one thousandth sample saved, giving a set of 2000 samples. The three chains were examined for evidence of lack of convergence (A11. 9 – A11. 12), and concatenated and systematically thinned to produce a 2000 sample chain for projections. Posterior distributions of trawl survey catchability were well within the prior distribution (A11. 13), with the MPD estimates also located within the posterior distributions, but the posterior distribution for the photo survey catchability for SCI 2 was again towards the upper range of the prior, although lower than the single area model. For SCI 1, the posterior trajectory of SSB (A11. 14 and Figure 64) suggests a decline from about 1994 to about 2003, with the stock remaining stable to 2012, and showing a slight increase in the most recent years. The median estimate of current status (SSB_{2015}/SSB_0) is 75% (95% confidence interval 62%–88%), with 0% probability that SSB_{2015} is below 40% SSB_0. The single area and combined area model outputs for SCI 1 are very similar (Figure 64). For SCI 2, the posterior trajectory of SSB (A11. 15 and Figure 65) suggests a decline from about 1994 to about 2003, with the stock increasing slightly to 2005, remaining stable to 2008, but then increasing to 2013, and subsequently remaining stable. The median estimate of current status (SSB_{2015}/SSB_0) is 107% (95% confidence interval 93%–124%), with 0% probability that SSB_{2015} is below 40% SSB_0. The combined area model estimates a slightly higher SSB_0 and biomass trajectory than the single area model, but with a very similar pattern in stock status, other than the combined area model suggesting stability in the most recent years, while the single area model suggests a slight decline in biomass (Figure 65). No projections were presented for this model.

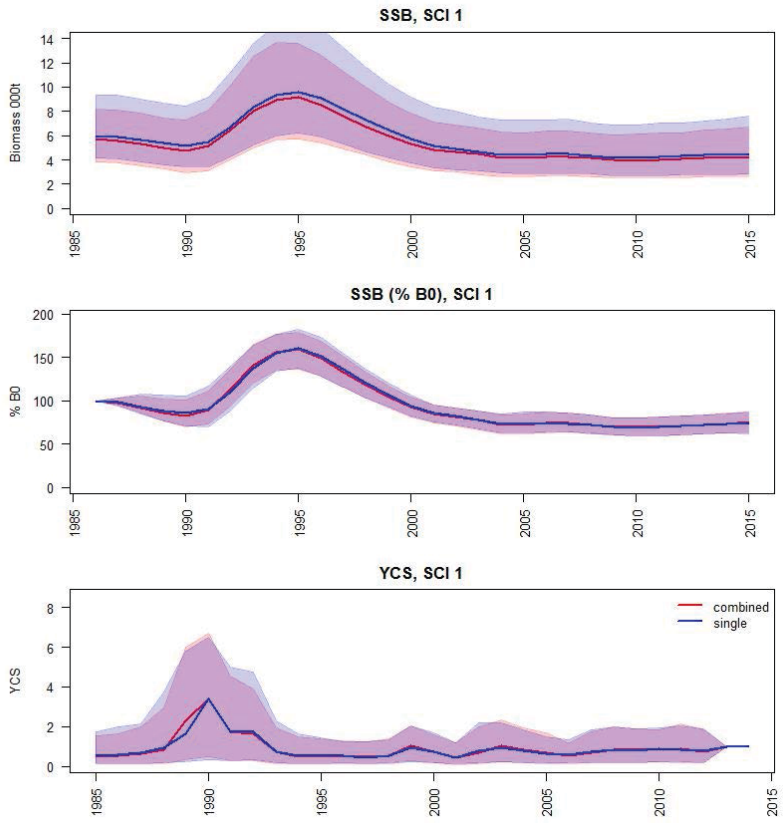

Figure 64: Posterior trajectories of SSB, SSB as a percentage of B_0, and YCS from the MCMC run for the SCI 1 for combined area and Base30 model.

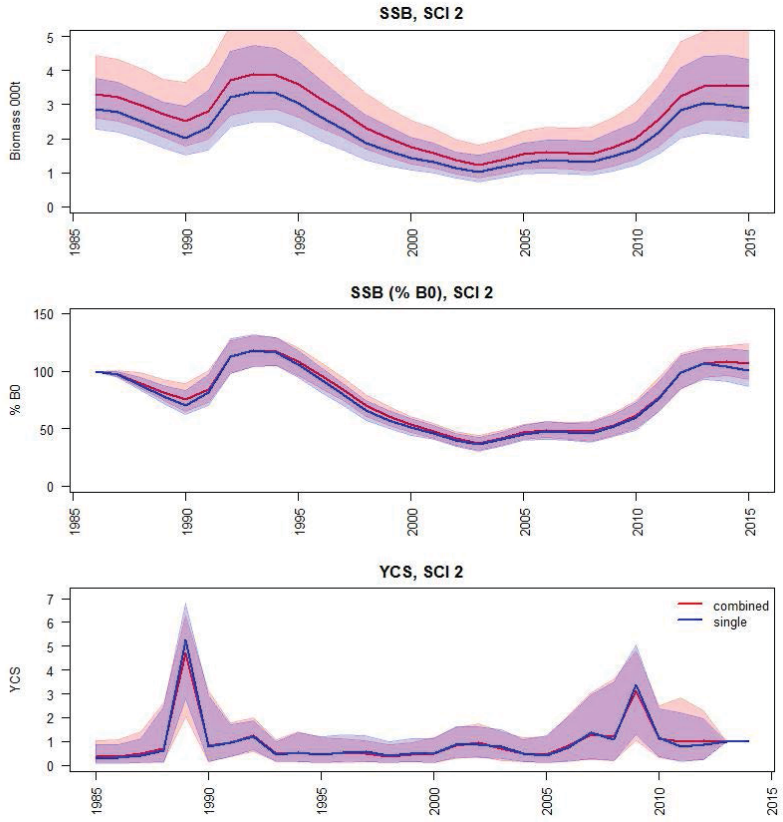

Figure 65: Posterior trajectories of SSB, SSB as a percentage of B_0, and YCS from the MCMC run for the SCI 2 for combined area and Base30 model.

7. DISCUSSION

Assessments of SCI 1 and SCI 2 stocks were last conducted in 2013 (Tuck 2014), building on the previous investigations developing the model structure (Tuck & Dunn 2012). In the 2013 assessment, SCI 1 was estimated to be about 70% SSB_0, while SCI 2 was estimated to be between 65% and 75% SSB_0.

The first accepted models for SCI 1 and SCI 2 included spatial structure, based on survey strata (Tuck & Dunn 2012), but the revised assessment in 2013 adopted a simpler spatial structure (Tuck 2014), and the SFAWG agreed that a single area model was appropriate for both separate assessments, although a combined area model was also examined. Models estimating M were not considered to generate realistic outputs, and base models were developed for both areas with M fixed at 0.25, 0.3 and 0.35. For each area, single annual standardised CPUE indices were calculated, and, along with trawl survey and photo survey data using revised priors for catchability (Tuck et al. 2015), were fitted as abundance indices, with associated length frequency distributions. The revised catchability priors had greater uncertainty than the previous parameters, and resulted in lower catchability estimates, and higher biomass for SCI 1, but no change in the stock trajectory (relative to SSB_0). The effect of this change was not as apparent for the SCI 2 model. Likelihood profiles suggest that the abundance indices data provide little information on biomass for SCI 1. Catches have been very stable throughout the history of the fishery, and do not appear to have had an effect on abundance. In SCI 2, both catches and abundance have changed markedly throughout the history of the fishery, and likelihood profiles suggest that the abundance indices data provide a reasonably consistent signal on biomass. Projections, up to 2021, were conducted for both stocks under a range of catch scenarios.

For SCI 1, the MPD estimate of SSB_0 was about 5600 t, but although the likelihood profiles were somewhat U shaped, most of the signal appears to come from the priors rather than the data. The estimated stock trajectory was sensitive to the value of M (higher M allowing the model to better fit rapid changes in CPUE), but all models showed an increase in biomass up to the mid 1990s (associated with very high recruitment a few years earlier) and a decline to the early 2000s, followed by a very stable period where SSB was around 70% SSB_0, but increasing slightly in the most recent years. The MCMC estimate of SSB_0 was between 5570 and 6150 t. SSB_{2015} was estimated to be between 3970 and 4600 t, and MCMC posteriors suggest a 0% probability that SSB_{2015} is below 40% SSB_0. Annual fishing intensity (equivalent annual F) has consistently been estimated to be below F 40% B_0. Sensitivity analyses suggested that the assessment is sensitive to the exclusion of the different survey data (e.g., excluding the photo survey leads to a lower biomass estimate), but stock status was not sensitive. For each of the models presented, future catches up to 156 tonnes are predicted to reduce the SSB relative to SSB_{2015}, but remain above 40% SSB_0 (the most pessimistic prediction giving a 98% probability of SSB exceeding 40% SSB_0 by 2021).

For SCI 2, the MPD estimate of SSB_0 was about 2700 t, with the likelihood profiles identifying a clear minimum, and more signal from the abundance data than was apparent for SCI 1. The models were sensitive to M, with a higher value resulting in a greater estimate of SSB_0, SSB_{2015}, and current stock status (relative to SSB_0). SSB is estimated to have increased through the early 1990s, peaking around 1993, and then declining to a minimum in 2003. Subsequently, it increased slightly to 2005, remained stable until about 2008, and increased rapidly to 2013, but has declined slightly since then. The MCMC estimate of SSB_0 was between 2730 and 3000 t. SSB_{2015} was estimated to be between 2430 and 3390 t, and MCMC posteriors suggest a 0% probability that SSB_{2015} is below 40% SSB_0. Annual fishing intensity (equivalent annual F) peaked in 2002, but has declined considerably in recent years, and SSB was at or below 40% SSB_0 between 2002 and 2004, but has increased considerably since this time. For each of the models presented, future catches up to 200 tonnes are predicted to reduce the SSB relative to SSB_{2015}, but maintain it above 40% SSB_0 (the most pessimistic prediction giving a 97% probability of SSB exceeding 40% SSB_0 by 2018).

A combined (SCI 1 and SCI 2) model was examined for the first time. Model outputs were very similar to equivalent single area models, although sharing catchability terms between stocks resulted in lower *q* values for SCI 2 (particularly for the *q-Photo* parameter), and an increased biomass estimate (and *vice versa* for SCI 1). Stock trajectories (relative to SSB_0) were very similar between the combined and single area models.

8. ACKNOWLEDGEMENTS

This work was funded by the Ministry for Primary Industries under project DEE2015-08SCI, and builds on a series of scampi assessment projects funded by the Ministry. I thank the many NIWA and Ministry of Fisheries staff who measured scampi over the years, and the members of the NIWA scampi image reading team. Development of the model structure benefitted greatly from comments members of the Shellfish Fisheries Assessment Working Group. This report was reviewed by Peter Horn (NIWA, Wellington).

9. REFERENCES

Bell, M.C., Redant, F., Tuck, I.D. (2006) *Nephrops* species. In: B. Phillips (Ed). *Lobsters: biology, management, aquaculture and fisheries*. Blackwell Publishing, Oxford: 412–461.

Bentley, N., Kendrick, T.H., Starr, P.J., Breen, P.A. (2012) Influence plots and metrics: tools for better understanding fisheries catch-per-unit-effort standardisations. *ICES Journal of Marine Science*, 69: 84–88.

Bull, B., Dunn, A. (2002) Catch-at-age: User manual v 1.06.2002/09/12. *NIWA Internal Report*, 114.

Bull, B., Francis, R.I.C.C., Dunn, A., McKenzie, A., Gilbert, D.J., Smith, M.H., Bian, R. (2008) CASAL (C++ algorithmic stock assessment laboratory). *NIWA Technical Report No.*, 130.

Bull, B., Francis, R.I.C.C., Dunn, A., McKenzie, A., Gilbert, D.J., Smith, M.H., Bian, R., Fu, D. (2012) CASAL (C++ algorithmic stock assessment laboratory). *NIWA Technical Report No.*, 135: 280.

Charnov, E.L., Berrigan, D., Shine, R. (1983) The M/*k* ratio is the same for fish and reptiles. *American Naturalist*, 142: 707–711.

Cordue, P.L. (2012) Fishing intensity metrics for use in overfishing determination. *ICES Journal of Marine Science: Journal du Conseil*, 69(4): 615-623. 10.1093/icesjms/fss036

Cryer, M., Coburn, R. (2000) Scampi stock assessment for 1999. *New Zealand Fisheries Assessment Report*, 2000/7.

Cryer, M., Dunn, A., Hartill, B. (2005) Length-based population model for scampi (*Metanephrops challengeri*) in the Bay of Plenty (QMA 1). *New Zealand Fisheries Assessment Report*, 2005/27: 55 p.

Cryer, M., Hartill, B., Drury, J., Armiger, H., Smith, M.D., Middleton, C. (2003) Indices of relative abundance for scampi, *Metanephrops challengeri*, based on photographic surveys in QMA 1 (1998–2003) and QMA 2 (2003). *Final Research Report for Ministry of Fisheries research project*, Objectives 1-3: 18.

Cryer, M., Oliver, M. (2001) Estimating age and growth in New Zealand scampi, *Metanephrops challengeri*. *Final Research Report for Ministry of Research Project*, Objective 2.

Cryer, M., Stotter, D.R. (1997) Trawling and tagging of scampi off the Alderman Islands, western bay of Plenty, September 1995 (KAH9511). *New Zealand Fisheries Data Report*, 84.

Cryer, M., Stotter, D.R. (1999) Movement and growth rates of scampi inferred from tagging, Alderman Islands, western Bay of Plenty. *NIWA Technical Report No.*, 49.

Fenaughty, C. (1989) Reproduction in *Metanephrops challengeri*. *Unpublished Report MAF Fisheries, Wellington*: 46.

Francis, R.I.C.C. (1999) The impact of correlations in standardised CPUE indices. *New Zealand Fisheries Assessment Research Document*: 30.

Francis, R.I.C.C. (2011) Data weighting in statistical fisheries stock assessment models. *Canadian Journal Fisheries and Aquatic Science*, 68: 1124–1138.

Francis, R.I.C.C., Bian, R. (2011) Catch-at-length and -age (CALA) User Manual: 83.

Hughes, D.J., Ansell, A.D., Atkinson, R.J.A. (1996) Sediment bioturbation by the echiuran worm Maxmuelleria lankesteri (Herdman) and its consequences for radionuclide dispersal in Irish Sea sediments. *Journal of Experimental Marine Biology and Ecology*, 195(2): 203-220. http://dx.doi.org/10.1016/0022-0981(95)00098-4

Hughes, D.J., Atkinson, R.J.A., Ansell, A.D. (1999) The annual cycle of sediment turnover by the echiuran worm Maxmuelleria lankesteri (Herdman) in a Scottish sea loch. *Journal of Experimental Marine Biology and Ecology*, 238(2): 209-223. http://dx.doi.org/10.1016/S0022-0981(98)00168-3

McCullagh, P., Nelder, J.A. (1989) *Generalised Linear Models*. Chapman and Hall, London: 511 p.

Morizur, Y. (1982) Estimation de la mortalité pour quelques stocks de langoustine, *Nephrops norvegicus*. *ICES CM*, 1982/K:10.

Nickell, L.A., Atkinson, R.J.A. (1995) Functional morphology of burrows and trophic modes of three thalassinidean shrimp species, and a new approach to the classification of thalassinidean burrow morphology. *Marine Ecology Progress Series*, 128: 181–197.

Nickell, L.A., Atkinson, R.J.A., Hughes, D.J., Ansell, A.D., Smith, C.J. (1995) Burrow morphology of the echiuran worm *Maxmuelleria lankesteri* (Echiura: Bonelliidae), and a brief review of burrow structure and related ecology of the Echiura. *Journal of Natural History*, 29: 871–885.

Pauly, D. (1980) On the interrelationships between natural mortality, growth parameters, and mean environmental temperature in 175 fish stocks. *Journal du Conseil International pour l'Exloration du Mer*, 39: 175–192.

Smith, C.R., Jumars, P.A., DeMaster, D.J. (1986) In situ studies of megafaunal mounds indicate rapid sediment turnover and community response at the deep-sea floor. *Nature*, 323(6085): 251-253. http://dx.doi.org/10.1038/323251a0

Starr, P.J. (2009) Rock lobster catch and effort data: summaries and CPUE standardisations, 1979–80 to 2007–08. *New Zealand Fisheries Assessment Report*, 2009/38: 73 p.

Starr, P.J., Breen, P.A., Kendrick, T.H., Haist, V. (2009) Model and data used for the 2008 stock assessment of rock lobsters (*Jasus edwardsii*) in CRA 3. *New Zealand Fisheries Assessment Report*, 2009/22: 62 p.

Tuck, I.D. (2009) Characterisation of scampi fisheries and the examination of catch at length and spatial distribution of scampi in SCI 1, 2, 3, 4A and 6A. *New Zealand Fisheries Assessment Report*, 2009/27: 102 p.

Tuck, I.D. (2010) Scampi burrow occupancy, burrow emergence and catchability. *Final Research Report for Ministry of Fisheries research project*: 58.

Tuck, I.D. (2013) Characterisation and length-based population model for scampi (*Metanephrops challengeri*) on the Mernoo Bank (SCI 3). *New Zealand Fisheries Assessment Report*, 2013/24: 165 p.

Tuck, I.D. (2014) Characterisation and length-based population model for scampi (*Metanephrops challengeri*) in the Bay of Plenty (SCI 1) and Hawke Bay/Wairaraoa (SCI 2). *New Zealand Fisheries Assessment Report*, 2014/33: 172 p.

Tuck, I.D. (2015) Characterisation and length-based population model for scampi (*Metanephrops challengeri*) at the Auckland Islands (SCI 6A). *New Zealand Fisheries Assessment Report*, 2015/21: 164 p.

Tuck, I.D. (in prep) Characterisation and length-based population model for scampi (*Metanephrops challengeri*) on the Mernoo Bank (SCI 3). *New Zealand Fisheries Assessment Report*: 221p.

Tuck, I.D., Atkinson, R.J.A., Chapman, C.J. (2000) Population biology of the Norway lobster, *Nephrops norvegicus* (L.) in the Firth of Clyde, Scotland. II. Fecundity and size at onset of maturity. *ICES Journal of Marine Science*, 57: 1222–1237.

Tuck, I.D., Dunn, A. (2006) Length based population model for scampi (*Metanephrops challengeri*) in the Bay of Plenty (SCI 1) and Wairarapa / Hawke Bay (SCI 2). *Final Research Report for Ministry of Fisheries research project SCI2005-01*, Objectives 2 & 3: 93.

Tuck, I.D., Dunn, A. (2009) Length-based population model for scampi (*Metanephrops challengeri*) in the Bay of Plenty (SCI 1) and Wairarapa / Hawke Bay (SCI 2). *Final Research Report for Ministry of Fisheries research project SCI2008-03*, Obj 1: 30.

Tuck, I.D., Dunn, A. (2012) Length-based population model for scampi (*Metanephrops challengeri*) in the Bay of Plenty (SCI 1), Wairarapa / Hawke Bay (SCI 2) and Auckland Islands (SCI 6A). *New Zealand Fisheries Assessment Report*, 2012/1: 125 p.

Tuck, I.D., Hartill, B., Drury, J., Armiger, H., Smith, M., Parkinson, D. (2006) Measuring the abundance of scampi - Indices of abundance for scampi, *Metanephrops challengeri*, based on photographic surveys in SCI 2 (2003-2006). *Final Research Report for Ministry of Fisheries research project SCI2005-01*, Obj 1: 21.

Tuck, I.D., Hartill, B., Parkinson, D., Harper, S., Drury, J., Smith, M., Armiger, H. (2009) Estimating the abundance of scampi - Relative abundance of scampi, *Metanephrops challengeri*, from a photographic survey in SCI 1 and SCI 6A (2008). *Final Research Report for Ministry of Fisheries research project SCI2008-01*, Objectives 1 & 2: 37.

Tuck, I.D., Parkinson, D., Armiger, H., Smith, M., Miller, A., Rush, N., Spong, K. (2016) Estimating the abundance of scampi in SCI 1 (Bay of Plenty) and SCI 2 (Wairarapa / Hawke Bay) in 2015. *New Zealand Fisheries Assessment Report*, 2016/17: 60 p.

Tuck, I.D., Parkinson, D., Drury, J., Armiger, H., Miller, A., Rush, N., Smith, M., Hartill, B. (2013) Estimating the abundance of scampi - Relative abundance of scampi, *Metanephrops challengeri*, from a photographic survey in SCI 1 and SCI 2 (2012). *Final Research Report for Ministry of Fisheries research project SCI2010-02A*: 54.

Tuck, I.D., Parsons, D.M., Hartill, B.W., Chiswell, S.M. (2015) Scampi (*Metanephrops challengeri*) emergence patterns and catchability. *ICES Journal of Marine Science*, 72 (Supplement 1): i199-i210. http://icesjms.oxfordjournals.org/content/early/2015/01/08/icesjms.fsu244.abstract

Tuck, I.D., Spong, K. (2013) Burrowing megafauna in SCI 3. *New Zealand Fisheries Assessment Report*, 2013/20: 50p.

Vignaux, M. (1994) Catch per unit effort (CPUE) analysis of west coast South Island and Cook Strait spawning hoki fisheries, 1987–93. *New Zealand Fisheries Assessment Research Document*: 29.

Wear, R.G. (1976) Studies on the larval development of *Metanephrops challengeri* (Balss, 1914) (Decapoda, Nephropidae). *Crustaceana*, 30: 113–122.

APPENDIX 1. CPUE standardisation diagnostics (SCI 1)

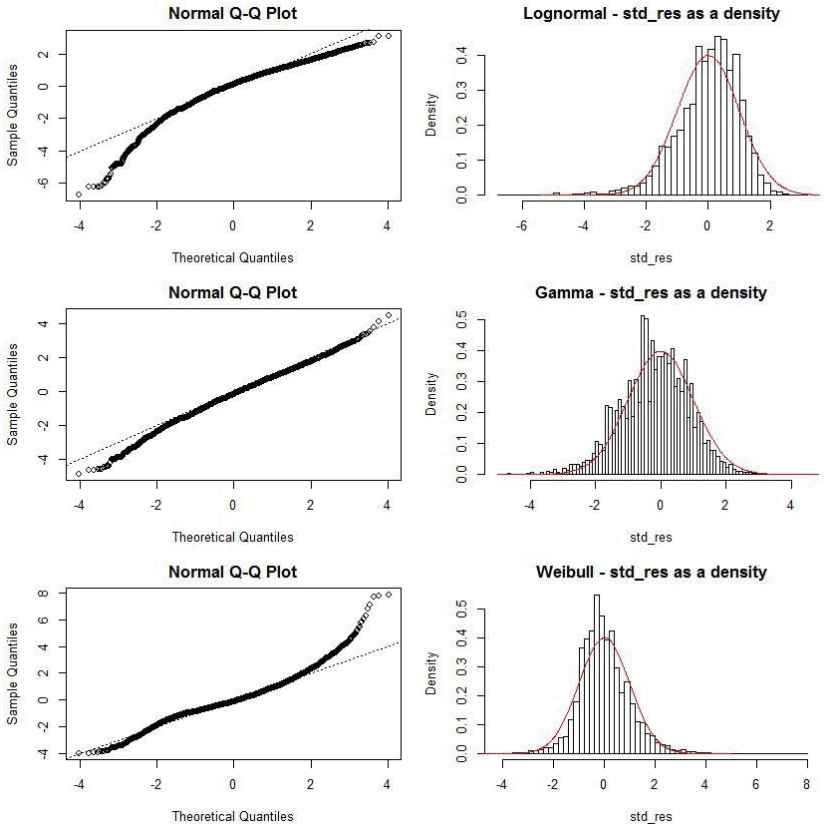

A1. 1: Plots of the distributions of standardised residuals for simple standardised CPUE models for SCI 1 with log normal (top panel), gamma (middle panel), and Weibull (bottom panel) error distributions.

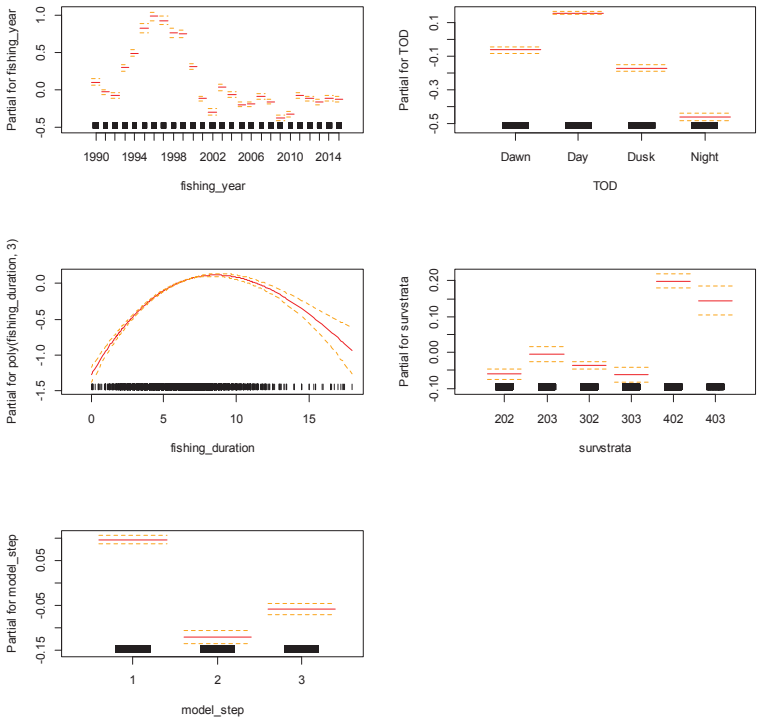

A1. 2: Termplot for final SCI 1 CPUE standardisation model (Table 5).

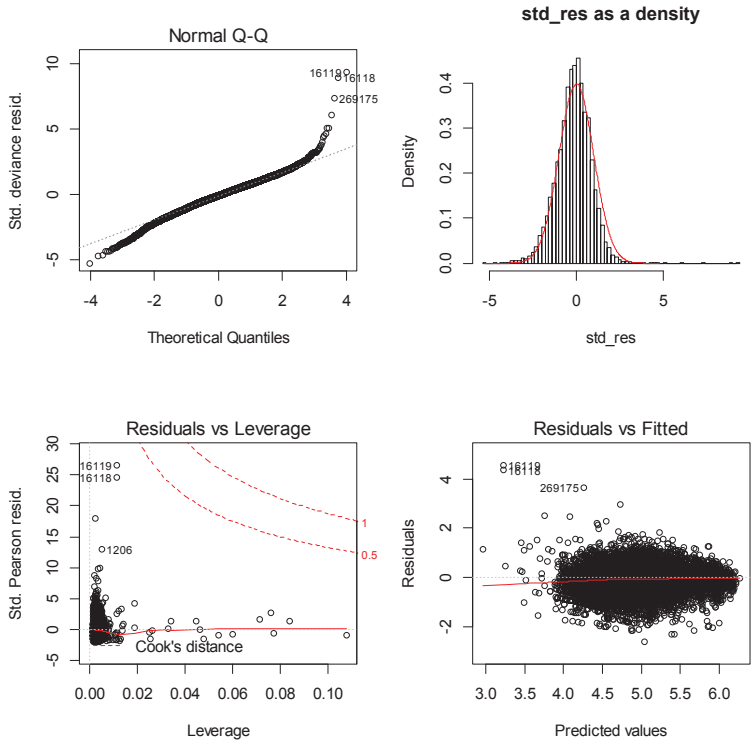

A1. 3: Diagnostic plots for final SCI 1 CPUE standardisation model (Table 5).

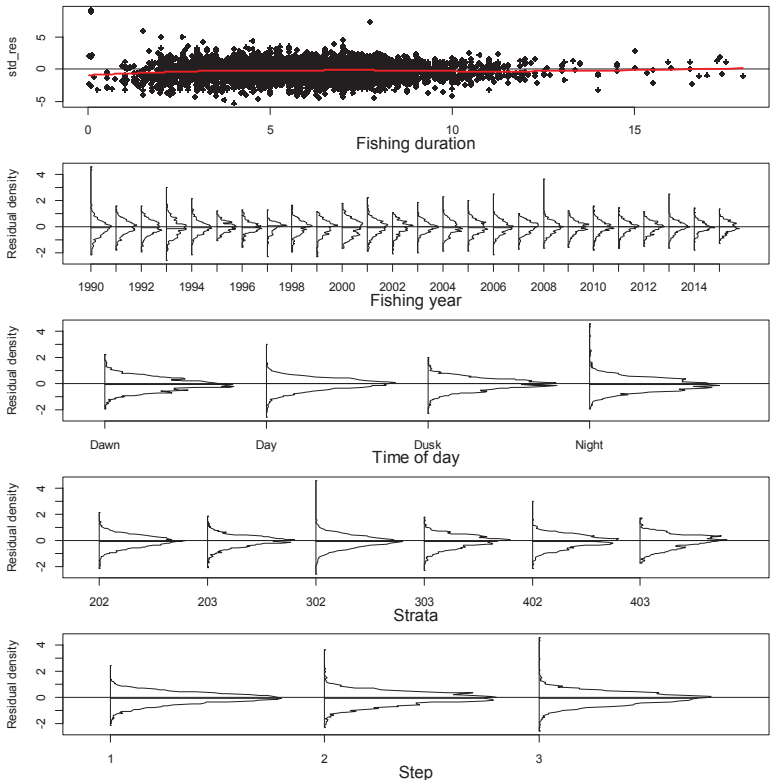

A1. 4: Distributions of residuals for final SCI 1 CPUE standardisation model (Table 5).

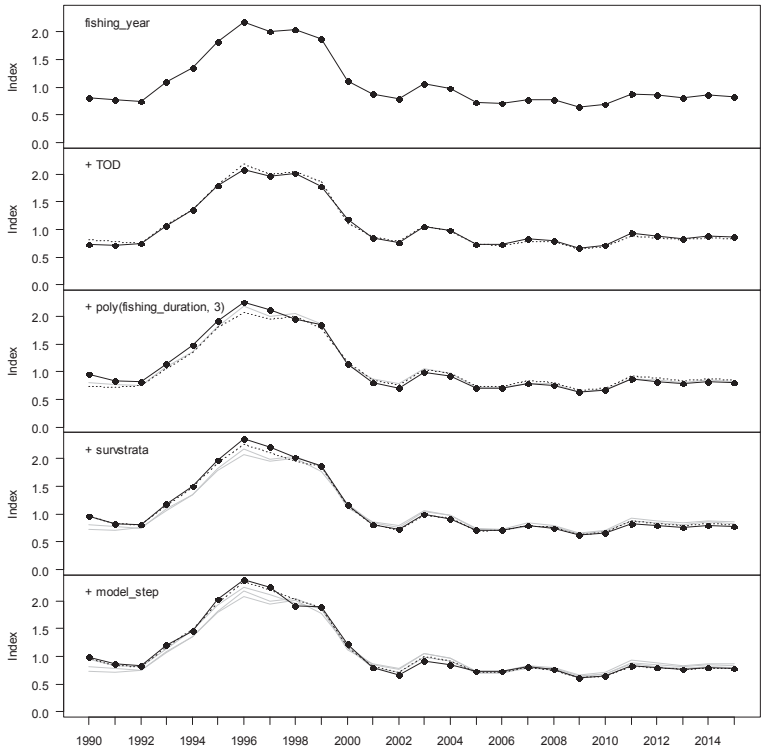

A1. 5: Step influence plot for final SCI 1 CPUE standardisation model (Table 5).

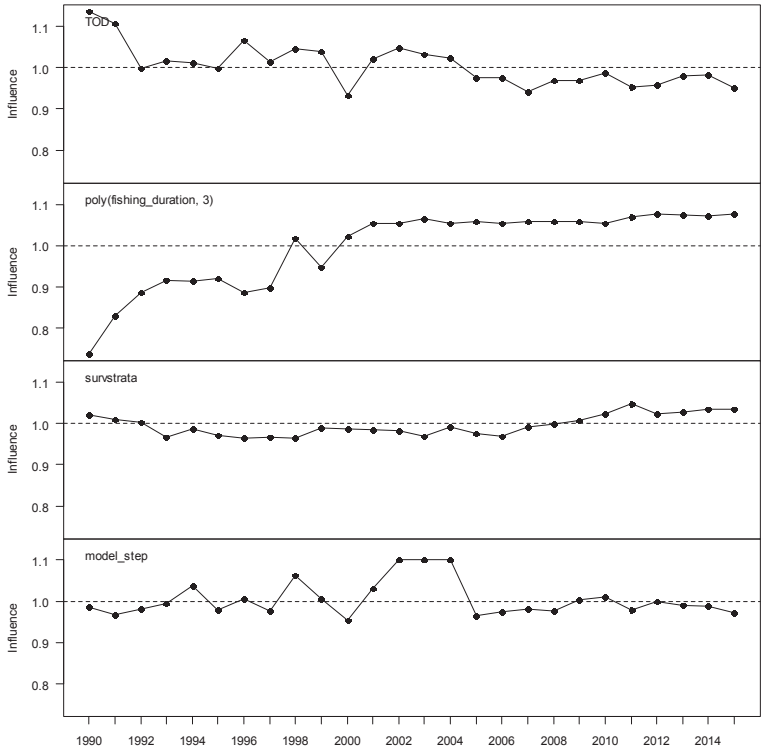

A1. 6: Year influence plots for each explanatory variable for final SCI 1 CPUE standardisation model (Table 5).

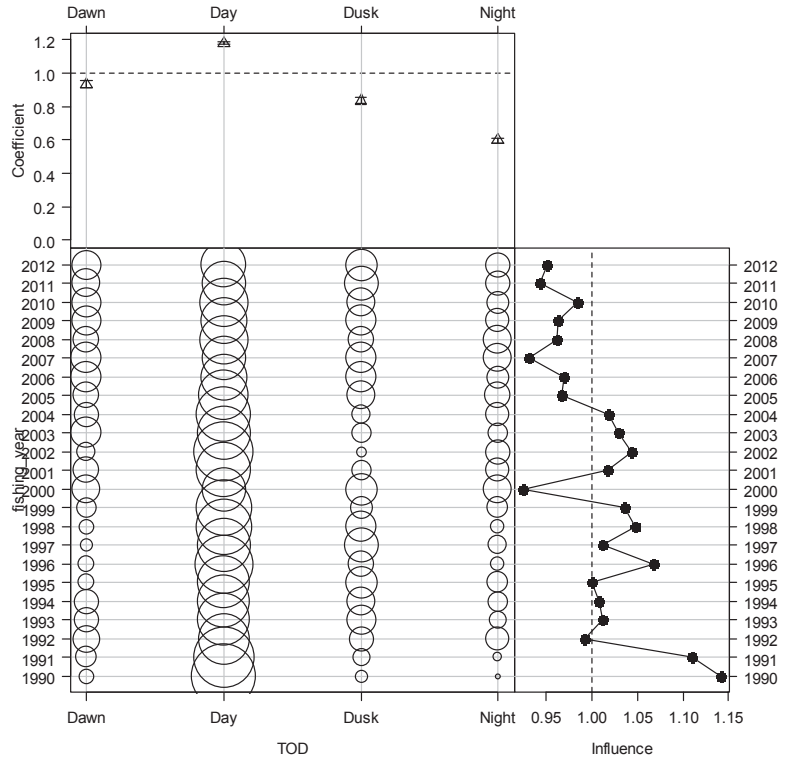

A1. 7: Coefficient-distribution influence plot for time of day for final SCI 1 CPUE standardisation model (Table 5).

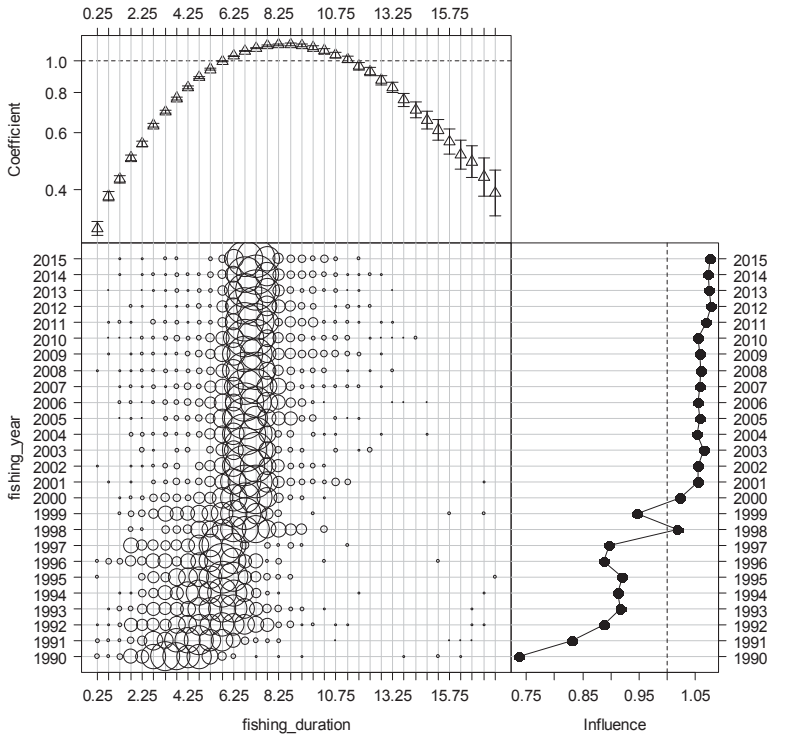

A1. 8: Coefficient-distribution influence plot for effort (fishing duration) for final SCI 1 CPUE standardisation model (Table 5).

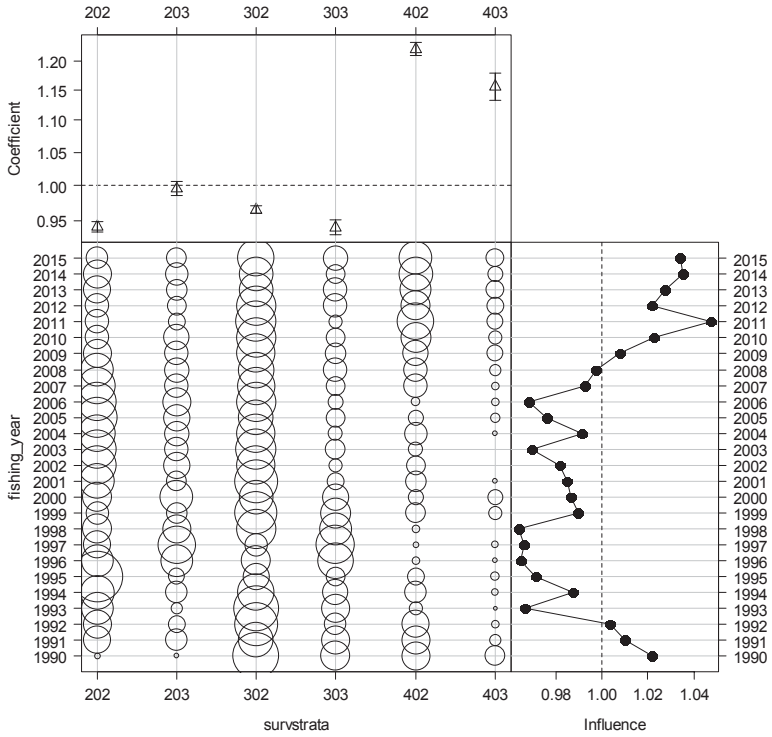

A1. 9: Coefficient-distribution influence plot for survstrata (survey strata) for final SCI 1 CPUE standardisation model (Table 5).

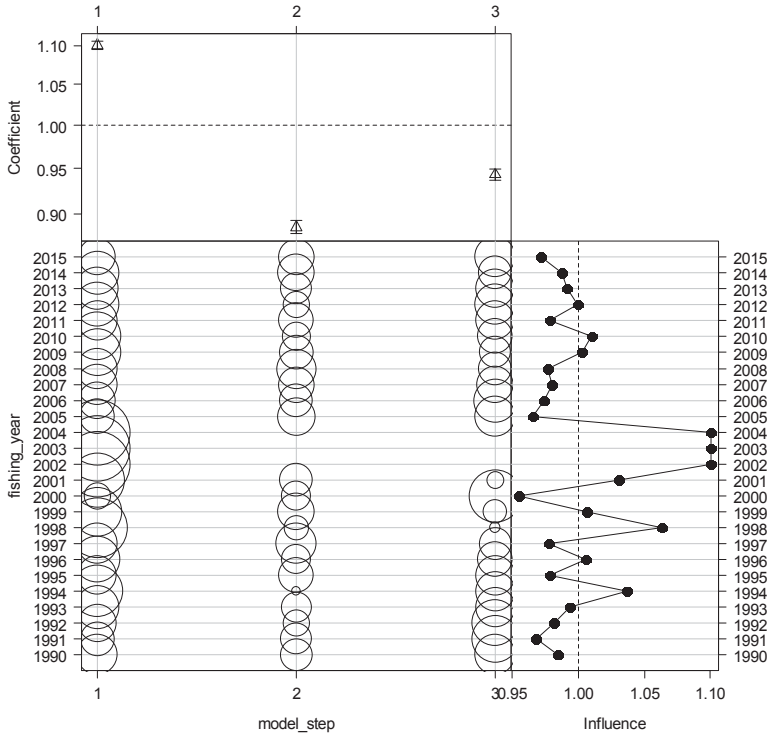

A1. 10: Coefficient-distribution influence plot for timestep for final SCI 1 CPUE standardisation model (Table 5).

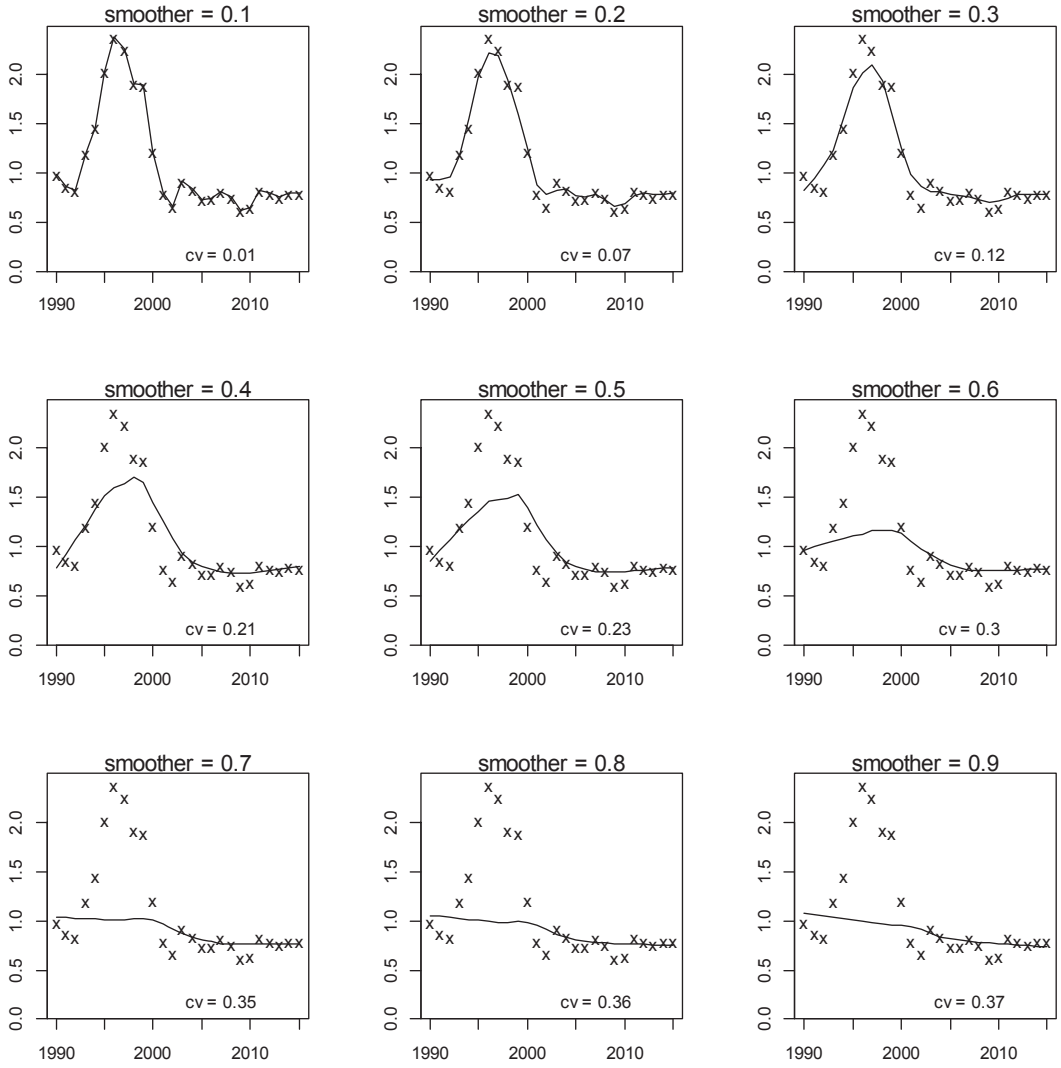

A1. 11: Range of smoothers fitted to index from the final SCI 1 CPUE standardisation model (Table 5).

APPENDIX 2. CPUE standardisation diagnostics (SCI 2)

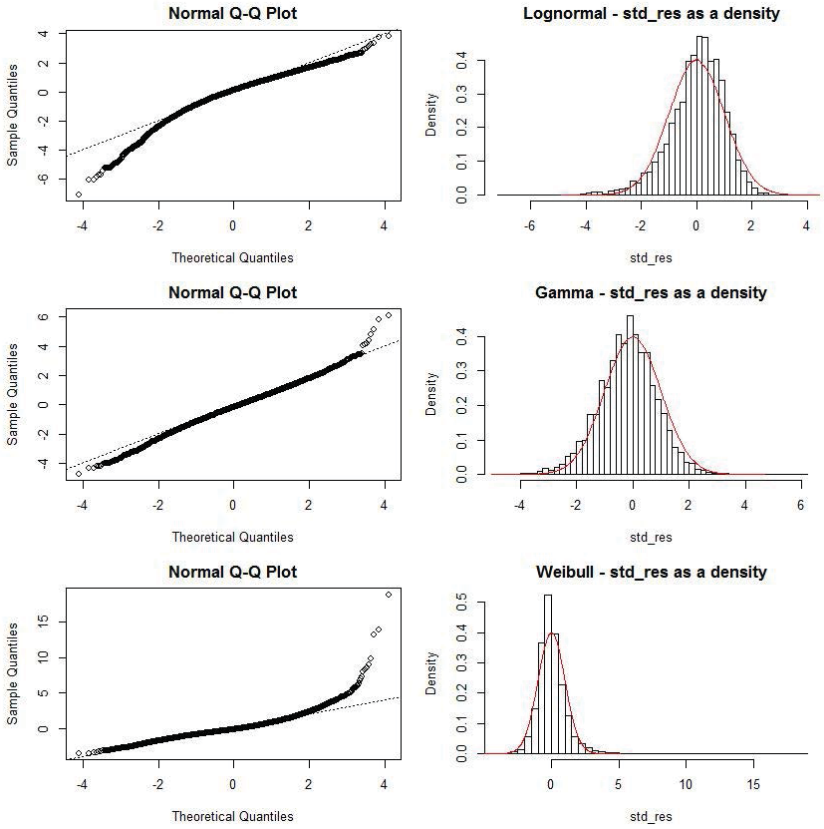

A2. 1: Plots of the distributions of standardised residuals for simple standardised CPUE models for SCI 2 with log normal (top panel), gamma (middle panel), and Weibull (bottom panel) error distributions.

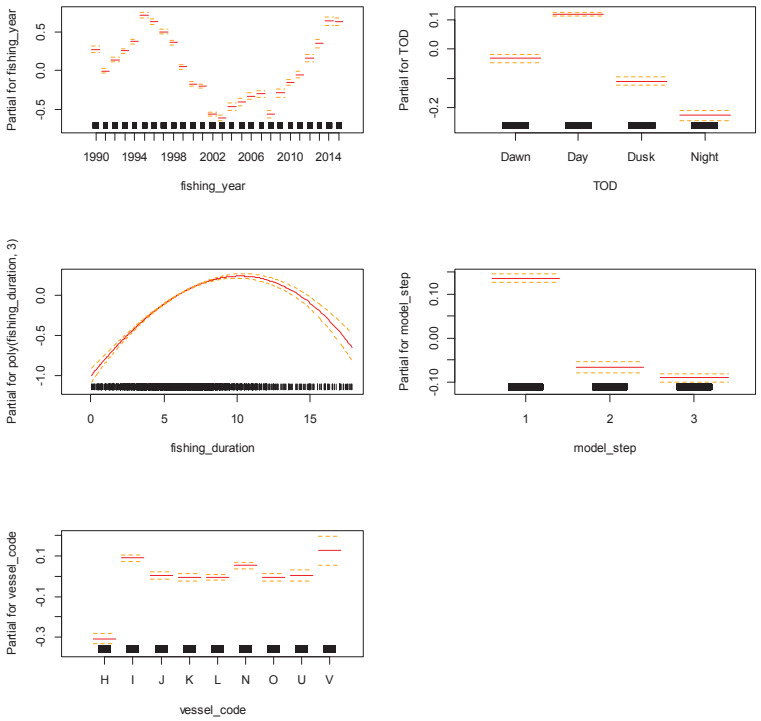

A2. 2: Termplot for final SCI 2 CPUE standardisation model (Table 8).

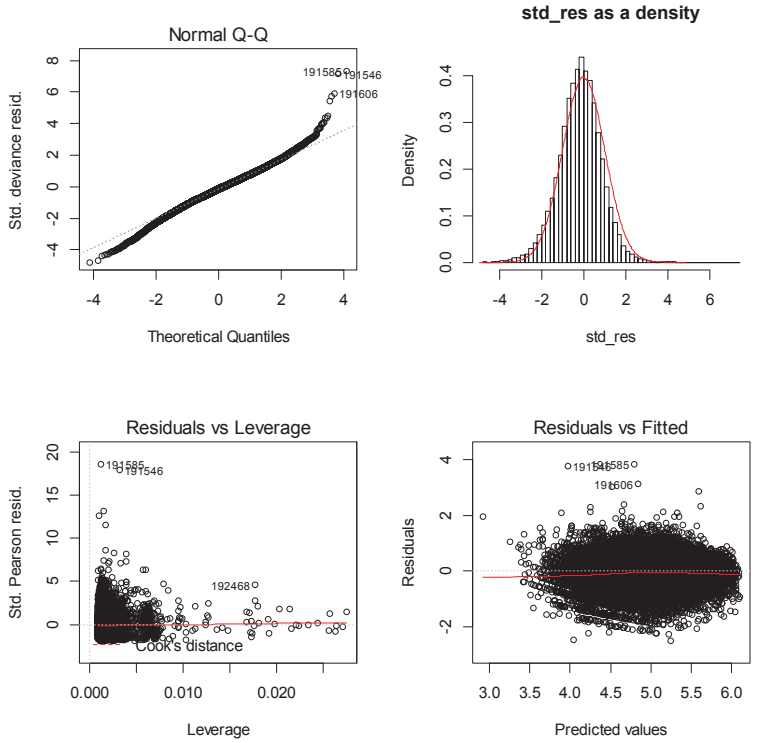

A2. 3: Diagnostic plots for final SCI 2 CPUE standardisation model (Table 8).

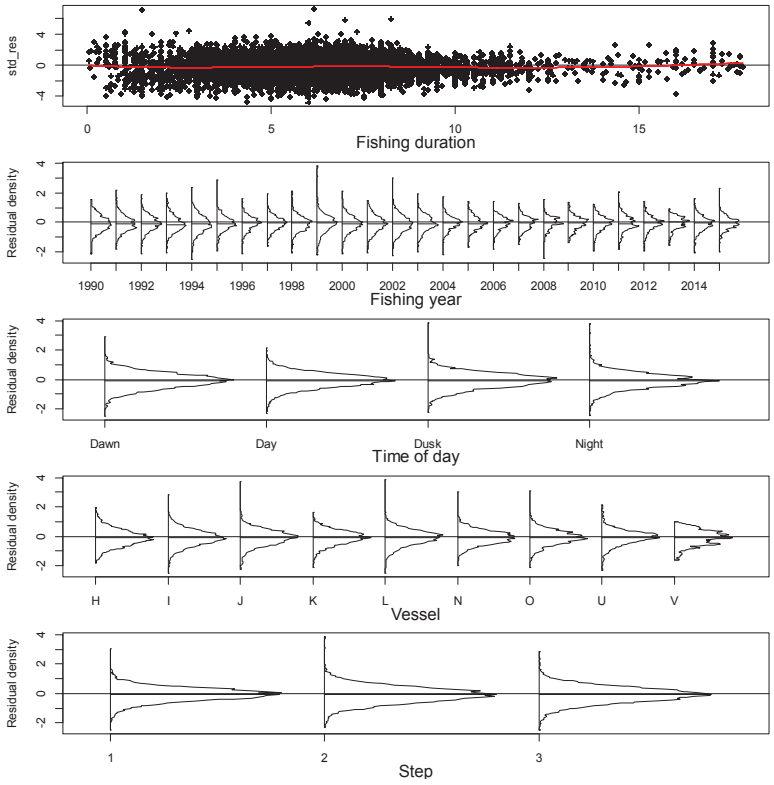

A2. 4: Distributions of residuals for final SCI 2 CPUE standardisation model (Table 8).

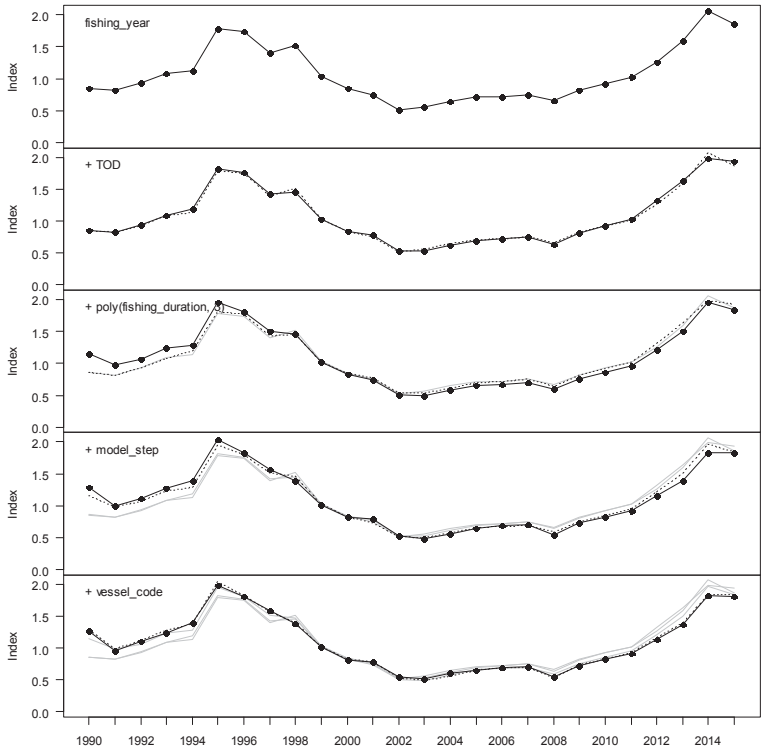

A2. 5: Step influence plot for final SCI 2 CPUE standardisation model (Table 8).

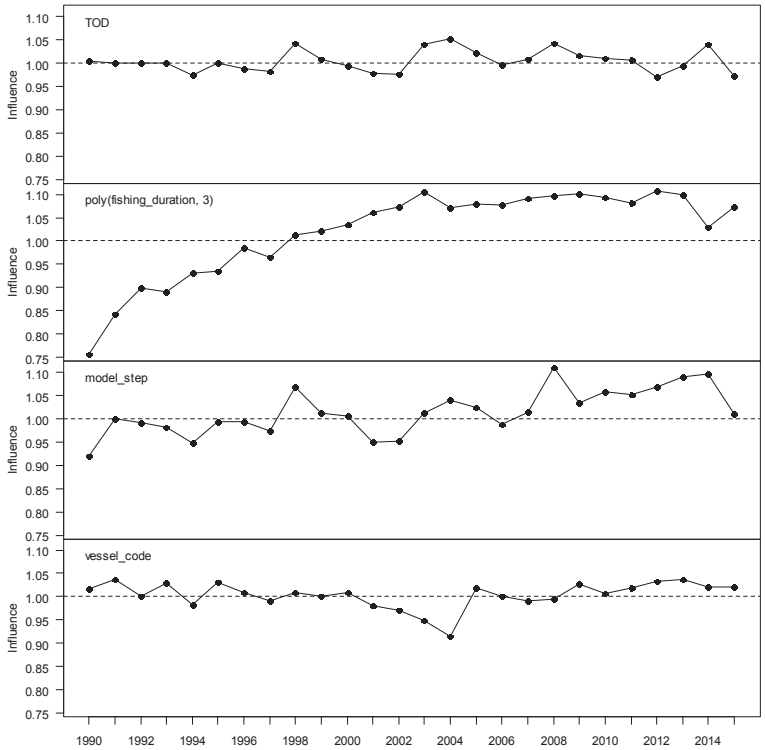

A2. 6: Year influence plots for each explanatory variable for final SCI 2 CPUE standardisation model (Table 8).

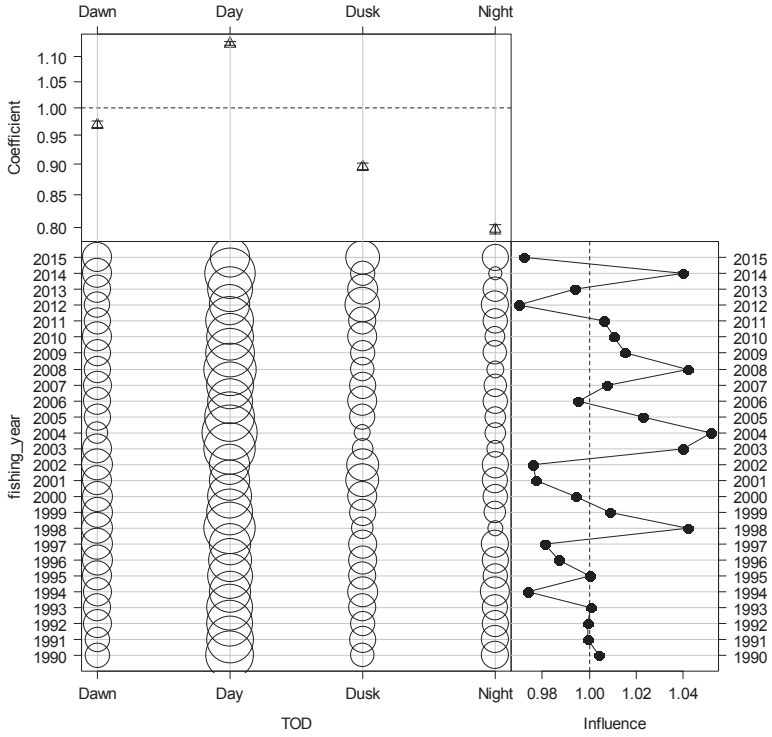

A2. 7: Coefficient-distribution influence plot for time of day for final SCI 2 CPUE standardisation model (Table 8).

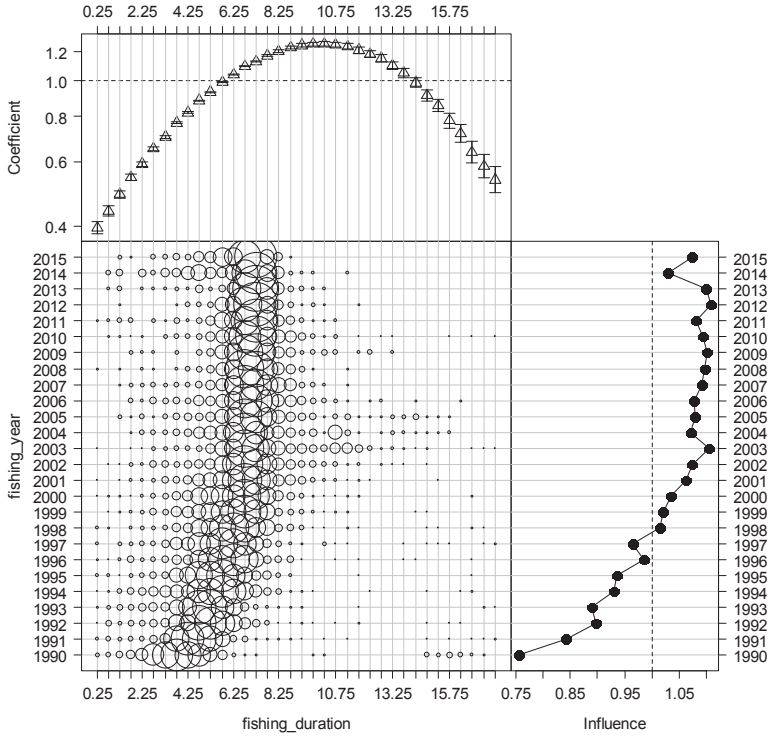

A2. 8: Coefficient-distribution influence plot for effort (fishing duration) for final SCI 2 CPUE standardisation model (Table 8).

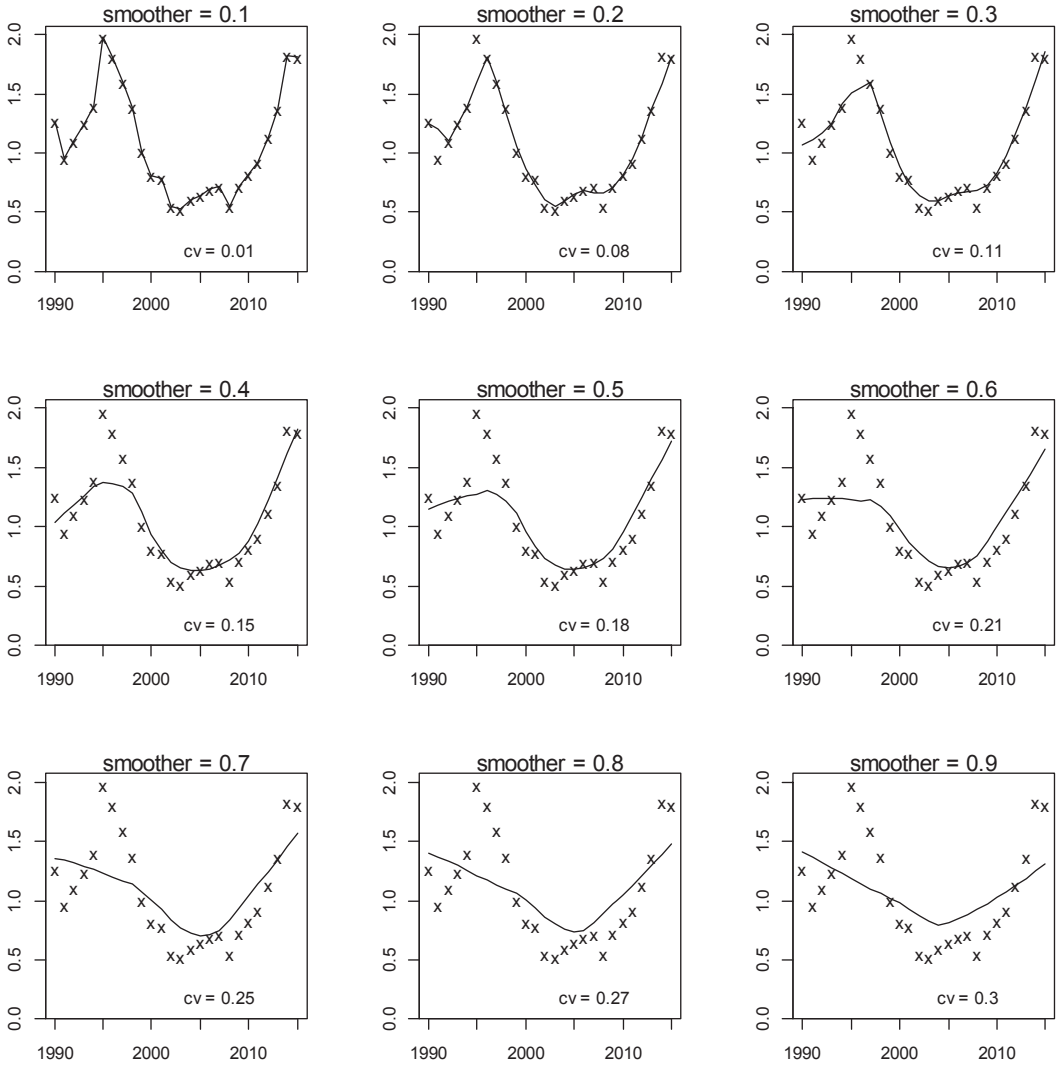

A2. 9: Range of smoothers fitted to the index from the final SCI 2 CPUE standardisation model (Table 8).

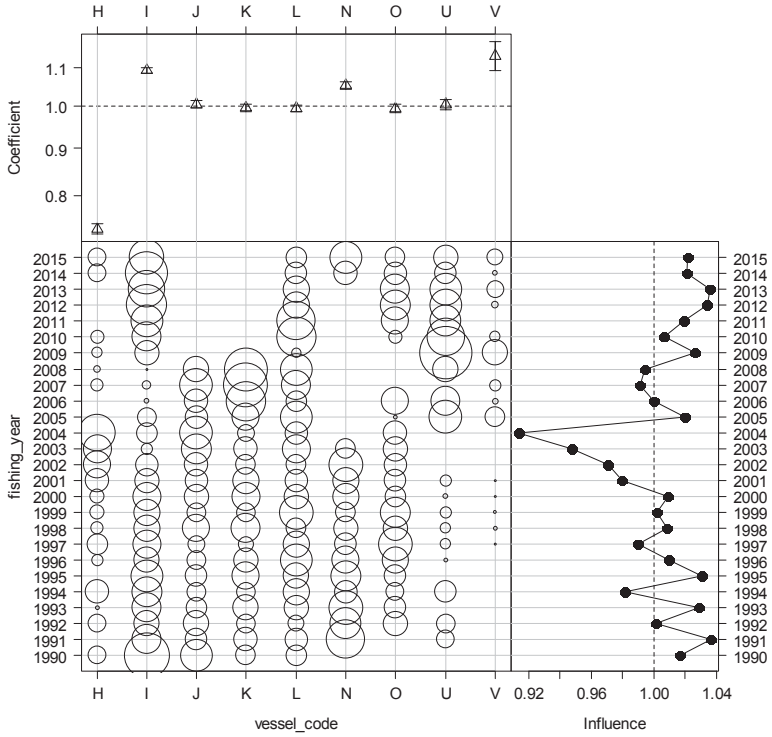

A2. 10: Coefficient-distribution influence plot for vessel for final SCI 2 CPUE standardisation model (Table 8).

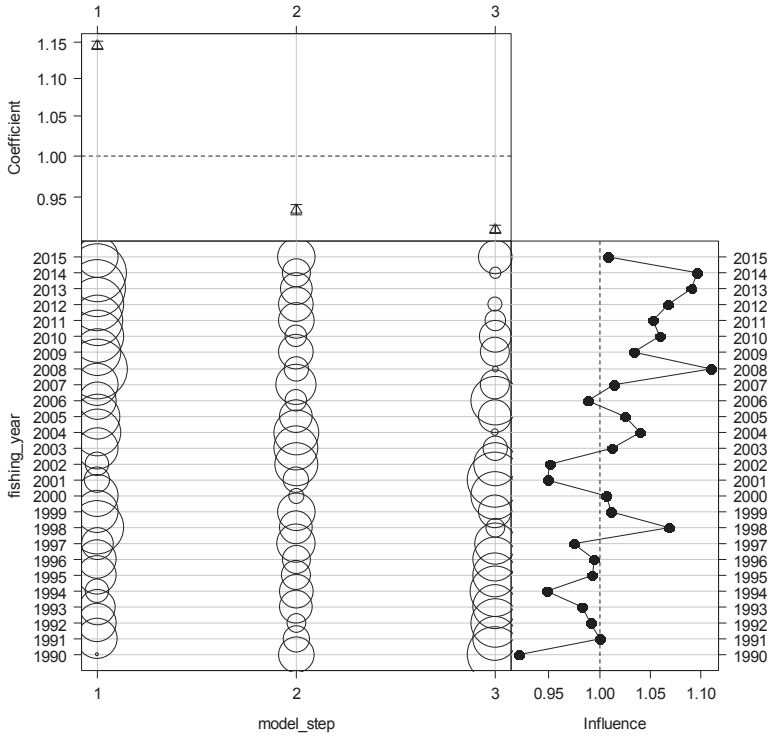

A2. 11: Coefficient-distribution influence plot for timestep for final SCI 2 CPUE standardisation model (Table 8).

APPENDIX 3. Analysis of length composition data (SCI 1)

Trawl survey length frequency

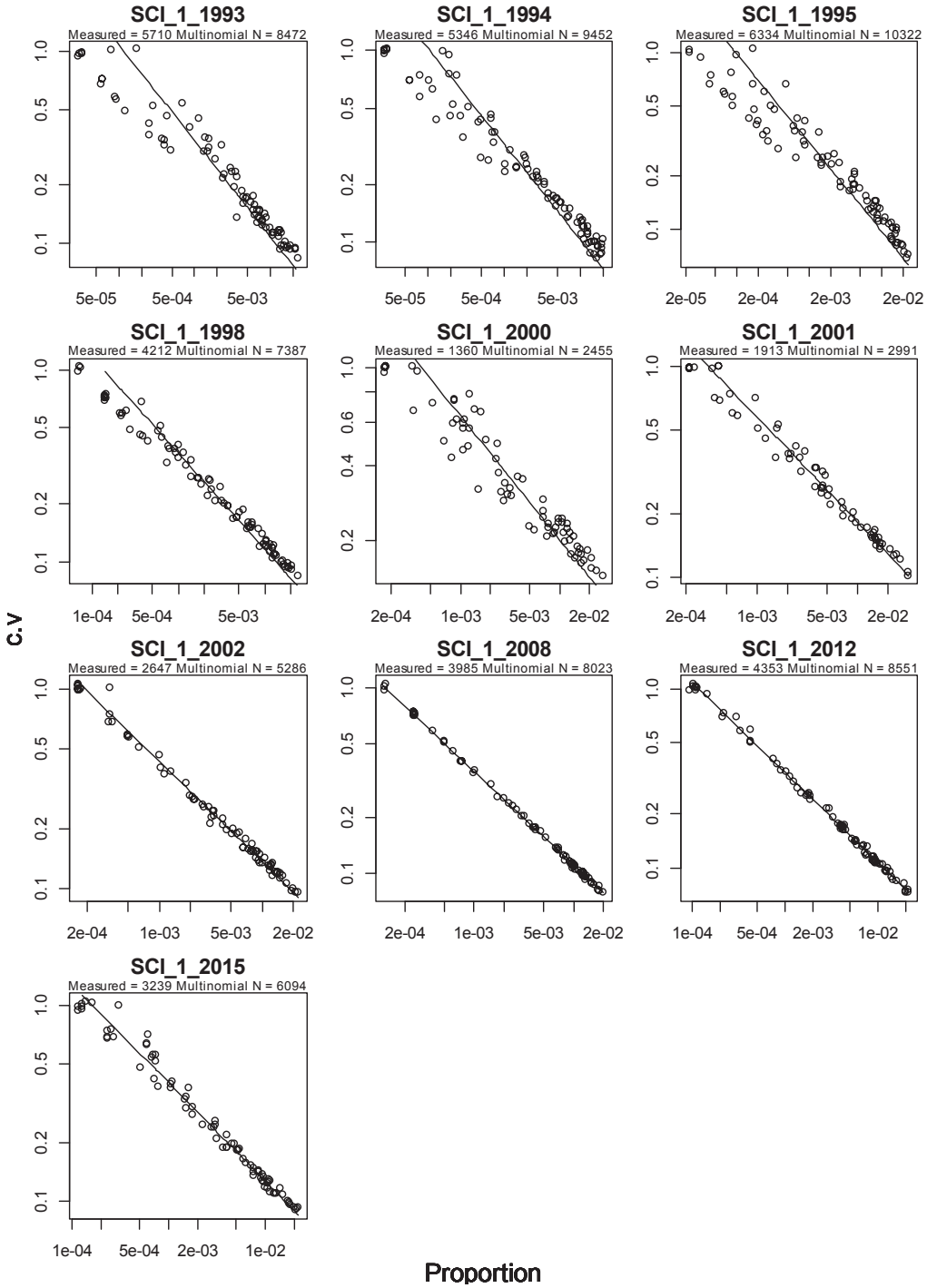

A3. 1: Observation-error CVs for the SCI 1 trawl survey proportions-at-length data sets. Each point represents a proportion at a specific length and sex for a given year. The diagonal line, which is the same in each panel, is added to aid comparison between panels; it shows the relationship between proportion and CV that would hold with simple multinomial sampling with sample size 500.

Observer length frequency

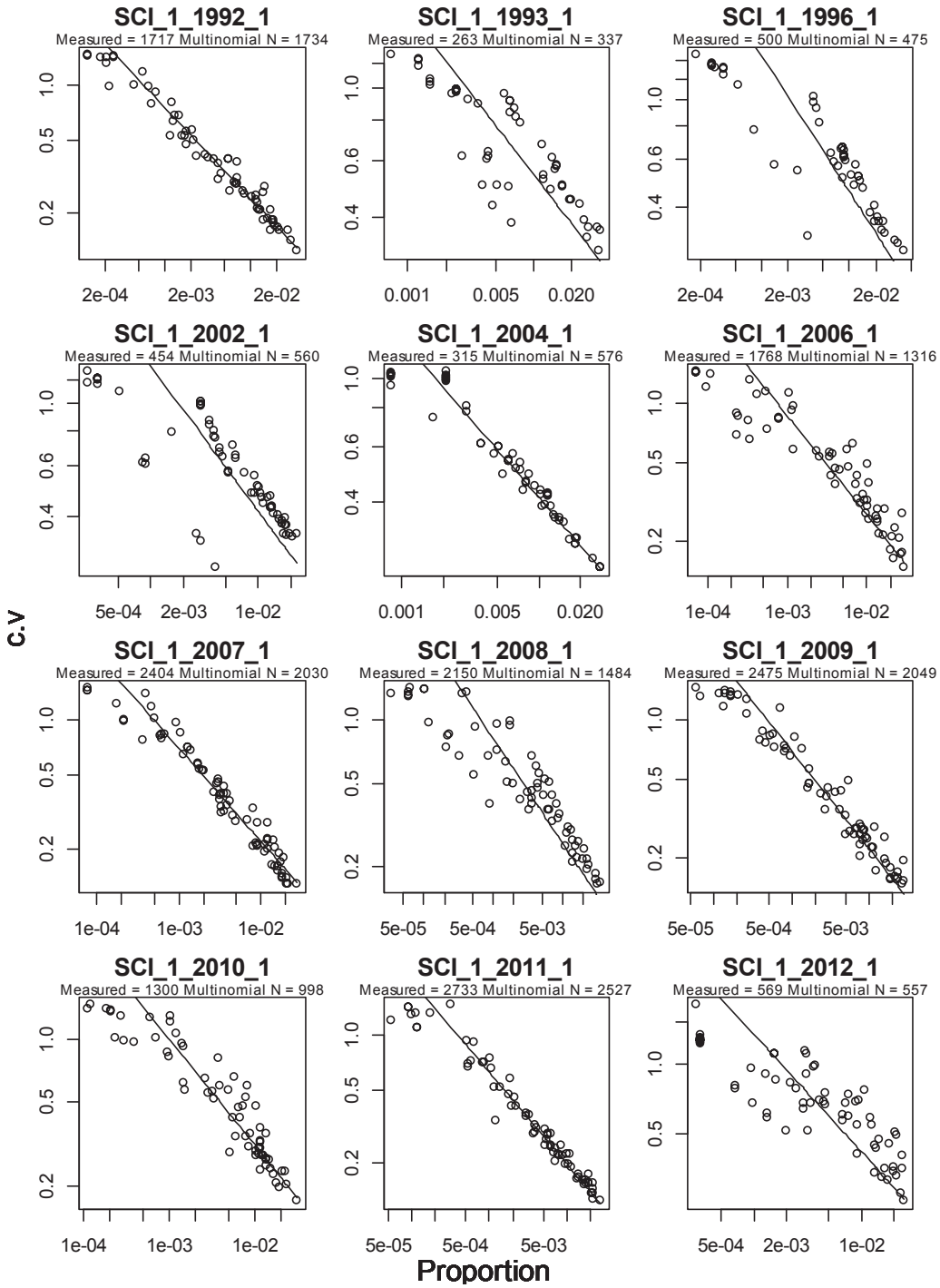

A3. 2: Observation-error CVs for the SCI 1 step 1 observer proportions-at-length data sets. Each point represents a proportion at a specific length and sex for a given year. The diagonal line, which is the same in each panel, is added to aid comparison between panels; it shows the relationship between proportion and CV that would hold with simple multinomial sampling with sample size 500.

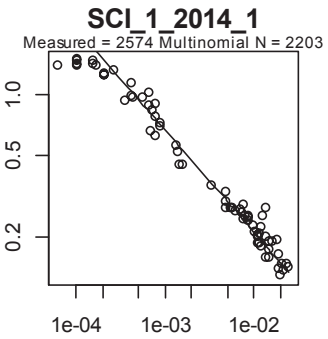

A3.2 (continued): Observation-error CVs for the SCI 1 step 1 observer proportions-at-length data sets. Each point represents a proportion at a specific length and sex for a given year. The diagonal line, which is the same in each panel, is added to aid comparison between panels; it shows the relationship between proportion and CV that would hold with simple multinomial sampling with sample size 500.

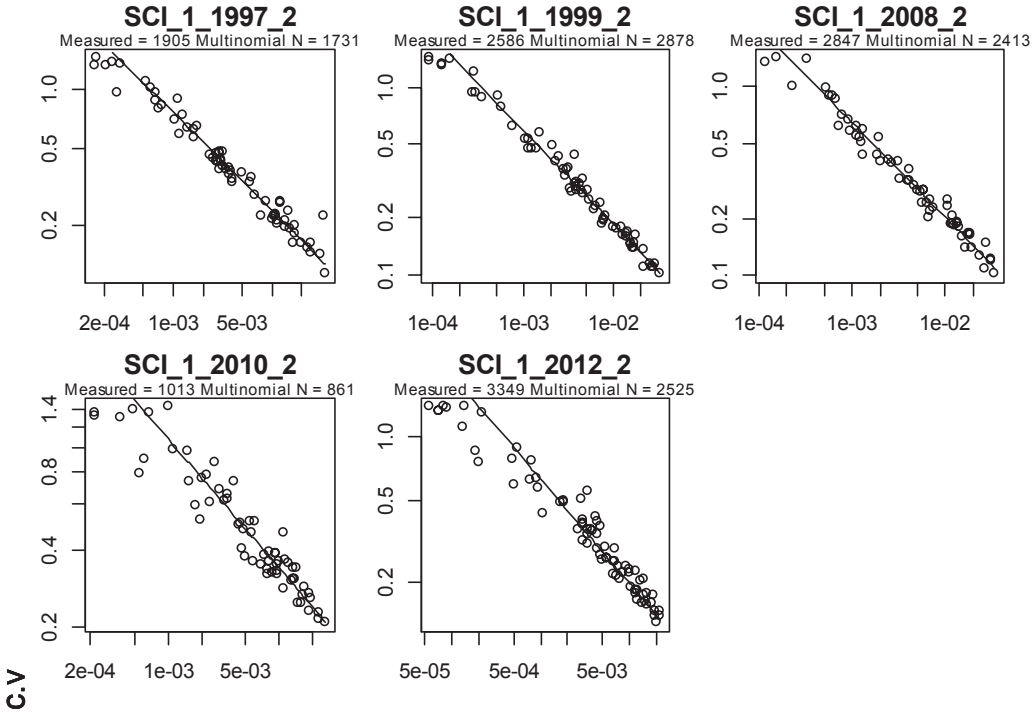

A3. 3: Observation-error CVs for the SCI 1 step 2 observer proportions-at-length data sets. Each point represents a proportion at a specific length and sex for a given year. The diagonal line, which is the same in each panel, is added to aid comparison between panels; it shows the relationship between proportion and CV that would hold with simple multinomial sampling with sample size 500.

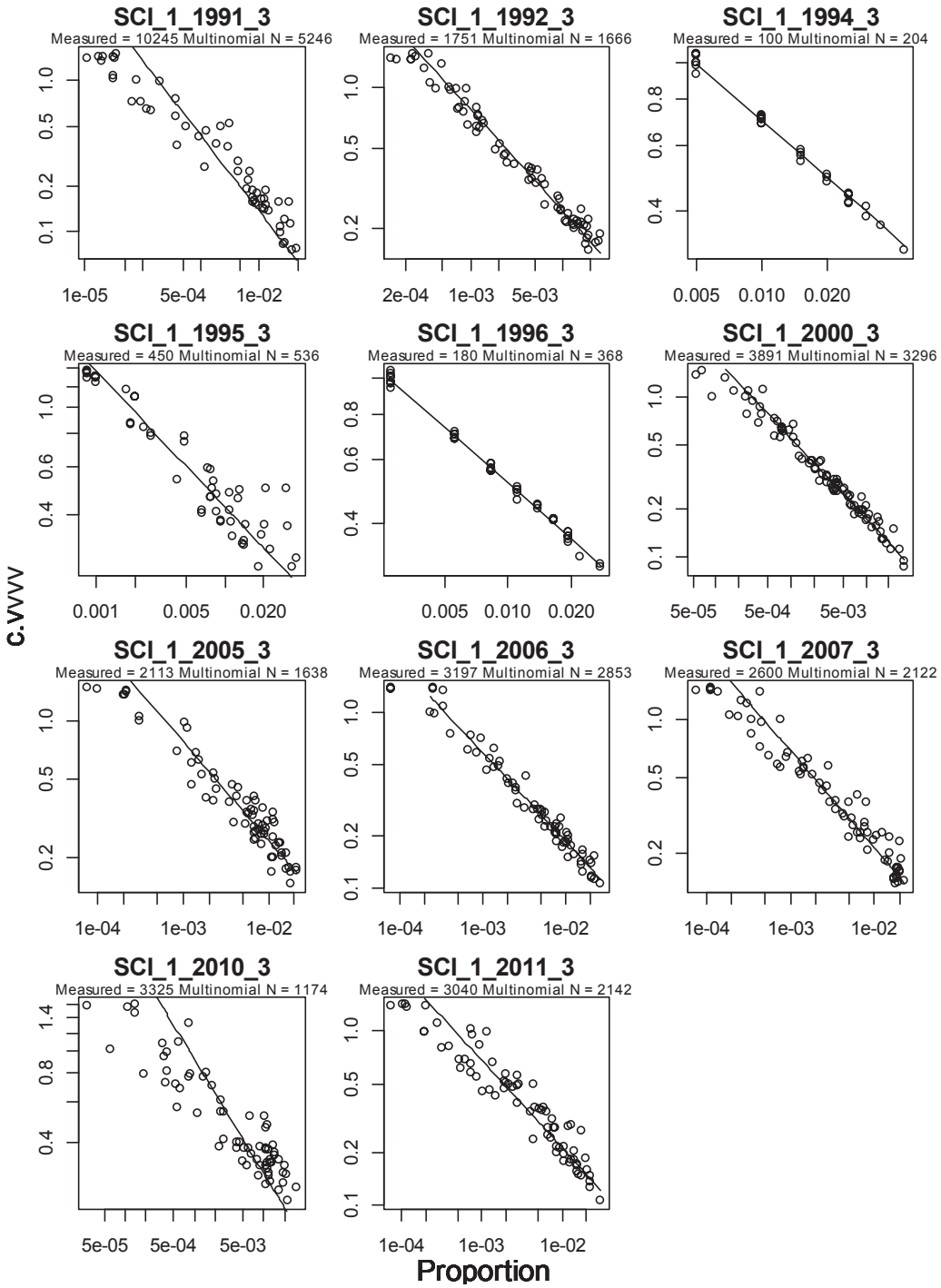

A3. 4: Observation-error CVs for the SCI 1 step 3 observer proportions-at-length data sets. Each point represents a proportion at a specific length and sex for a given year. The diagonal line, which is the same in each panel, is added to aid comparison between panels; it shows the relationship between proportion and CV that would hold with simple multinomial sampling with sample size 500.

Photo Survey

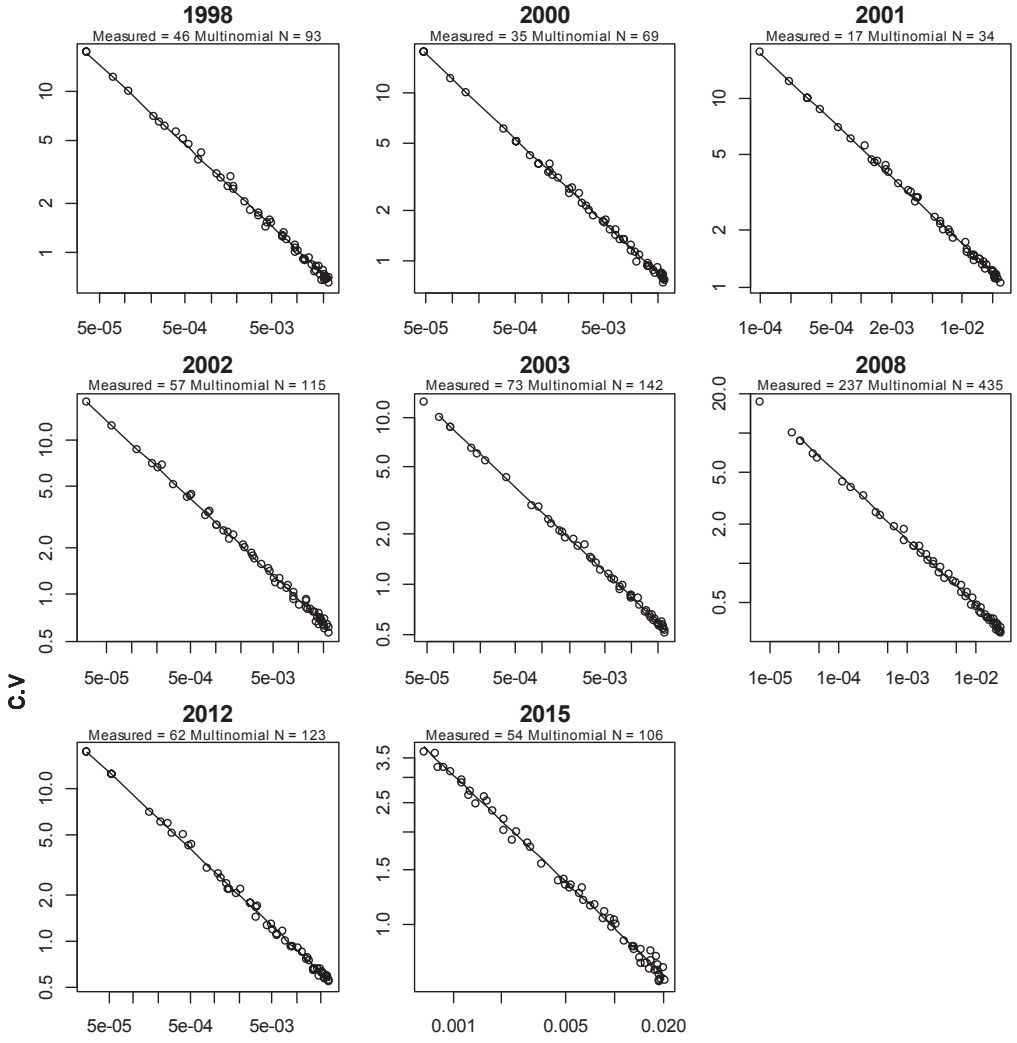

A3. 5: Observation-error CVs for the SCI 1 photo survey proportions-at-length data sets. Each point represents a proportion at a specific length and sex for a given year. The diagonal line, which is the same in each panel, is added to aid comparison between panels; it shows the relationship between proportion and CV that would hold with simple multinomial sampling with sample size 500.

APPENDIX 4. Analysis of length composition data (SCI 2)

Trawl survey length frequency

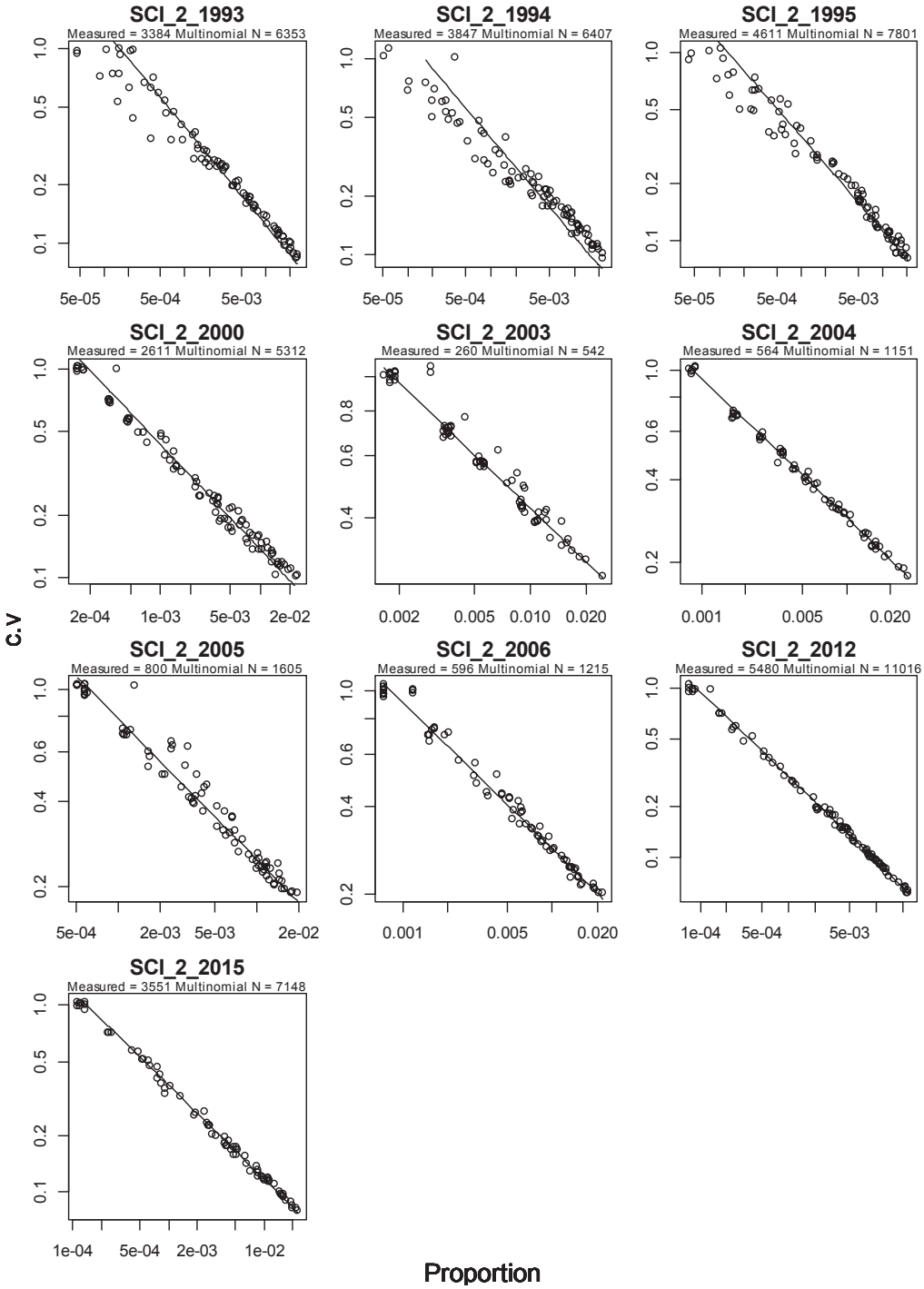

A4. 1: Observation-error CVs for the SCI 2 trawl survey proportions-at-length data sets. Each point represents a proportion at a specific length and sex for a given year. The diagonal line, which is the same in each panel, is added to aid comparison between panels; it shows the relationship between proportion and CV that would hold with simple multinomial sampling with sample size 500.

Observer length frequency

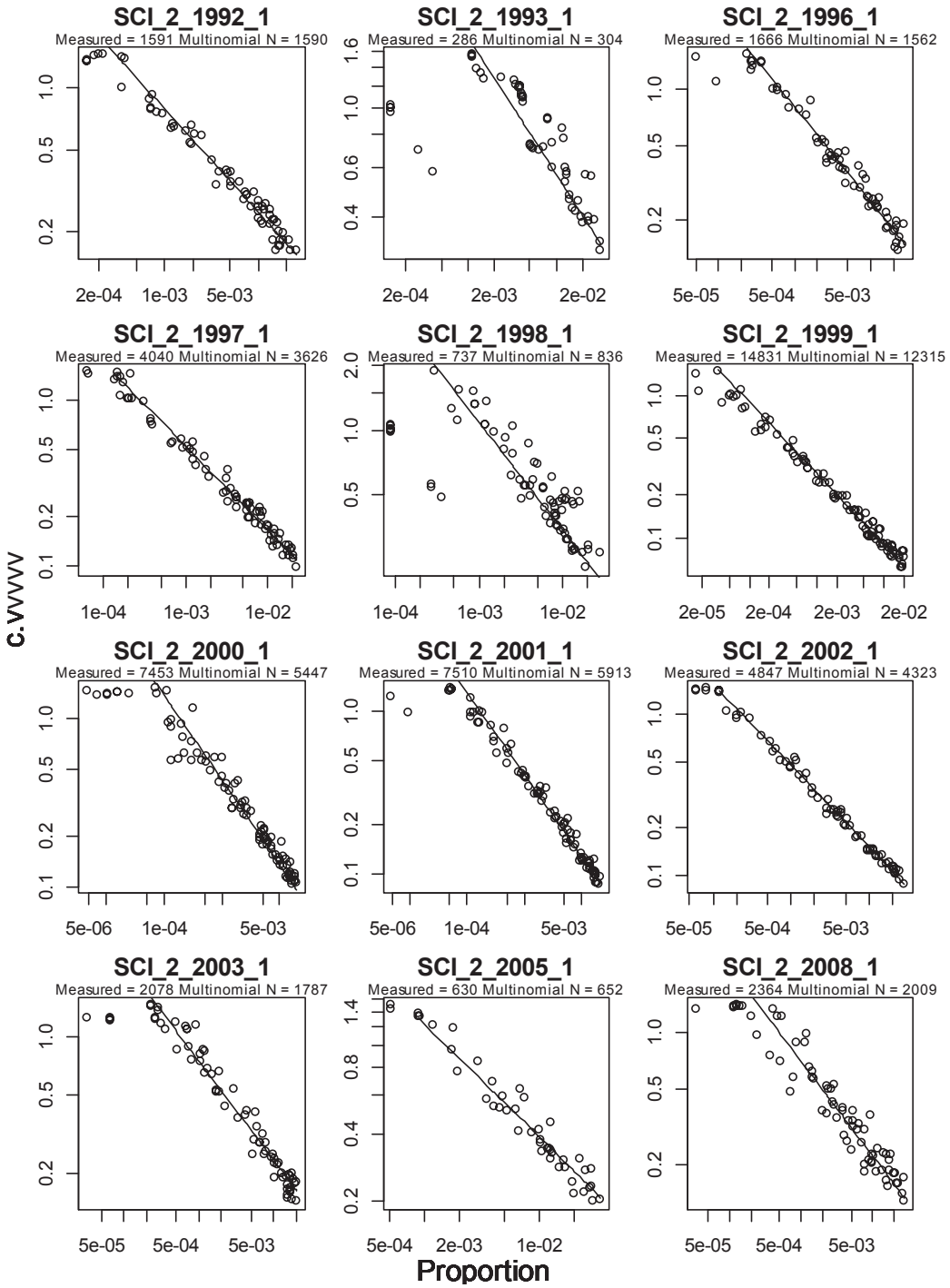

A4. 2: Observation-error CVs for the SCI 2 step 1 observer proportions-at-length data sets. Each point represents a proportion at a specific length and sex for a given year. The diagonal line, which is the same in each panel, is added to aid comparison between panels; it shows the relationship between proportion and CV that would hold with simple multinomial sampling with sample size 500.

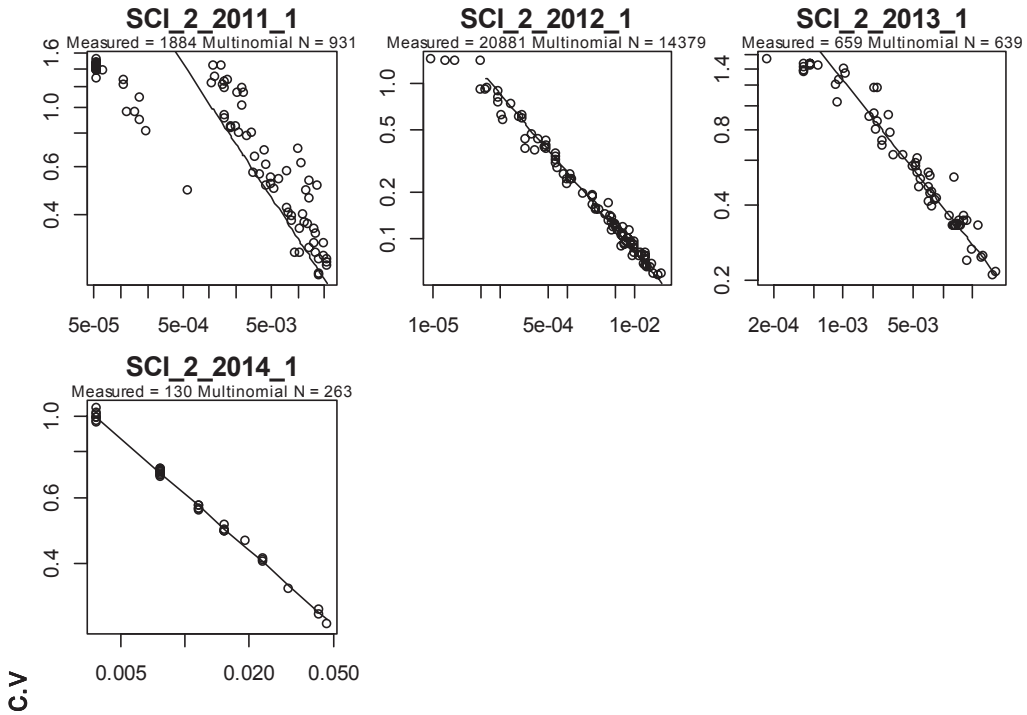

A4. 2 (continued): Observation-error CVs for the SCI 2 step 1 observer proportions-at-length data sets. Each point represents a proportion at a specific length and sex for a given year. The diagonal line, which is the same in each panel, is added to aid comparison between panels; it shows the relationship between proportion and CV that would hold with simple multinomial sampling with sample size 500.

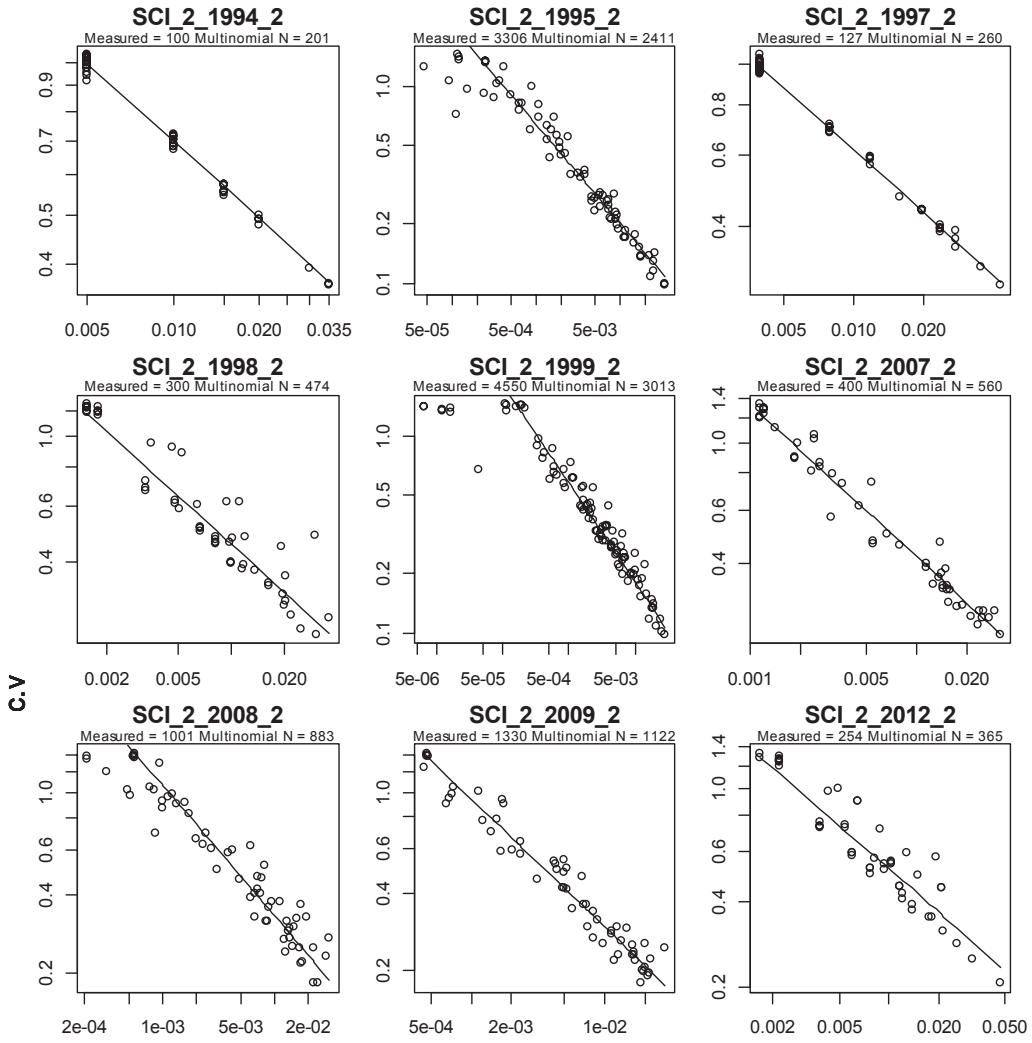

A4. 3: Observation-error CVs for the SCI 2 step 2 observer proportions-at-length data sets. Each point represents a proportion at a specific length and sex for a given year. The diagonal line, which is the same in each panel, is added to aid comparison between panels; it shows the relationship between proportion and CV that would hold with simple multinomial sampling with sample size 500.

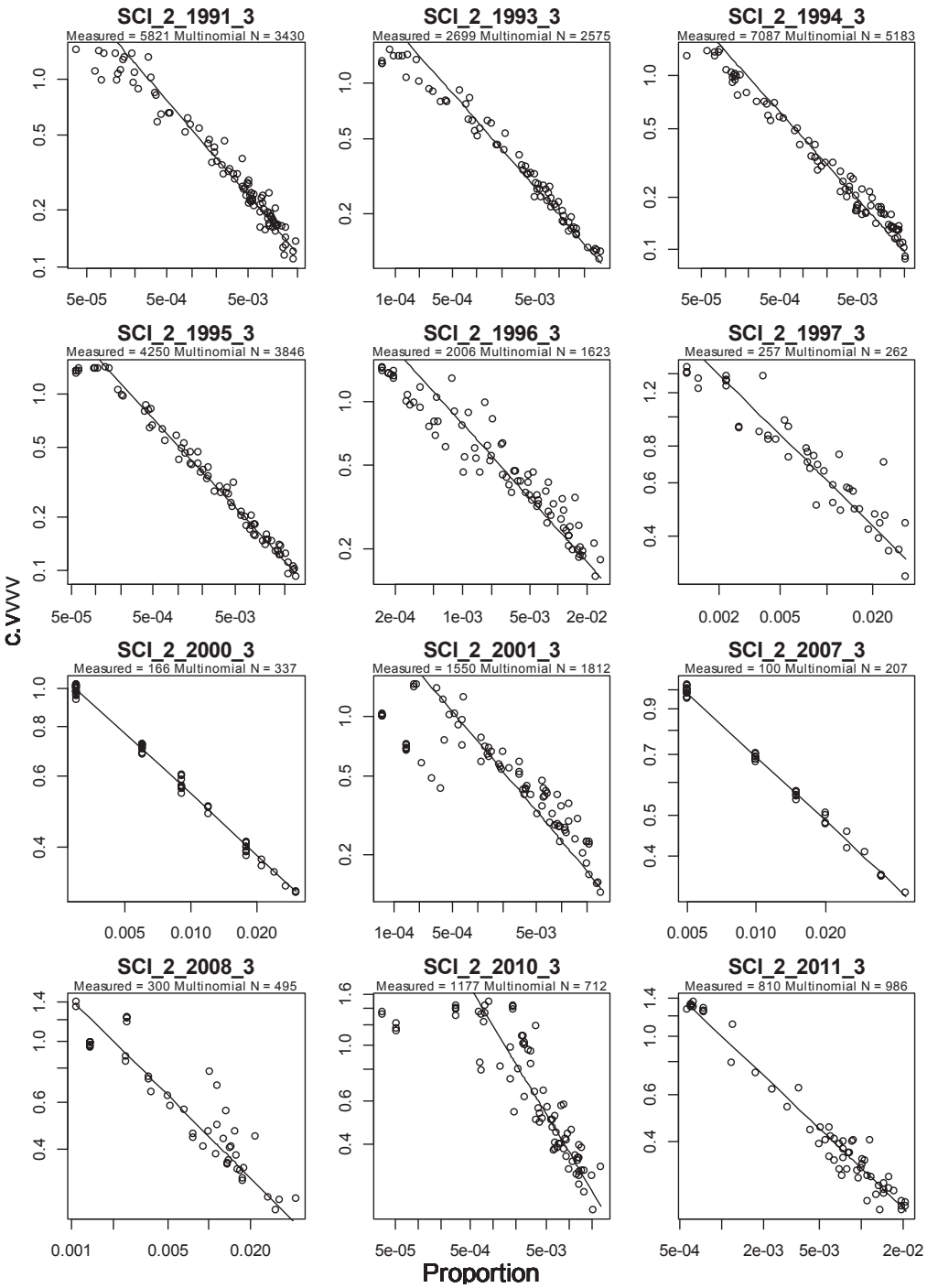

A4. 4: Observation-error CVs for the SCI 2 step 3 observer proportions-at-length data sets. Each point represents a proportion at a specific length and sex for a given year. The diagonal line, which is the same in each panel, is added to aid comparison between panels; it shows the relationship between proportion and CV that would hold with simple multinomial sampling with sample size 500.

Photo survey

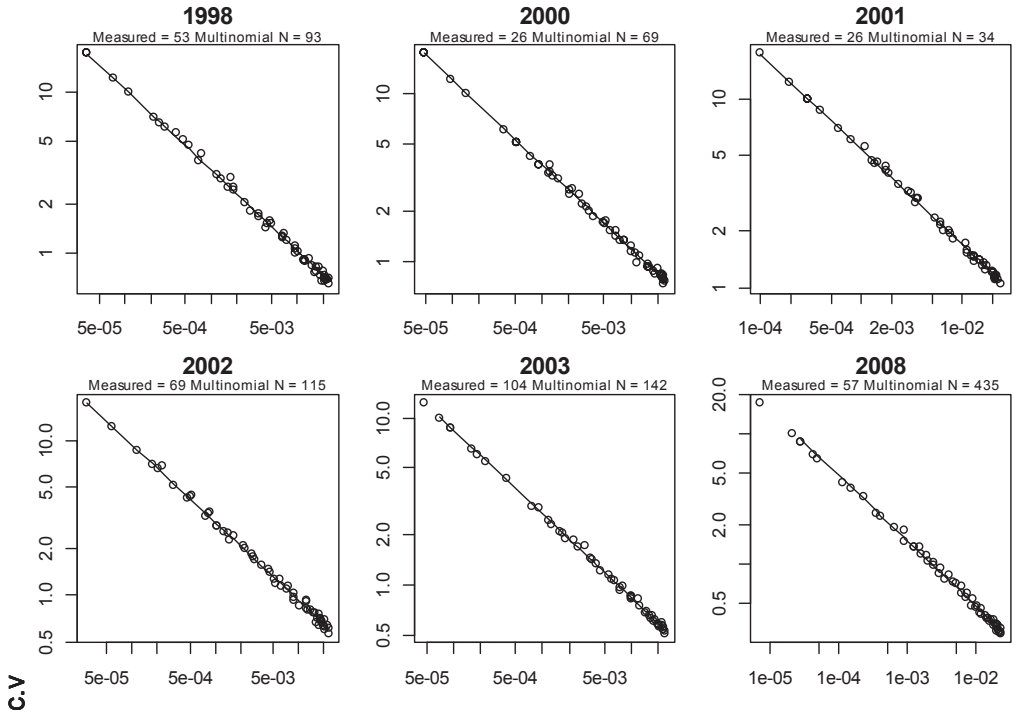

A4. 5: Observation-error CVs for the SCI 2 photo survey proportions-at-length data sets. Each point represents a proportion at a specific length and sex for a given year. The diagonal line, which is the same in each panel, is added to aid comparison between panels; it shows the relationship between proportion and CV that would hold with simple multinomial sampling with sample size 500.

APPENDIX 5. SCI 1 BASE25 model plots (M=0.25)

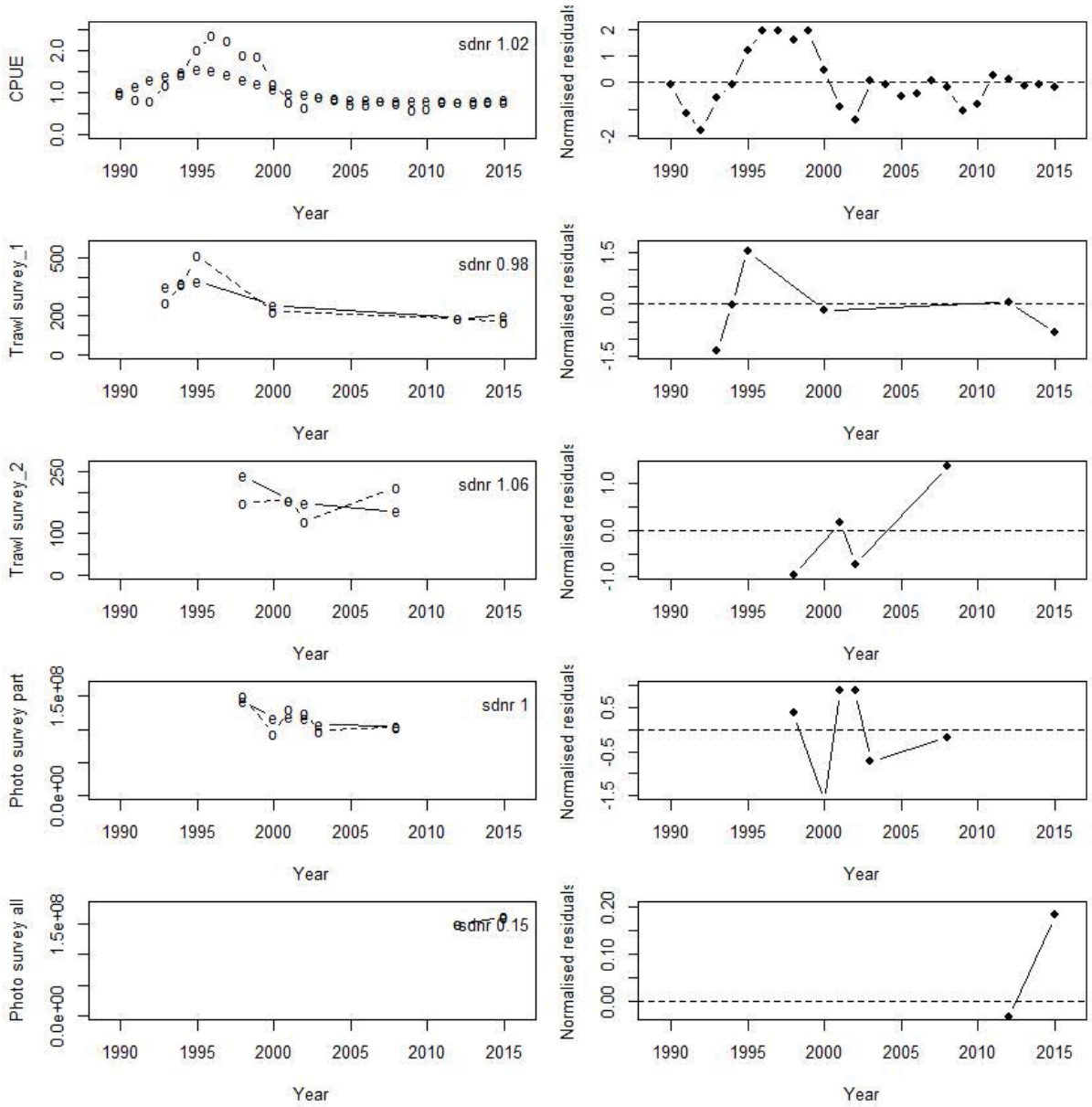

A5. 1: Fits to abundance indices (left column) and normalised residuals (right column) for standardised CPUE index (top row) trawl survey biomass index covering whole area (second row), trawl survey biomass index covering limited area (third row), photo survey abundance index covering limited area (fourth row) and photo survey abundance index covering whole area (fifth row) for SCI 1 Base25 model.

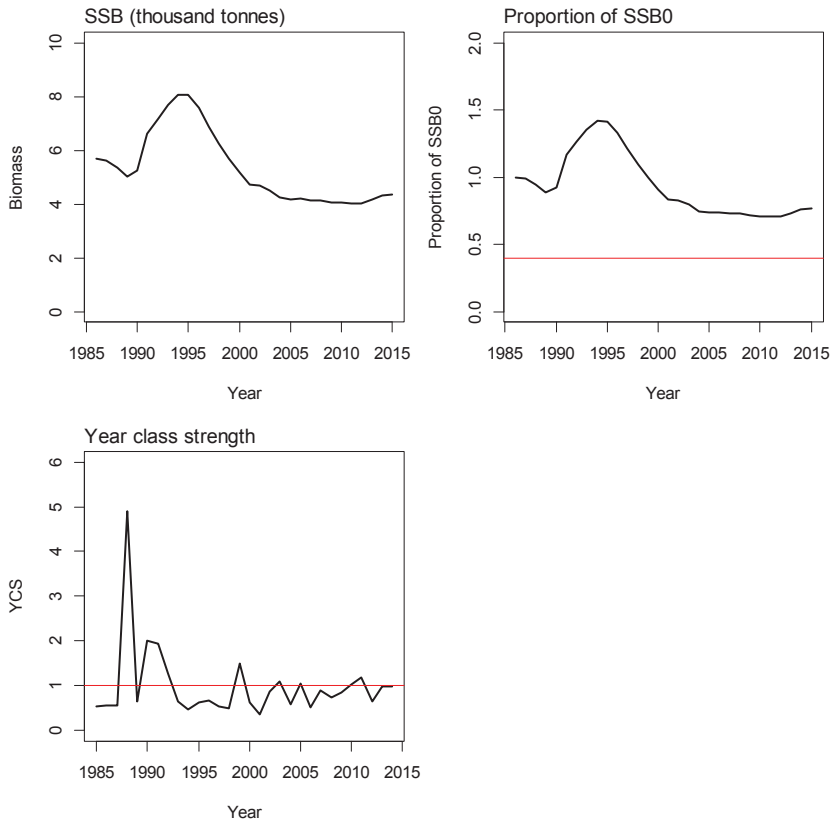

A5. 2: Spawning stock biomass trajectory (upper left), stock status (upper right), and year class strength (lower left) for SCI 1 Base25 model.

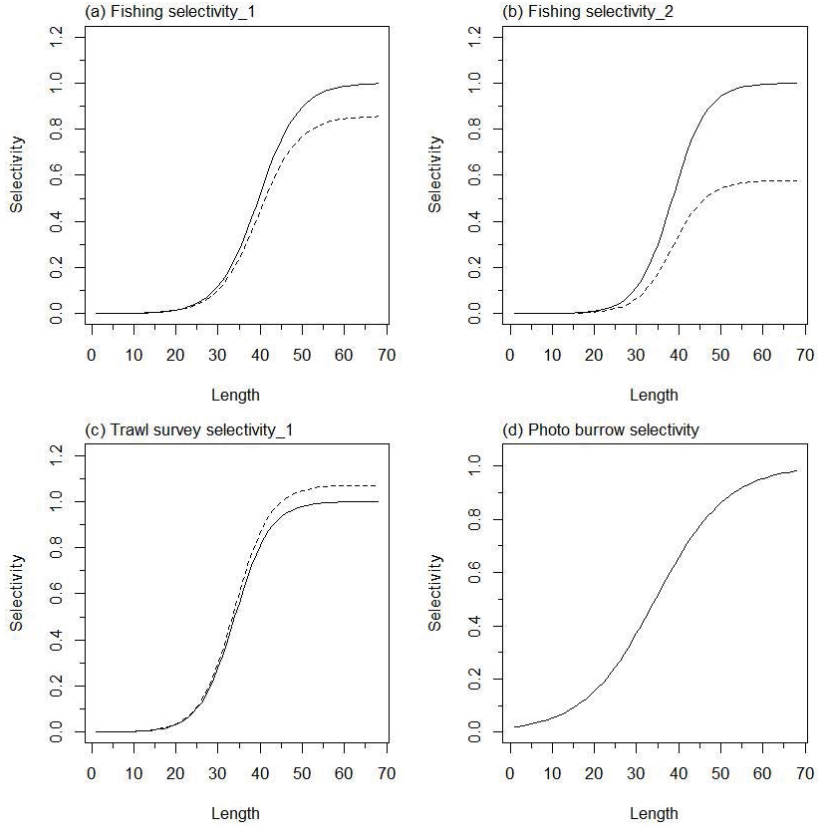

A5. 3: Fishery and survey selectivity curves for SCI 1 Base25 model. Solid line – females, dotted line – males. The scampi burrow index is not sexed, and a single selectivity applies.

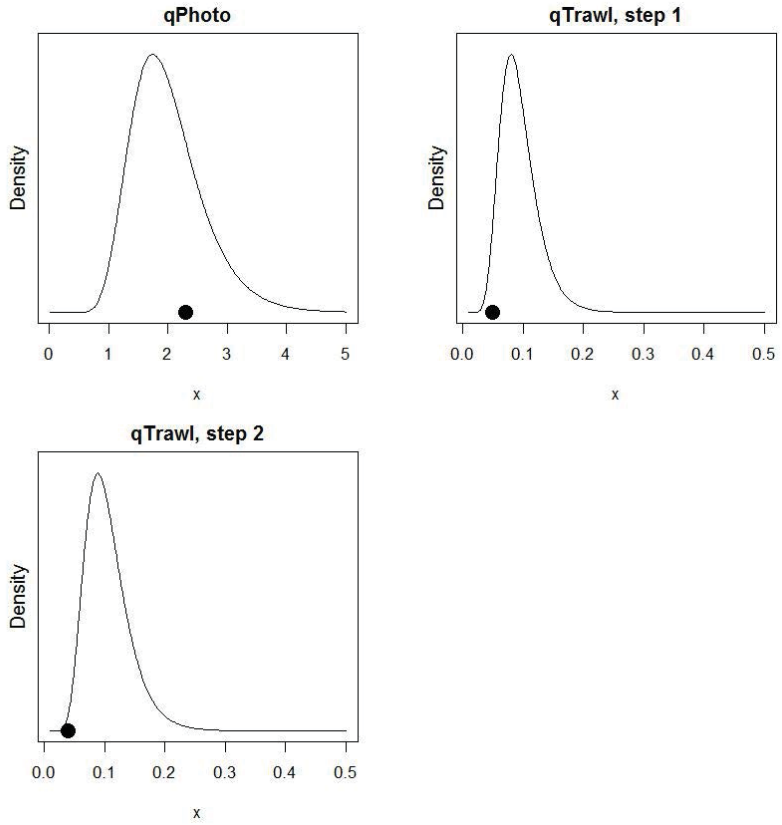

A5. 4: Catchability estimates from MPD model run, plotted in relation to prior distribution for SCI 1 Base25 model.

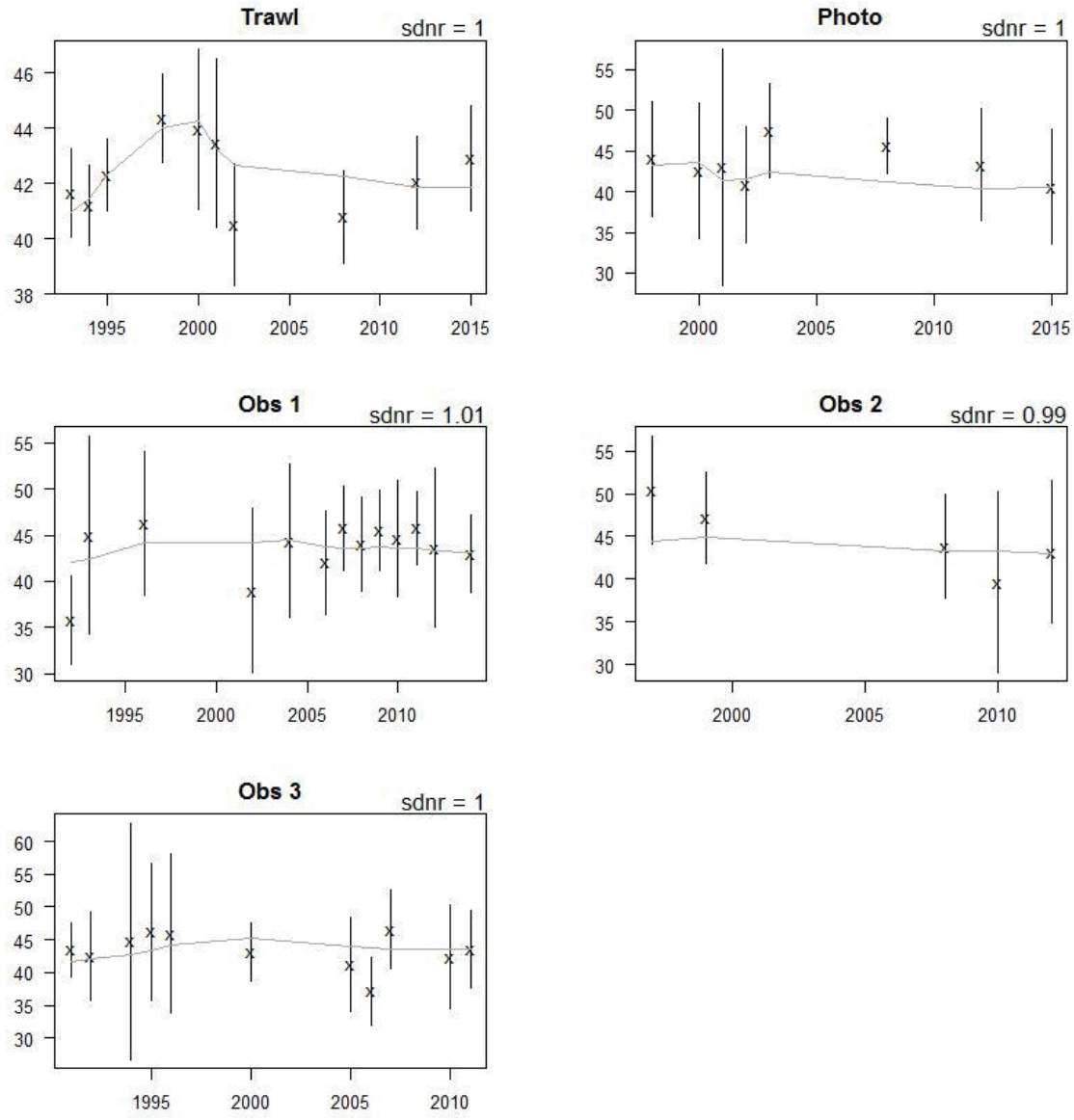

A5. 5: Observed (crosses, with vertical lines representing ± two standard errors) and fitted (grey line) mean length from length frequency distributions for survey and observer samples for SCI 1 Base25 model.

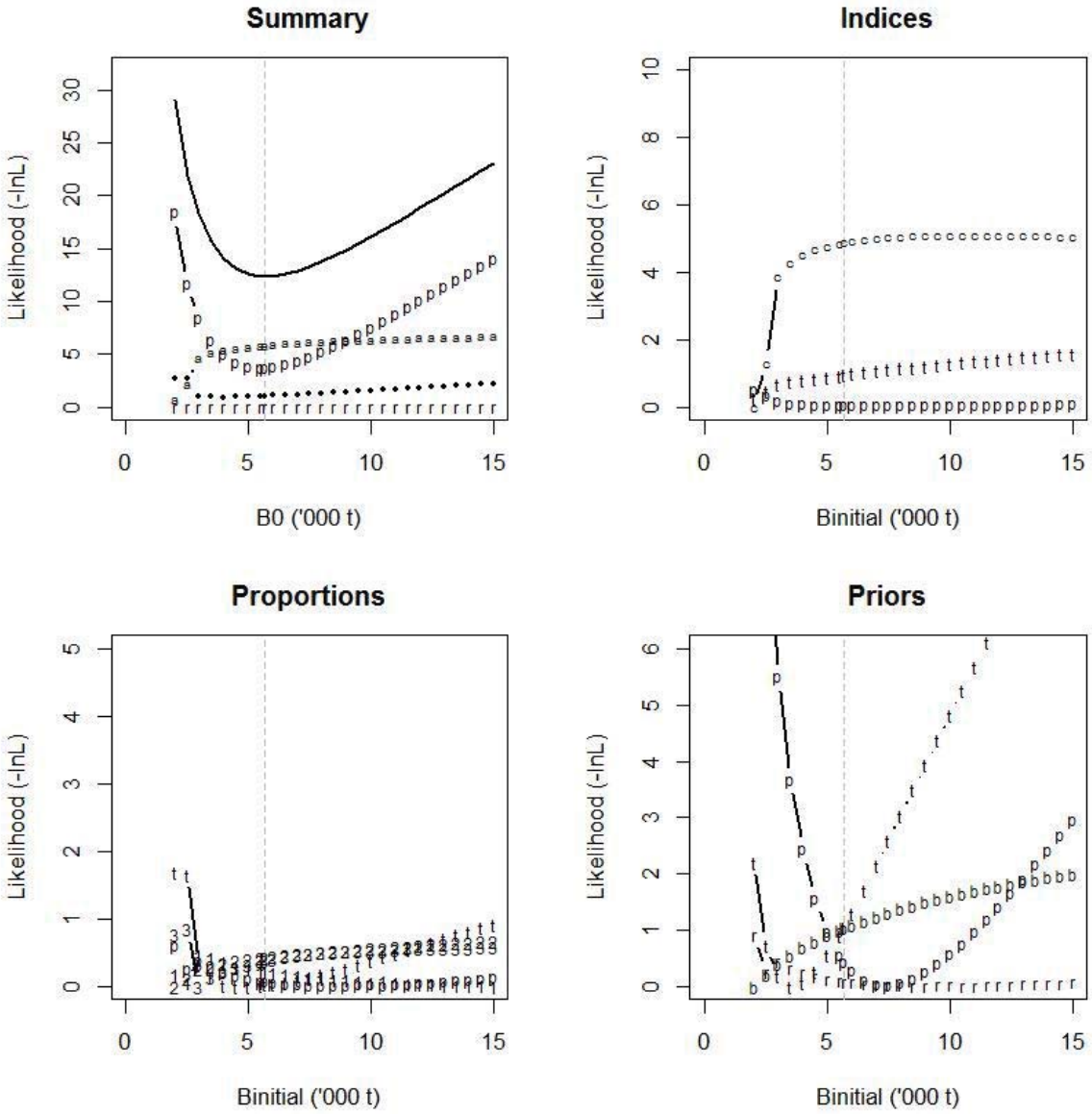

A5. 6: Likelihood profiles for model Base25 for SCI 1 when B_0 is fixed in the model. Figures show profiles for main priors (top left, p-priors, a – abundance indices, • – proportions at length, r-recapture data), abundance indices (top right, t - trawl survey step, c - CPUE, p – photo survey), proportion at length data (bottom left, p-photo, t-trawl, 1 – observer time step 1, 2 – observer time step 2, 3 – observer time step 3) and priors (bottom right, b- B_0, YCS - r, p- *q-Photo*, t – *q-Trawl*).

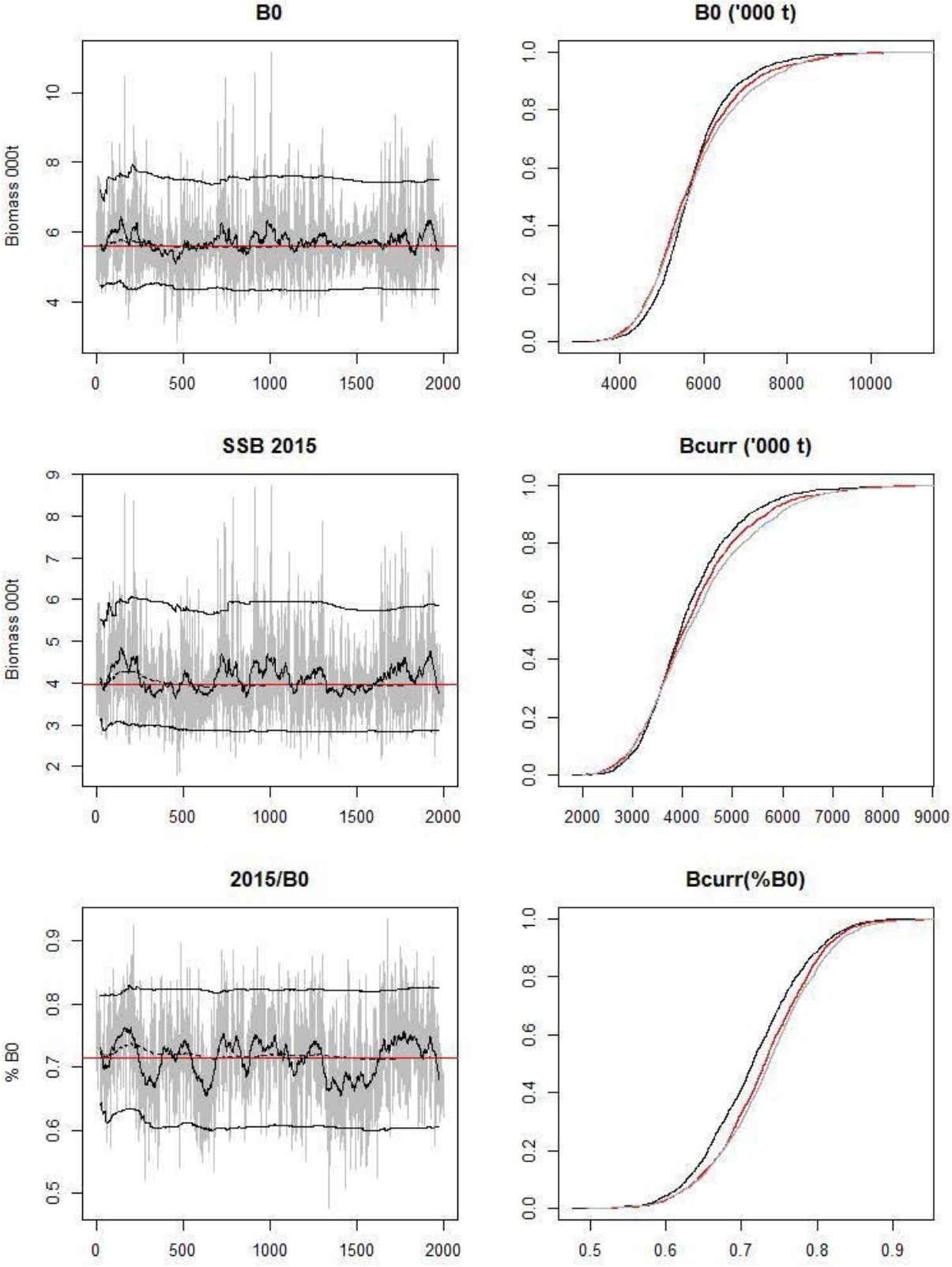

A5. 7: MCMC traces for B_0, SSB_{2015}, and SSB_{2015}/B_0 terms for SCI 1 Base25 model, along with cumulative frequency distributions for three independent MCMC chains.

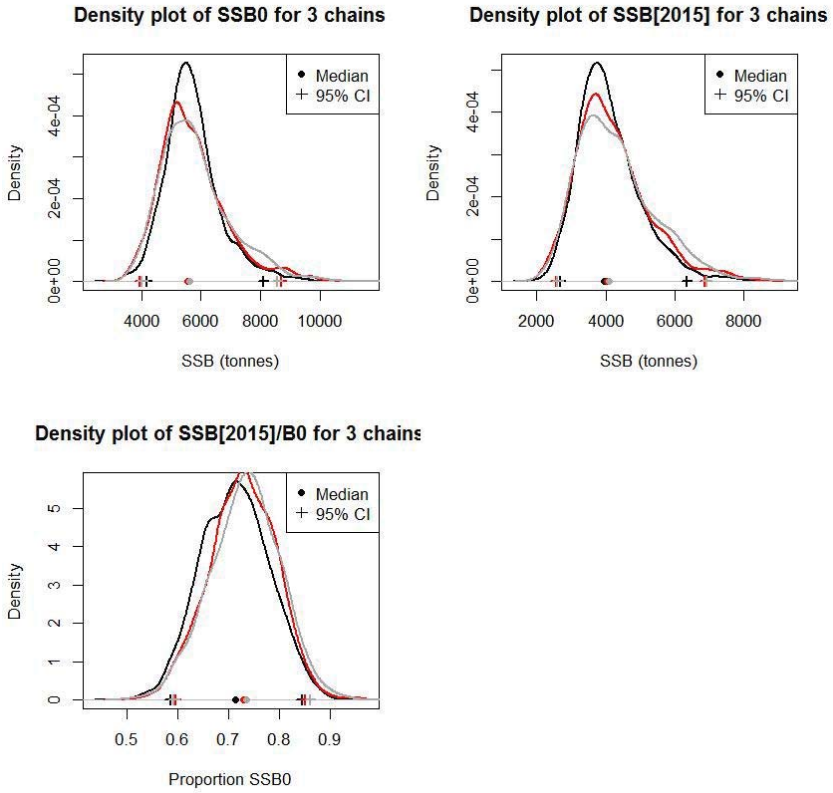

A5. 8: Density plots for B_0, SSB_{2015}, and SSB_{2015}/B_0 terms SCI 1 Base25 model for three independent MCMC chains, with median and 95% confidence intervals.

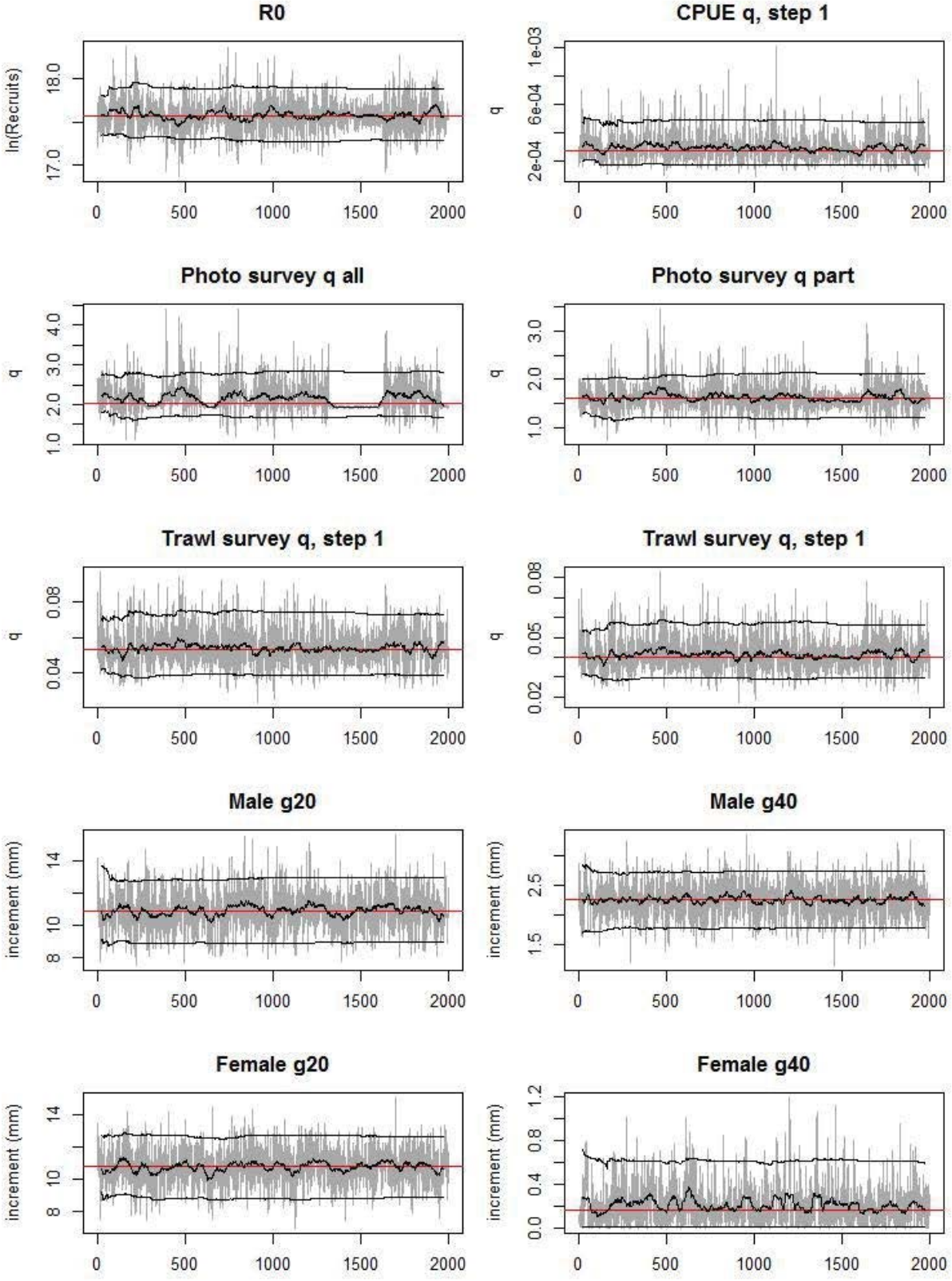

A5. 9: MCMC traces for R_0, catchability and growth terms for SCI 1 Base25 model.

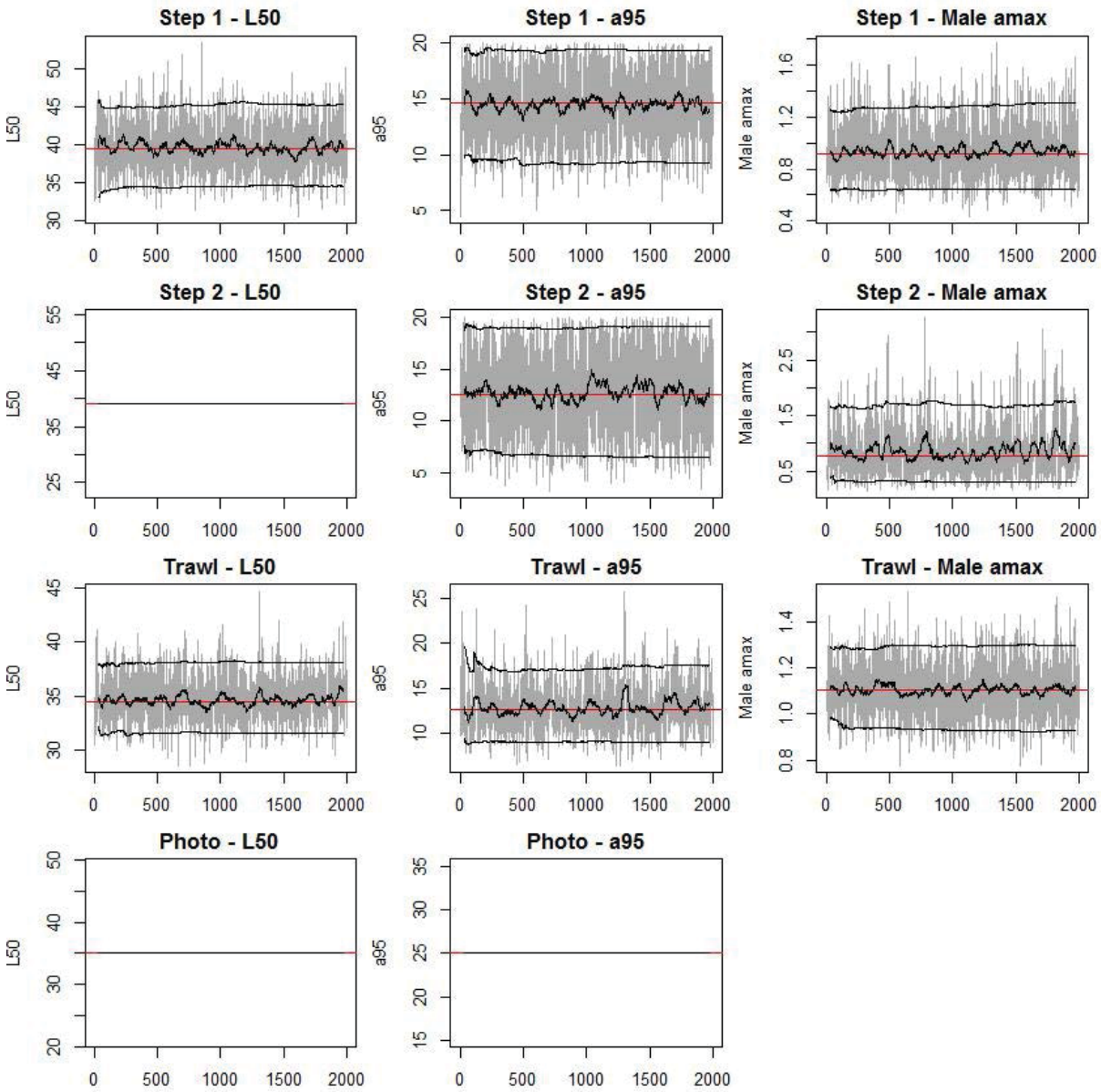

A5. 10: MCMC traces for selectivity terms for SCI 1 Base25 model. Horizontal lines represent terms fixed in the model.

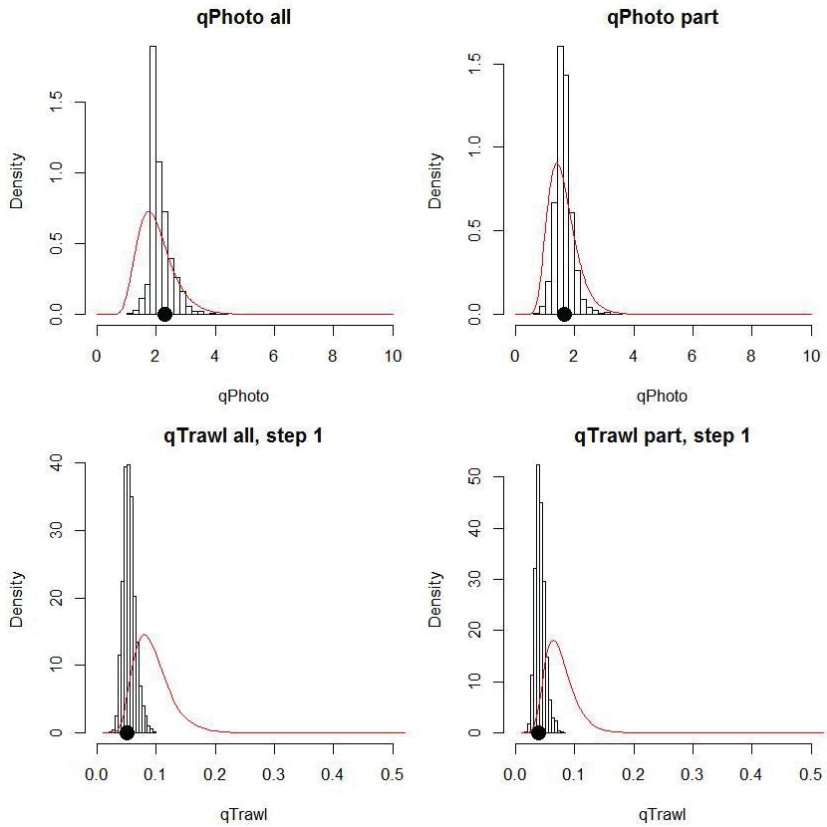

A5. 11: Marginal posterior distributions (histograms), MPD estimates (solid symbols) and distributions of priors (lines) for catchability terms SCI 1 Base25 model.

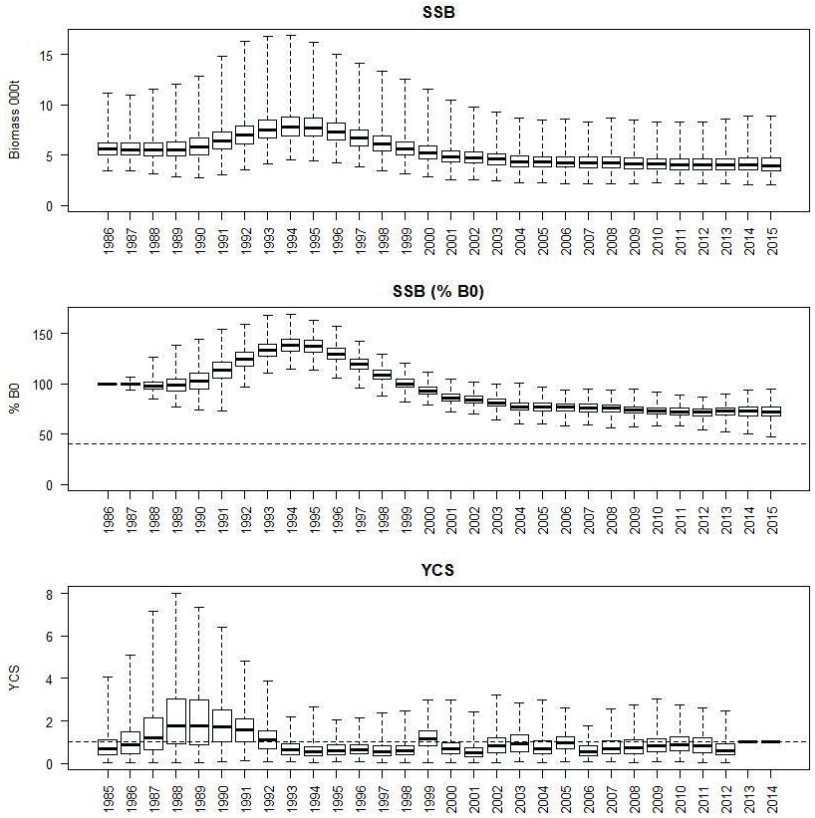

A5. 12: Posterior trajectory of SSB, SSB/SSB$_0$ and YCS SCI 1 Base25 model.

APPENDIX 6. SCI 1 Base30 model plots (M=0.3)

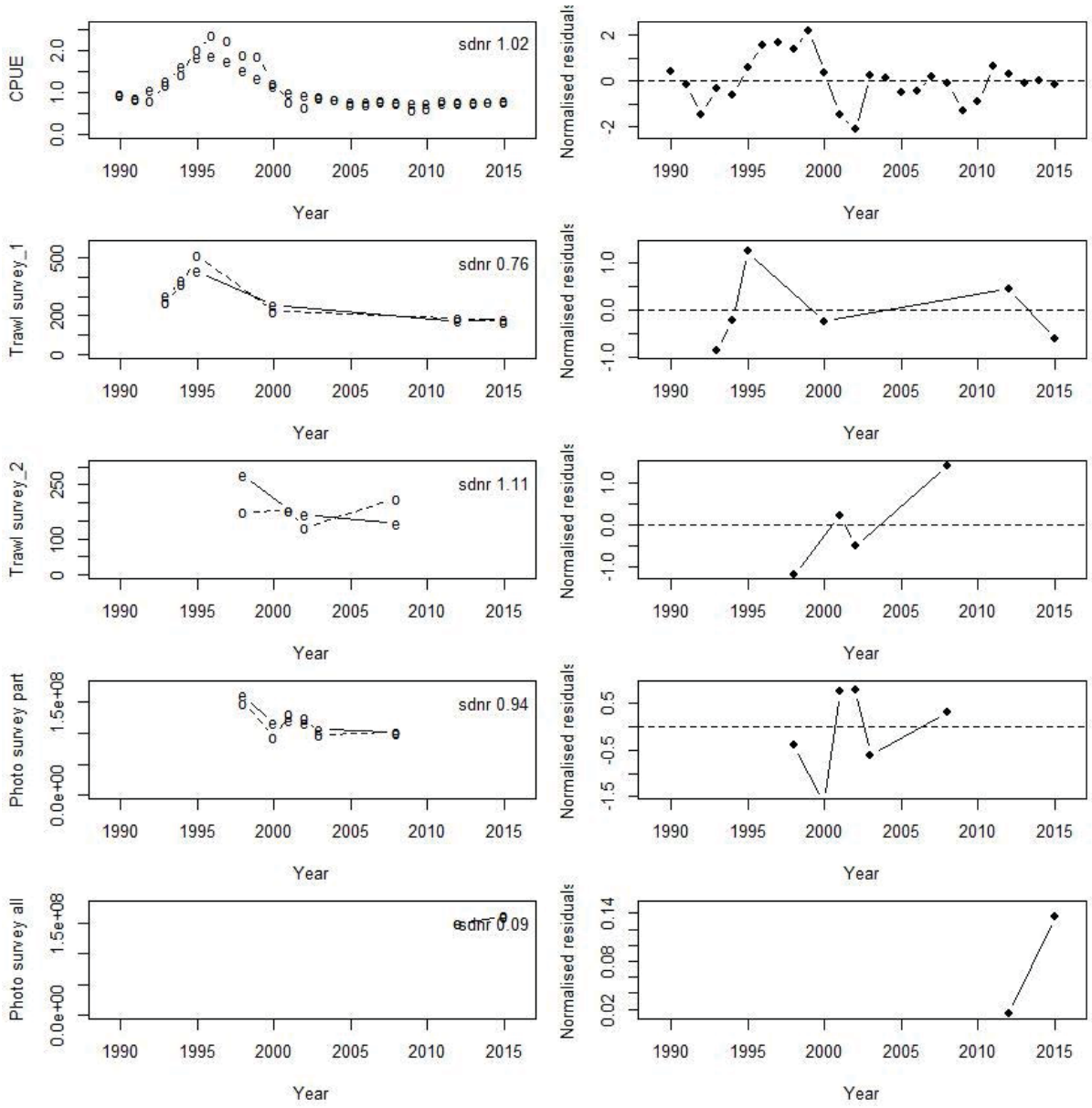

A6. 1: Fits to abundance indices (left column) and normalised residuals (right column) for standardised CPUE index (top row) trawl survey biomass index covering whole area (second row), trawl survey biomass index covering limited area (third row), photo survey abundance index covering limited area (fourth row) and photo survey abundance index covering whole area (fifth row) for the SCI 1 Base30 model.

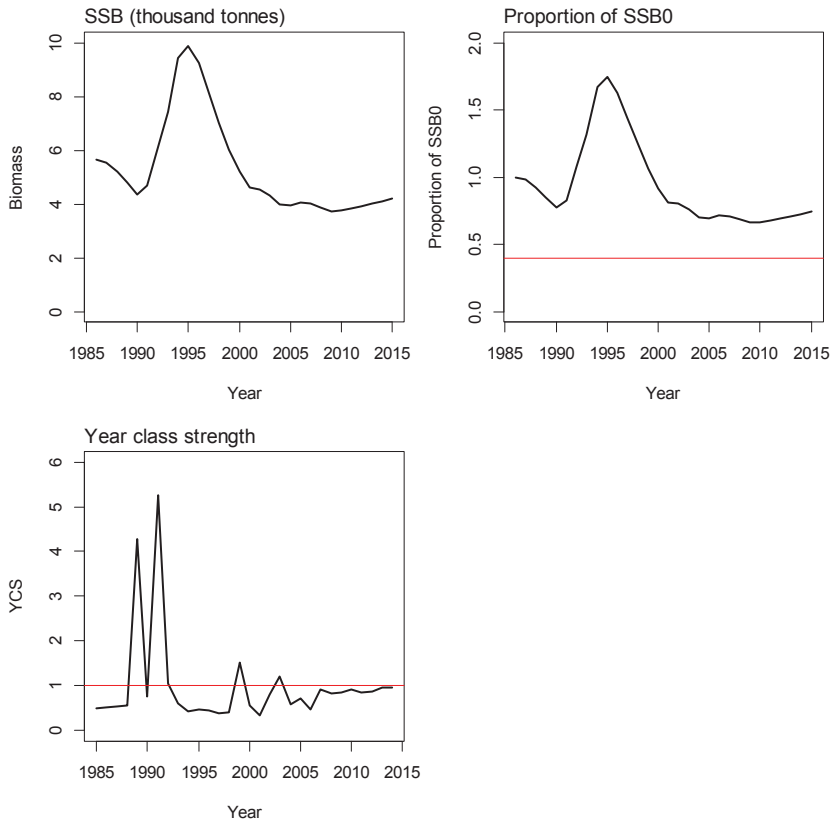

A6. 2: Spawning stock biomass trajectory (upper left), stock status (upper right), and year class strength (lower left) for the SCI 1 Base25 model.

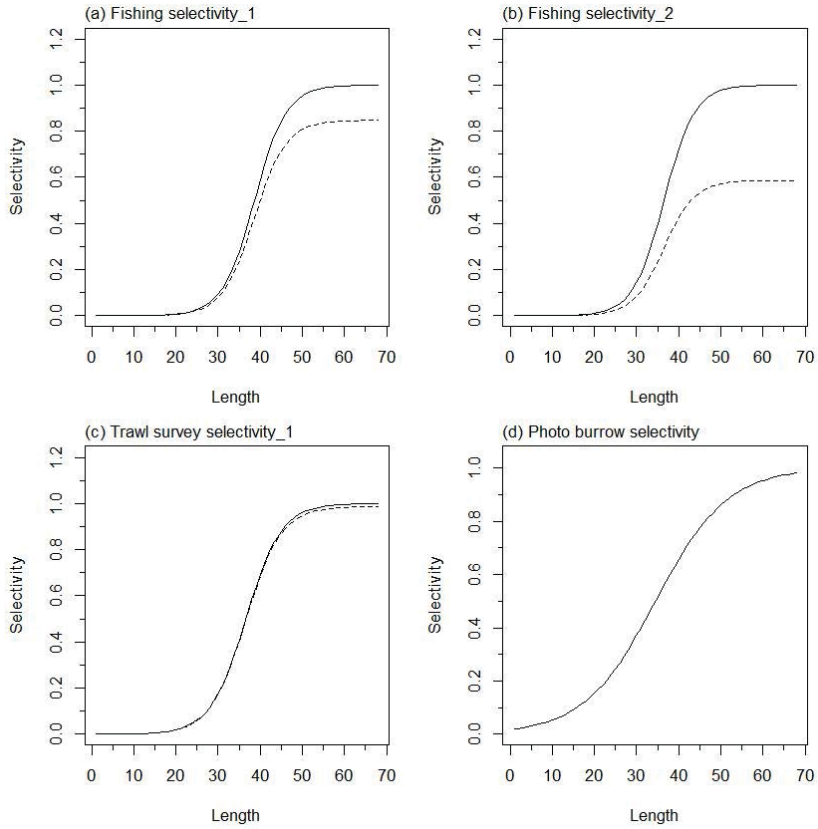

A6. 3: Fishery and survey selectivity curves for the SCI 1 Base30 model. Solid line – females, dotted line – males. The scampi burrow index is not sexed, and a single selectivity applies.

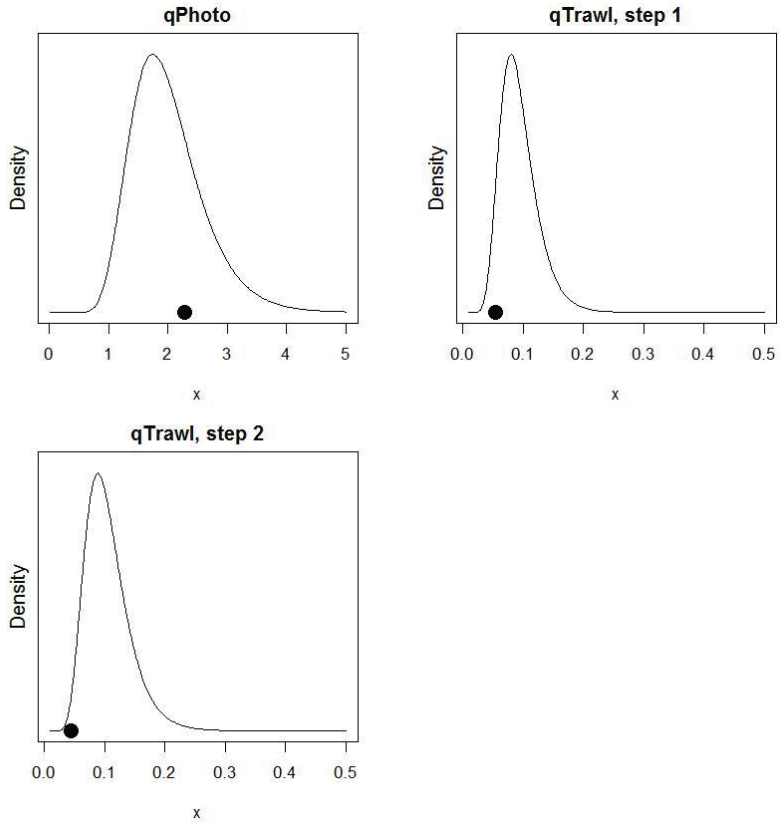

A6. 4: Catchability estimates from MPD model run, plotted in relation to prior distribution for the SCI 1 Base30 model.

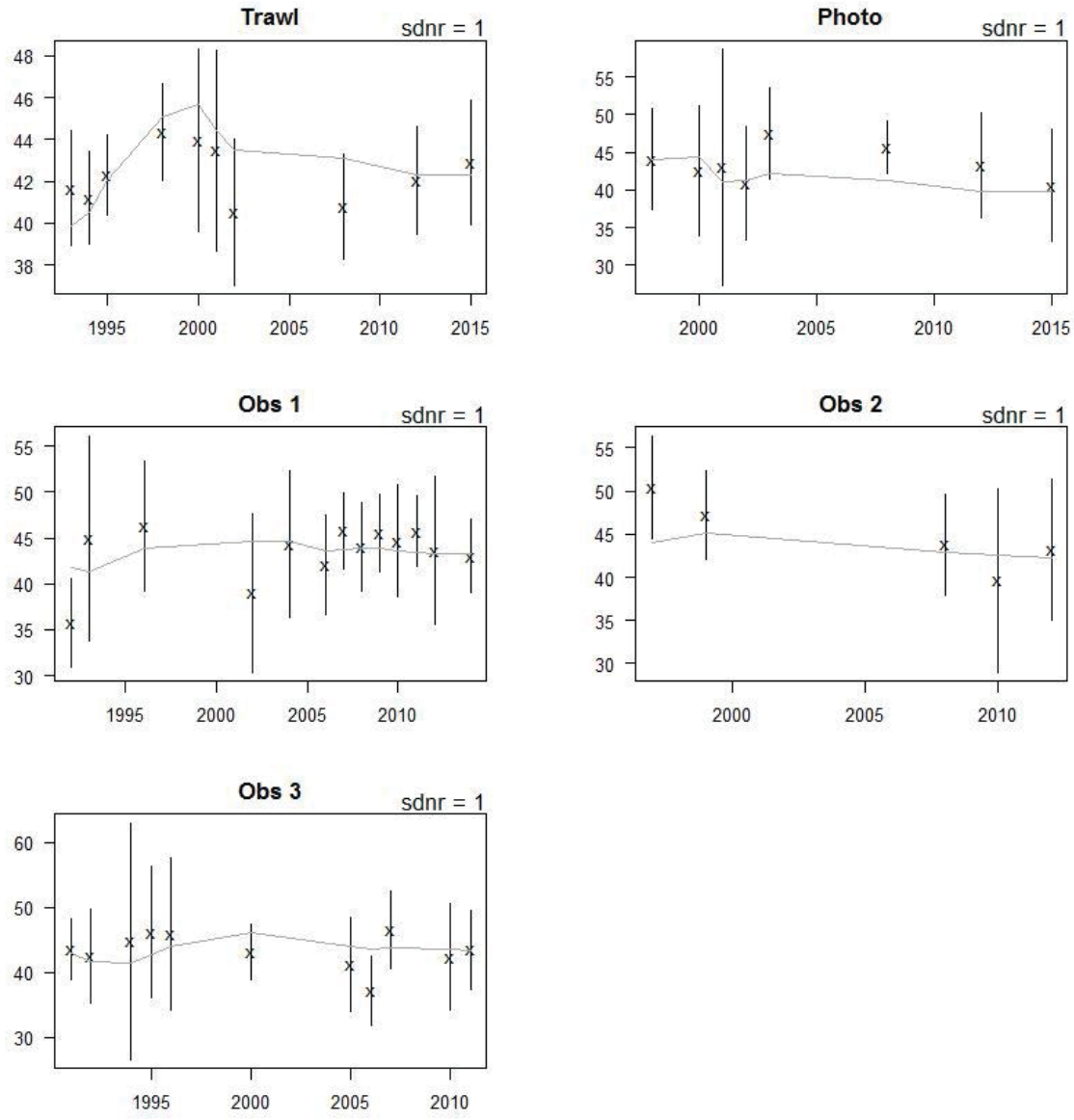

A6. 5: Observed (solid line) and fitted (grey line) mean length from length frequency distributions for survey and observer samples for the SCI 1 Base30 model.

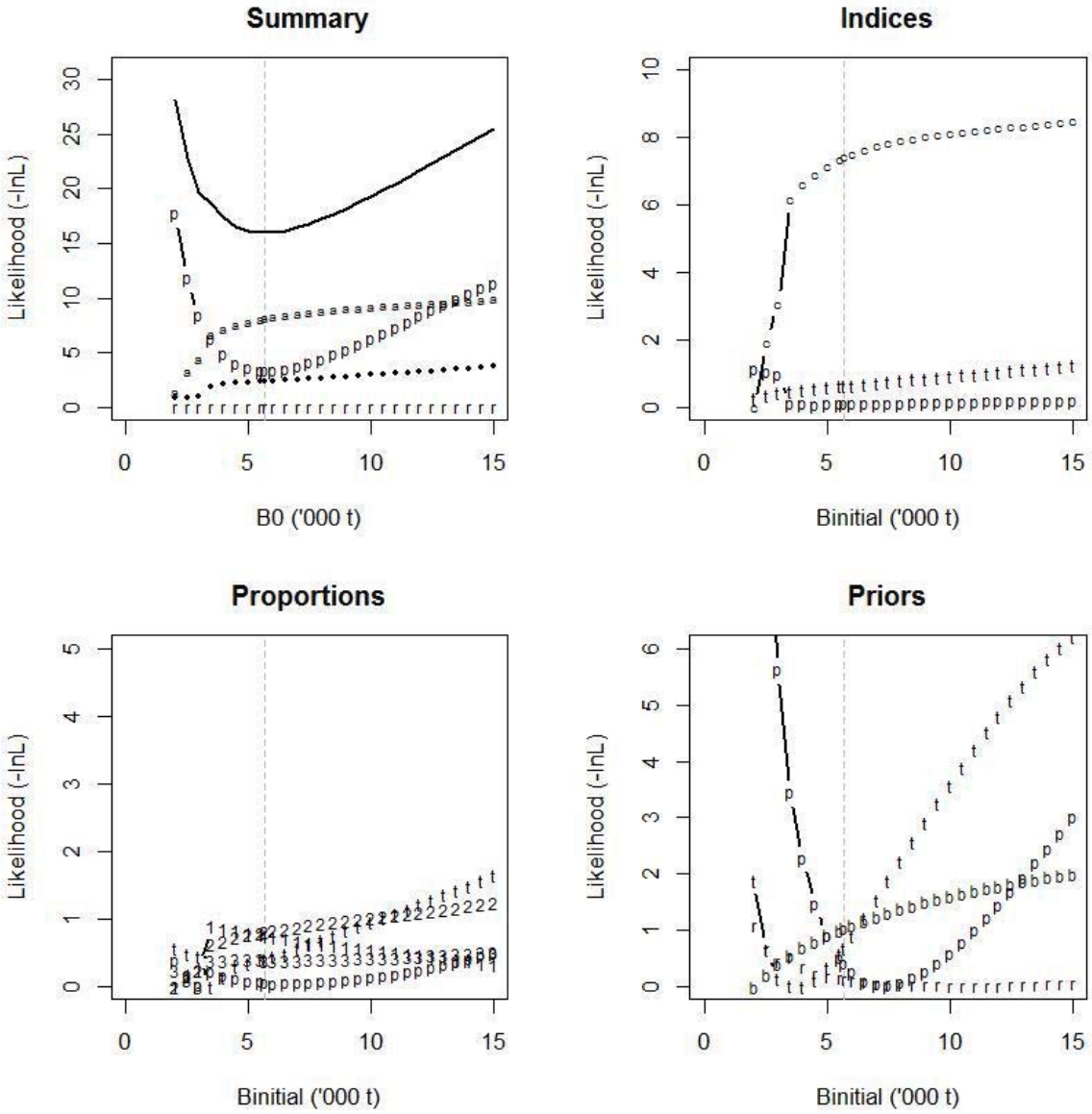

A6. 6: Likelihood profiles for model Base30 for SCI 1 when B_0 is fixed in the model. Figures show profiles for main priors (top left, p-priors, a – abundance indices, • – proportions at length, r-recapture data), abundance indices (top right, t - trawl survey step, c - CPUE, p – photo survey), proportion at length data (bottom left, p-photo, t-trawl, 1 – observer time step 1, 2 – observer time step 2, 3 – observer time step 3) and priors (bottom right, b- B_0, YCS - r, p- *q-Photo*, t – *q-Trawl*).

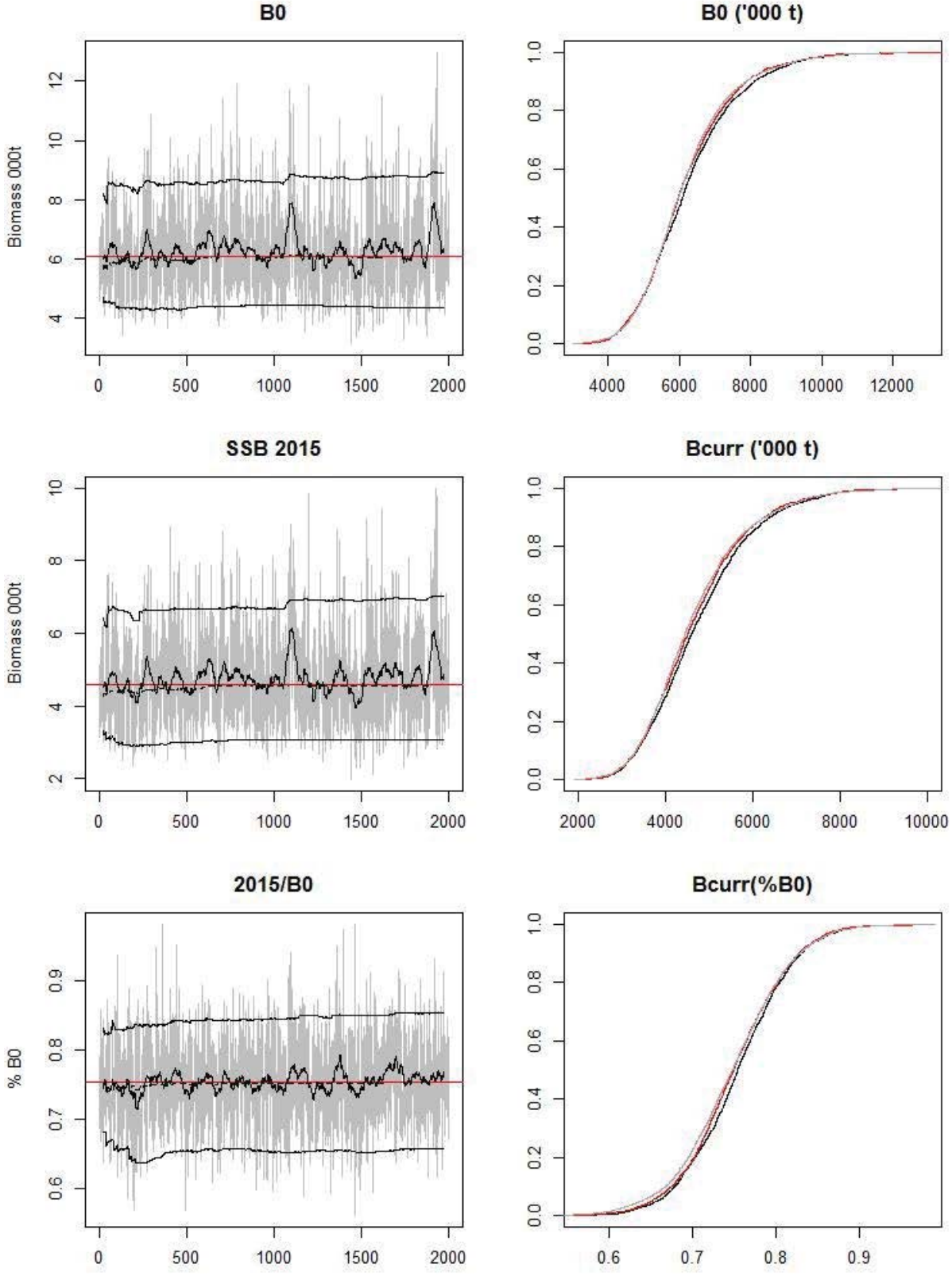

A6. 7: MCMC traces for B_0, SSB_{2015}, and SSB_{2015}/B_0 terms for the SCI 1 Base30 model, along with cumulative frequency distributions for three independent MCMC chains.

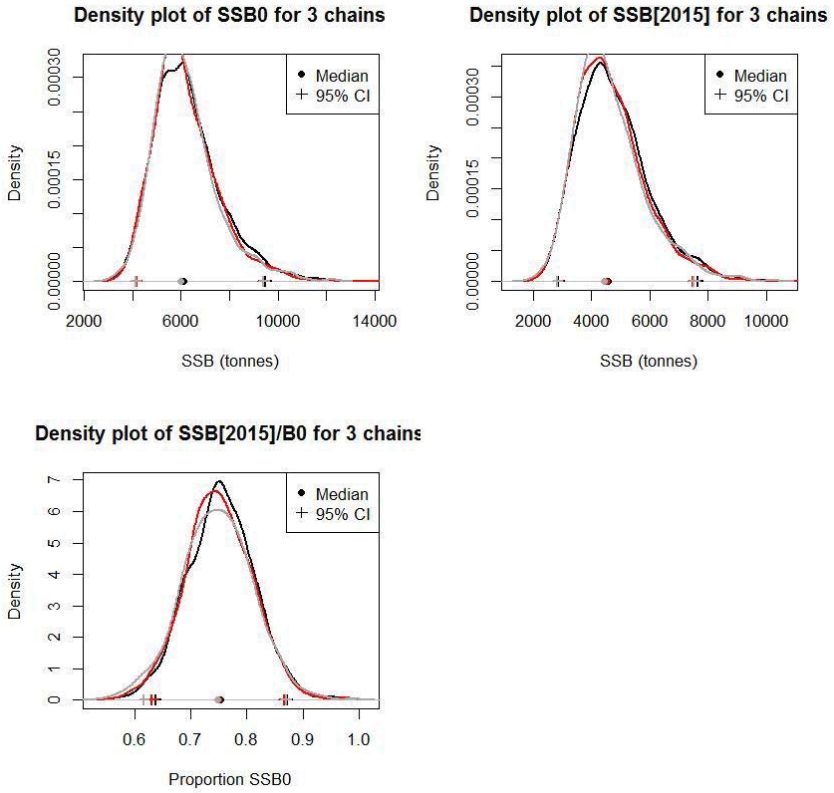

A6. 8: Density plots for B_0, SSB_{2015}, and SSB_{2015}/B_0 terms for the SCI 1 Base30 model for three independent MCMC chains, with median and 95% confidence intervals.

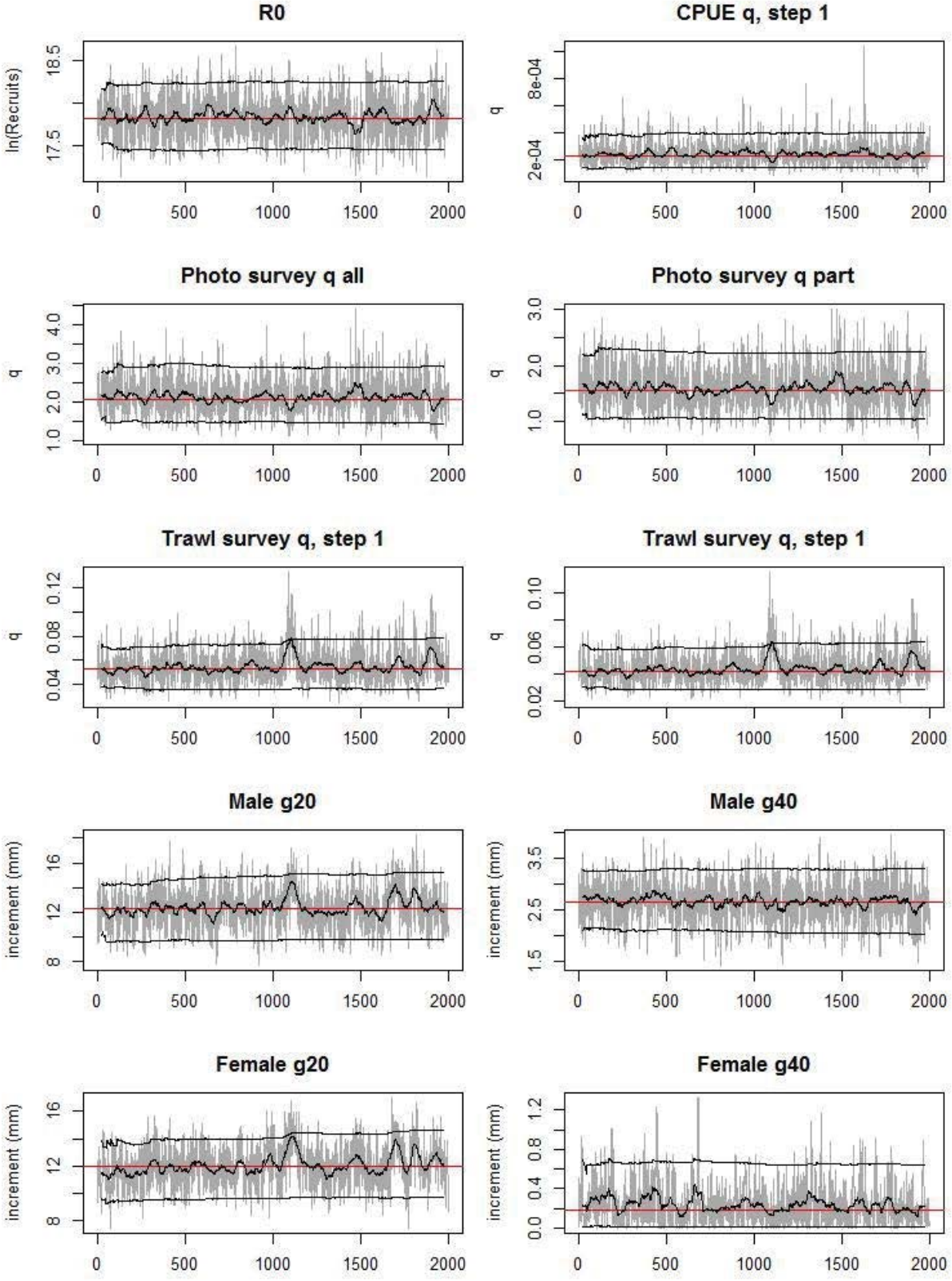

A6. 9: MCMC traces for R_0, catchability and growth terms for the SCI 1 Base30 model.

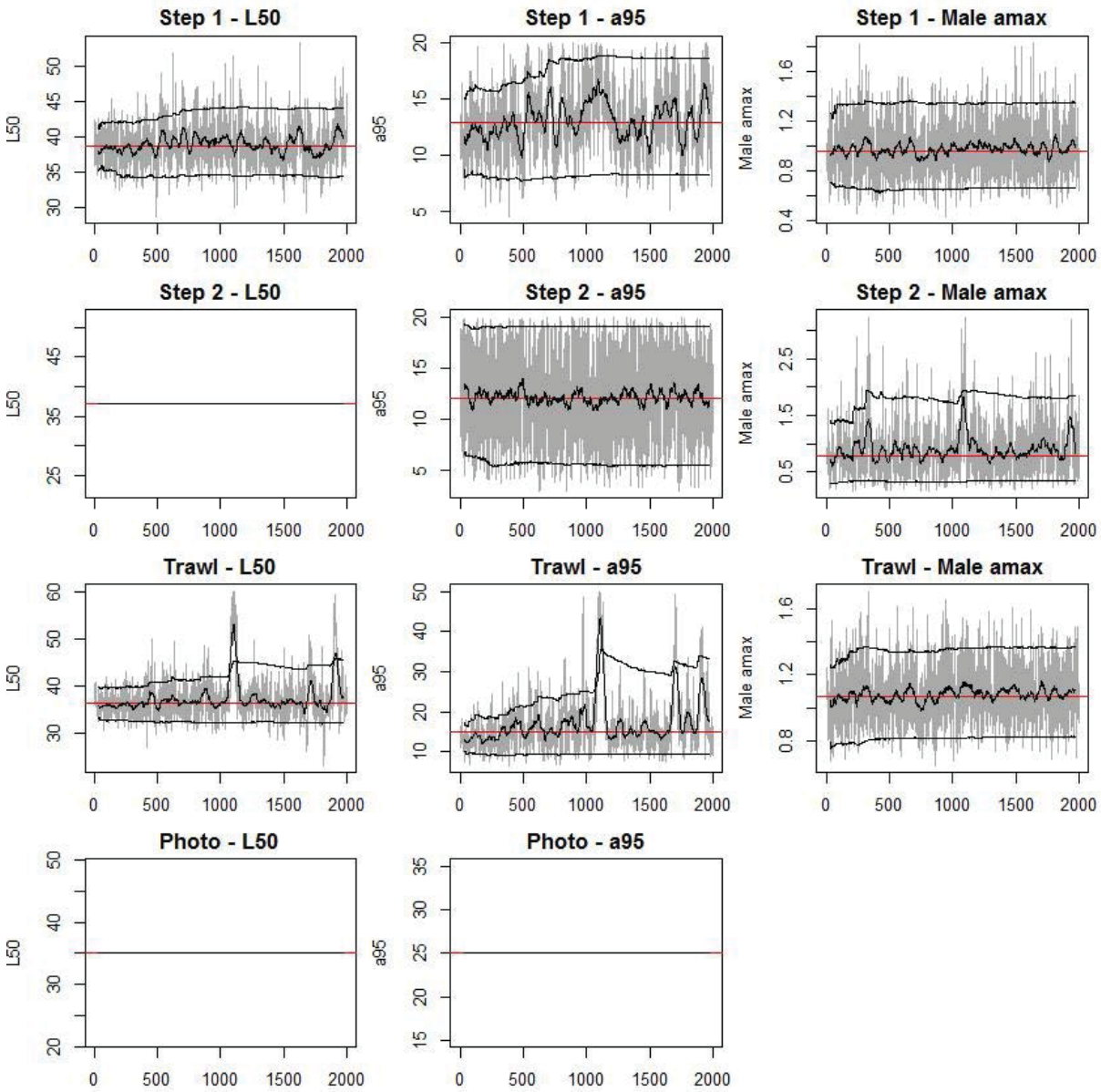

A6. 10: MCMC traces for selectivity terms for the SCI 1 Base30 model. Horizontal lines represent terms fixed in the model.

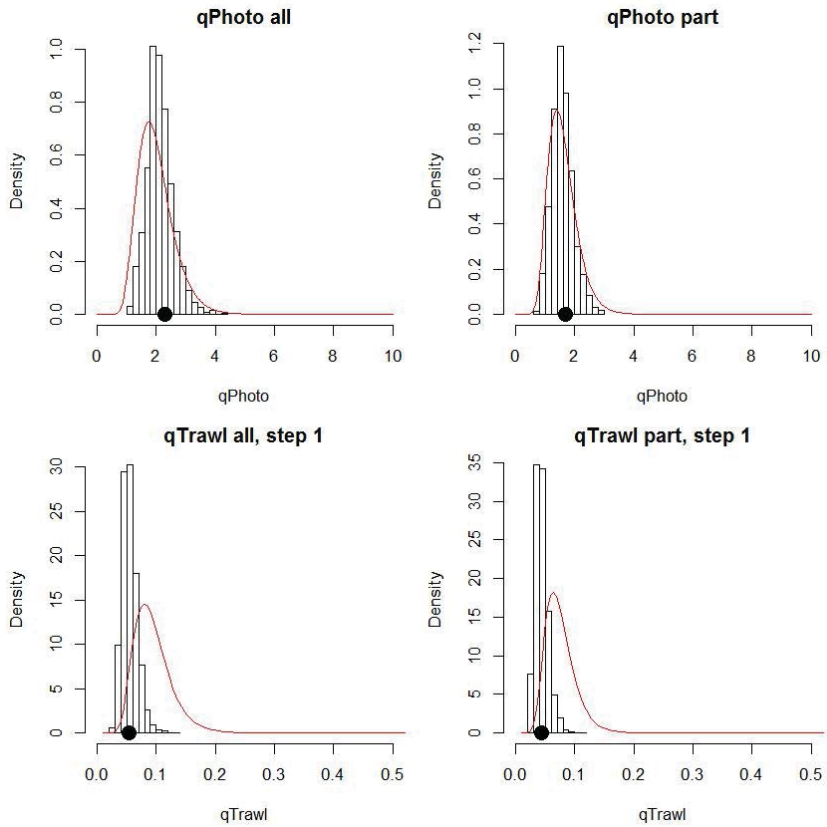

A6. 11: Marginal posterior distributions (histograms), MPD estimates (solid symbols) and distributions of priors (lines) for catchability terms for the SCI 1 Base30 model.

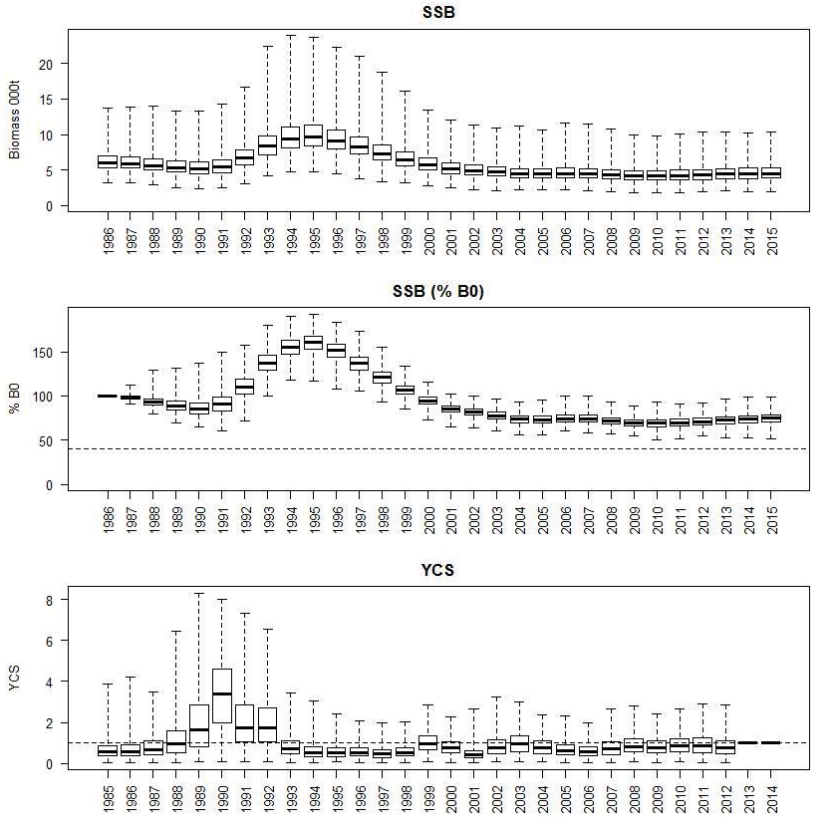

A6. 12: Posterior trajectory of SSB, SSB/SSB$_0$ and YCS for the SCI 1 Base30 model.

APPENDIX 7. SCI 1 Base35 model plots (M=0.35)

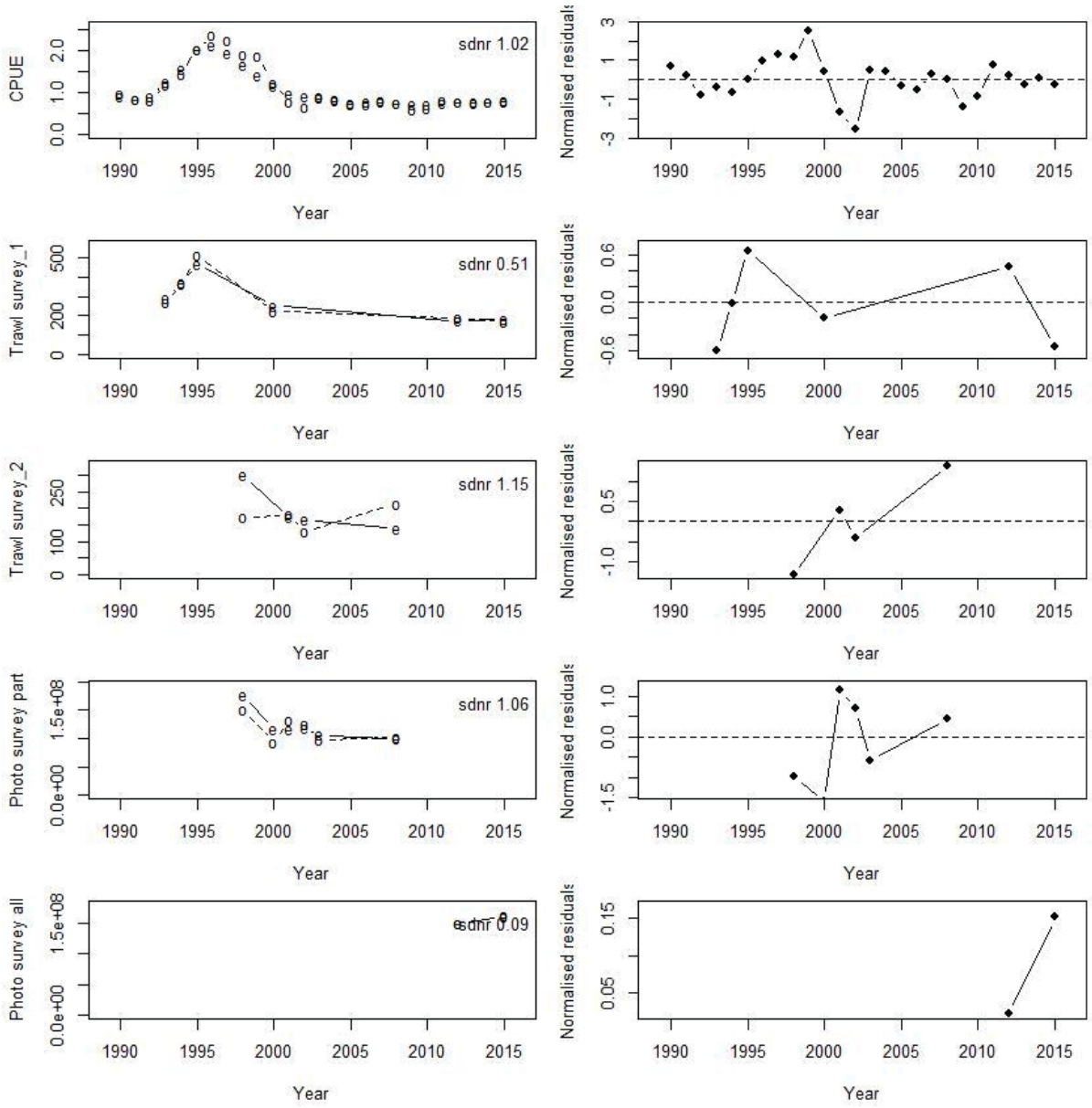

A7. 1: Fits to abundance indices (left column) and normalised residuals (right column) for standardised CPUE index (top row) trawl survey biomass index covering whole area (second row), trawl survey biomass index covering limited area (third row), photo survey abundance index covering limited area (fourth row) and photo survey abundance index covering whole area (fifth row) for the SCI 1 Base35 model.

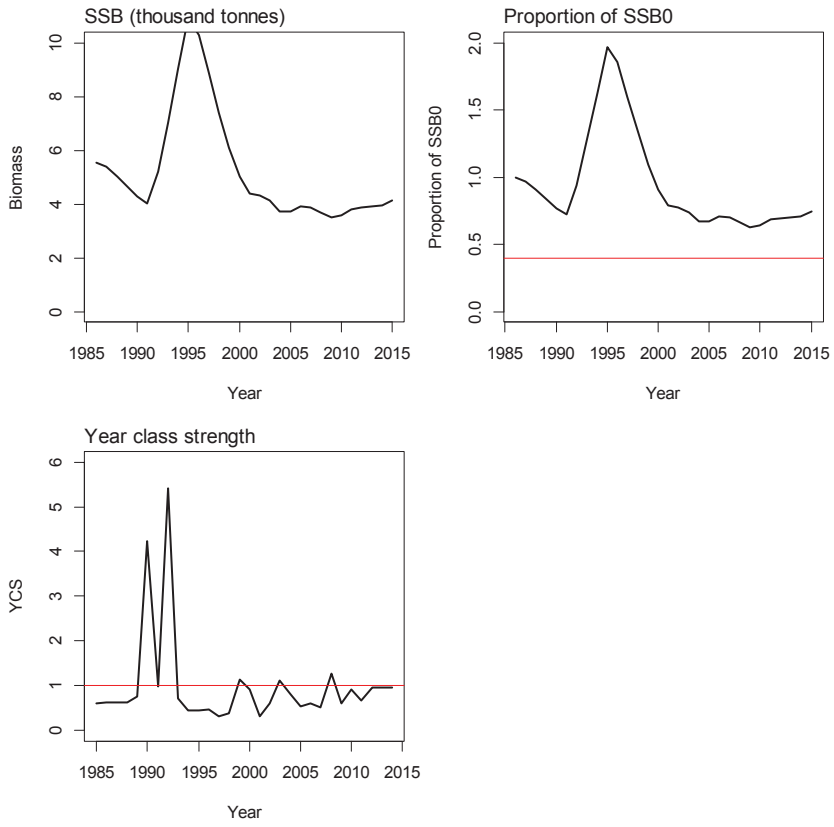

A7. 2: Spawning stock biomass trajectory (upper left), stock status (upper right), and year class strength (lower left) for the SCI 1 Base35 model.

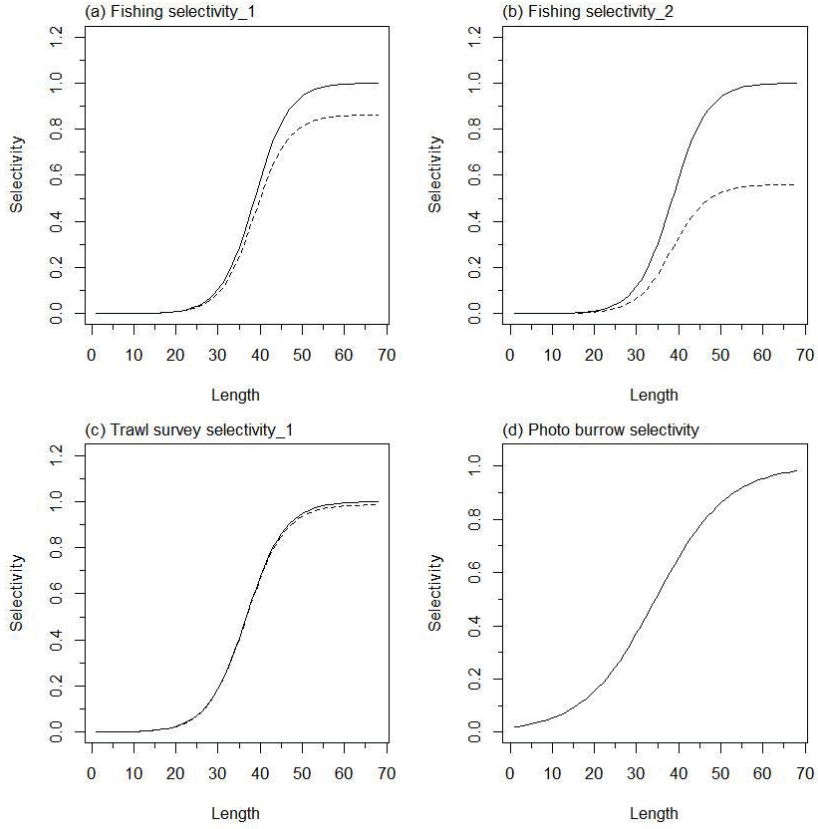

A7. 3: Fishery and survey selectivity curves for the SCI 1 Base35 model. Solid line – females, dotted line – males. The scampi burrow index is not sexed, and a single selectivity applies.

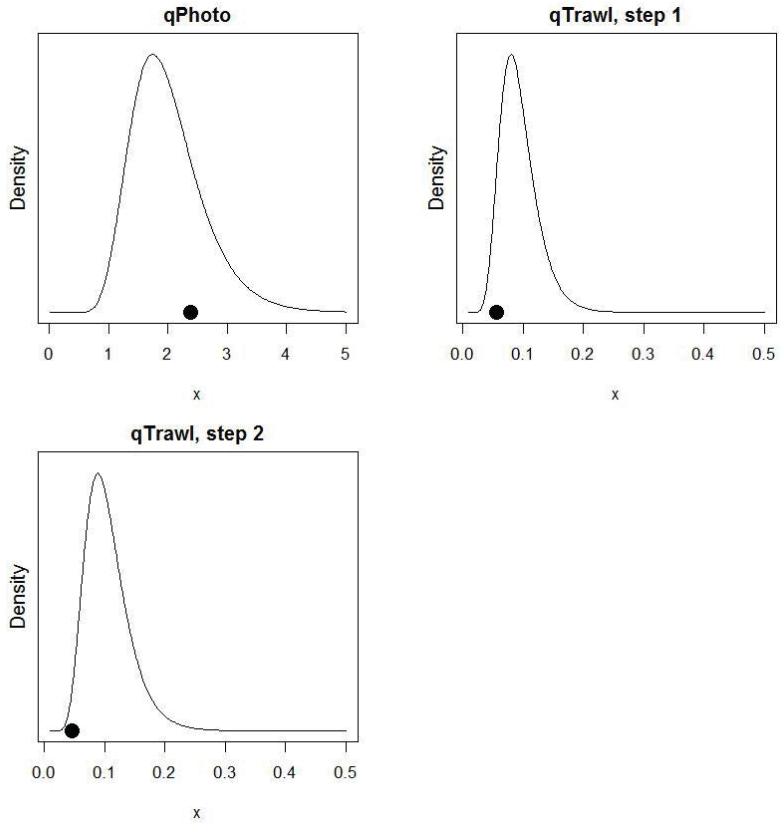

A7. 4: Catchability estimates from MPD model run, plotted in relation to prior distribution for the SCI 1 Base35 model.

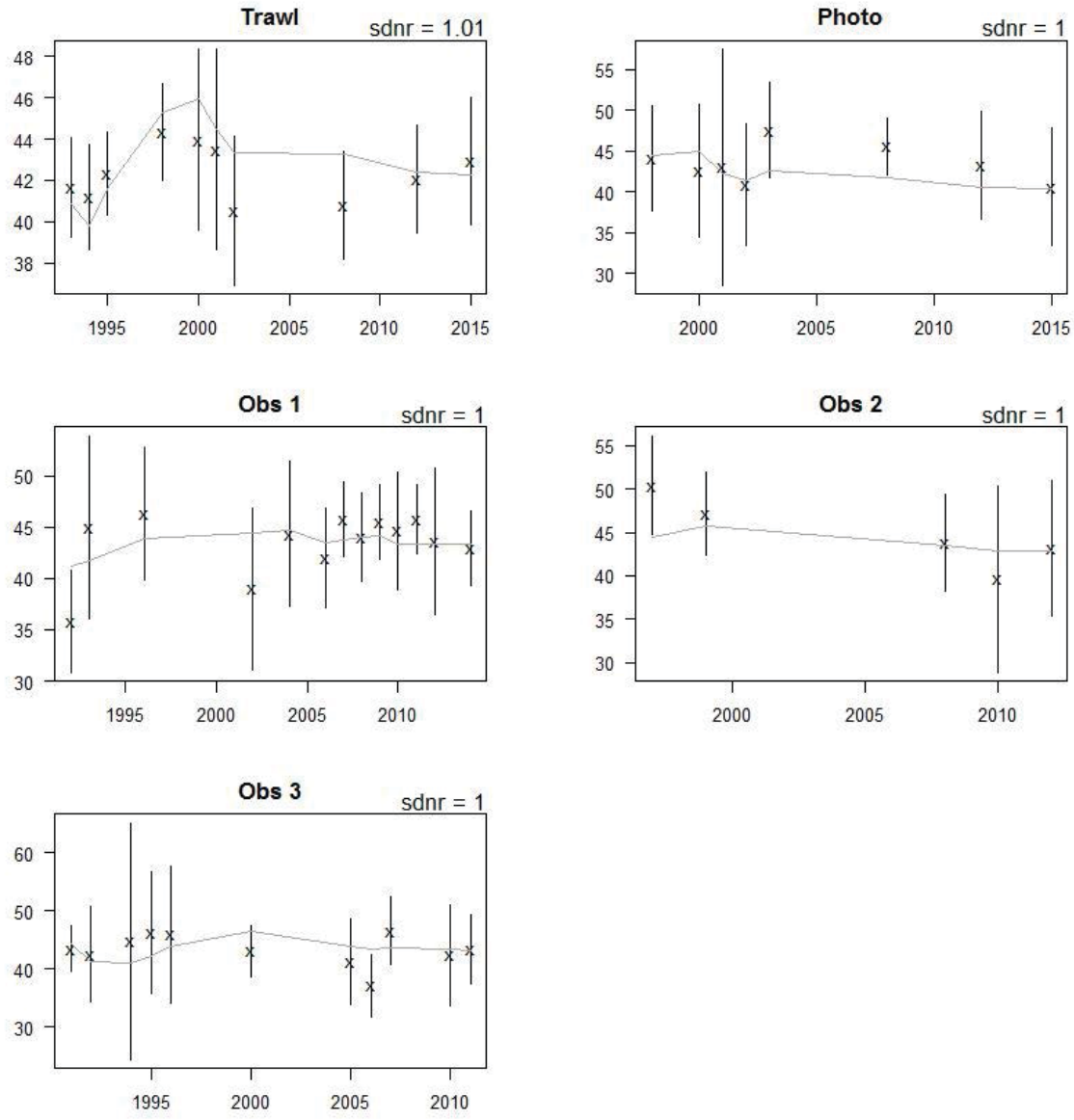

A7. 5: Observed (crosses, with vertical lines representing ± two standard errors) and fitted (grey line) mean length from length frequency distributions for survey and observer samples for the SCI 1 Base35 model.

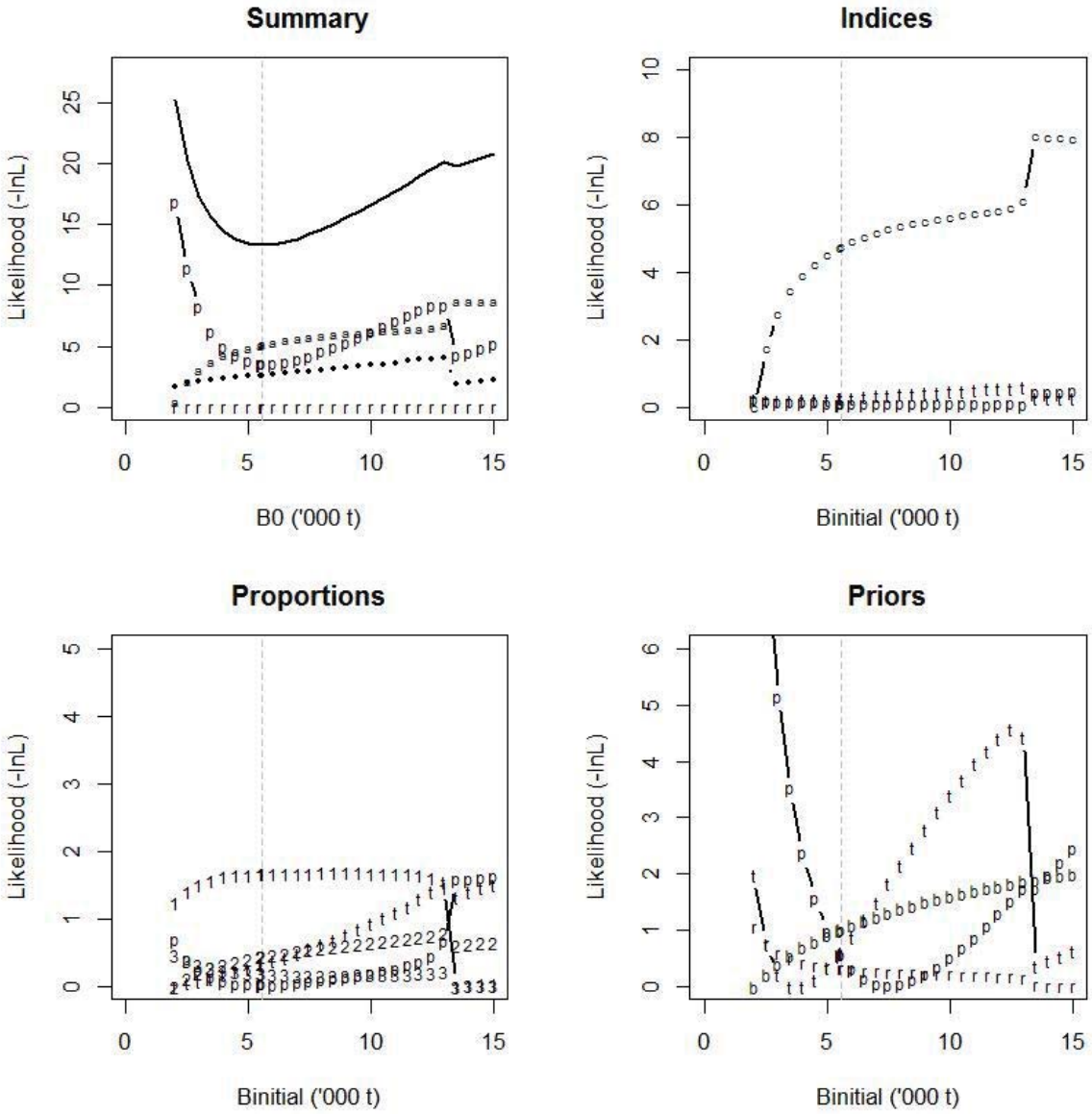

A7. 6: Likelihood profiles for model Base35 for SCI 1 when B_0 is fixed in the model. Figures show profiles for main priors (top left, p-priors, a – abundance indices, • – proportions at length, r-recapture data), abundance indices (top right, t - trawl survey step, c - CPUE, p – photo survey), proportion at length data (bottom left, p-photo, t-trawl, 1 – observer time step 1, 2 – observer time step 2, 3 – observer time step 3) and priors (bottom right, b- B_0, YCS - r, p- *q-Photo*, t – *q-Trawl*).

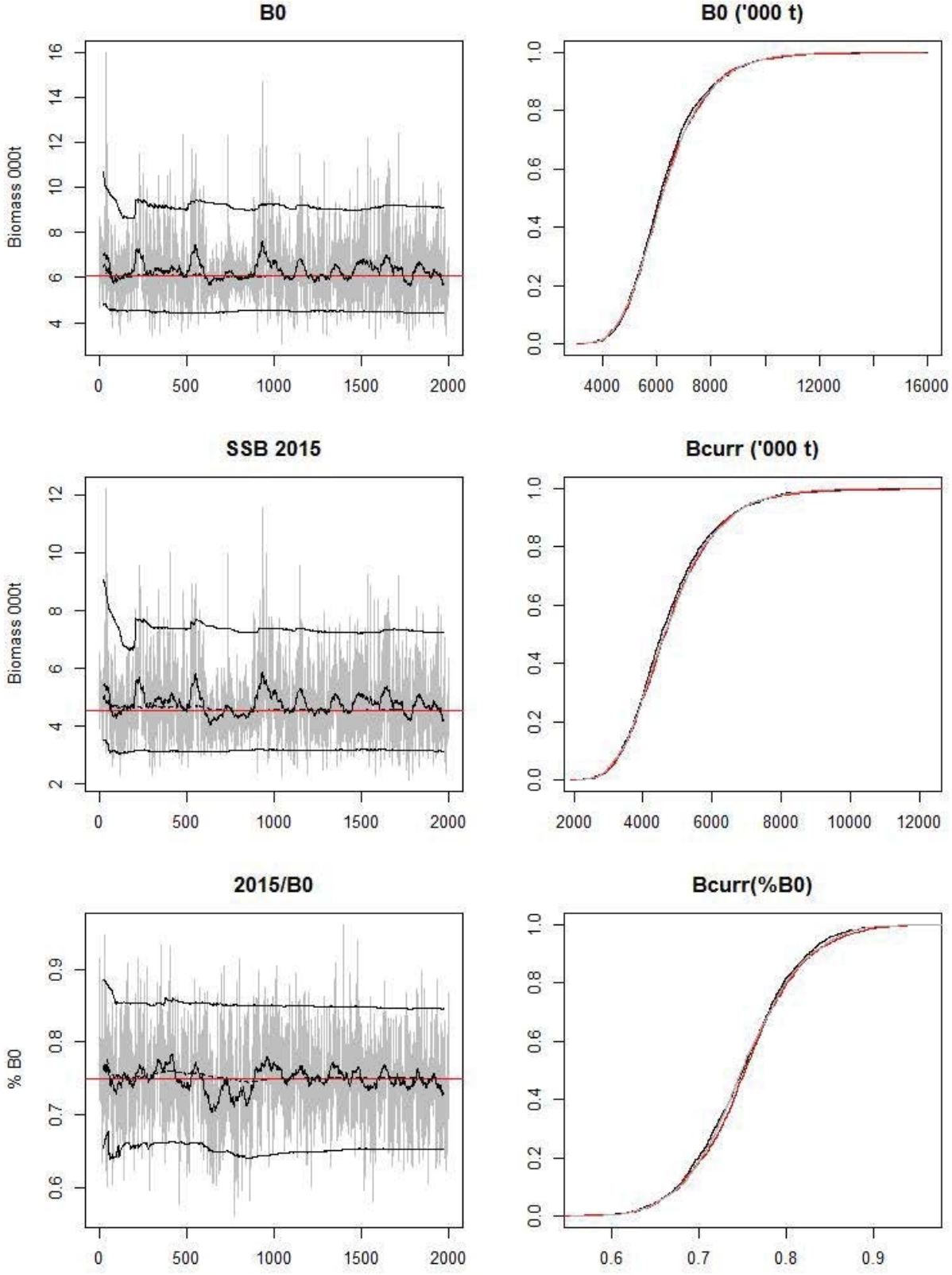

A7. 7: MCMC traces for B_0, SSB_{2015}, and SSB_{2015}/B_0 terms for the SCI 1 Base35 model, along with cumulative frequency distributions for three independent MCMC chains.

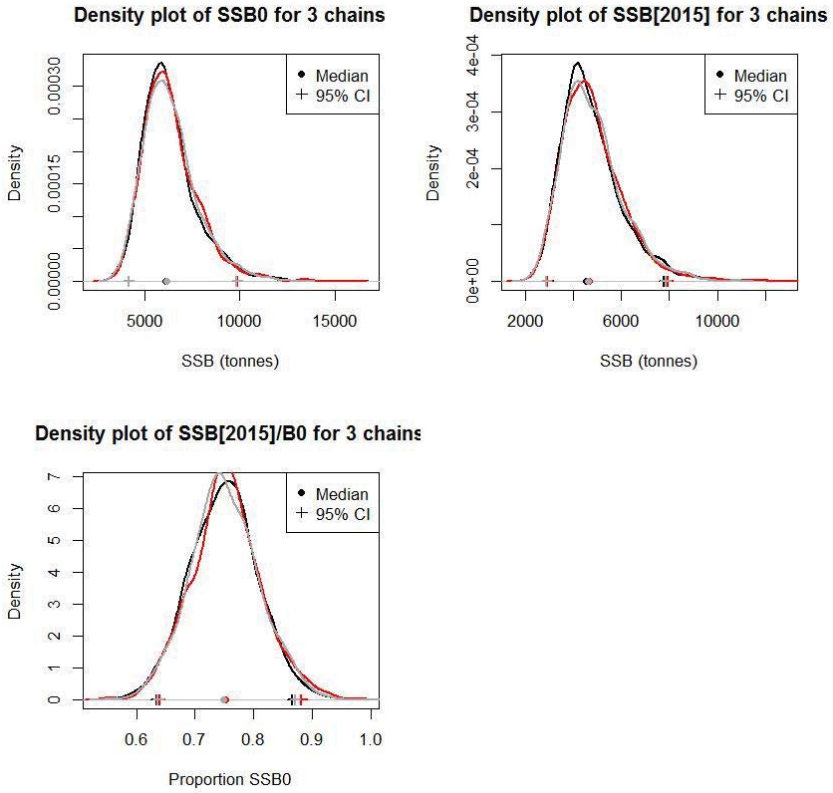

A7. 8: Density plots for B_0, SSB_{2015}, and SSB_{2015}/B_0 terms for the SCI 1 Base35 model for three independent MCMC chains, with median and 95% confidence intervals.

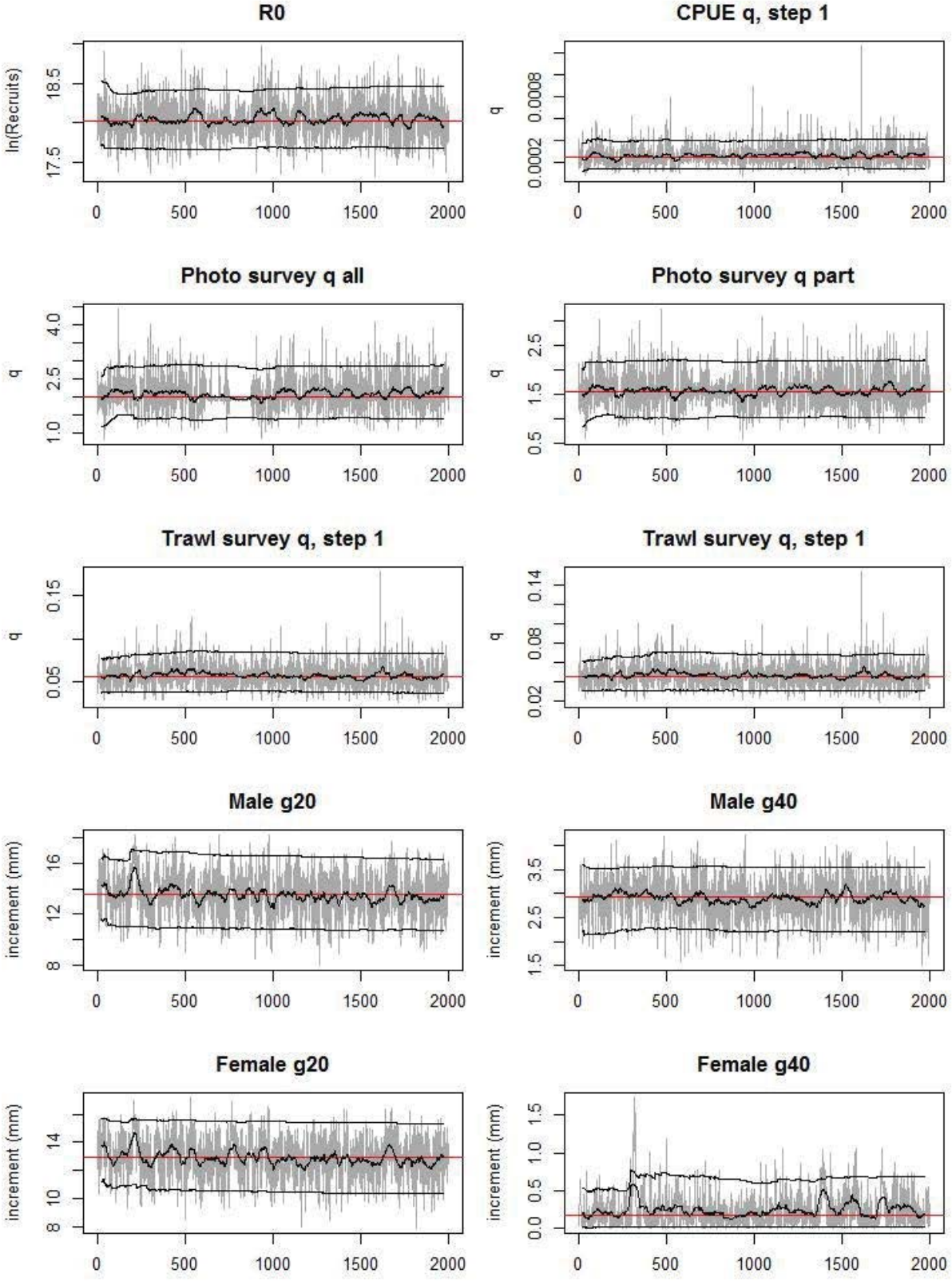

A7. 9: MCMC traces for R_0, catchability and growth terms for the SCI 1 Base35 model.

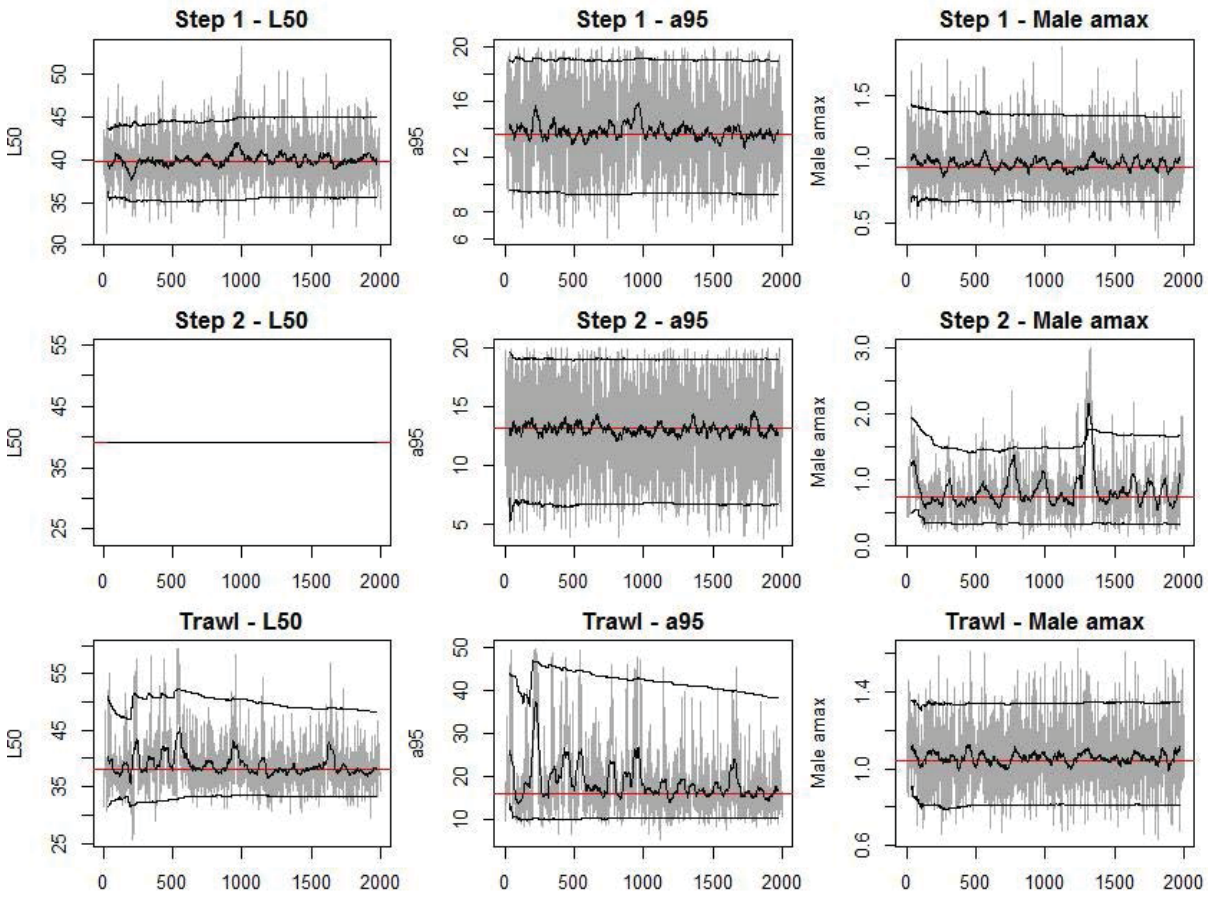

A7. 10: MCMC traces for selectivity terms for the SCI 1 Base35 model. Horizontal lines represent terms fixed in the model.

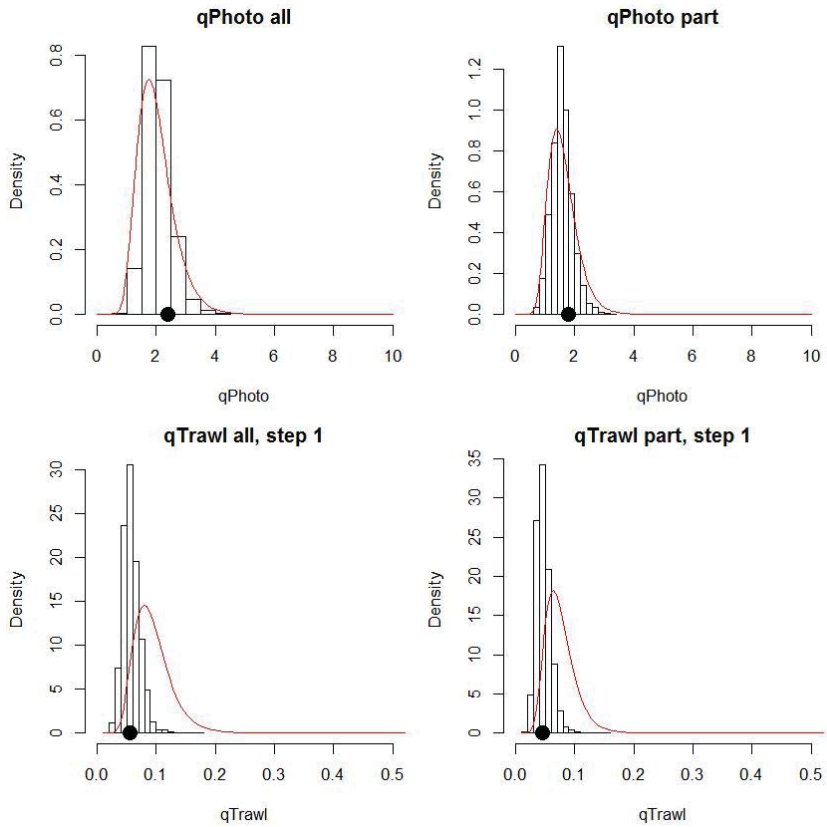

A7. 11: Marginal posterior distributions (histograms), MPD estimates (solid symbols) and distributions of priors (lines) for catchability terms for the SCI 1 Base35 model.

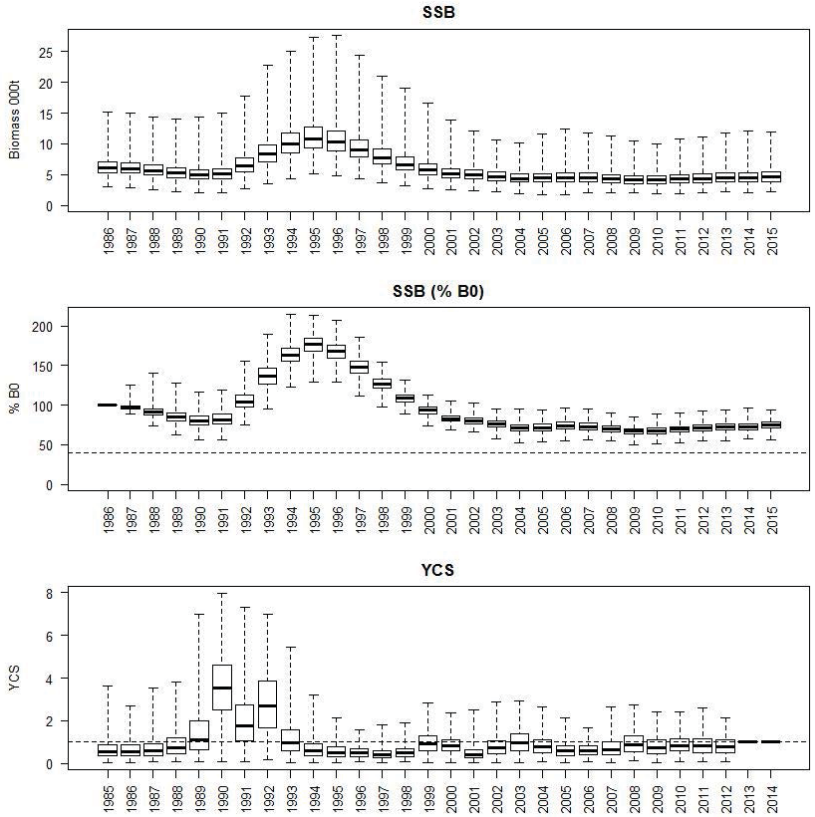

A7. 12: Posterior trajectory of SSB, SSB/SSB$_0$ and YCS for the SCI 1 Base35 model.

APPENDIX 8. SCI 2 model plots (M=0.25)

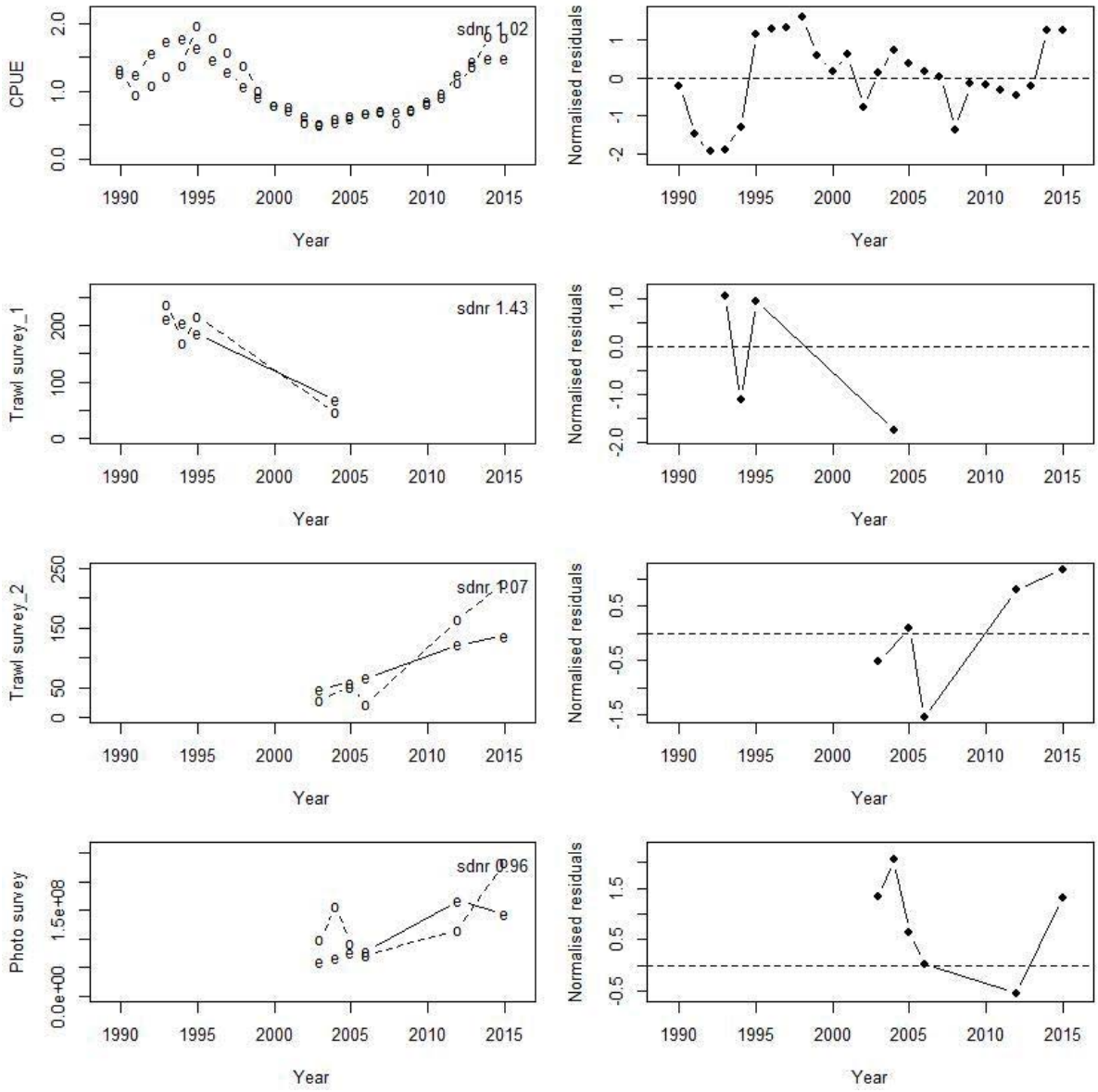

A8. 1: Fits to abundance indices (left column) and normalised residuals (right column) for standardised CPUE index (top row) trawl survey biomass index time step 1 (second row), trawl survey biomass index time step 2 (third row), and photo survey abundance index (fourth row) for the SCI 2 Base25 model.

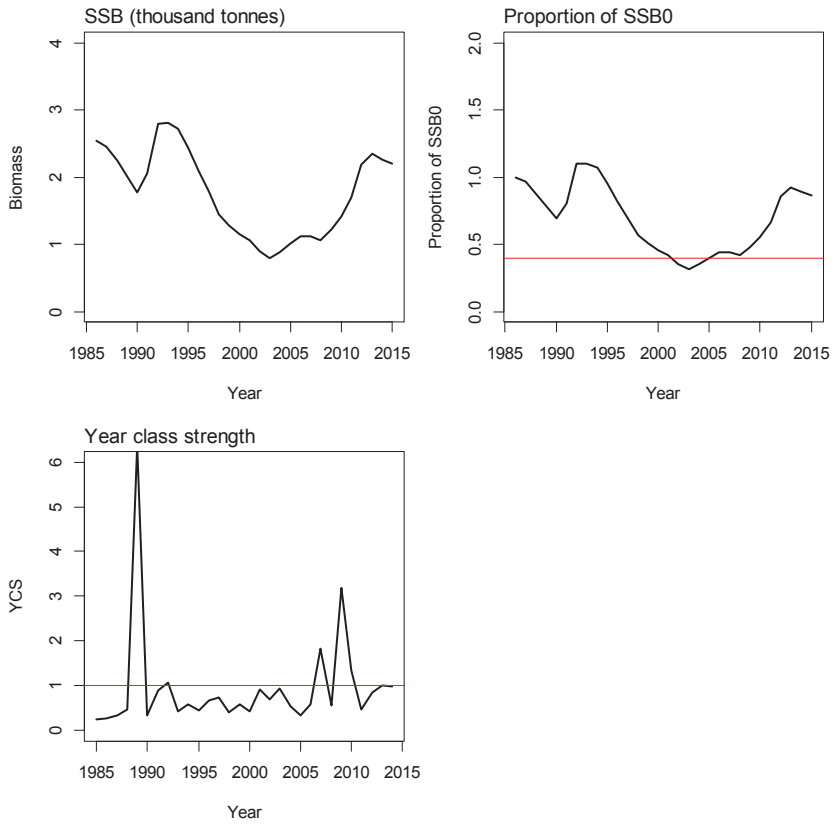

A8. 2: Spawning stock biomass trajectory (upper left), stock status (upper right), and year class strength (lower left) for the SCI 2 Base25 model.

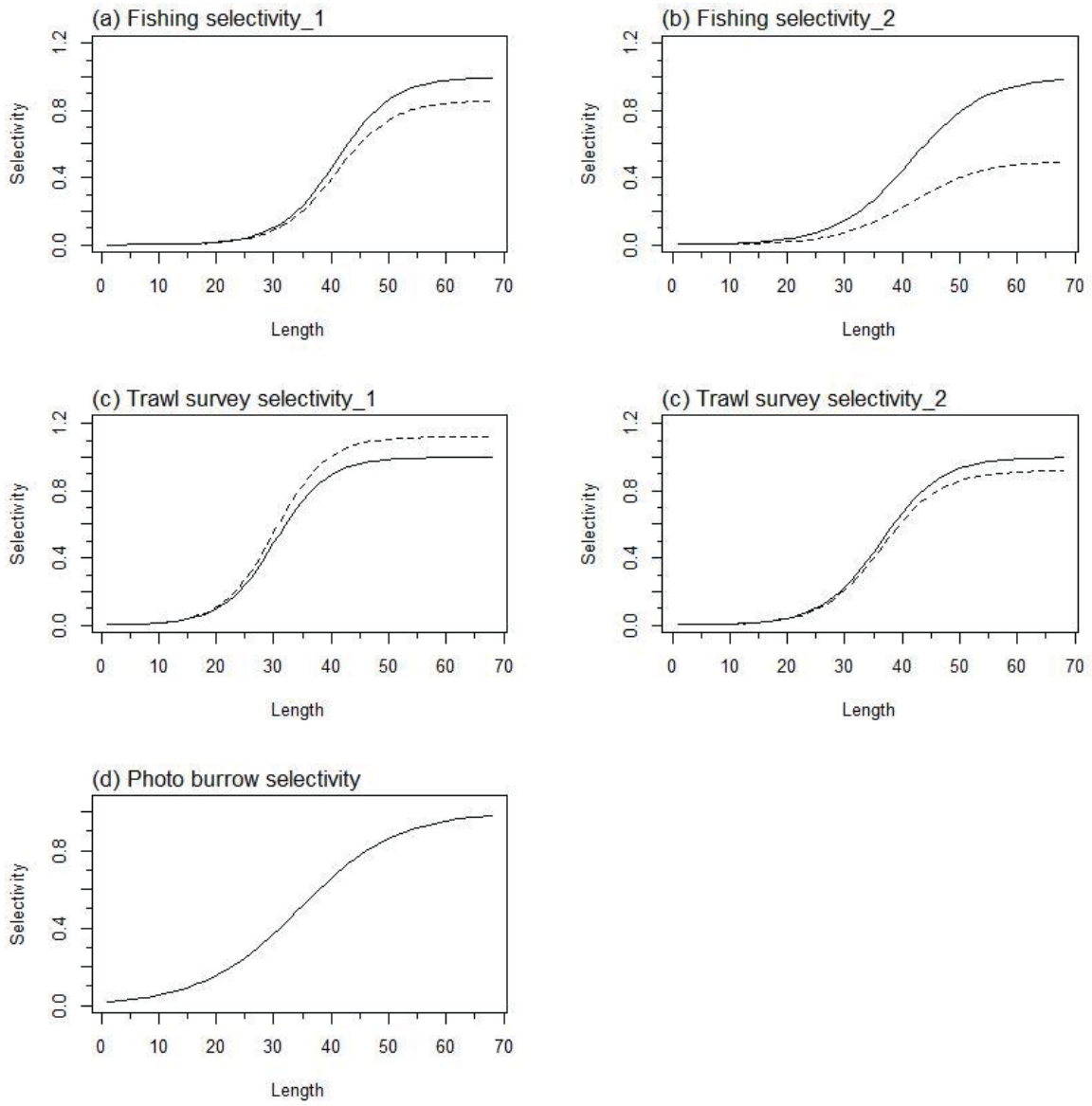

A8. 3: Fishery and survey selectivity curves for the SCI 2 Base25 model. Solid line – females, dotted line – males. The scampi burrow index is not sexed, and a single selectivity applies.

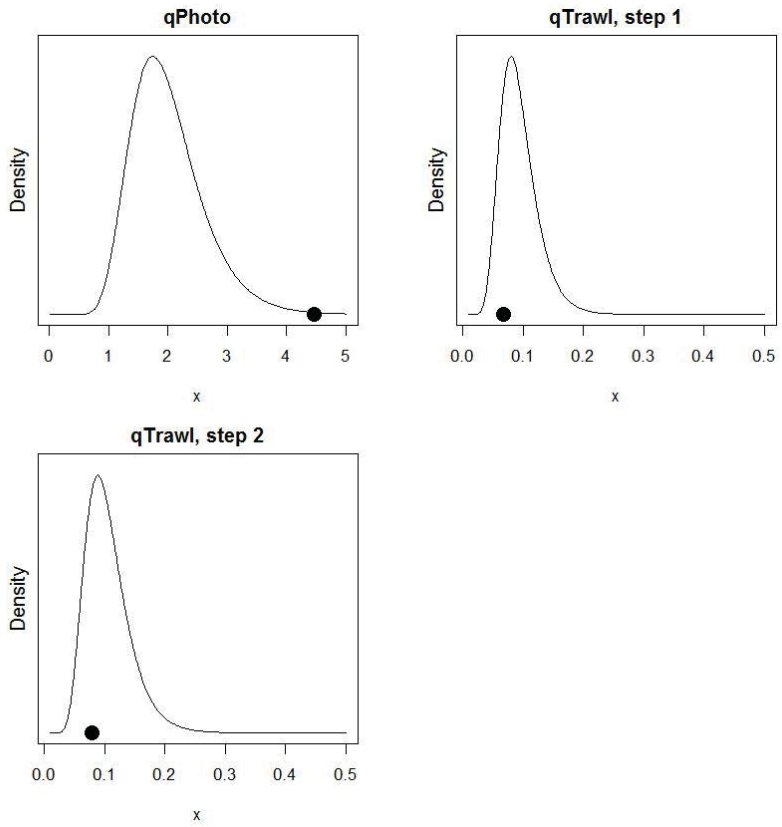

A8. 4: Catchability estimates from MPD model run, plotted in relation to prior distribution for the SCI 2 Base25 model.

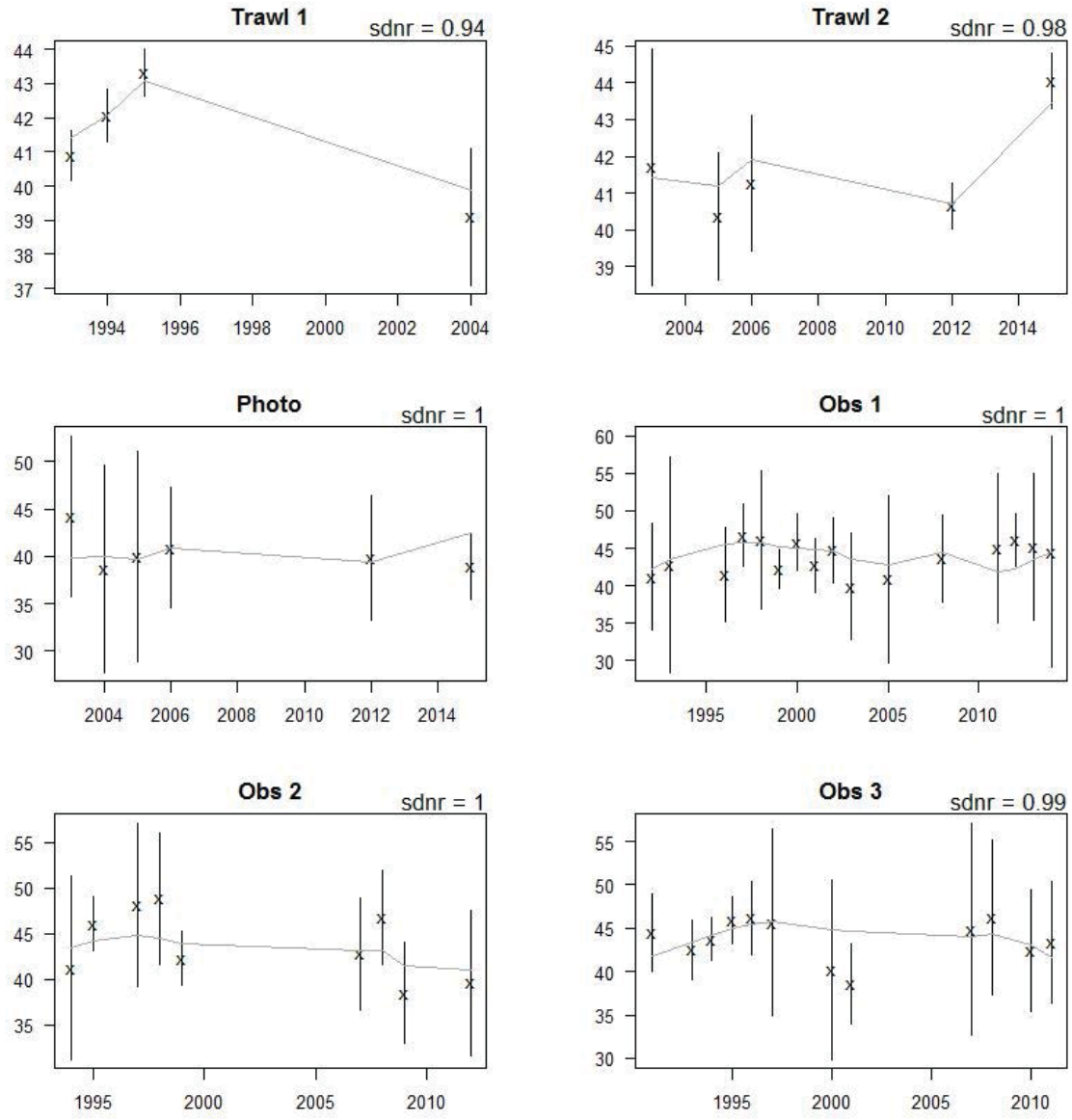

A8. 5: Observed (solid line) and fitted (grey line) mean length from length frequency distributions for survey and observer samples for the SCI 2 Base25 model.

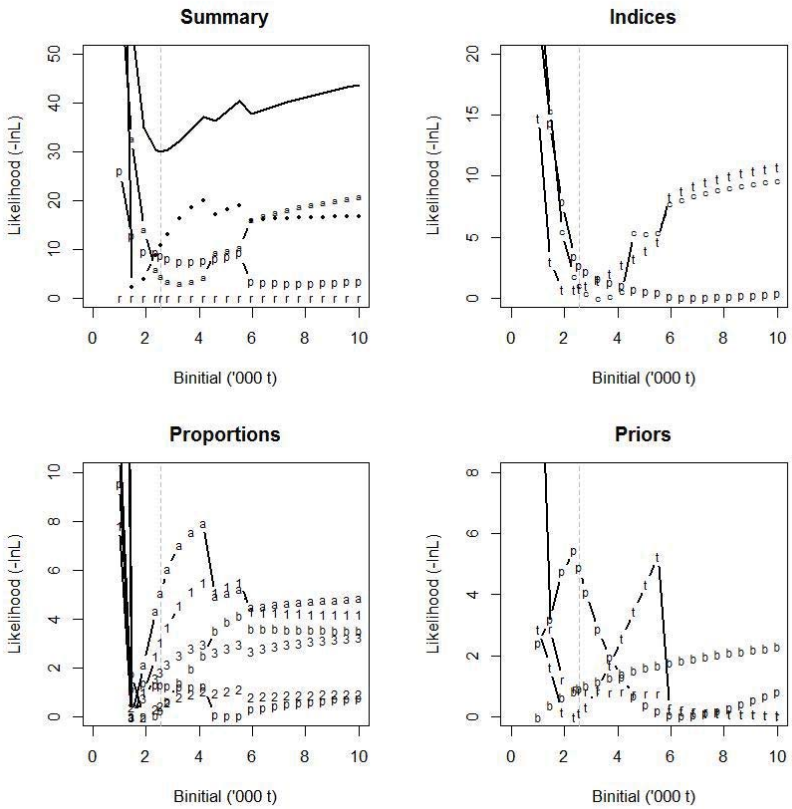

A8. 6: Likelihood profiles for model Base25 for SCI 2 when B_0 is fixed in the model. Figures show profiles for main priors (top left, p-priors, a – abundance indices, • – proportions at length, r-recapture data), abundance indices (top right, t - trawl survey step, c - CPUE, p – photo survey), proportion at length data (bottom left, p-photo, t-trawl, 1 – observer time step 1, 2 – observer time step 2, 3 – observer time step 3) and priors (bottom right, b- B_0, YCS - r, p- *q-Photo*, t – *q-Trawl*).

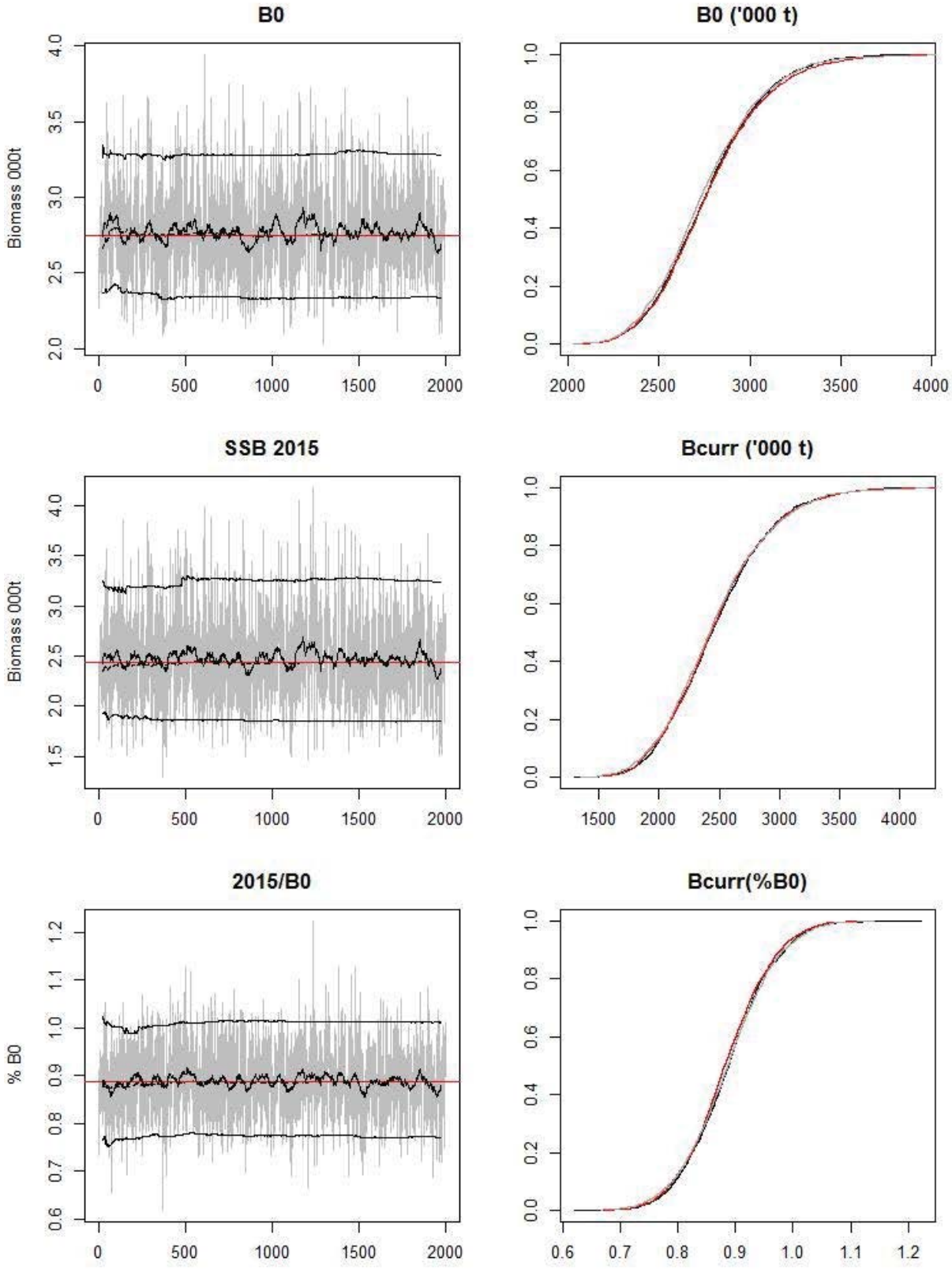

A8. 7: MCMC traces for B_0, SSB_{2015}, and SSB_{2015}/B_0 terms for the SCI 2 Base25 model, along with cumulative frequency distributions for three independent MCMC chains.

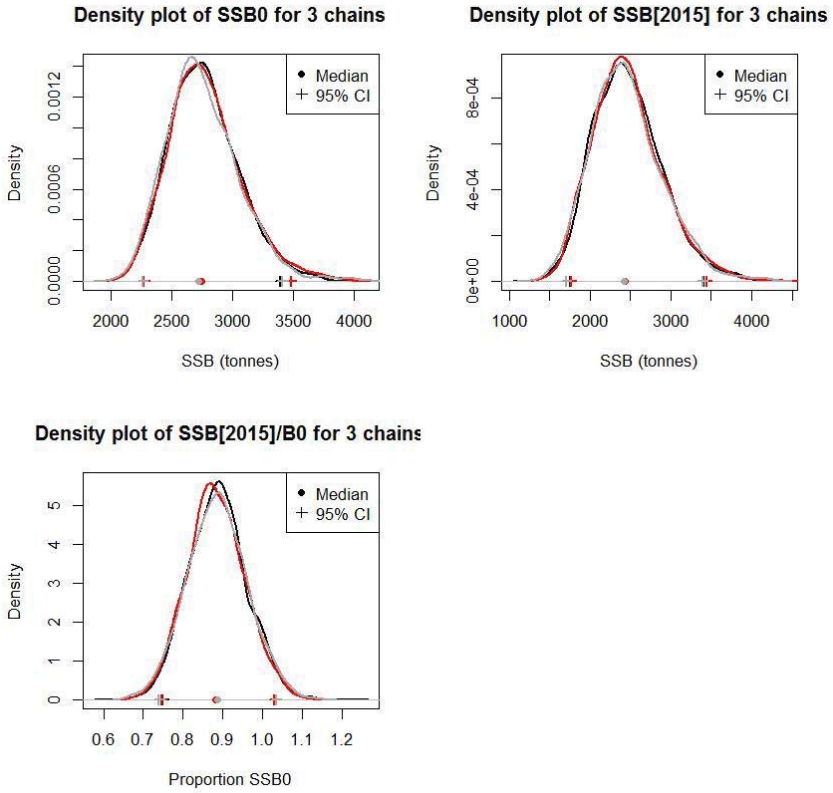

A8. 8: Density plots for B_0, SSB_{2015}, and SSB_{2015}/B_0 terms for the SCI 2 Base25 model for three independent MCMC chains, with median and 95% confidence intervals.

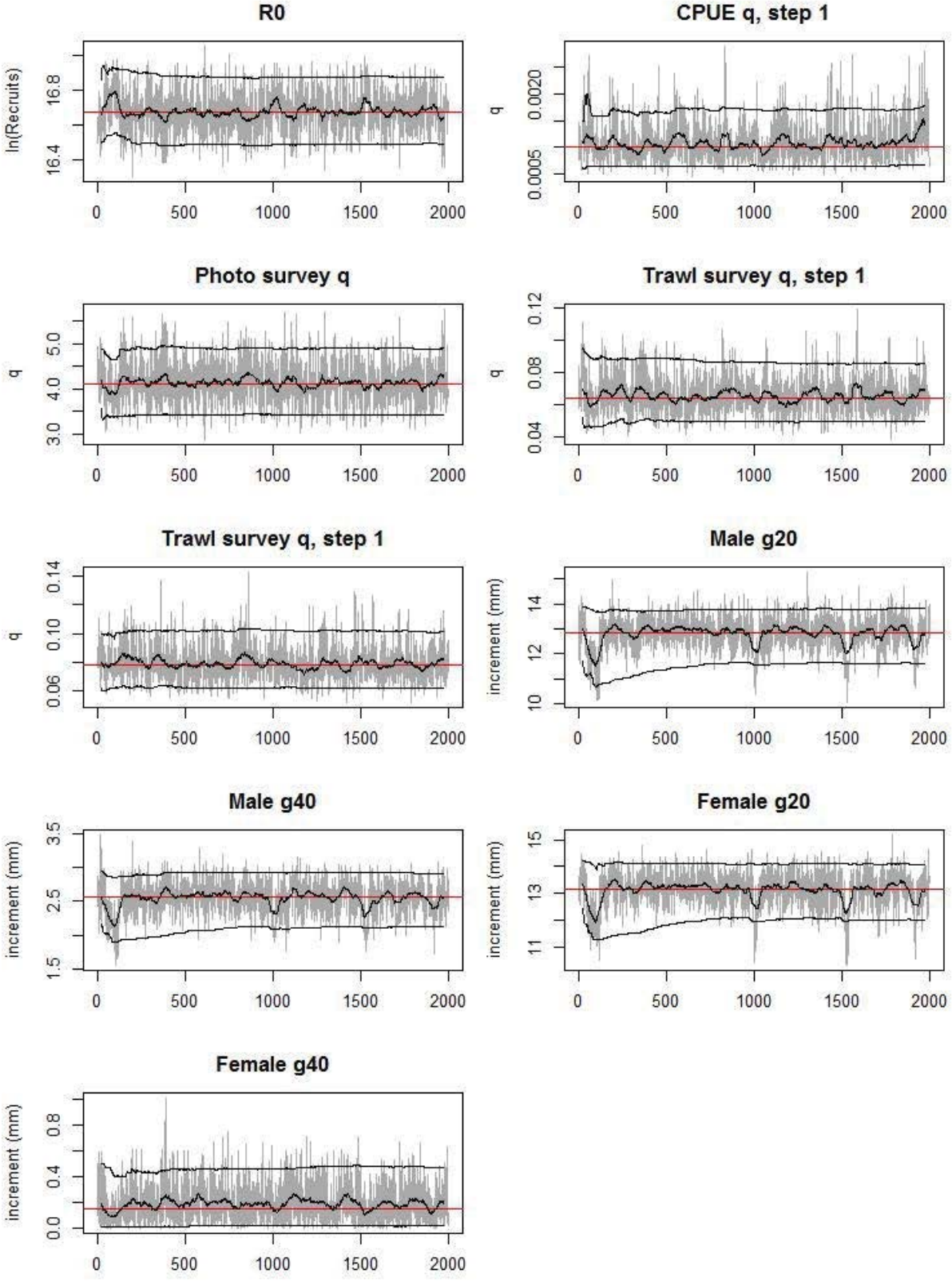

A8. 9: MCMC traces for R_0, catchability and growth terms for the SCI 2 Base25 model.

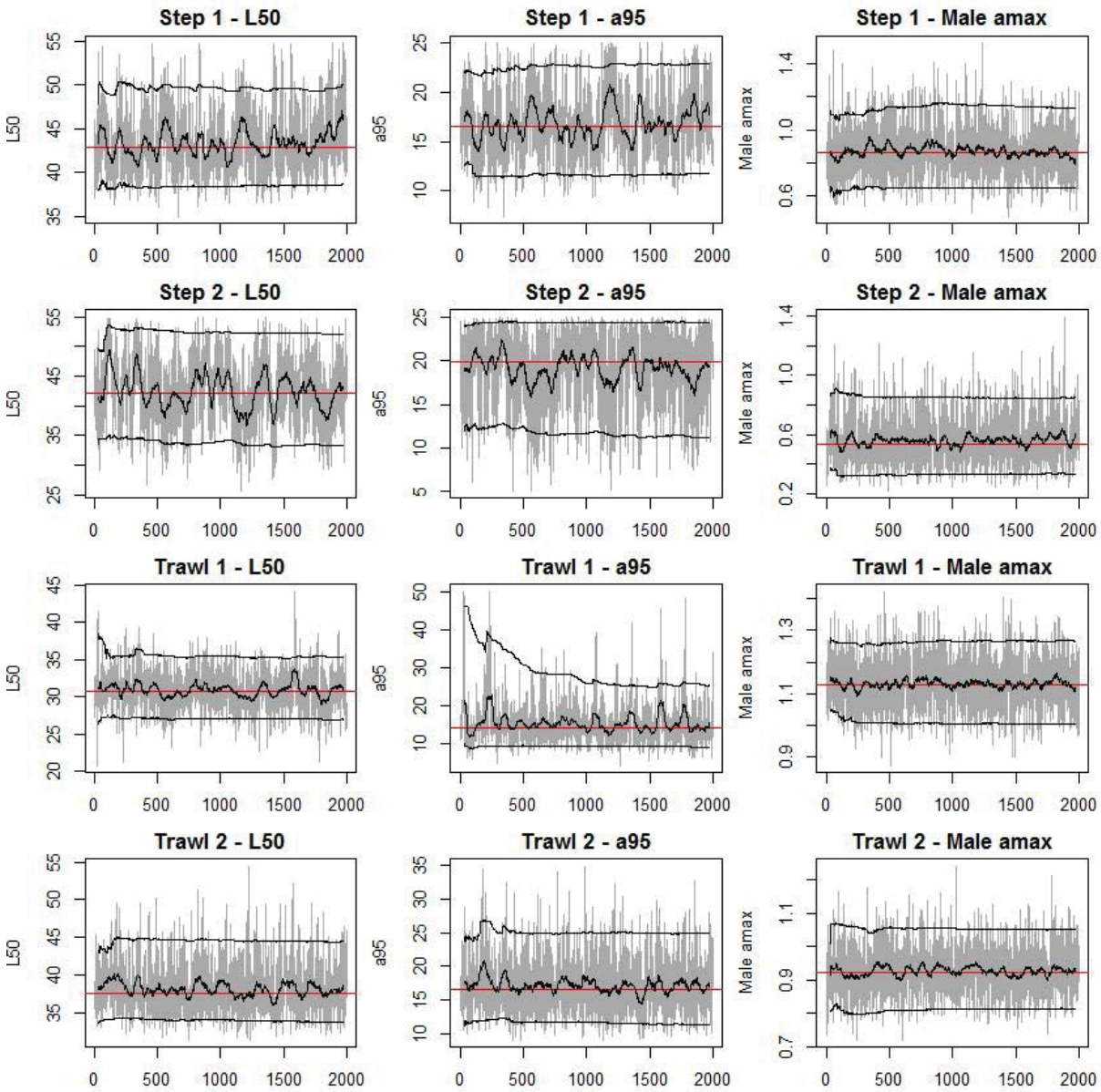

A8. 10: MCMC traces for selectivity terms for the SCI 2 Base25 model. Horizontal lines represent terms fixed in the model.

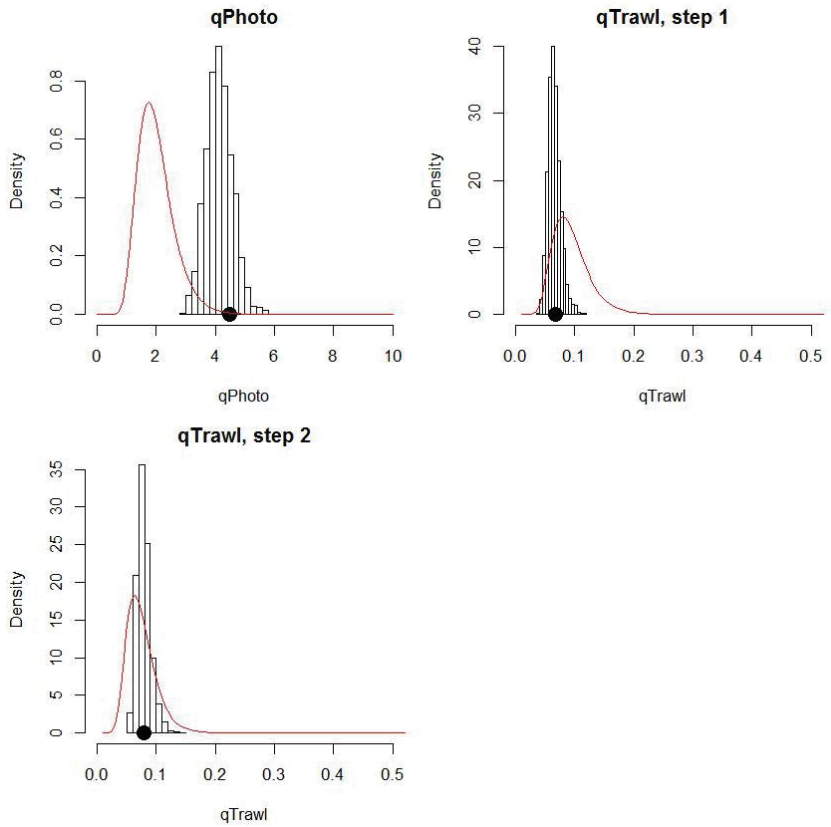

A8. 11: Marginal posterior distributions (histograms), MPD estimates (solid symbols) and distributions of priors (lines) for catchability terms for the SCI 2 Base25 model.

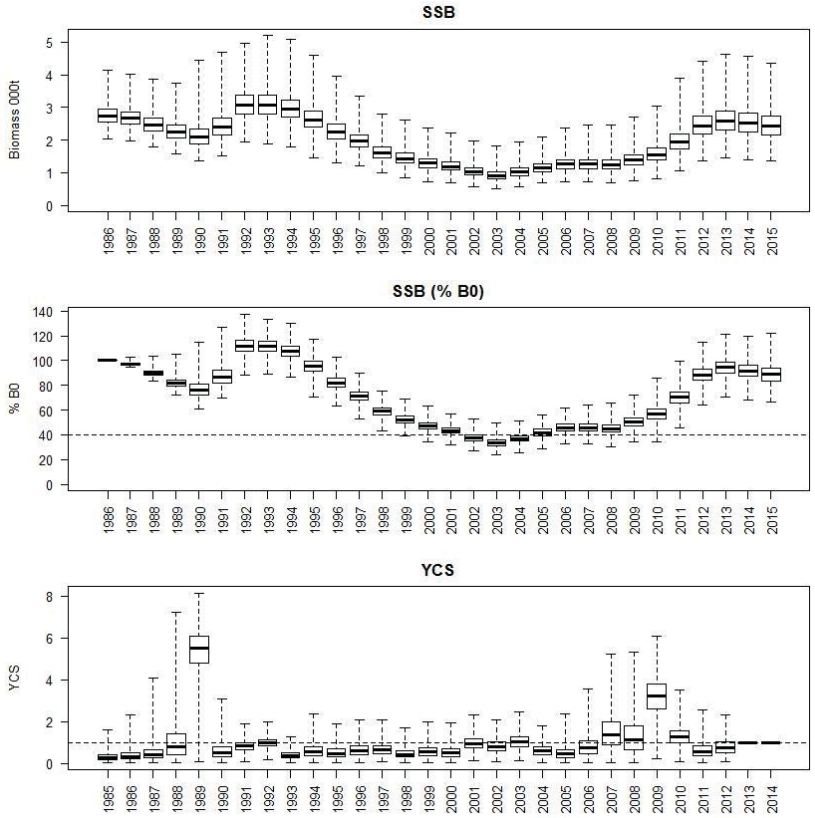

A8. 12: Posterior trajectory of SSB, SSB/SSB$_0$ and YCS for the SCI 2 Base25 model.

APPENDIX 9. SCI 2 model plots (M=0.3)

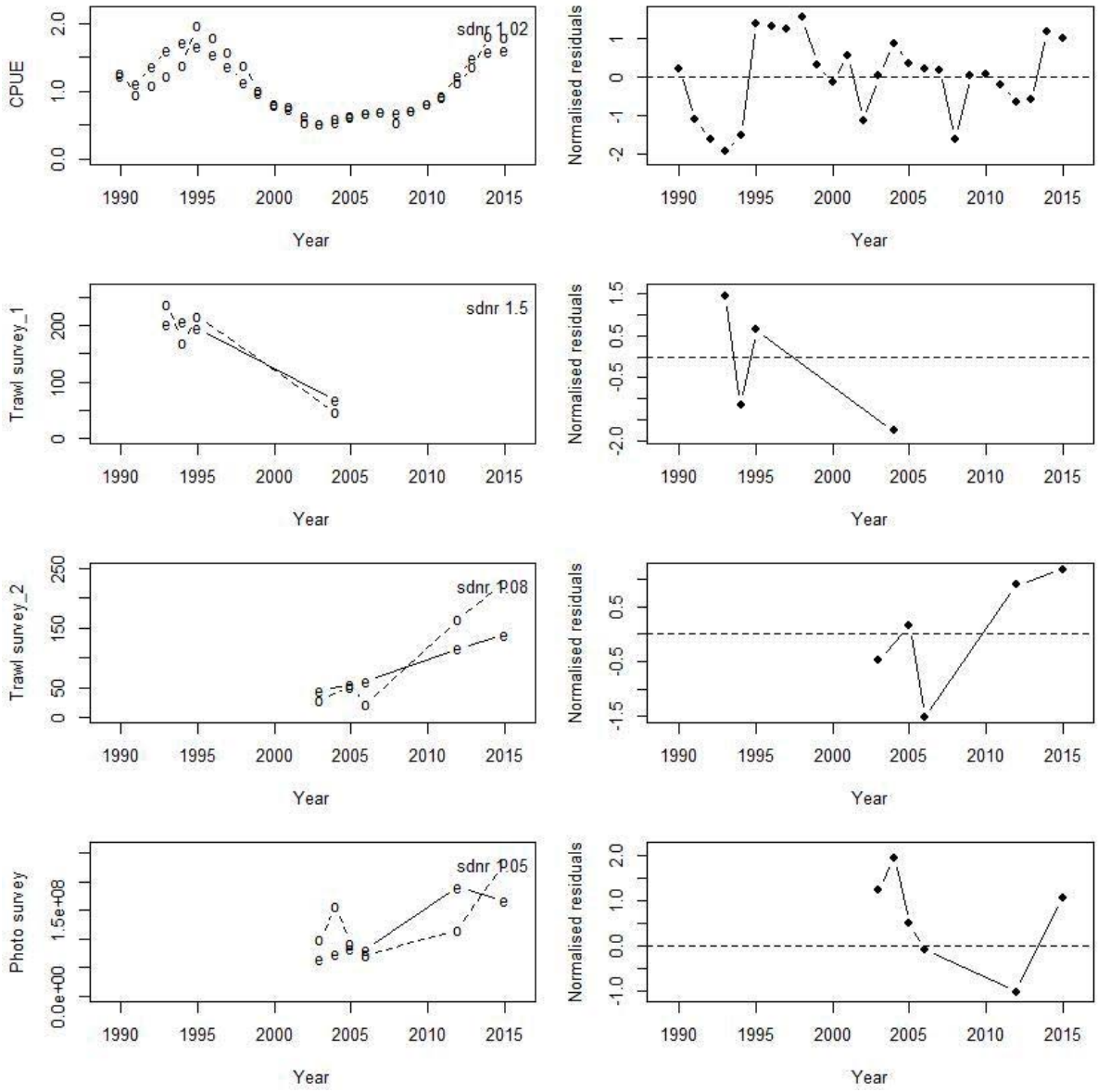

A9. 1: Fits to abundance indices (left column) and normalised residuals (right column) for standardised CPUE index (top row) trawl survey biomass index time step 1 (second row), trawl survey biomass index time step 2 (third row), and photo survey abundance index (fourth row) for the SCI 2 Base30 model.

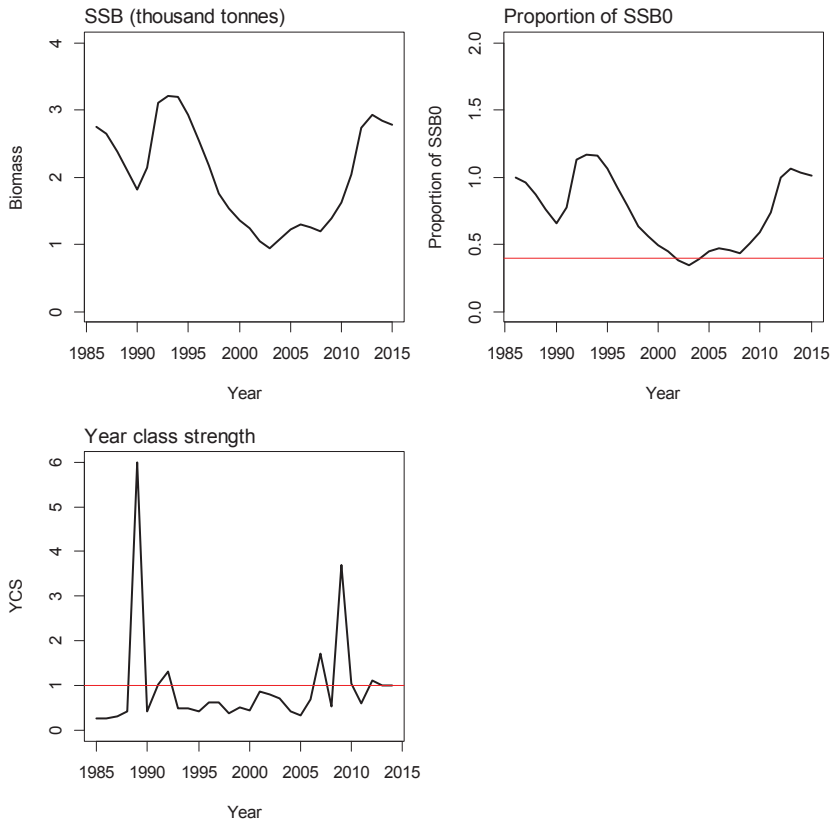

A9. 2: Spawning stock biomass trajectory (upper left), stock status (upper right), and year class strength (lower left) for the SCI 2 Base30 model.

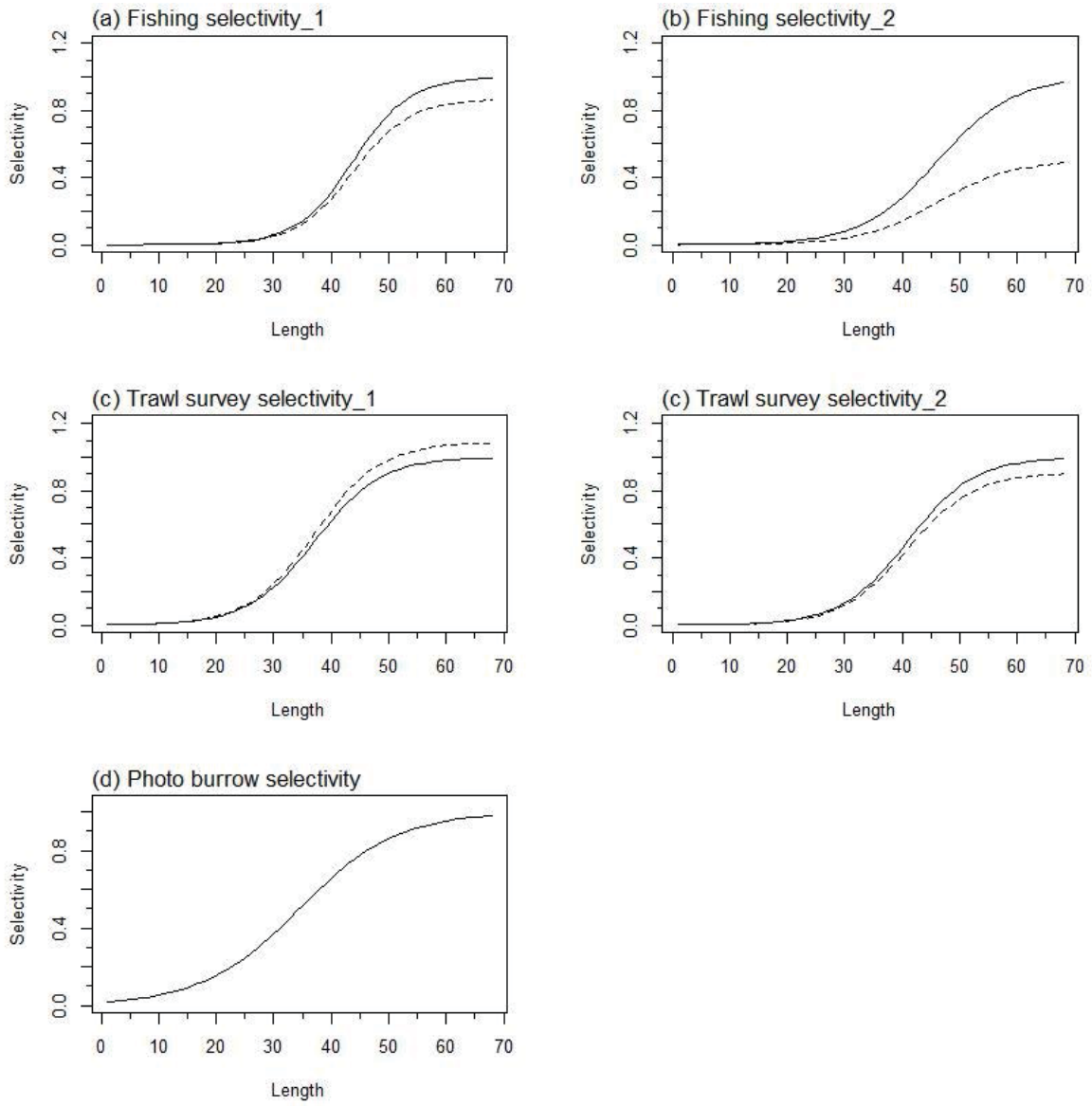

A9. 3: Fishery and survey selectivity curves for the SCI 2 Base30 model. Solid line – females, dotted line – males. The scampi burrow index is not sexed, and a single selectivity applies.

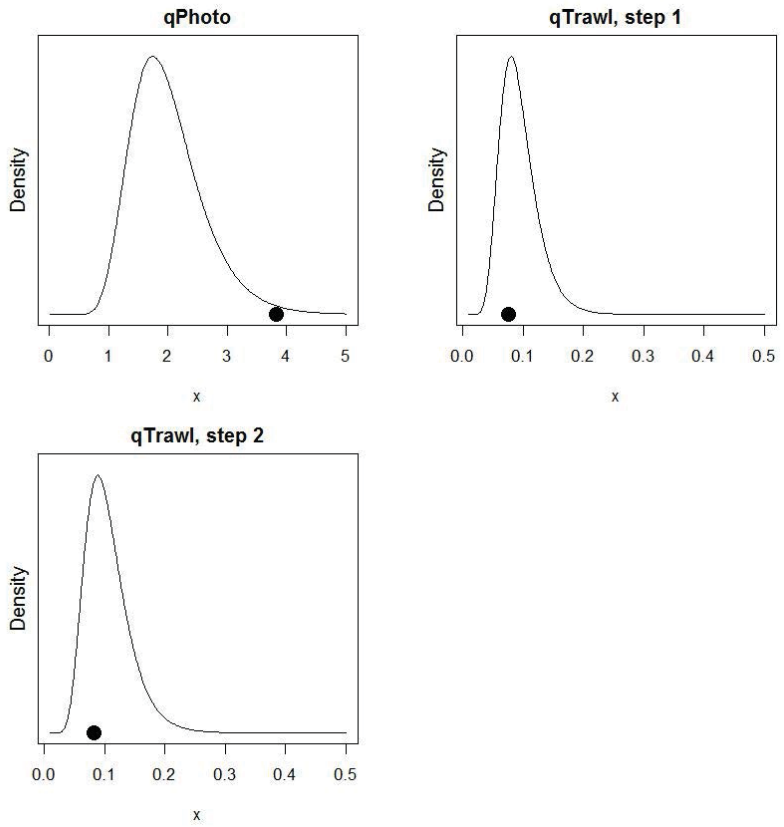

A9. 4: Catchability estimates from MPD model run, plotted in relation to prior distribution for the SCI 2 Base30 model.

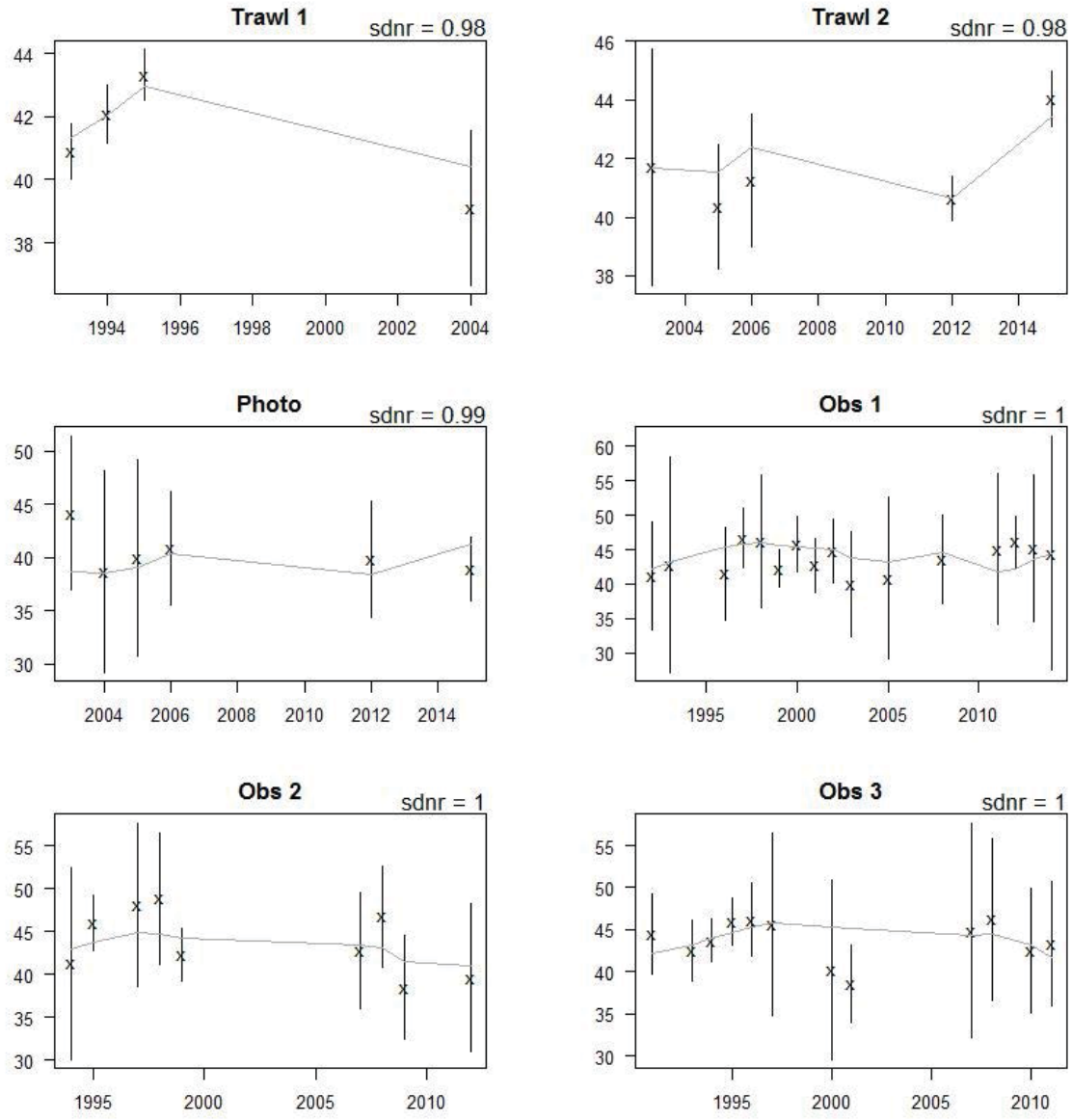

A9. 5: Observed (solid line) and fitted (grey line) mean length from length frequency distributions for survey and observer samples for the SCI 2 Base30 model.

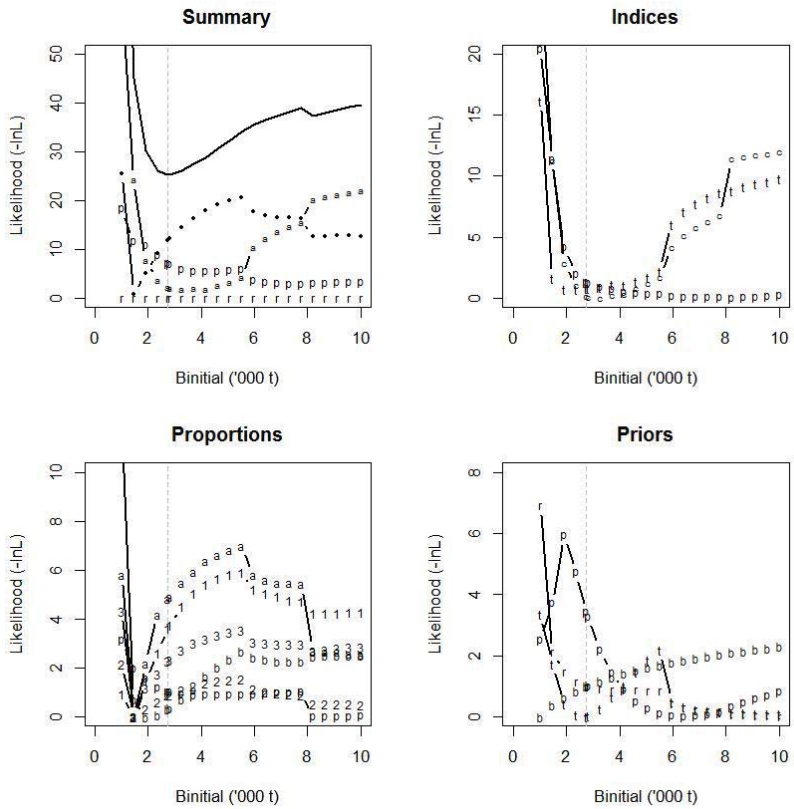

A9. 6: Likelihood profiles for model Base25 for SCI 2 when B_0 is fixed in the model. Figures show profiles for main priors (top left, p-priors, a – abundance indices, • – proportions at length, r-recapture data), abundance indices (top right, t - trawl survey step, c - CPUE, p – photo survey), proportion at length data (bottom left, p-photo, t-trawl, 1 – observer time step 1, 2 – observer time step 2, 3 – observer time step 3) and priors (bottom right, b- B_0, YCS - r, p- *q-Photo*, t – *q-Trawl*).

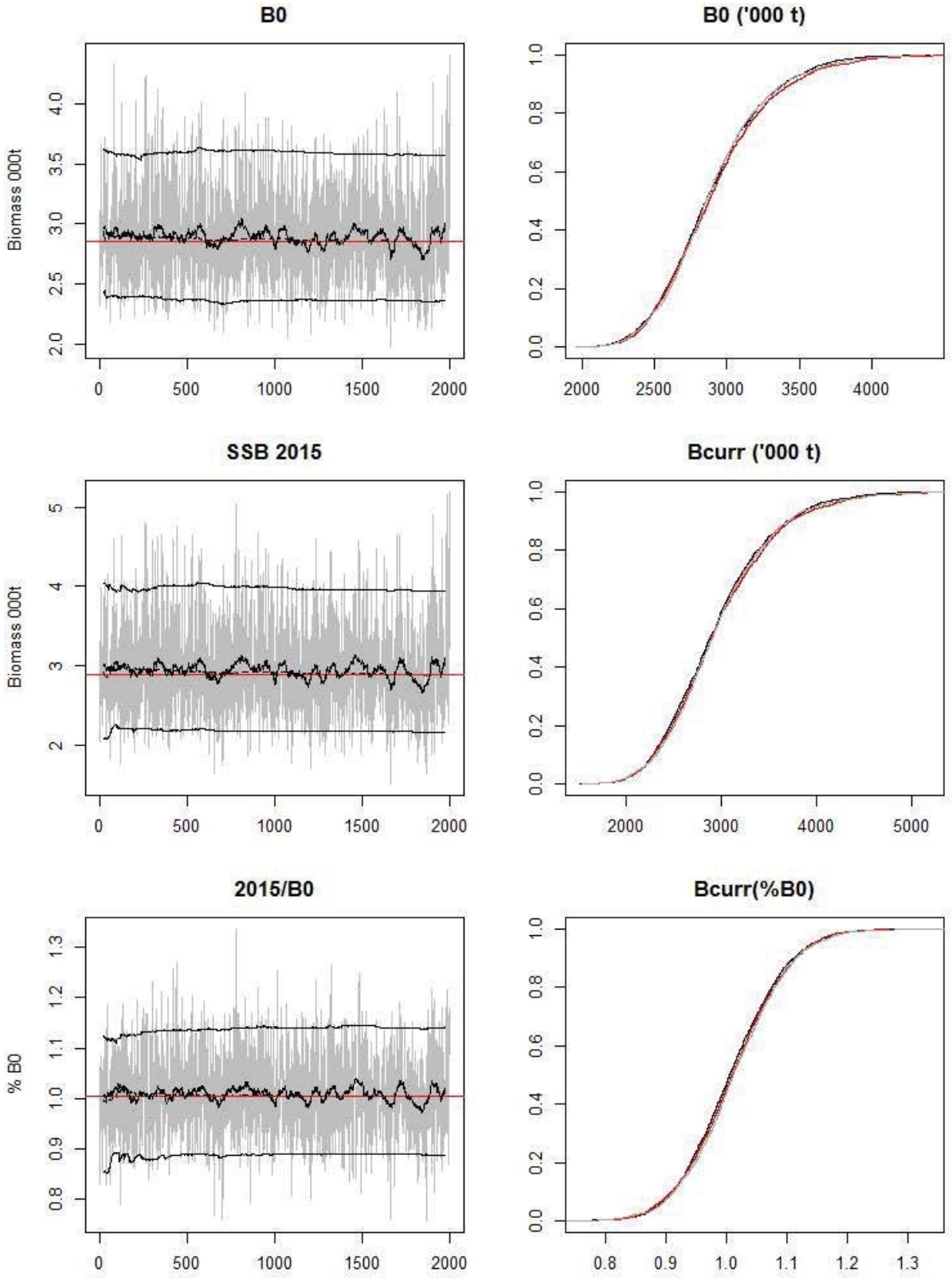

A9. 7: MCMC traces for B_0, SSB_{2015}, and SSB_{2015}/B_0 terms for the SCI 2 Base30 model, along with cumulative frequency distributions for three independent MCMC chains.

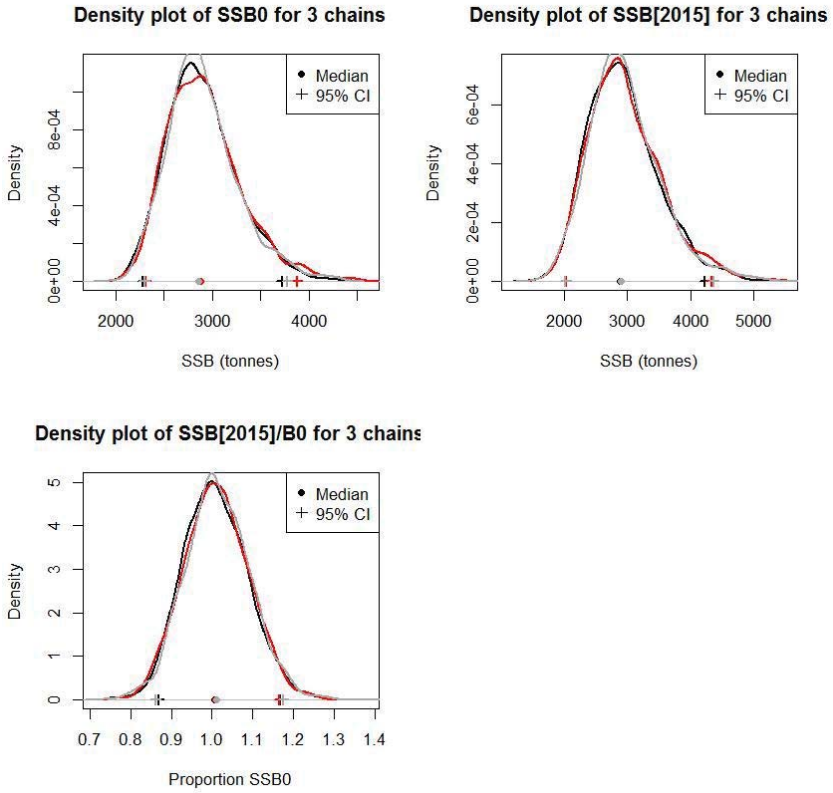

A9. 8: Density plots for B_0, SSB_{2015}, and SSB_{2015}/B_0 terms for the SCI 2 Base30 model for three independent MCMC chains, with median and 95% confidence intervals.

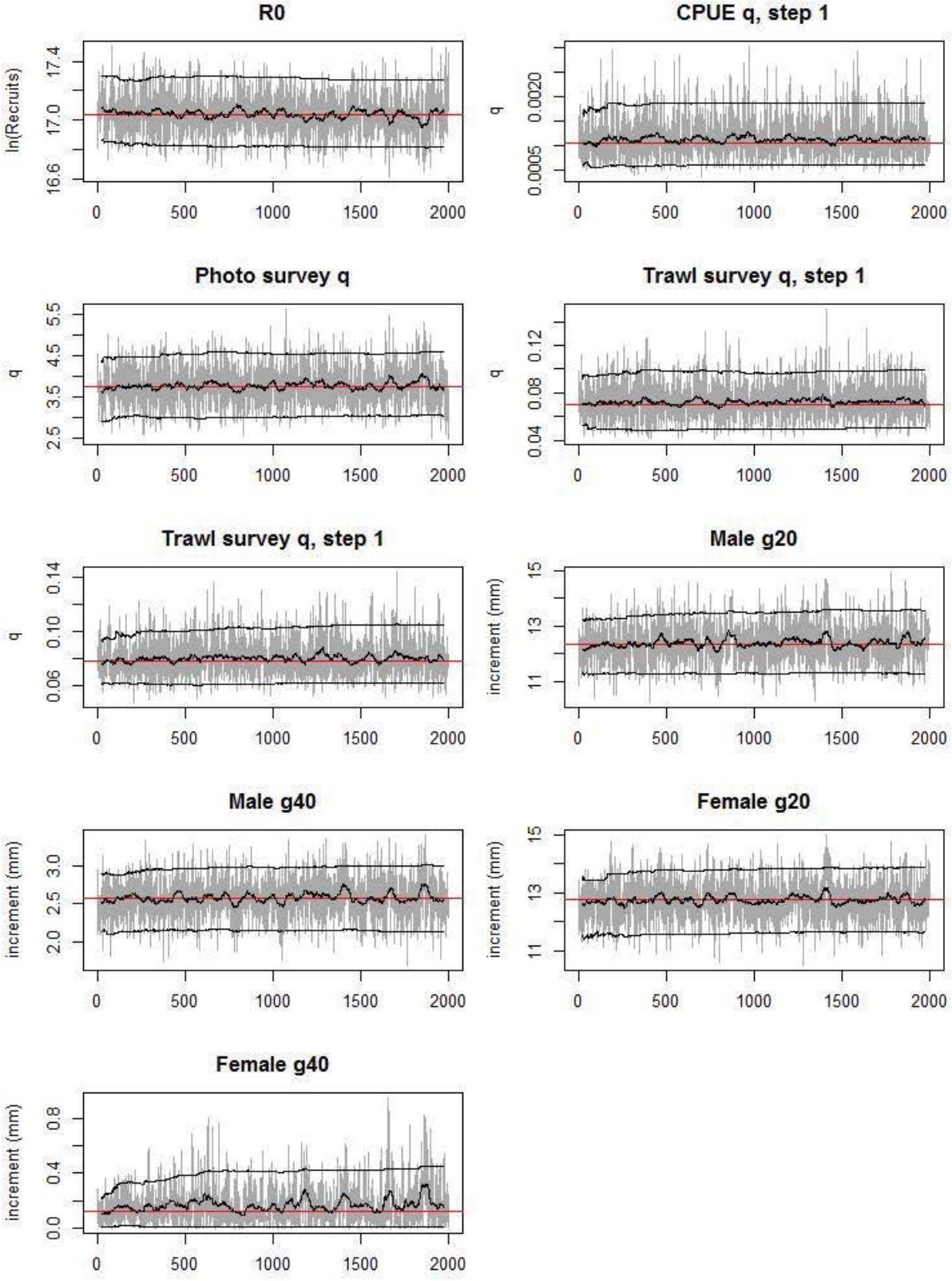

A9. 9: MCMC traces for R_0, catchability and growth terms for the SCI 2 Base30 model.

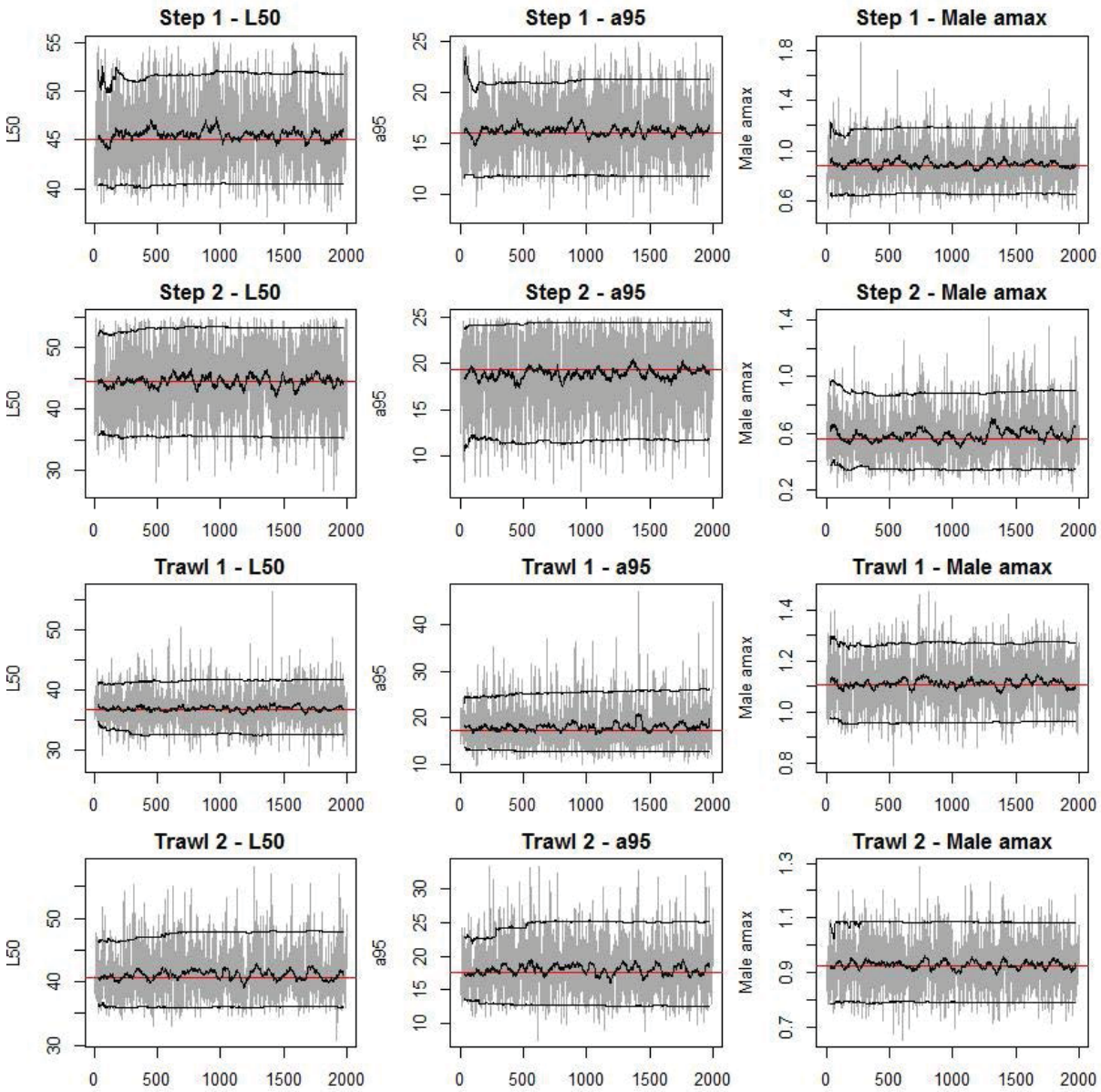

A9. 10: MCMC traces for selectivity terms for the SCI 2 Base30 model. Horizontal lines represent terms fixed in the model.

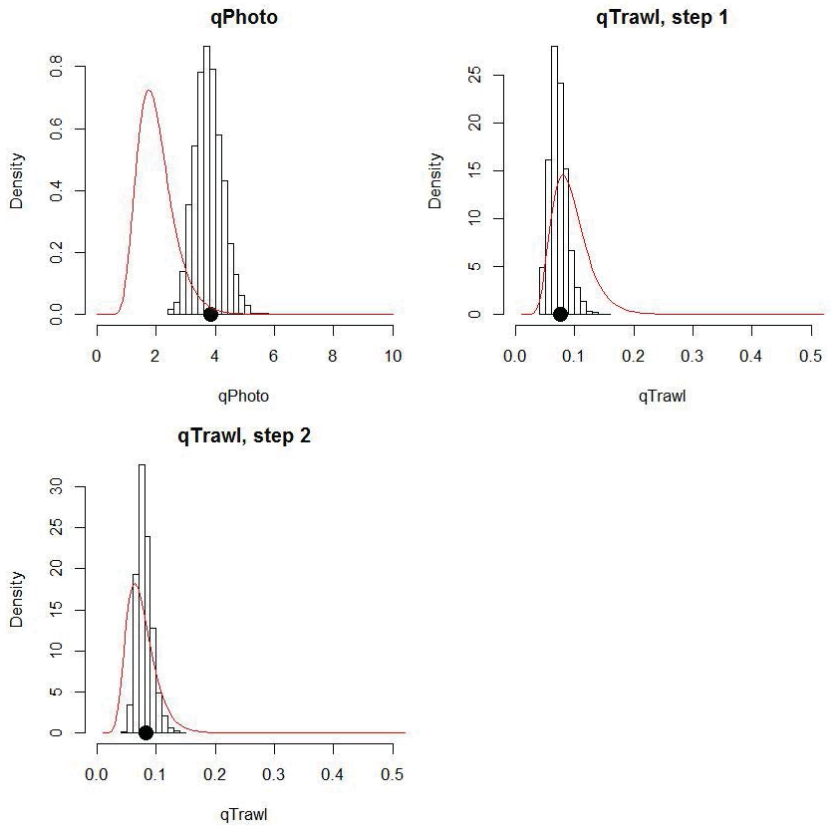

A9. 11: Marginal posterior distributions (histograms), MPD estimates (solid symbols) and distributions of priors (lines) for catchability terms for the SCI 2 Base30 model.

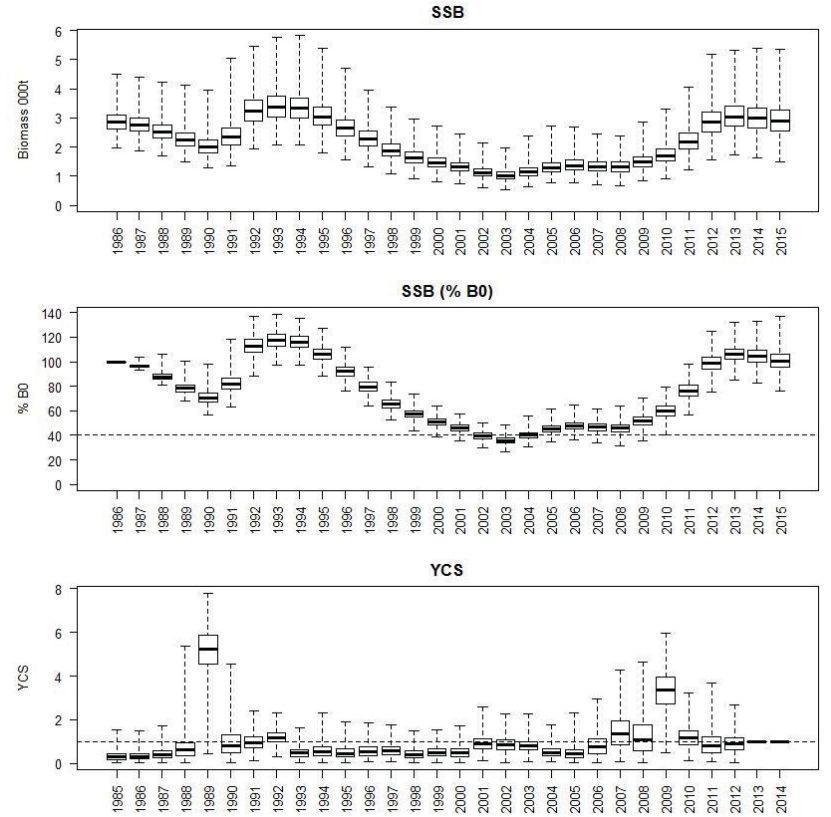

A9. 12: Posterior trajectory of SSB, SSB/SSB$_0$ and YCS for the SCI 2 Base30 model.

APPENDIX 10. SCI 2 model plots (M=0.35)

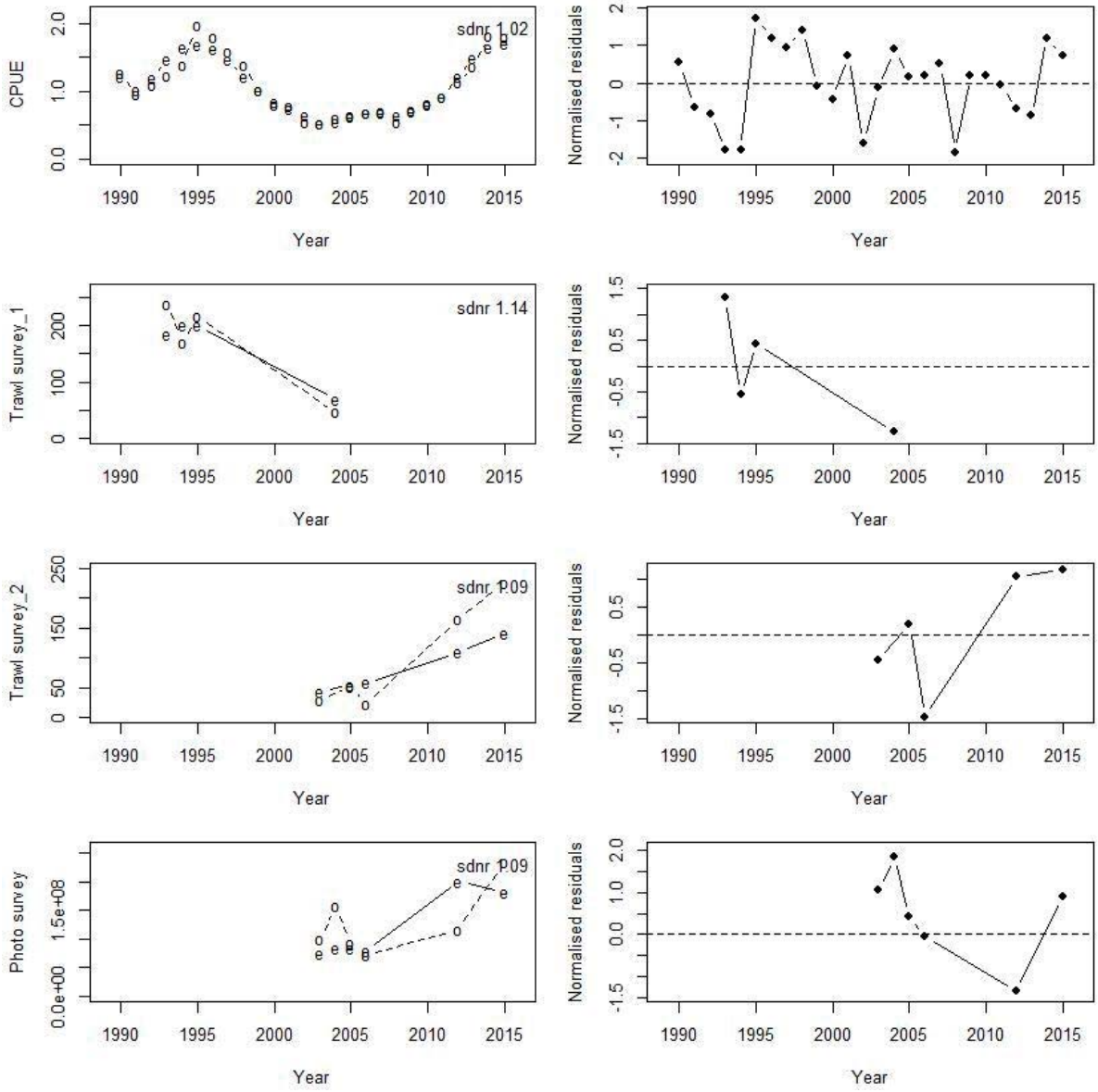

A10. 1: Fits to abundance indices (left column) and normalised residuals (right column) for standardised CPUE index (top row) trawl survey biomass index time step 1 (second row), trawl survey biomass index time step 2 (third row), and photo survey abundance index (fourth row) for the SCI 2 Base35 model.

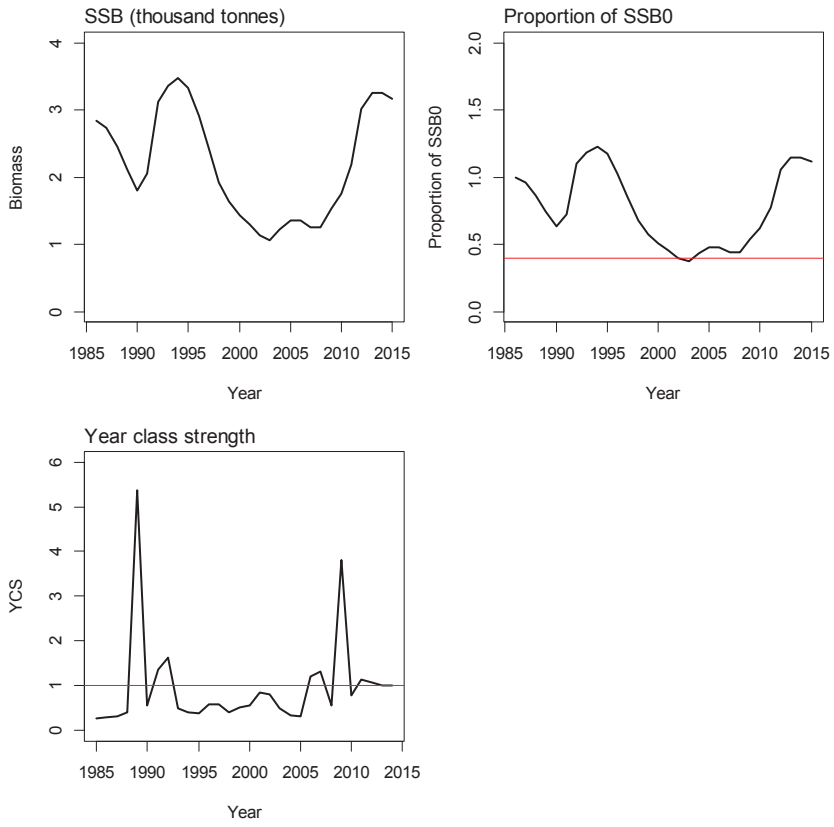

A10. 2: Spawning stock biomass trajectory (upper left), stock status (upper right), and year class strength (lower left) for the SCI 2 Base35 model.

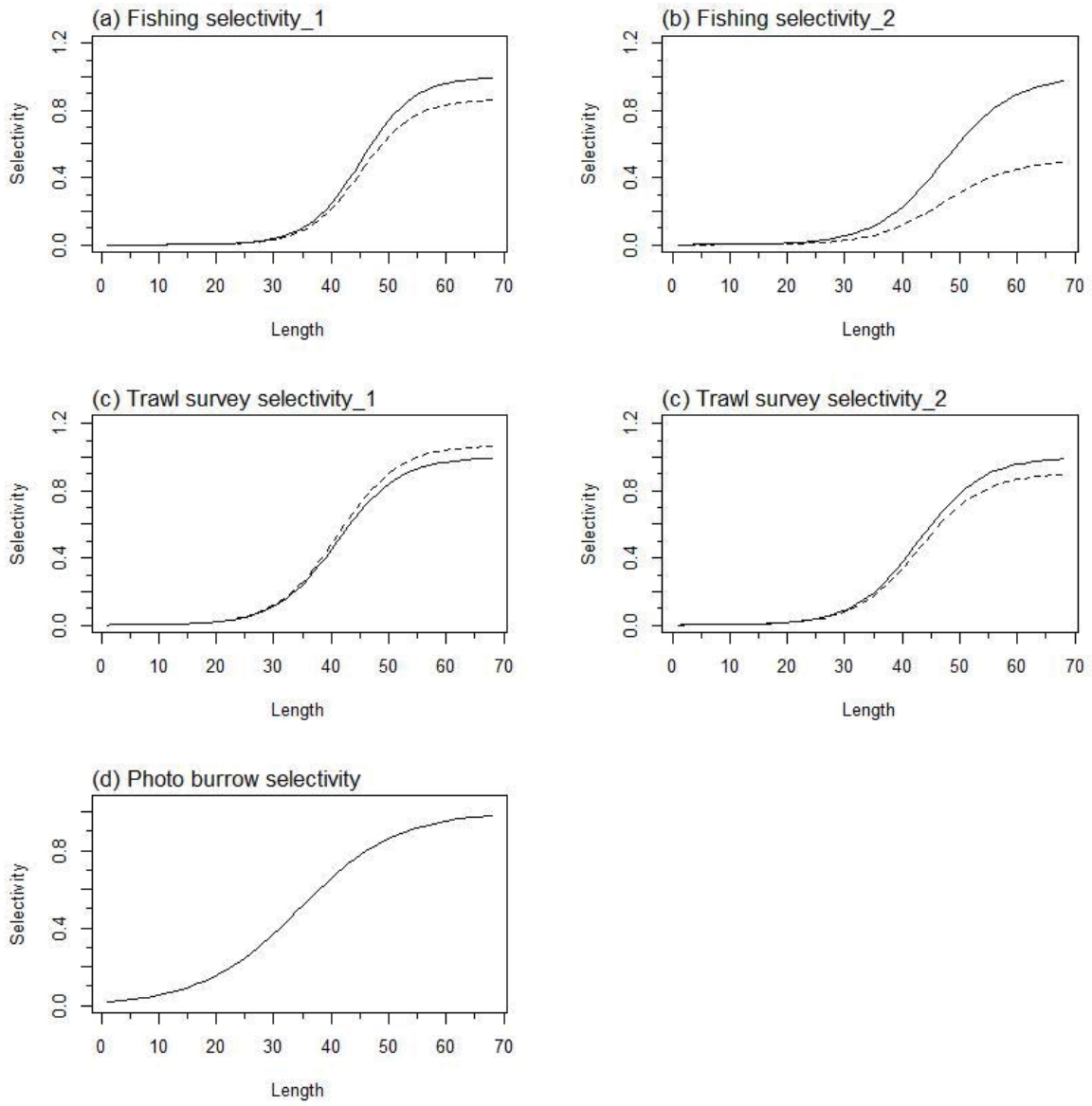

A10. 3: Fishery and survey selectivity curves for the SCI 2 Base35 model. Solid line – females, dotted line – males. The scampi burrow index is not sexed, and a single selectivity applies.

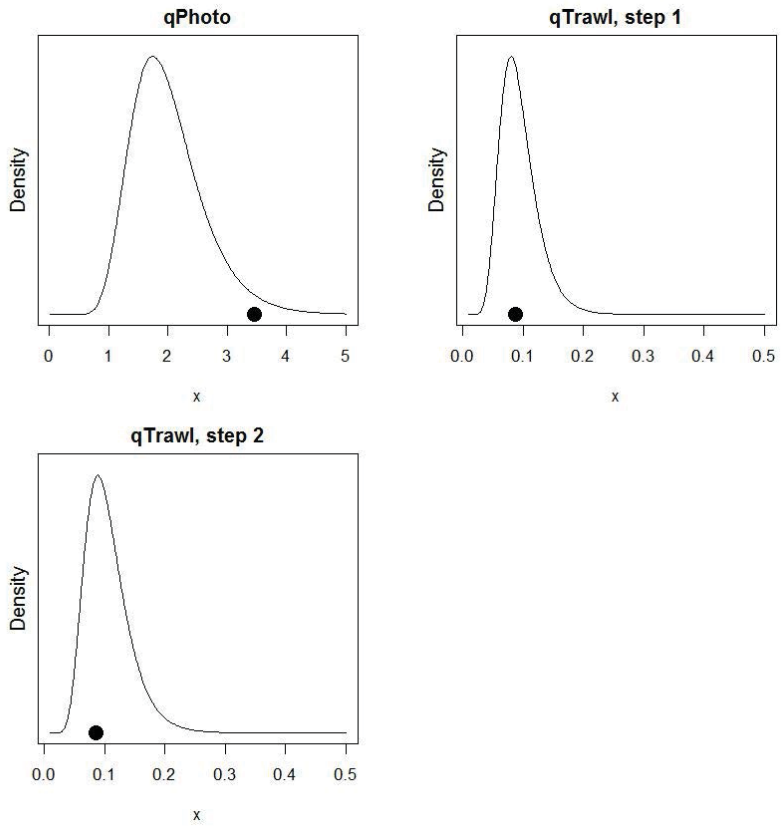

A10. 4: Catchability estimates from MPD model run, plotted in relation to prior distribution for the SCI 2 Base35 model.

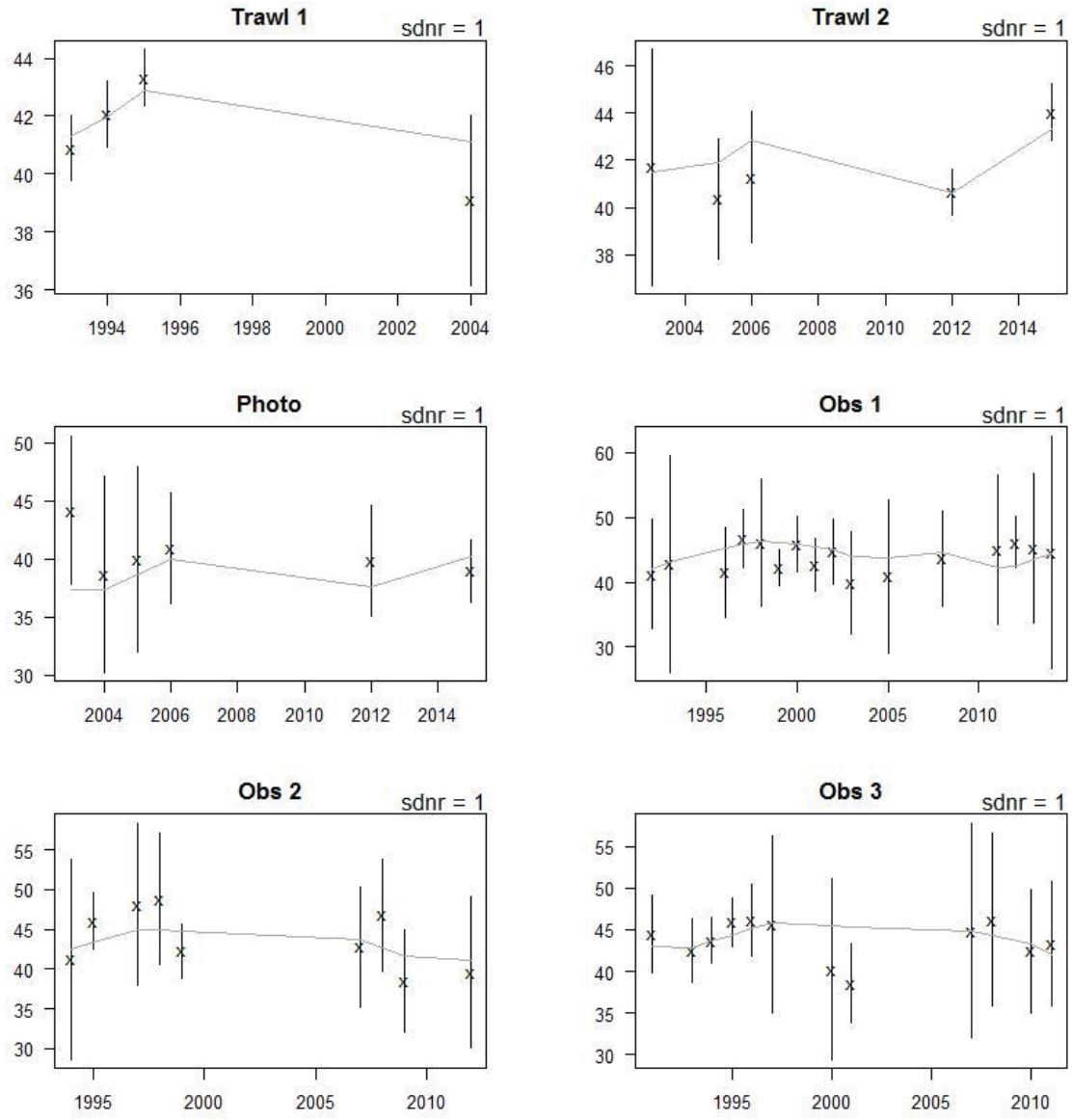

A10. 5: Observed (solid line) and fitted (grey line) mean length from length frequency distributions for survey and observer samples for the SCI 2 Base35 model.

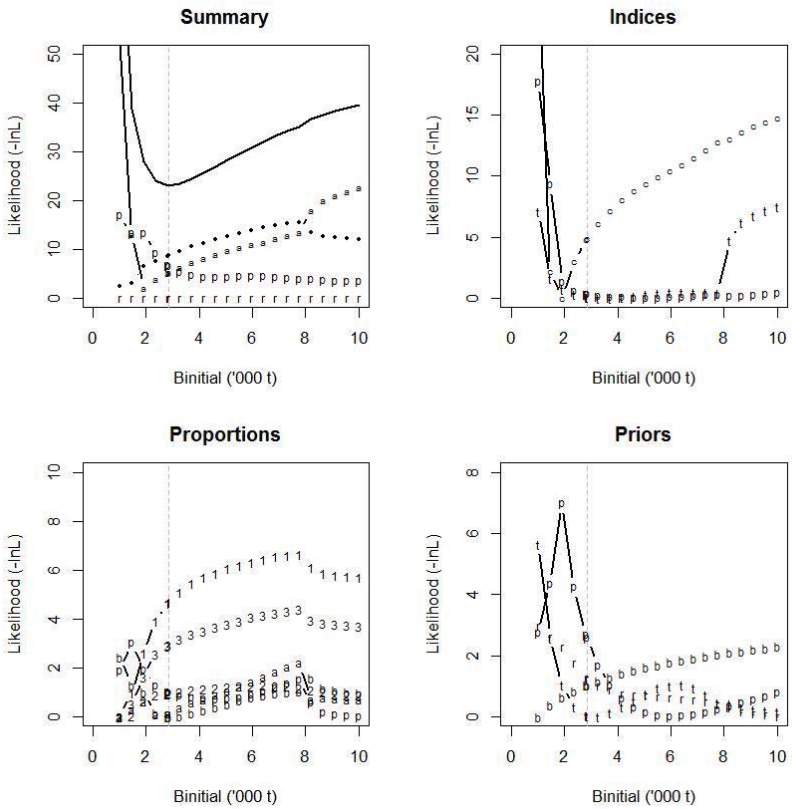

A10. 6: Likelihood profiles for model Base35 for SCI 2 when B_0 is fixed in the model. Figures show profiles for main priors (top left, p-priors, a – abundance indices, • – proportions at length, r-recapture data), abundance indices (top right, t - trawl survey step, c - CPUE, p – photo survey), proportion at length data (bottom left, p-photo, t-trawl, 1 – observer time step 1, 2 – observer time step 2, 3 – observer time step 3) and priors (bottom right, b- B_0, YCS - r, p- *q-Photo*, t – *q-Trawl*).

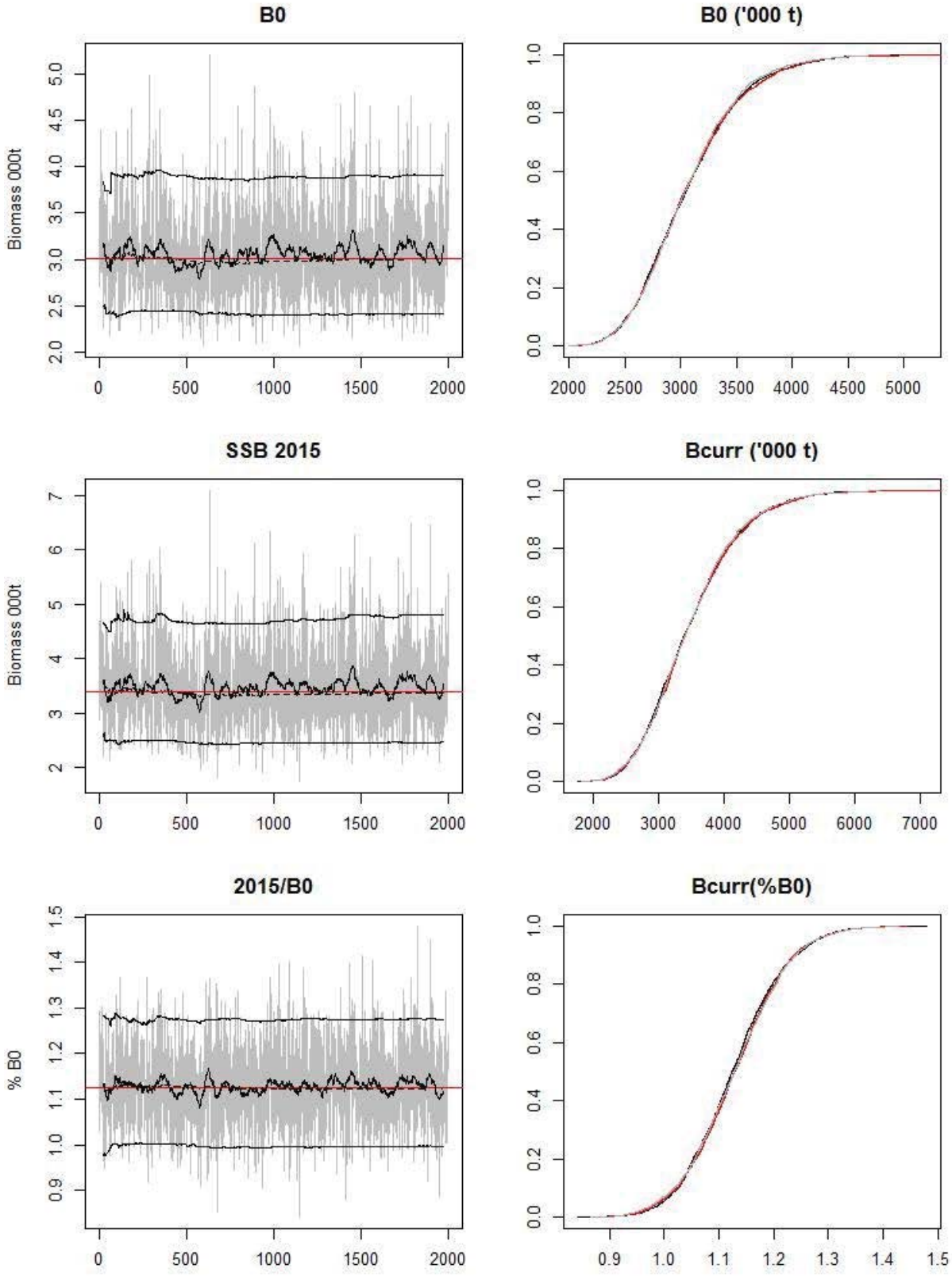

A10. 7: MCMC traces for B_0, SSB_{2015}, and SSB_{2015}/B_0 terms for the SCI 2 Base35 model, along with cumulative frequency distributions for three independent MCMC chains.

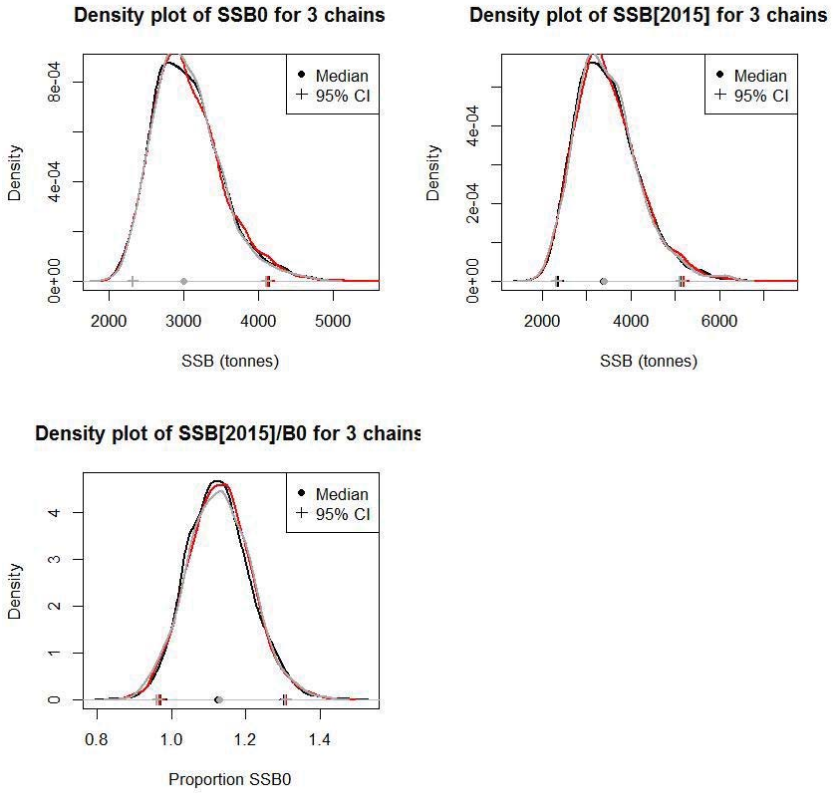

A10. 8: Density plots for B_0, SSB_{2015}, and SSB_{2015}/B_0 terms for the SCI 2 Base35 model for three independent MCMC chains, with median and 95% confidence intervals.

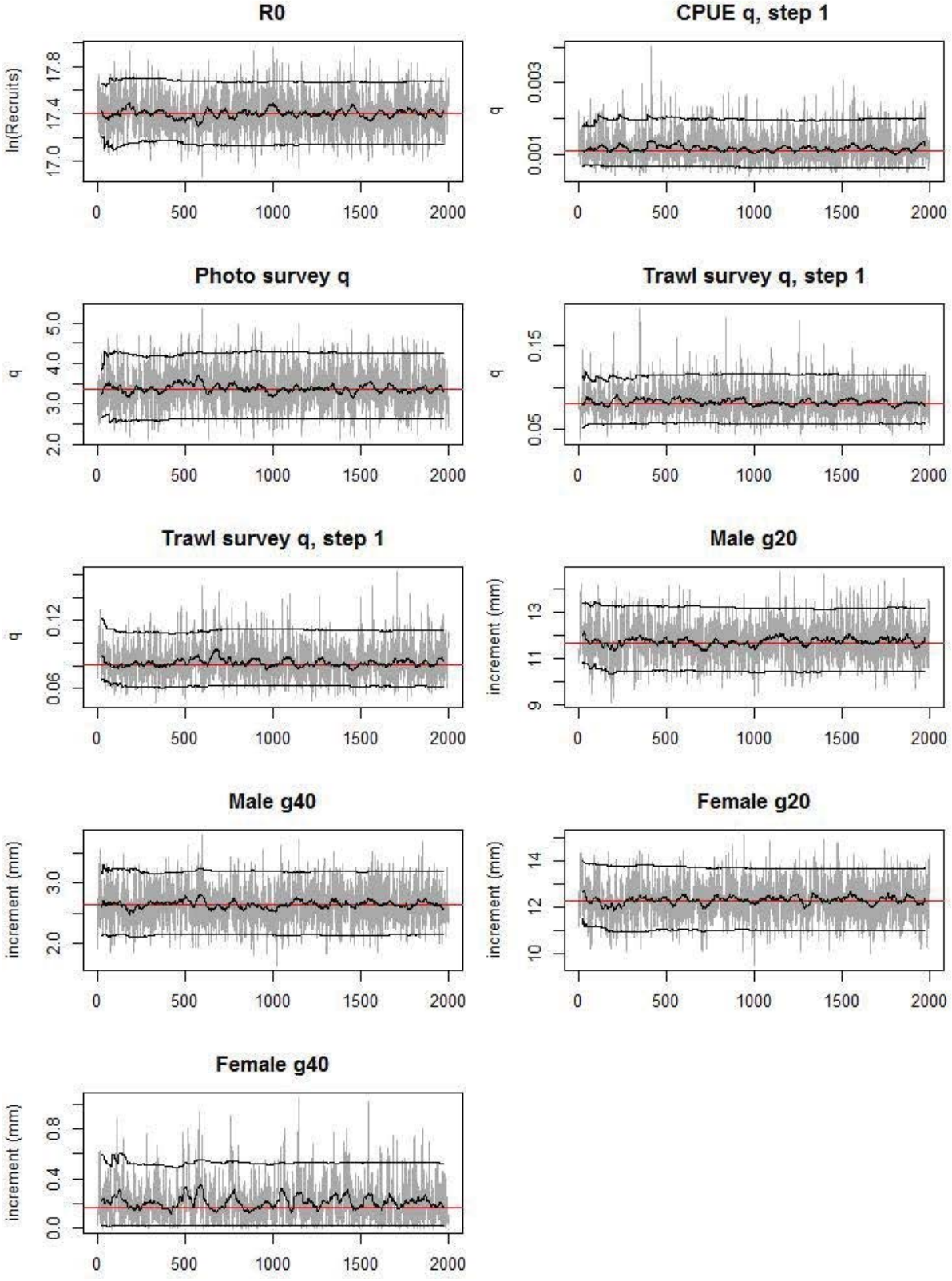

A10. 9: MCMC traces for R_0, catchability and growth terms for the SCI 2 Base35 model.

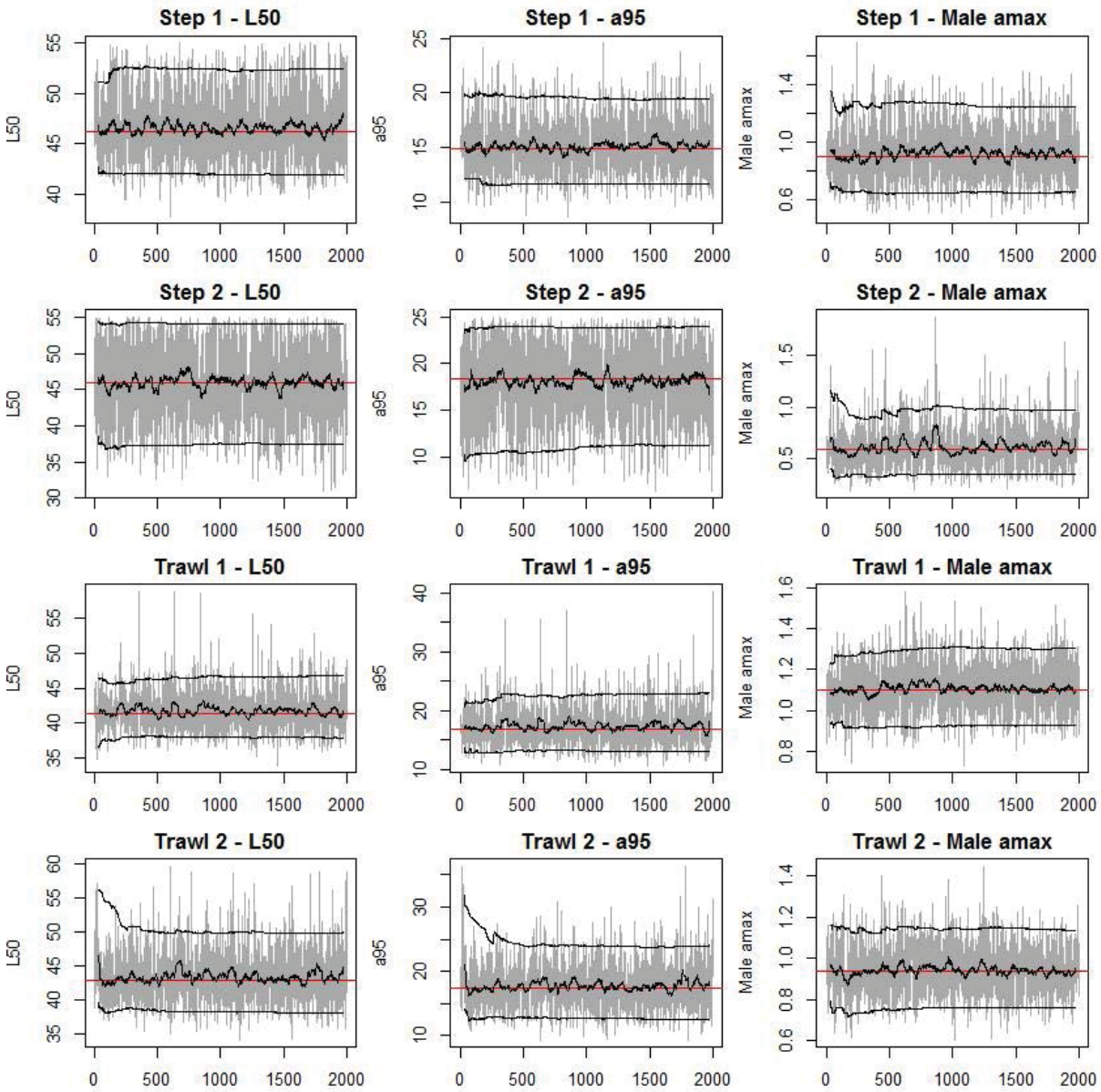

A10. 10: MCMC traces for selectivity terms for the SCI 2 Base35 model. Horizontal lines represent terms fixed in the model.

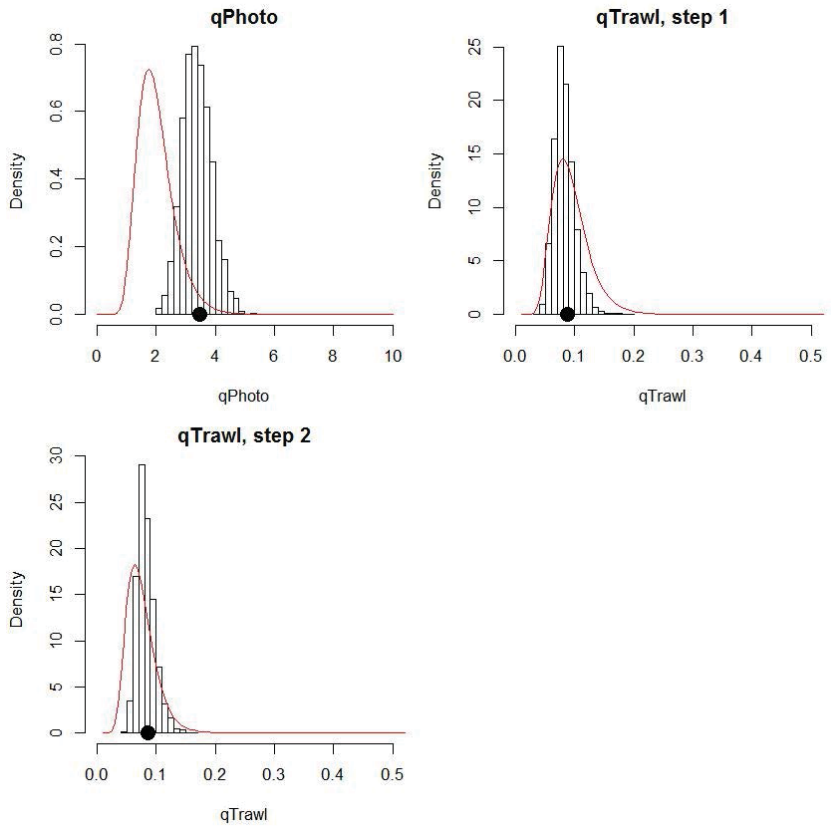

A10. 11: Marginal posterior distributions (histograms), MPD estimates (solid symbols) and distributions of priors (lines) for catchability terms for the SCI 2 Base35 model.

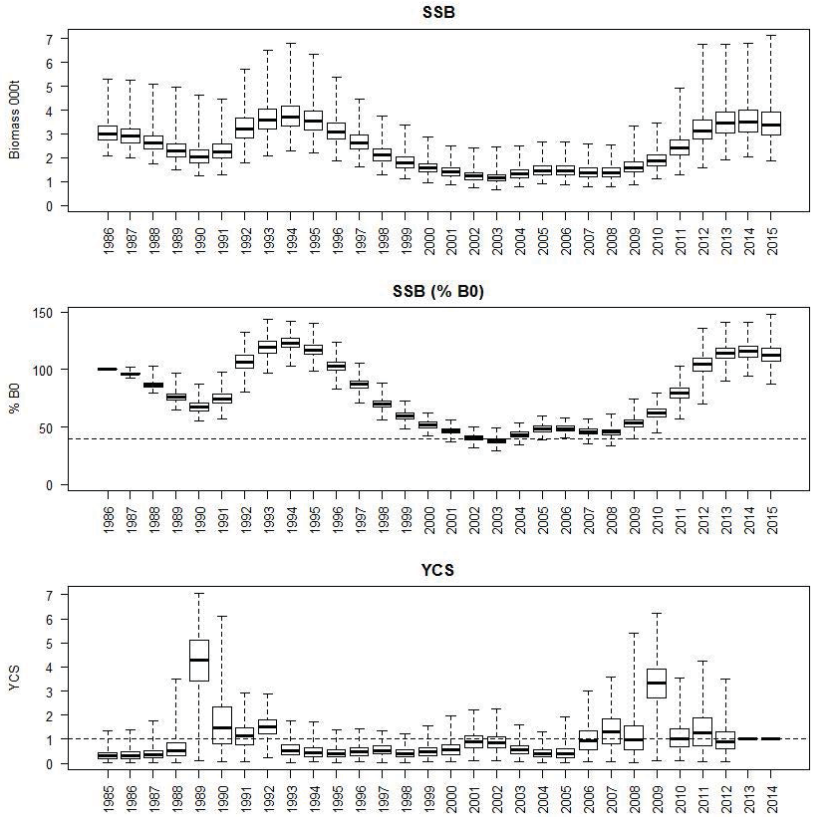

A10. 12: Posterior trajectory of SSB, SSB/SSB$_0$ and YCS for the SCI 2 Base35 model.

APPENDIX 11. Combined area model plots (M=0.30)

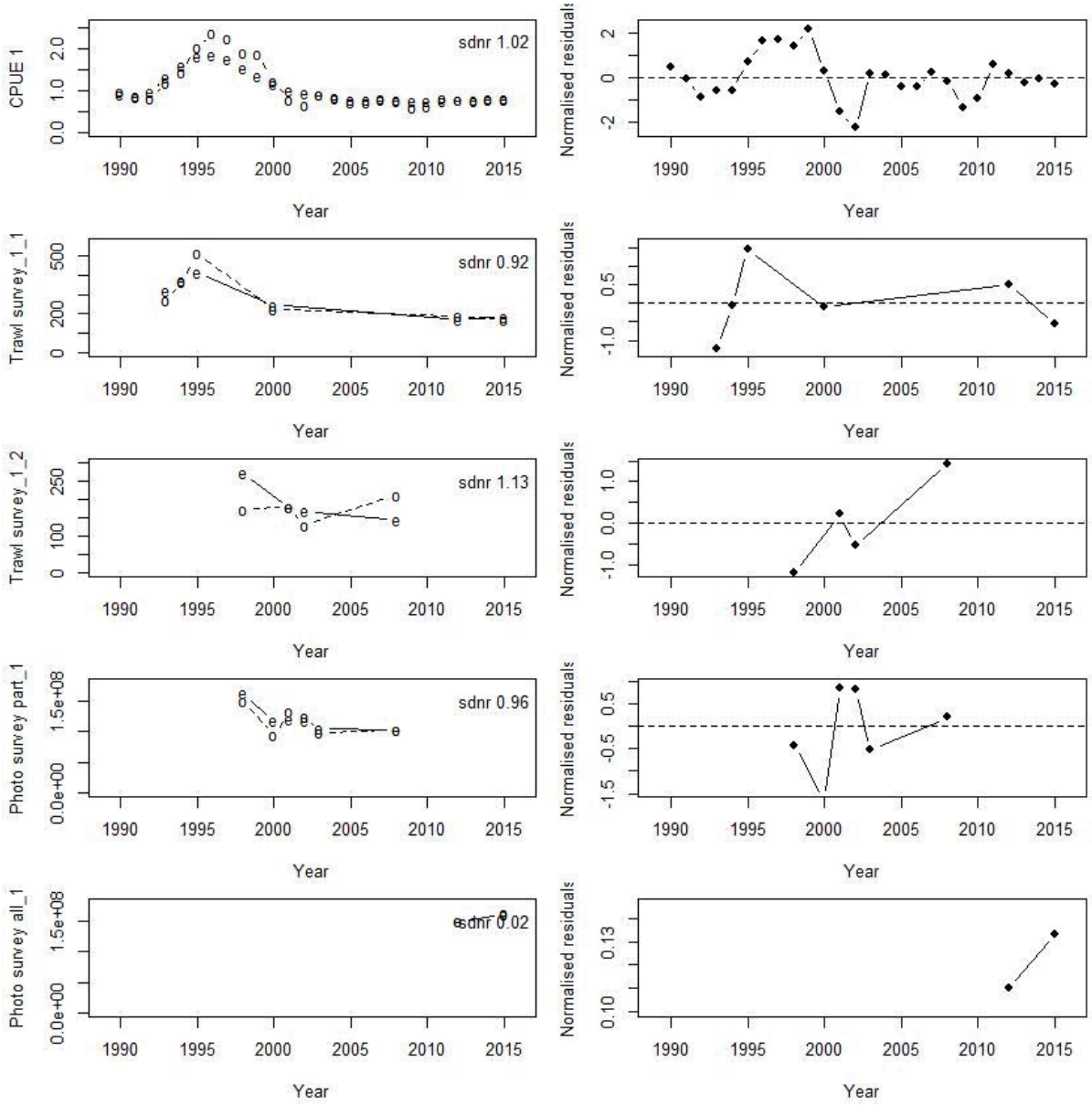

A11. 1: Fits to abundance indices (left column) and normalised residuals (right column) for standardised CPUE index (top row) trawl survey biomass index time step 1 (second row), trawl survey biomass index time step 2 (third row), and photo survey abundance index (fourth row) for SCI 1 within the Combined area Base30 model.

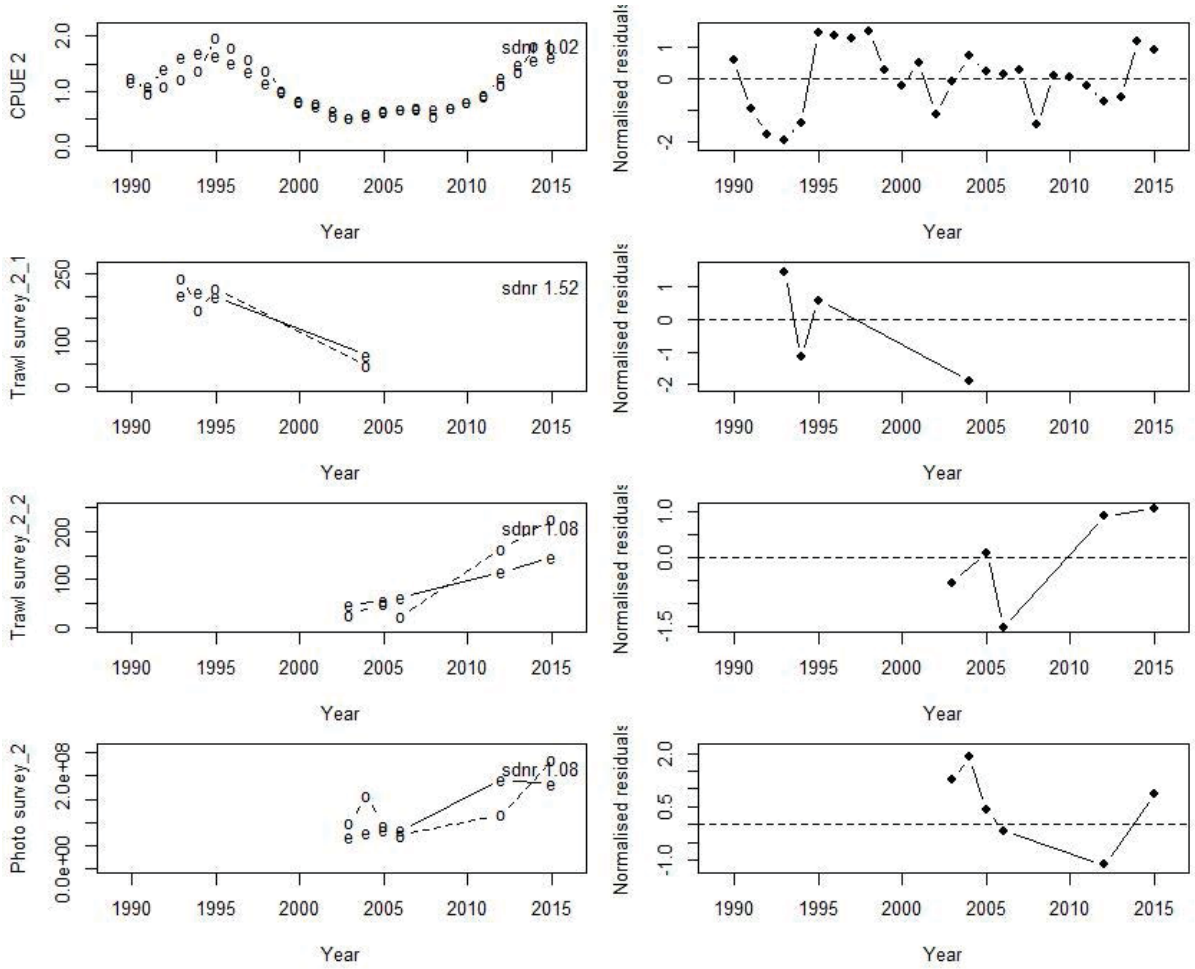

A11. 2: Fits to abundance indices (left column) and normalised residuals (right column) for standardised CPUE index (top row) trawl survey biomass index time step 1 (second row), trawl survey biomass index time step 2 (third row), and photo survey abundance index (fourth row) for SCI 2 within the Combined area Base30 model.

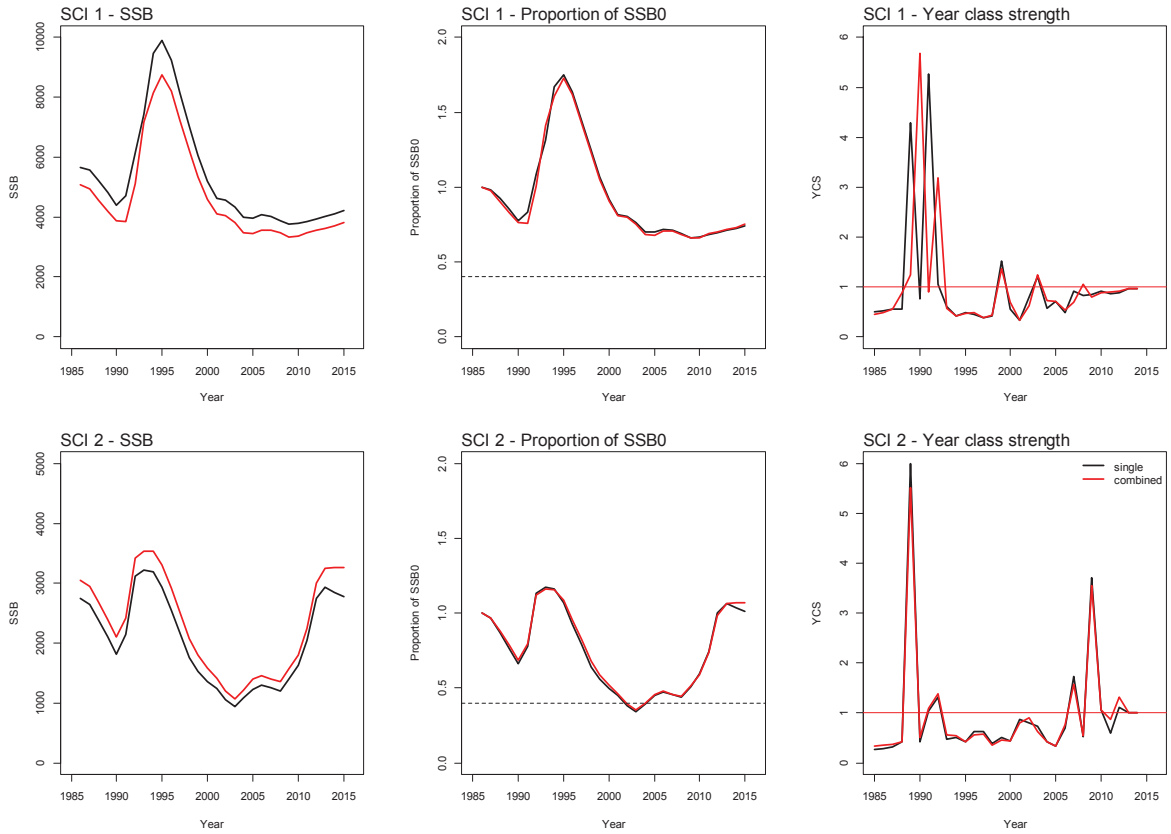

A11. 3: Spawning stock biomass trajectory (left), stock status (middle), and year class strength (right) for SCI 1 (top) and SCI 2 (bottom) from Combined area (red) and equivalent single area (black) models.

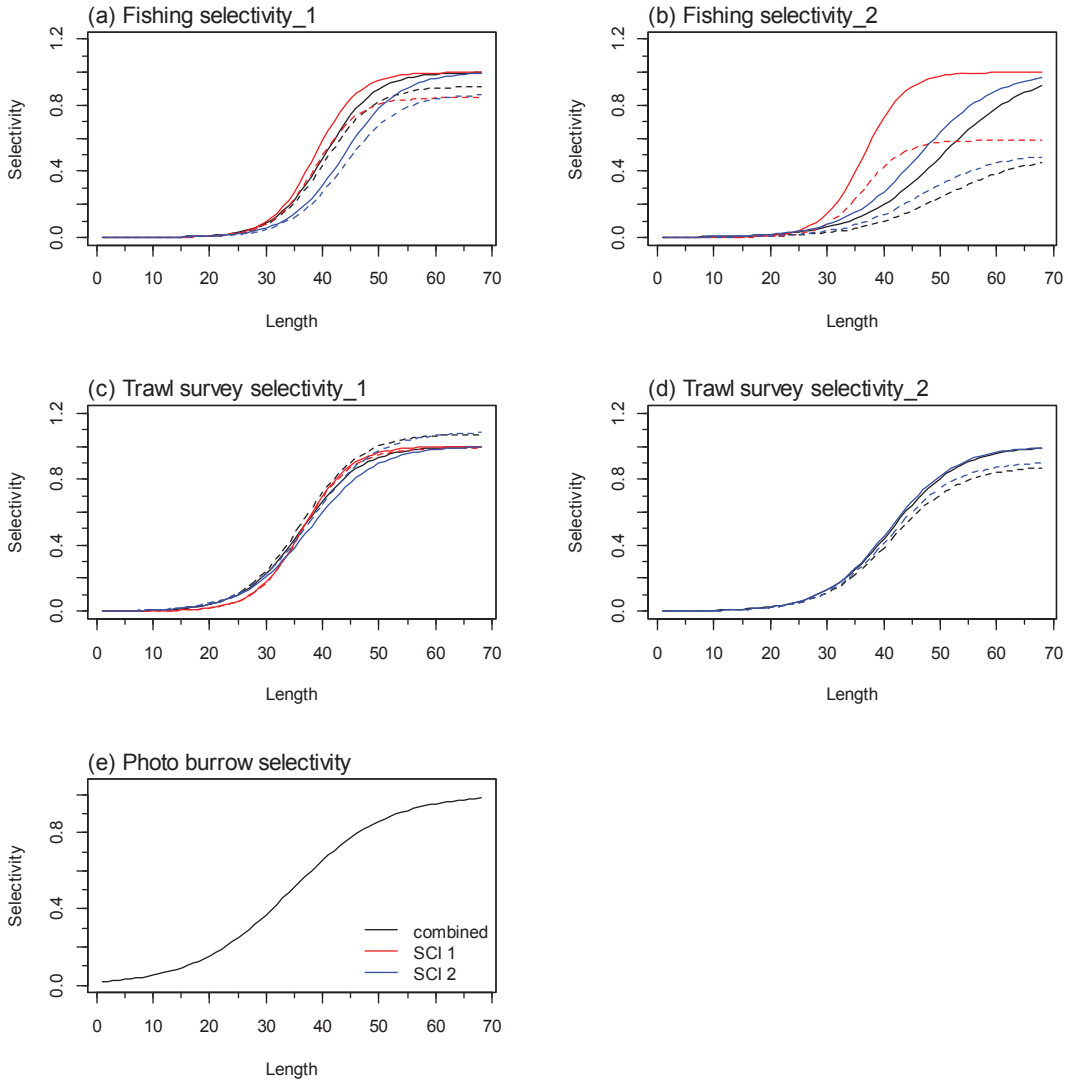

A11. 4: Fishery and survey selectivity curves for the Combined area (black) and equivalent single area (red/blue) models. Solid line – females, dotted line – males. The scampi burrow index is not sexed, and a single fixed selectivity applies. SCI 1, step 2 L_{50} was also fixed.

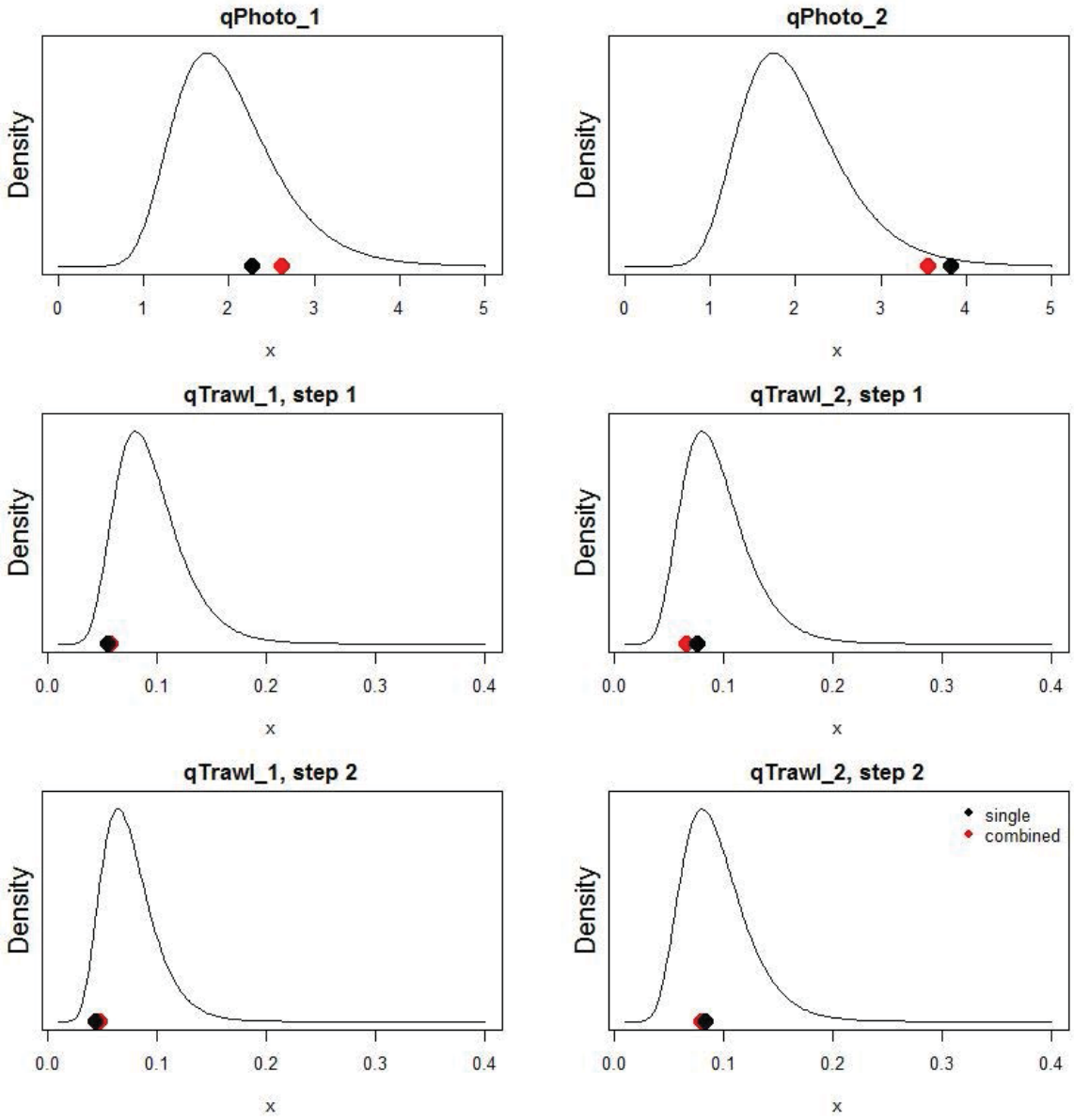

A11. 5: Catchability estimates from MPD model run, plotted in relation to prior distribution for the Combined area (red) and equivalent single area (black) models.

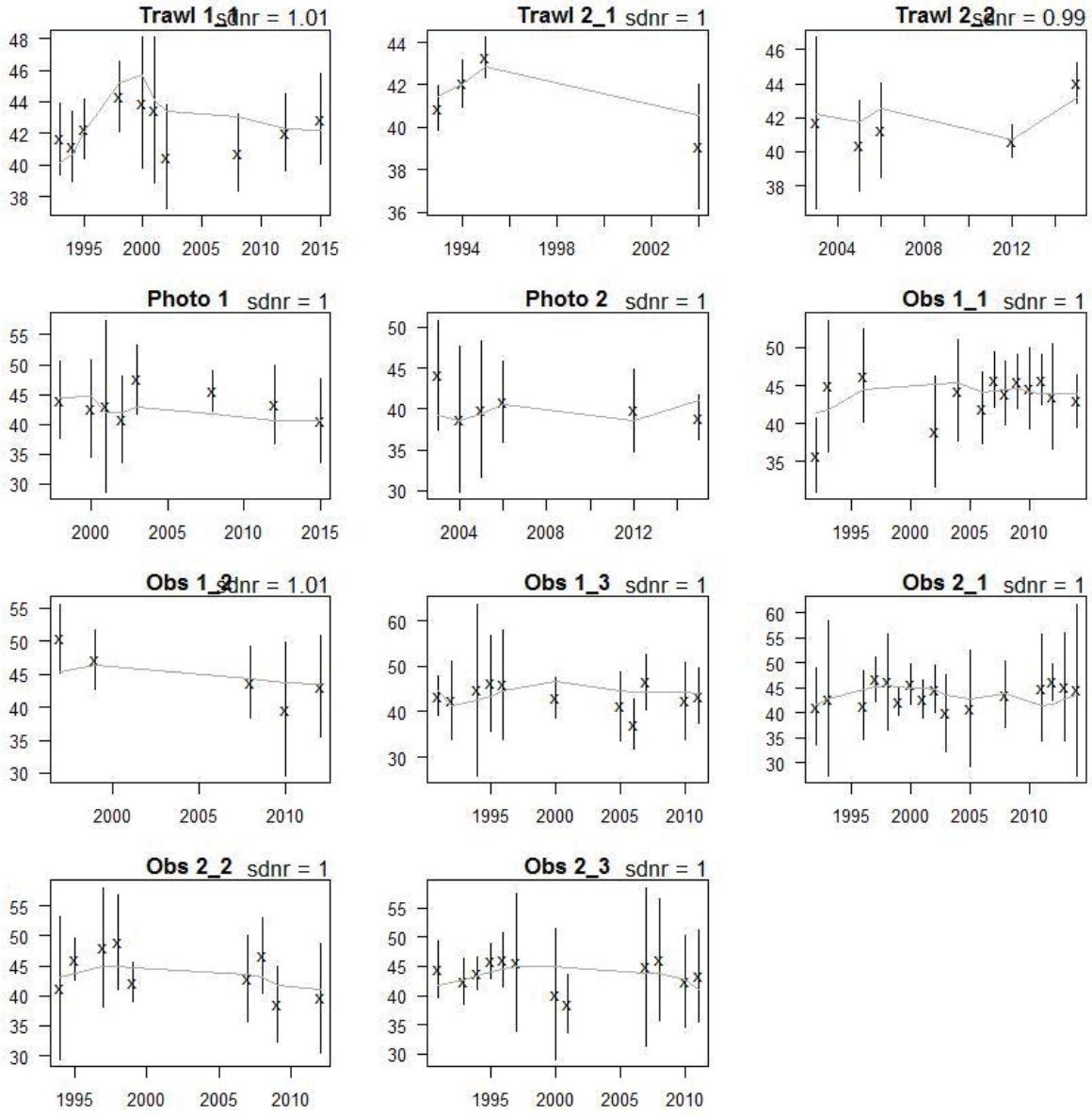

A11. 6: Observed (crosses, with vertical lines representing ± two standard errors) and fitted (grey line) mean length from length frequency distributions for survey and observer samples for the Combined area model.

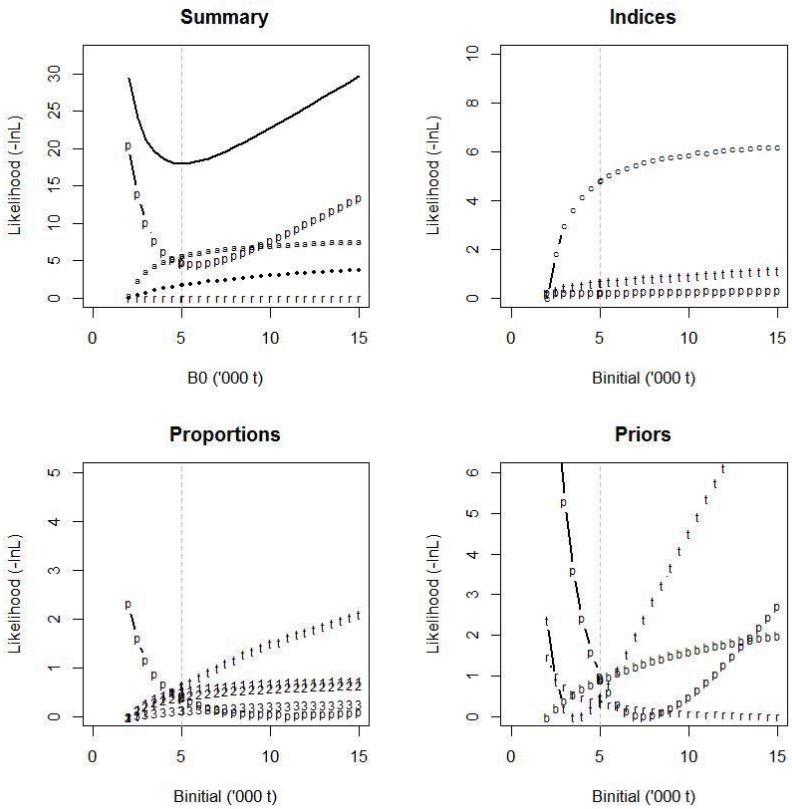

A11. 7: Likelihood profiles for the combined area model for SCI 1 when B_0 is fixed in the model. Figures show profiles for main priors (top left, p-priors, a – abundance indices, • – proportions at length, r-recapture data), abundance indices (top right, t - trawl survey step, c - CPUE, p – photo survey), proportion at length data (bottom left, p-photo, t-trawl, 1 – observer time step 1, 2 – observer time step 2, 3 – observer time step 3) and priors (bottom right, b- B_0, YCS - r, p- *q-Photo*, t – *q-Trawl*).

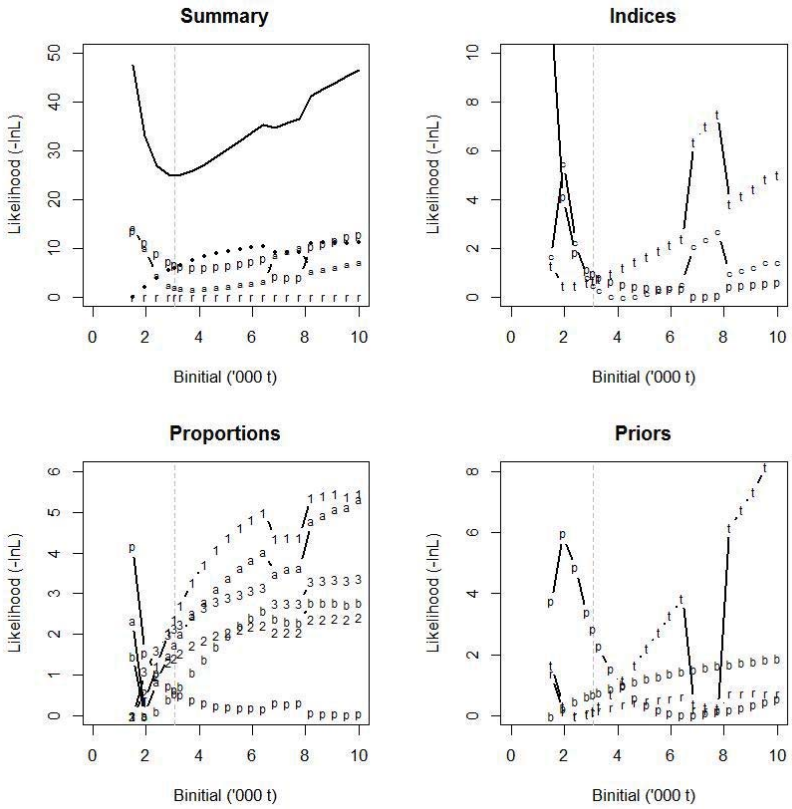

A11. 8: Likelihood profiles for the combined area model for SCI 2 when B_0 is fixed in the model. Figures show profiles for main priors (top left, p-priors, a – abundance indices, • – proportions at length, r-recapture data), abundance indices (top right, t - trawl survey step, c - CPUE, p – photo survey), proportion at length data (bottom left, p-photo, t-trawl, 1 – observer time step 1, 2 – observer time step 2, 3 – observer time step 3) and priors (bottom right, b- B_0, YCS - r, p- *q-Photo*, t – *q-Trawl*).

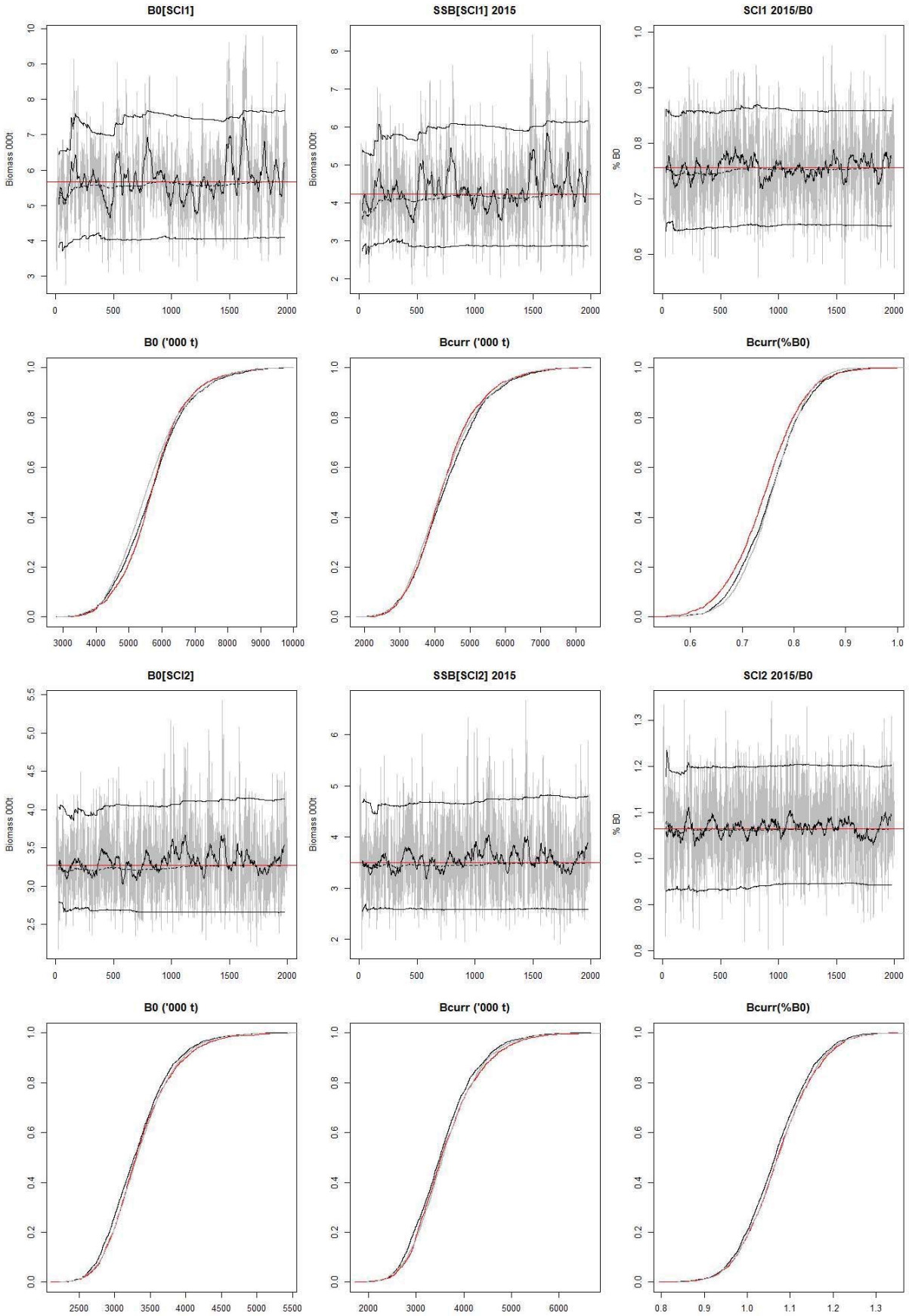

A11. 9: MCMC traces for B_0, SSB_{2015}, and SSB_{2015}/B_0 terms for the combined area model, along with cumulative frequency distributions for three independent MCMC chains.

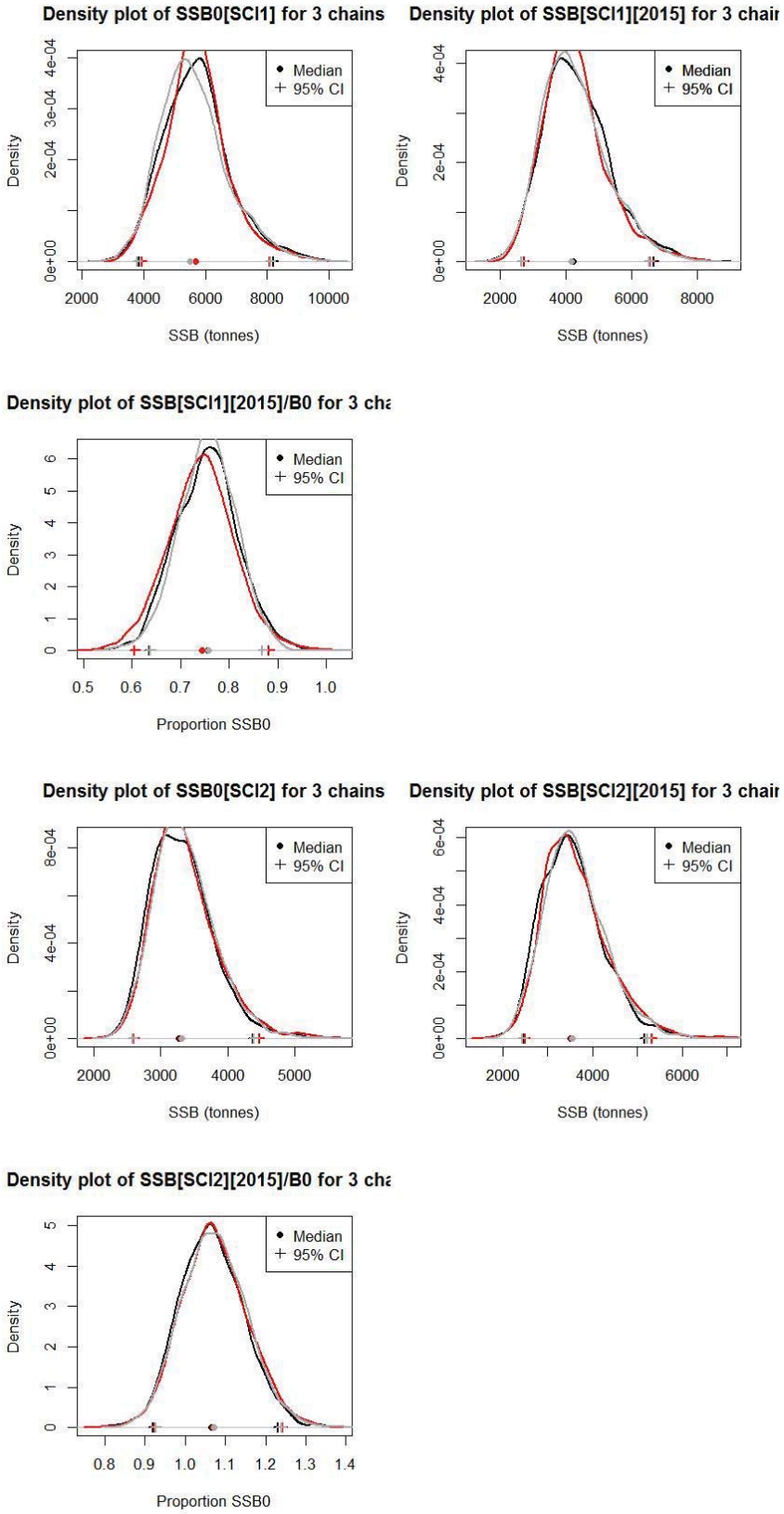

A11. 10: Density plots for B_0, SSB_{2015}, and SSB_{2015}/B_0 terms for SCI 1 and SCI 2 the combined area model for three independent MCMC chains, with median and 95% confidence intervals.

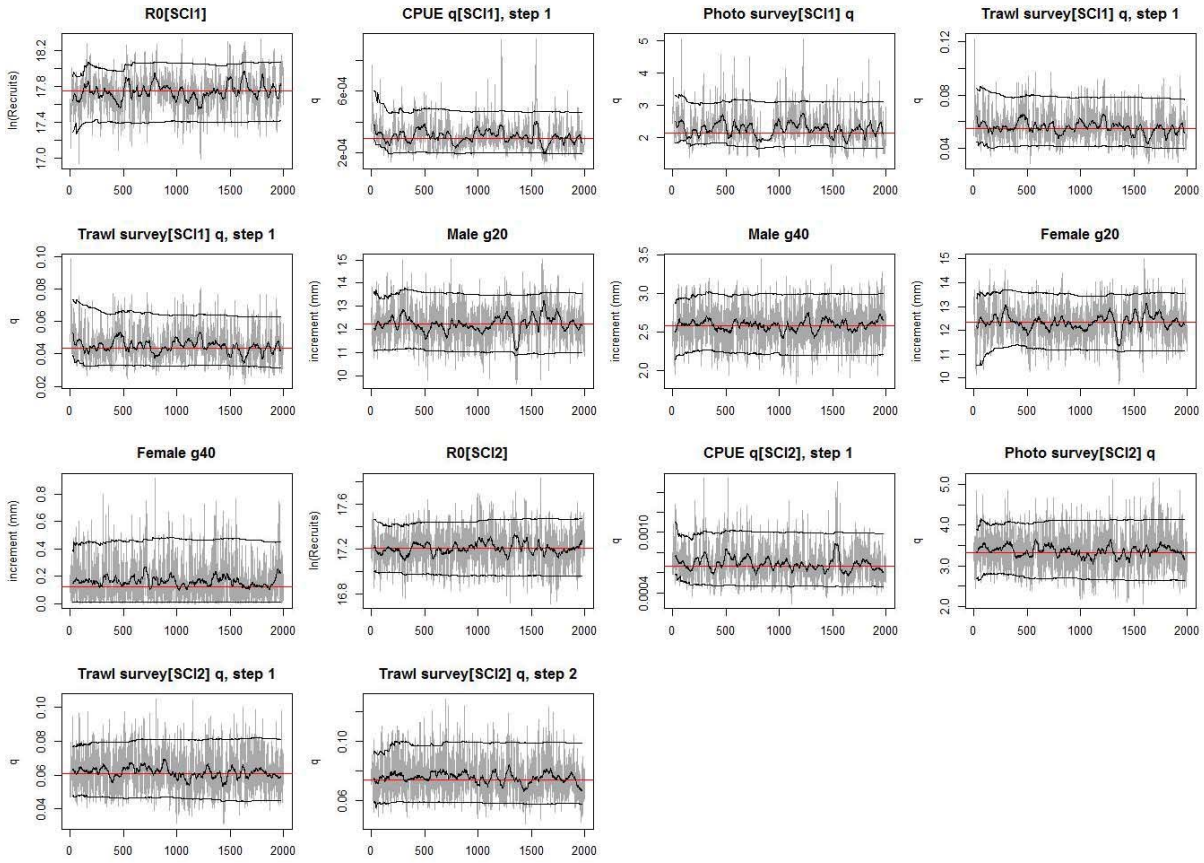

A11. 11: MCMC traces for R_0, catchability and growth terms for the combined area model.

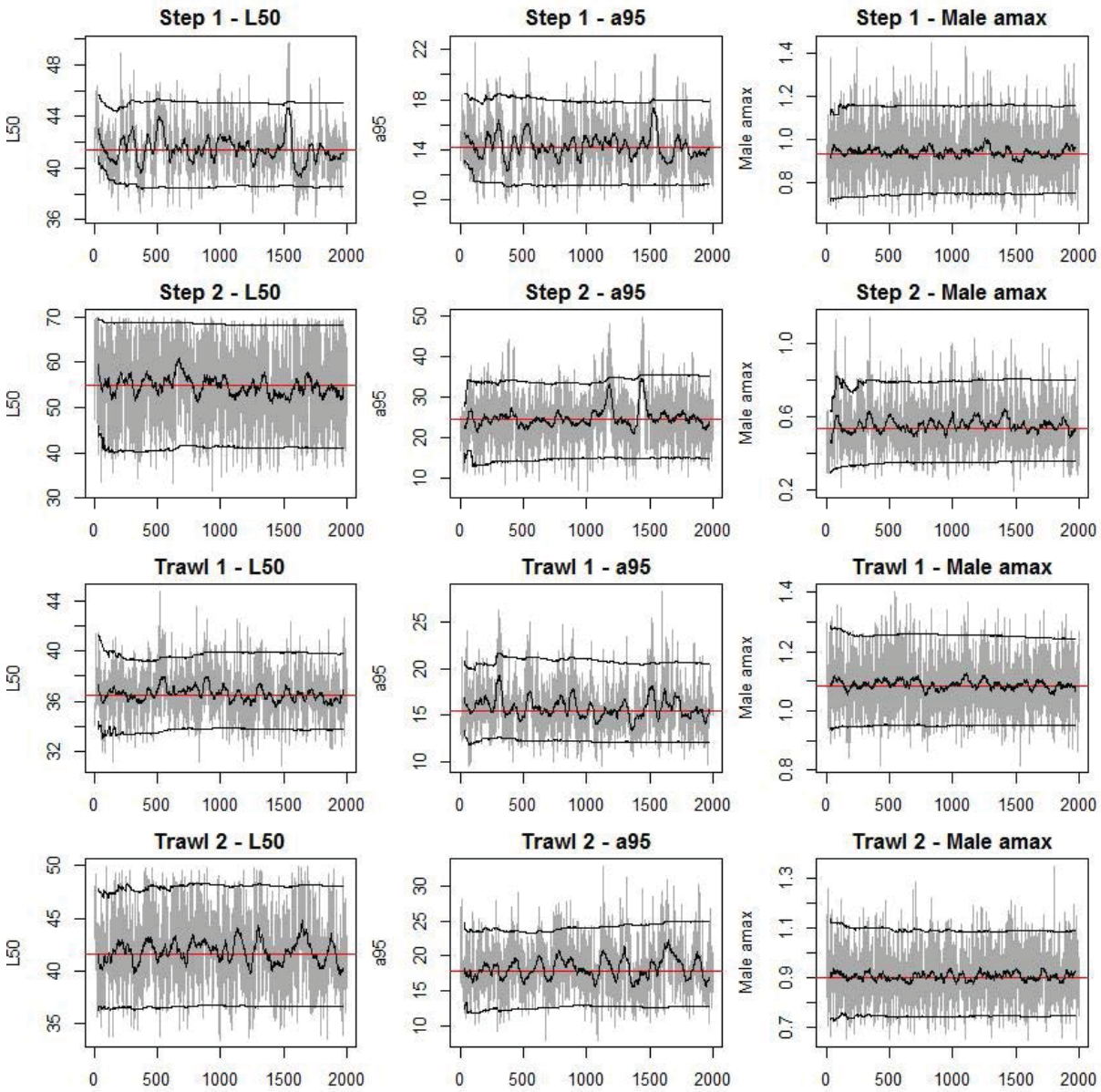

A11. 12: MCMC traces for selectivity terms for the combined area model.

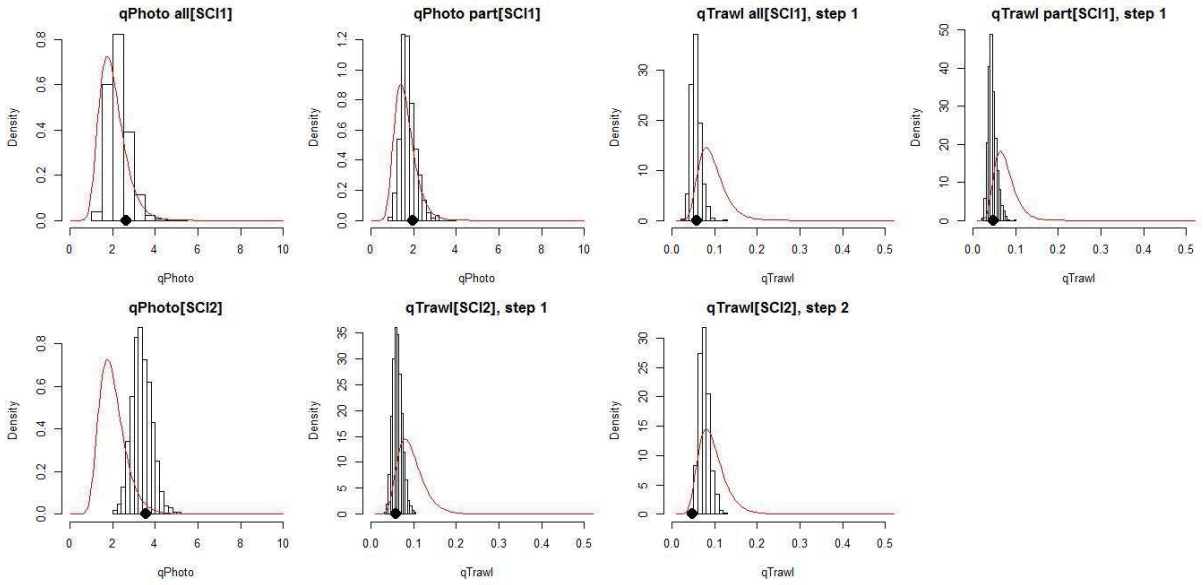

A11. 13: Marginal posterior distributions (histograms), MPD estimates (solid symbols) and distributions of priors (lines) for catchability terms for the combined area model.

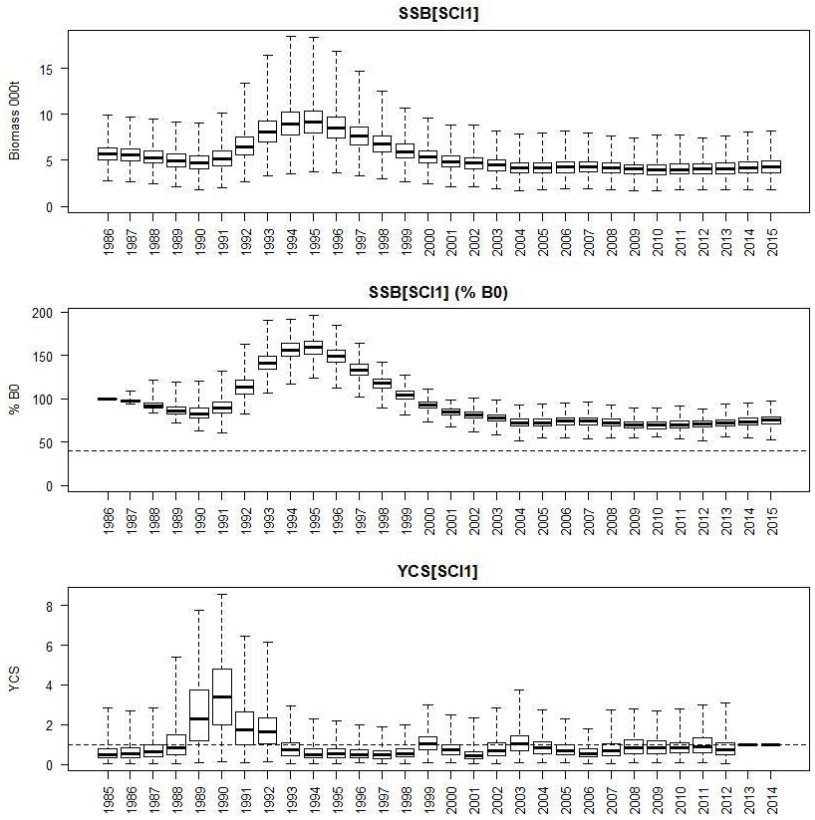

A11. 14: Posterior trajectory of SSB, SSB/SSB$_0$ and YCS for SCI 1 for the combined area model.

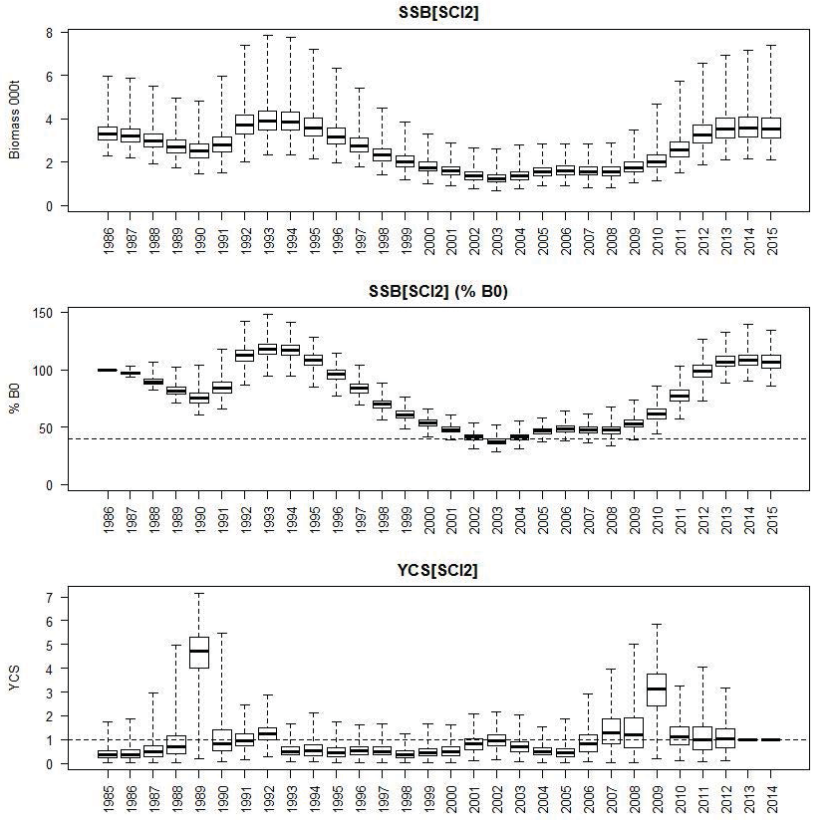

A11. 15: Posterior trajectory of SSB, SSB/SSB$_0$ and YCS for SCI 2 for the combined area model.